

1-1-2013

A Silylation Based Kinetic Resolution of Secondary Alcohols And The Synthesis And Structural Characterization of Pyridyl-oxazolidine Compounds

Cody Ian Sheppard
University of South Carolina

Follow this and additional works at: <https://scholarcommons.sc.edu/etd>

 Part of the [Chemistry Commons](#)

Recommended Citation

Sheppard, C. I.(2013). *A Silylation Based Kinetic Resolution of Secondary Alcohols And The Synthesis And Structural Characterization of Pyridyl-oxazolidine Compounds*. (Doctoral dissertation). Retrieved from <https://scholarcommons.sc.edu/etd/734>

This Open Access Dissertation is brought to you by Scholar Commons. It has been accepted for inclusion in Theses and Dissertations by an authorized administrator of Scholar Commons. For more information, please contact digres@mailbox.sc.edu.

A SILYLATION BASED KINETIC RESOLUTION OF SECONDARY ALCOHOLS AND
THE SYNTHESIS AND STRUCTURAL CHARACTERIZATION OF PYRIDYL-
OXAZOLIDINE COMPOUNDS

by

Cody Sheppard

Bachelor of Science
North Georgia College and State University, 2007

Submitted in Partial Fulfillment of the Requirements

For the Degree of Doctor of Philosophy in

Chemistry and Biochemistry

College of Arts and Sciences

University of South Carolina

2013

Accepted by:

Sheryl L. Wiskur, Major Professor

Ken D. Shimizu, Committee Member

Andrew B. Greytak, Committee Member

Campbell McInnes, Committee Member

Lacy Ford, Vice Provost and Dean of Graduate Studies

© Copyright by Cody Sheppard, 2013
All Rights Reserved

ACKNOWLEDGEMENTS

“Human speech is like a cracked kettle on which we tap crude rhythms for bears to dance to, while we long to make music that will melt the stars”

-Gustave Flaubert, “Madame Bovary”

First, I would like to thank Dr. Sheryl Wiskur for accepting me into her group and for the multitude of occasions in which her input helped my research; it has been a pleasure being able to work in her group. I would also like to thank my Grandmother. Any words I find myself writing to express my feeling of gratitude for the sacrifice and love she has given to me throughout my life falls short. All I can say is simply, thank you. To the rest of my family, I would also like to thank you all for your love and support. I would like to specifically thank my brother Todd. You are one of the most thought-provoking and intellectually stimulating persons I know. The conversations and debates we have, which would go on indefinitely if we were to let them, demand of me to maintain an open mind as well as a sharp one. I look forward to our discussions continuing for many years to come. To my dear friends, even though I favor quality over quantity, I have managed to end up with many fantastic friends. You have all made my life more interesting and enjoyable. I hope I have done the same for you. To the past and present Wiskur group members, it is tough to overstate the impact you all have had on my approach to chemistry. I am proud to have been able to work alongside you all. To my best friend and wife Meredith, it did not take long for me to realize that you are the most beautiful, smartest, wittiest, funniest, and kindest person I know. You have played no small part in me getting to where I am today and I cannot be more grateful.

ABSTRACT

Described herein is the first enantioselective silylation based kinetic resolution of monofunctional secondary alcohols to achieve useful levels of enantioselectivity. Using commercially available reagents, the reaction conditions were optimized and found to successfully resolve several secondary alcohols with high enantioselectivity. It was discovered that the nucleophilic isothioureia compound (-)-tetramisole, with Ph_3SiCl as the silyl source, gave superior results to other nucleophilic catalysts and was capable of performing the kinetic resolution in as little as 45 minutes using mild reaction conditions. The structural and electronic characteristics of successful and less successful substrates are also discussed.

Chapter three discusses mechanistic investigations and the characterization of the reactive silylating compounds for the enantioselective silylation of monofunctional secondary alcohols with (-)-tetramisole and other nucleophiles. Solid state and solution based ^1H and ^{29}Si NMR techniques were utilized as well as a modified ^1H - ^{29}Si gHSQC NMR technique. Evidence to support a tetravalent silicon intermediate between (-)-tetramisole and Ph_3SiCl is presented. Then, circular dichroism studies were performed on some chiral silyl ethers to see if a nearby chiral center can cause the aryl groups to favor a single helical conformation.

Chapter four presents the synthesis and structural characteristics of chiral 2-pyridyloxazolidine and 2,6-pyridylbisoxazolidine compounds. These compounds were

found to be viable ligands in the formation of metal complexes. Their ability to behave as colorimetric sensors for chiral monofunctional alcohols and amines is also reported. In addition, their use as an organocatalyst for the kinetic resolution of secondary alcohols by enantioselective silylation is also discussed.

TABLE OF CONTENTS

ACKNOWLEDGEMENTS.....	iii
ABSTRACT	iv
LIST OF TABLES	ix
LIST OF FIGURES	xi
CHAPTER 1 INTRO AND BACKGROUND	1
1.1 INTRODUCTION	1
1.2 METHODS FOR THE OBTAINMENT OF ENANTIOMERICALLY ENRICHED COMPOUNDS.....	3
1.3 ORGANOCATALYZED KINETIC RESOLUTIONS OF SECONDARY ALCOHOLS BY LEWIS BASES	13
1.4 CONCLUSIONS	23
1.5 REFERENCES.....	24
CHAPTER 2 KINETIC RESOLUTION OF SECONDARY ALCOHOLS BY ENANTIOSELECTIVE SILYLATION.....	28
2.1 INTRODUCTION	28
2.2 TRANSITION METAL CATALYZED KINETIC RESOLUTIONS BY ENANTIOSELECTIVE SILYLATION.....	29
2.3 ORGANOCATALYZED ENANTIOSELECTIVE SILYLATION.....	31
2.4 IDENTIFYING A SELECTIVE CATALYST FOR THE ENANTIOSELECTIVE SILYLATION OF SECONDARY ALCOHOLS.....	45
2.5 OPTIMIZING REACTION CONDITIONS FOR THE ENANTIOSELECTIVE SILYLATION OF SECONDARY ALCOHOLS WITH (-)-TETRAMISOLE (2.12).....	52

2.6 DETERMINING THE SUBSTRATE SCOPE FOR THE ENANTIOSELECTIVE Silylation OF SECONDARY ALCOHOLS WITH 2.12	61
2.7 CONCLUSIONS	66
2.8 EXPERIMENTAL	68
2.9 REFERENCES	101
CHAPTER 3 MECHANISTIC INVESTIGATIONS INTO THE ENANTIOSELECTIVE Silylation OF SECONDARY ALCOHOLS WITH Ph ₃ SiCl BY Levamisole (2.12)	106
3.1 INTRODUCTION	110
3.2 DETERMINING THE VALENCY OF THE REACTIVE Silylating INTERMEDIATE BY NMR ANALYSIS	131
3.3 DETERMINING THE EXISTENCE OF A SINGLE PROPELLER CONFORMATION OF Silyl ETHERS BY CIRCULAR DICHROISM	138
3.4 STUDYING THE PROPELLER CONFORMATION OF Silyl ETHER COMPOUNDS IN THE SOLID STATE	141
3.5 CONCLUSIONS	141
3.6 EXPERIMENTAL	143
3.7 REFERENCES	222
CHAPTER 4 THE SYNTHESIS AND CHARACTERIZATION OF 2-PYRIDYL-OXAZOLIDINE LIGANDS AND THEIR APPLICATION AS CHIRAL SENSORS AND CATALYSTS	229
4.1 INTRODUCTION	229
4.2 SYNTHESIS AND CHARACTERIZATION OF CHIRAL 2-PYRIDYL-OXAZOLIDINE (MONOX) AND 2-PYRIDYL-BISOXAZOLIDINE (BISOX) COMPLEXES	232
4.3 THE SYNTHESIS OF NOVEL METAL COMPLEXES WITH THE DIMETHYL-BISOX LIGAND AND THEIR APPLICATION IN THE COLORIMETRIC SENSING OF CHIRAL ALCOHOLS	236
4.4 THE SYNTHESIS OF NOVEL BISOX-NICKEL AND BISOX-ZINC COMPLEXES AND THEIR USE AS SENSORS FOR MONOFUNCTIONAL CHIRAL AMINES	240
4.5 APPLICATION OF BISOX AS AN ORGANOCATALYST IN THE KINETIC RESOLUTION OF SECONDARY ALCOHOLS VIA ENANTIOSELECTIVE Silylation	247

4.6 CONCLUSIONS	248
4.7 EXPERIMENTAL	249
4.8 REFERENCES.....	271
WORKS CITED	275

LIST OF TABLES

Table 1.1 The conversion required to achieve 90%, 95%, and 99% ee at a given selectivity factor	12
Table 2.1 The substrate scope reported for the enantioselective silylation of meso diols with catalyst 2.7	40
Table 2.2 Reaction conditions and substrate screening of the RRRM silylation reported by the Tan group	42
Table 2.3 Testing bases for the enantioselective silylation of 2.11 with CD-TMS and Et ₃ Si-Cl.	49
Table 2.4 Testing various catalysts for the enantioselective silylation of 2.11 with Et ₃ Si-Cl.	51
Table 2.5 The effect of different silyl substituents on the enantioselective silylation of 2.11 with 2.12	53
Table 2.6 The effect of base upon the selectivity factor for the enantioselective silylation of 2.11 with 2.12	55
Table 2.7 Testing the solvent effect on the enantioselective silylation of 2.11	57
Table 2.8 Determining the length of the reaction for the enantioselective silylation of 2.11 with 2.12	58
Table 2.9 Testing other nucleophilic catalysts with the optimized conditions developed for the enantioselective silylation of 1-indanol (2.11)	60

Table 2.10 Testing the substrate scope with the optimized reaction conditions for enantioselective silylation with 2.12	63
Table 3.1 Solid State MAS- ²⁹ Si-SSNMR analysis of 2.12 /Ph ₃ SiCl and hydrolysis products.....	116
Table 3.2 ¹ H- ²⁹ Si gHSQC NMR analysis at -78°C of several 2.12 /silylchloride complexes and their potential hydrolysis products	121
Table 3.3 ¹ H- ²⁹ Si gHSQC NMR analysis of Ar ₃ SiCl with electron donating, electron withdrawing, and <i>p</i> <i>t</i> Bu- substituents at -78 °C in CD ₂ Cl ₂	124
Table 3.4 Enantioselective silylation of (±)-4-chroman-3-ol with 2.12	125
Table 3.5 ¹ H- ²⁹ Si gHSQC NMR analysis at -78 °C of complexes formed with different nucleophiles	129

LIST OF FIGURES

Figure 1.1 The enantiomers of the commercially available drugs Chloramphenicol and Ethambutol have undesired effects	2
Figure 1.2 The enantiopure blockbuster drug Nexium was once sold as the racemate: Prilosec.....	3
Figure 1.3 Some commercially available drugs with their D-amino acid fragment highlighted in red	4
Figure 1.4 Paclitaxel	5
Figure 1.5 Catalytic cycle for the kinetic resolution of secondary alcohols via acylation.	14
Figure 1.6 The planar chiral ferrocene catalysts developed by the Fu group and their application as a acyl transfer catalyst.....	17
Figure 1.7 Peptide based catalysts screened in the enantioselective acylation of 1.13	19
Figure 1.8 Proposed mechanism for the kinetic resolution of secondary alcohols with the peptide based catalysts developed by the Miller group	20
Figure 1.9 Proposed transition state for the enantioselective acylation by 1.14	21
Figure 1.10 The evolution of the amidine and isothioureia catalysts developed by the Birman group	22
Figure 1.11 Kinetic resolution of secondary alcohols via 1.15	22
Figure 2.1 Catalytic pathway for the enantioselective Si–O coupling proposed by the Oestreich group.....	31

Figure 2.2 The proposed transition state for the enantioselective silylation of 1,2-syn diols by the bifunctional catalyst, 2.6	39
Figure 2.3 The proposed catalytic cycle for the desymmetrization of cyclic syn-1,2-diols using the bifunctional catalyst 2.7 with Et ₃ Si-Cl	41
Figure 2.4 Initial findings of the Wiskur group which suggest that the silylation step was the enantiomerically enriching step.	43
Figure 2.5 The mechanism proposed by the Wiskur group for the generation of enantiomerically enriched trimethylsilyl protected β-hydroxy esters from the Mukiyama aldol reaction catalyzed by a quaternary cinchona alkaloid salt.....	44
Figure 2.6 The product observed from the deprotection of ((6-methoxy-1,2,3,4-tetrahydronaphthalen-1-yl)oxy)triphenylsilane	66
Figure 3.1 The nucleophilic isothioureia based catalyst (-)-tetramisole (2.12)	107
Figure 3.2 Mechanistic questions to be investigated	107
Figure 3.3 A valence bond visualization of a 3c-4e bond between silicon and its axial ligands in a pentavalent silicon species	110
Figure 3.4 A comparison of the bicyclic ring protons in CD ₂ Cl ₂ of (a) 2.12 and (b) the isolated solid that forms from the addition of 2.12 and Ph ₃ SiCl	111
Figure 3.5 nOe-difference spectrum of the isolated solid from the addition of 2.12 to Ph ₃ SiCl in THF and the observed nOe correlations.....	112
Figure 3.6 ²⁹ Si-SSNMR and ²⁹ Si-NMR resonances for the known pentavalent isothioureia/silylchloride (3.3)	113
Figure 3.7 The obtained and literature MAS- ²⁹ Si-SSNMR spectra of Ph ₃ SiOH.....	115

Figure 3.8 Reported ^{29}Si resonances for Ph_3SiCl ⁴⁴ and some hypervalent silicon containing compounds of the formula Ph_3SiX_2	117
Figure 3.9 Presumed nucleophilic attack of the chiral alcohol	131
Figure 3.10 Ph_3SiCl undergoes a rapid interconversion between helical propeller conformations	132
Figure 3.11 By attaching a chiral ligand to Ph_3SiCl , it may be possible to get a single helical arrangement of the phenyl groups.	133
Figure 3.12 The proposed origin of enantiodiscrimination for the enantioselective silylation of secondary alcohols with 2.12 and Ph_3SiCl	133
Figure 3.13 Three representative chiral trityl ethers and the reported aryl configuration	134
Figure 3.14 $\text{Ph}_3\text{Si-}$ derivatized silyl ether compounds analyzed via CD spectroscopy.....	135
Figure 3.15 The acquired CD spectrum of 3.15 showing a Cotton effect	136
Figure 3.16 The acquired CD spectrum of 3.16	137
Figure 3.17 The acquired CD spectrum of 3.17 & 3.18	138
Figure 3.18 The two crystal structures isolated from 3.16 showing both potential helical conformations of the silyl ether group	139
Figure 3.19 The only crystal structures obtained from 3.17 and 3.18	140
Figure 4.1 The oxazoline functionality	230
Figure 4.2 The two potential diastereomers of the oxazolidine complexes MonOx and methyl-MonOx.....	236
Figure 4.3 Chiral monofunctional alcohols tested as analytes with 4.22	240

Figure 4.4 Examples of chiral pseudo crown ethers reported for the colorimetric enantiodiscrimination of chiral amines	242
Figure 4.5 The enantioselective indicator displacement assays (eIDA) developed by the Anslyn group. The indicator, chrome azurol S, is shown in red.....	240
Figure 4.6 Chiral monofunctional amines tested as analytes with 4.22	243
Figure 4.7 The transition metal and lanthanide salts used with 4.8 in the discrimination of 4.31 and 4.22 (acac = acetylacetone)	244
Figure 4.8 The monofunctional chiral amines used as analytes with 4.44	247

Chapter 1. Introduction and Background

1.1 Introduction

The obtainment of enantiomerically pure compounds has been a major endeavor in organic chemistry for the last several decades. The demand for these compounds is driven mainly by their biological activity. These properties are exploited primarily in the pharmaceutical industry where they are employed for their pharmacological properties.^{1, 2} Historically, chiral drugs were often sold as a racemate;¹ however, it is often only one enantiomer that possesses the desired biological activity, or shows much activity at all. It is also noteworthy that in some cases, one enantiomer of the desired compound can have the desired properties while its opposite enantiomer can have harmful or even fatal effects. For example, (R,R)-chloramphenicol possesses antibacterial properties while its enantiomer is inactive. However, (S,S)-Ethambutol has been used in the treatment of tuberculosis, while the enantiomer causes blindness¹ (Figure 1.1).

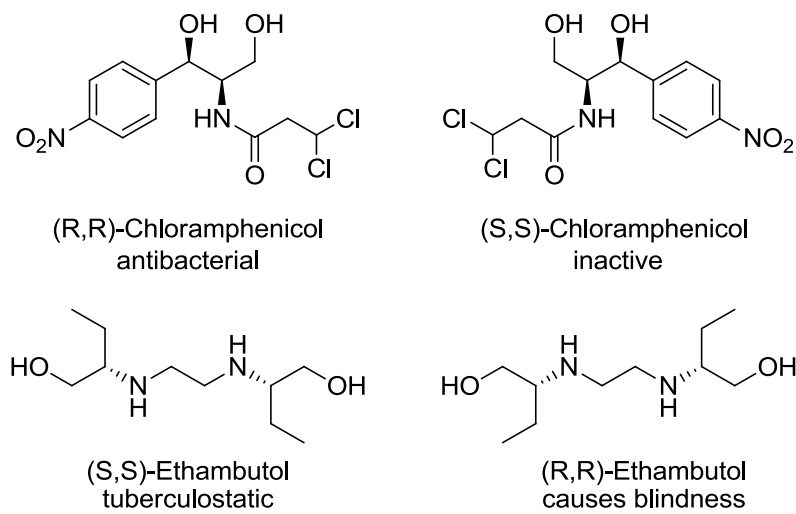


Figure 1.1 The enantiomers of the commercially available drugs Chloramphenicol and Ethambutol have undesired effects.¹

Due to the potential negative effects of certain enantiomers, the USFDA requires both enantiomers of a racemic drug to be analyzed for their potential pharmacological effects.³ This requires the synthesis or separation of enantiomers even for screening purposes. With these considerations in mind, there have been major research efforts by many research groups to develop methods for the creation and isolation of homochiral compounds. As a result of this research, many previously racemic drugs are now being released as single enantiomer compounds, leading to formulations that are considerably more pharmacologically active and require lower dosages, such as in the case of Esomeprazole and Omeprazole (**Figure 1.2**).⁴ Several of the most common methods for the procurement of enantiomerically enriched compounds will be discussed herein.

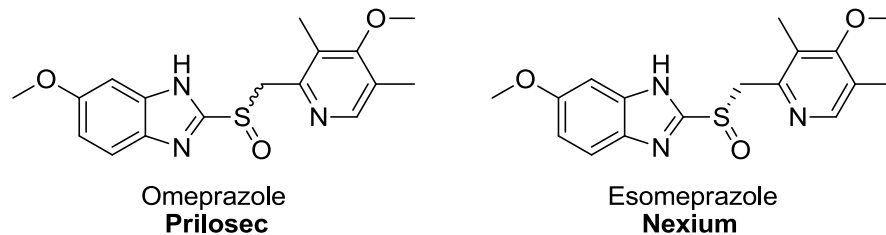


Figure 1.2 The enantiopure blockbuster drug Nexium was once sold as the racemate: Prilosec

1.2 Methods for the obtainment of enantiomerically enriched compounds

1.2.1 Nature ('the chiral pool')

When looking for a specific enantiomer of a molecule, it is quite often that one may need to look no further than nature. In fact, screening natural products for their medicinal properties remains one of the most important methods for determining basic pharmacores for modern drug discovery.⁵ The chiral building blocks of new biologically active molecules can also be obtained from natural sources, but there are some major limitations to this method. First, Nature's chiral pool is limited and may not contain the desired building block. It is also possible that nature makes the opposite enantiomer of the needed chiral compound. Perhaps the best example of this is the fact that most α -amino acids found in nature are levorotary. However, it was discovered that dextrorotary amino acids can have antibacterial properties when incorporated into peptides and small molecules, which can lead to antimicrobial selectivity.⁶⁻⁸ Due to these properties, there has been a large demand for D-amino acids in the production of a number of antibiotics and other drugs such as Nateglinide, penicillins, Seromycin, and Alitame (Figure 1.3).⁹ Secondly, there is the potential that the demand for the natural product is much greater

than the supply. This can be exemplified by the production of the cancer drug Paclitaxel (Taxol).

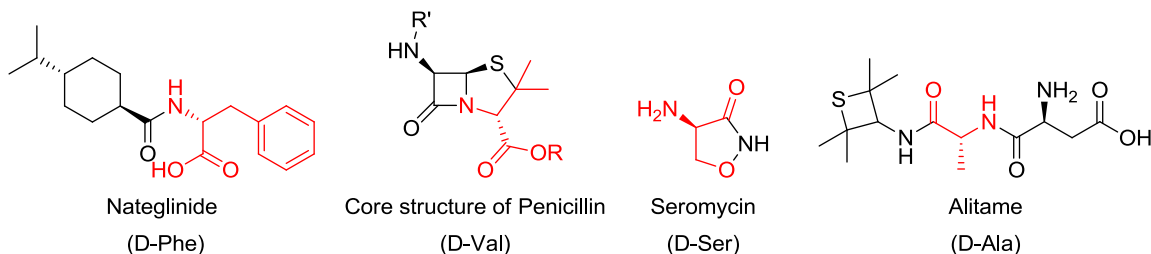


Figure 1.3 Some commercially available drugs with their D-amino acid fragment highlighted in red.

Paclitaxel (Figure 1.4), which was originally obtained solely by extraction from the Pacific yew tree *Taxus brevifolia*, was found to have potent anti-cancer activity.¹⁰ This property has led to the drug becoming a highly sought after natural product. Although Paclitaxel is readily found in nature, it was reported to require 16,000 pounds of bark to extract only 1 kg of Paclitaxel.¹¹ This renders direct access to this product unfeasible in the quantities required for commercial sale. As a result, other methods for the production of Paclitaxel have since been developed.¹² All of the above shortcomings listed have led to the development of several other methods to synthesize chirally enriched compounds.

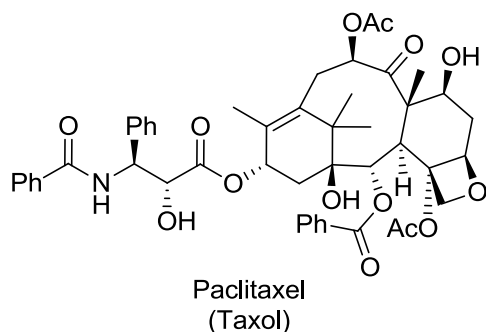
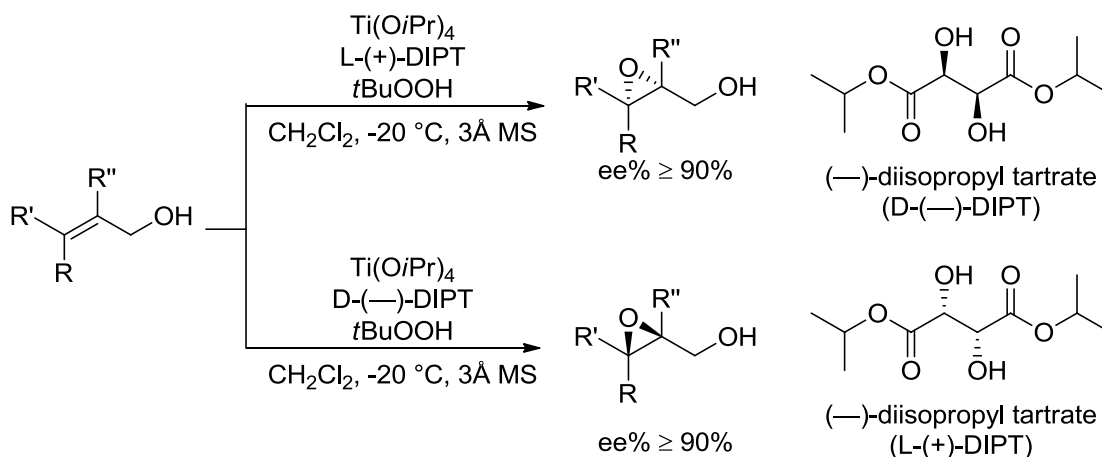


Figure 1.4 Paclitaxel

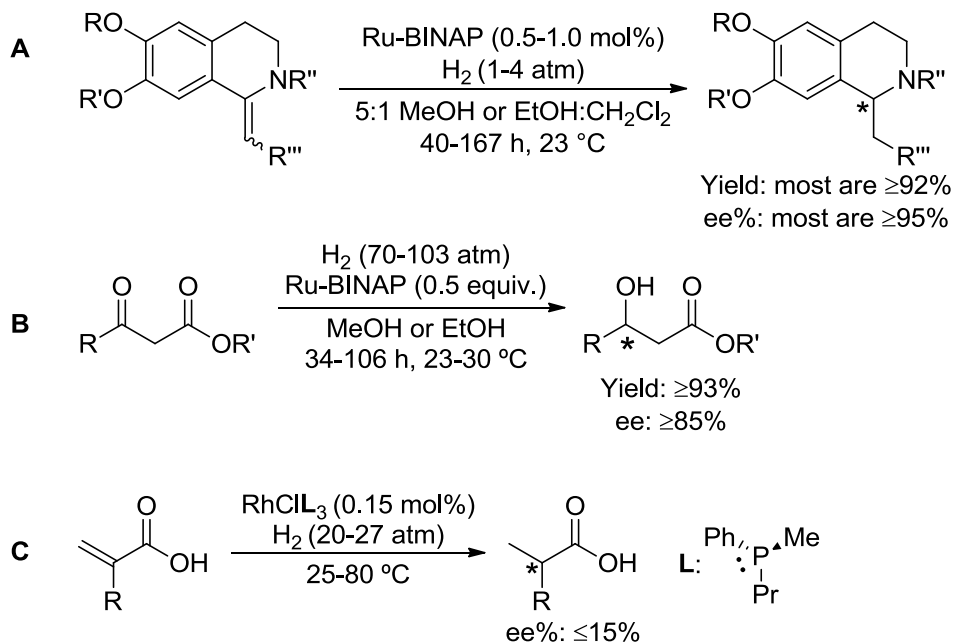
1.2.2 Asymmetric Catalysis

One of the most common methods for the production of optically active molecules is via asymmetric reactions.¹³⁻¹⁵ These reactions occur through the use of a chiral catalyst to perform a reaction on a prochiral substrate resulting in enantiomerically enriched chiral products. Asymmetric reactions are also some of the most common methods to obtain enantiomerically enriched products. In this family of reactions, one of the most well-known asymmetric reactions is the enantioselective epoxidation reaction that was developed by the Sharpless group (Scheme 1.1).¹⁶⁻¹⁸ In this reaction, titanium tetrakisopropoxide was combined with (-)-diisopropyl tartrate with tertbutoxide as an oxidant to enantioselectively oxidize allylic alcohols giving enantiomerically enriched epoxides. Another important class of asymmetric reactions is the asymmetric hydrogenation reactions developed by the Noyori group¹⁹⁻²² and Knowles et al²²⁻²⁵ (Scheme 1.2). In these reactions, rhodium and ruthenium metals are combined with chiral phosphine ligands with H₂ to reduce alkenes and carbonyls to give enantiomerically enriched carbon centers. These asymmetric transformations were also

mentioned as the key reactions which led to Drs. Barry Sharpless, Ryōji Noyori, and William S. Knowles sharing the Nobel Prize in 2001. Undoubtedly, these reactions and subsequent international recognition has brought even more attention to this already nascent field.



Scheme 1.1 The general reaction scheme for the Sharpless asymmetric epoxidation including the predicted product's stereochemistry.



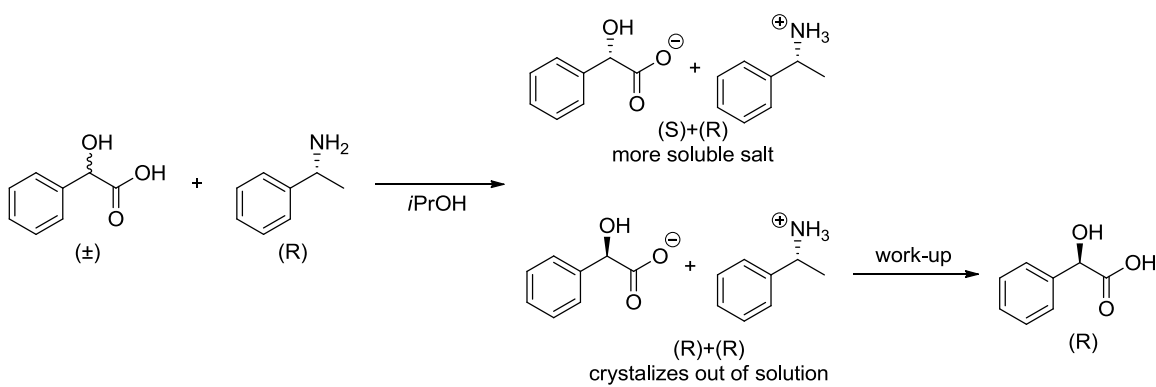
Scheme 1.2 Selected early examples of the Noyori (**A** and **B**) and Knowles (**C**) asymmetric hydrogenation.

The advantage of using asymmetric reactions to procure enantiomerically enriched compounds lies in its potential to achieve a yield of up to 100% with an enantiomeric excess (ee%) of up to 100%. In a finely tuned system, a quantitative yield of a single enantiomer can be obtained. Furthermore, one of the key goals of any methodology is to minimize the catalyst loading. This method can use catalytic loadings down to a fraction of a percent. Such low catalyst loadings, however, are found mostly in the case of transition metal catalysts, as opposed to organocatalysts which frequently require higher catalyst loadings.²⁶ The main drawback of transition metal catalyzed asymmetric reactions is the toxicity for some of the most common transition metals that are used, and necessitating extensive purification to ensure removal of all transition metal residue. If high ee%, yield, and low catalyst loading are found in the same system, this would be an ideal system for the generation of enantiomerically pure compounds. However, this is not often the case. As a result, either the yields or enantioselectivity may not be good enough for the substrate being reacted. Also, it is common in asymmetric reactions that there is a need for achiral additives which can generate waste byproducts that can be undesirable on a large, industrial scale.¹ Therefore, despite all of the advances in asymmetric catalysis over the past several decades there remains a demand for alternative methods for procuring enantioenriched compounds.

1.2.3 Classical Resolution

One of the oldest methods for procuring a single enantiomer of a compound is classical resolution. In this technique, a racemic compound, usually an amine or acid

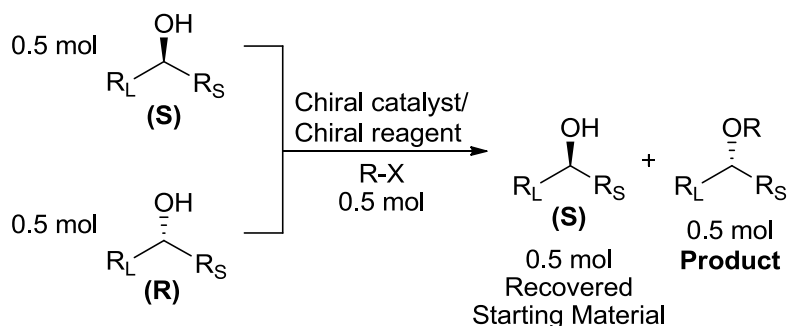
containing compound, is selectively crystallized by the addition of a chiral compound that is usually the other half of the subsequent acid-base pair, to form a diastereomeric salt. These diastereomers can then have very different solubility which can cause a diastereomer to crystallize. The diastereomers can then be easily converted to the original compound that is now of high enantiopurity (Scheme 1.3). This technique is commonly implemented in the pharmaceutical industry. However, there remain some key limitations with this resolution method. First, it is currently very difficult to predict what the optimal resolving agent, since there is no guarantee that the resulting diastereomer salt or compound will crystallize in a selective manner. Therefore, the method development strategy for identifying suitable resolution conditions involve simple trial and error.² Also, we are limited by the number of known and readily available resolving agents.²⁷ Another problem is the relatively small number of functional groups that lend themselves to this method. For example, functional groups such as alcohols are very difficult to resolve in this method. The other issue, which is also a problem with most resolution techniques, is that, since we are starting with a racemic mixture (and there is no interconversion between enantiomers), the highest yield theoretically possible is 50%.



Scheme 1.3 Classical resolution of mandelic acid with (R) -1-phenylethylamine²⁸

1.2.4 Kinetic Resolution

The final technique discussed herein is kinetic resolution. In this method, a racemic substrate is reacted with a chiral catalyst or reagent that selectively reacts with one enantiomer leaving the unreacted starting material enantiomerically enriched and, depending on the type of kinetic resolution being performed, also gives an enantioenriched product as well (Scheme 1.4). This form of resolution can be accomplished three different ways, each with their own drawbacks. One of the most popular forms of kinetic resolution is enzymatic kinetic resolution. This form of kinetic resolution most commonly involves using a natural enzyme to catalyze an enantioselective reaction of a racemic substrate. This method has three main drawbacks, the relatively high cost of enzymes, the limited pool of selective substrates and the potential for solvent incompatibility with the substrate or the enzyme.



Scheme 1.4 Example of a kinetic resolution of a racemic secondary alcohol.

Another common kinetic resolution method is the use of enantioselective transition metal catalysts. However, as mentioned before, one of the main drawbacks of this method is the potential for residual toxic metal contamination of the desired products or unreacted starting materials. Finally, there are kinetic resolutions catalyzed by organic

catalysts. This field is now well established, but it is still evolving. The key benefit of organocatalyzed kinetic resolutions is the low toxicity of most of the catalysts used, however, they usually require higher catalyst loadings.

The advantage and disadvantage of kinetic resolutions is in the dependence of enantiomeric excess (ee) upon conversion (conv.). As the reaction proceeds (and conv. increases), the ee of the starting material increases, and the ee of the product (ee') diminishes. This "tuneability" of the ee% allows for the achievement of very high ee's using reactions that have low or moderate enantioselectivity. In order to predict the required amount of conversion that would be required to achieve a desired ee, there must be a way to correlate ee and conv.. This value is called selectivity factor (s), which is simply the ratio of the rates of the individual enantiomers (k_{rel}) (Equation 1.1). This also happens to correlate to the $\Delta\Delta G^\ddagger$ between the diastereomeric transition states of the enantiomers in the selectivity-determining step and correlates to the selectivity factor as well (Equation 1.1).^{29, 30}

With a $s = 10$, an ee of 98% is achievable with a conversion of 70%. For an ee of 99% the conversion falls only slightly to 28%.^{31, 32} When the selectivity factor increases higher than 10, the resulting increase in enantiomeric excess at a given conversion increases at smaller amounts as s approaches infinity. Therefore, a $s \geq 10$ is often considered the benchmark with which to determine if a reaction is efficient enough to be practical.

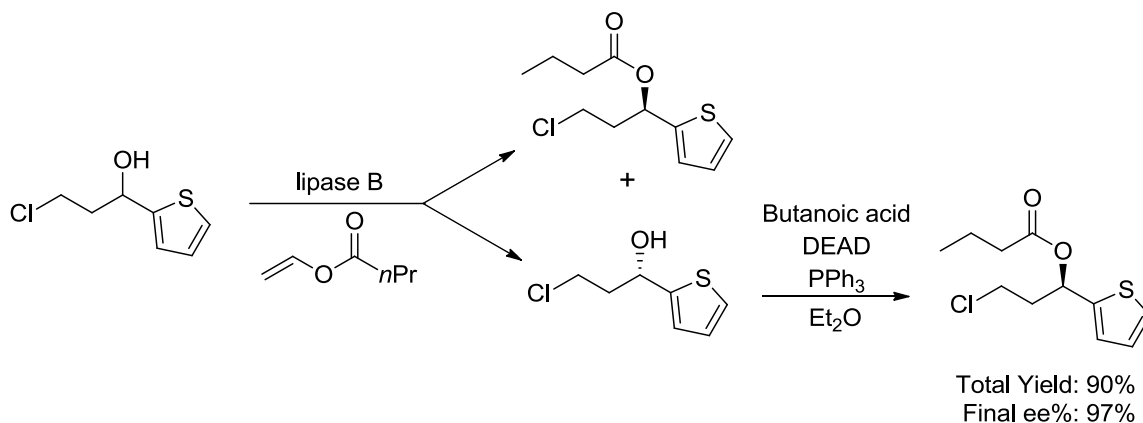
$$s = k_{\text{rel}} = \frac{k_{\text{fast}}}{k_{\text{slow}}} = e^{\frac{\Delta\Delta G^\ddagger}{RT}} = \frac{\ln[(1-\text{Conv.})(1-\text{ee})]}{\ln[(1-\text{Conv.})(1+\text{ee})]}$$

Equation 1.1 The relation between selectivity factor (s), rate, conversion (conv.), ee, and $\Delta\Delta G^\ddagger$. R refers to the gas constant and T is temperature in kelvin.

Energetically, the $\Delta\Delta G^\ddagger$ required to reach a $s = 10$ is only 1.35 kcal/mol at 23 °C or 0.89 kcal/mol at -78 °C. For comparison, the energy difference between an axial and equatorial methyl group on cyclohexane is 1.74 kcal/mol.³³ With the relationship between ee and conv. established, it now becomes possible to predict the required conversion needed to get the desired ee (Table 1.1). The key drawback of this method is the same as with classical resolutions, which is a maximum yield of 50%. However, this can be overcome in the case of alcohols through the use of a tandem kinetic resolution/Mitsunobu reaction such as seen in Scheme 1.5. One example of this can be shown in work of the Anthonsen group, where the sequential acylation via enzymatic kinetic resolution then inversion of the stereochemistry of the remaining starting material via Mitsunobu reaction gave the desired chiral ester with 90% yield and ee% of 97% (Scheme 1.5).³⁴

Table 1.1 The conversion required to achieve 90%, 95%, and 99% ee at a given selectivity factor.

s	Conv. required for the given ee at the indicated selectivity factor		
	ee = 90%	ee = 95%	ee = 99%
2	97.2	98.6	99.7
10	62.0	65.8	72.0
20	54.9	57.7	61.9
30	52.4	54.8	58.1
40	51.1	53.3	56.1
50	50.4	52.4	54.8



Scheme 1.5 The enzymatic acylation of a racemic secondary alcohol followed by a Mitsunobu reaction to give high ee and a yield greater than the theoretical 50% maximum yield.

With the advantage of a tunable ee and yields of up to 50%, kinetic resolution methodology becomes an incredibly powerful means to achieve highly enantiomerically pure molecules. This has led to the development of many different kinetic resolution methodologies^{13,31,32,35} and with the potential for the use of lower toxicity organocatalysts, has led the Wiskur group and other groups to target new organocatalyzed kinetic resolution techniques.

1.3 Organocatalyzed Kinetic Resolutions of Secondary Alcohols by Lewis Bases

1.3.1 Organocatalyzed Enantioselective Acylation

The most common method type of organocatalyzed kinetic resolution of secondary alcohols is by enantioselective acylation.^{36, 37} In these reactions, either a chiral Lewis base or a chiral Lewis acid/achiral Lewis base system³⁷ is used to generate a diastereomeric transition state that proceeds at different rates in the acylation reaction. In this report, the term organocatalysis is defined as a catalyst where the reaction center is, either a nitrogen, sulfur, phosphorous, or carbon. It is possible that some organocatalysts may contain a transition metal but the metal center is not part of the reaction center. Reported herein will be a brief overview of some of the most important Lewis base activated acylation reactions to date.

The general scheme for the kinetic resolution of secondary alcohols via enantioselective acylation is shown in Figure 1.5. The catalytic cycle begins with the nucleophilic acyl substitution by a chiral nucleophile, typically an anhydride or acyl chlorides, to form an enantiomerically pure acyl donor complex. This activated acylating compound will then undergo nucleophilic attack by a chiral secondary alcohol. Due to the chiral nucleophile, one secondary alcohol will be preferentially acylated, releasing the chiral catalyst and yielding enantiomerically enriched alcohol and ester.

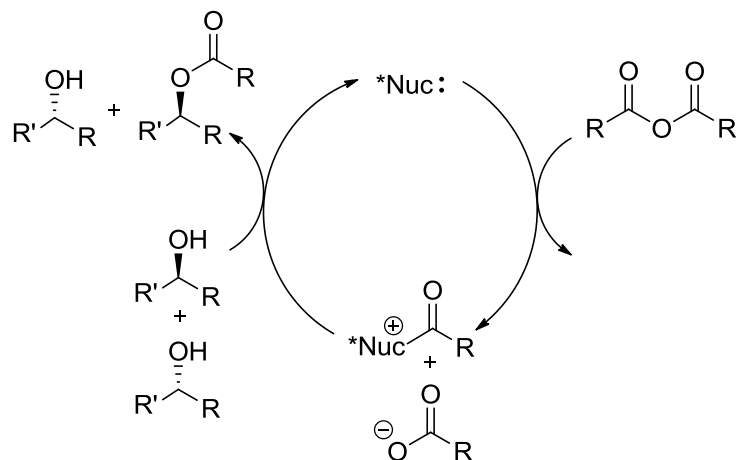
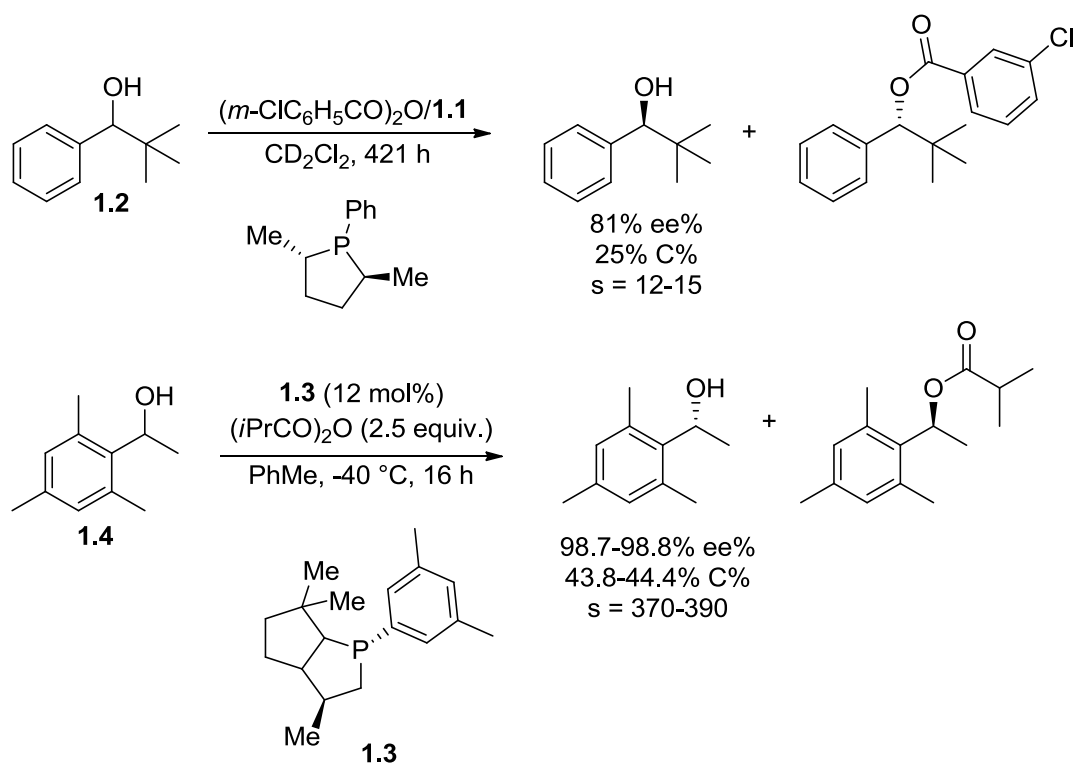


Figure 1.5 Catalytic cycle for the kinetic resolution of secondary alcohols via acylation.

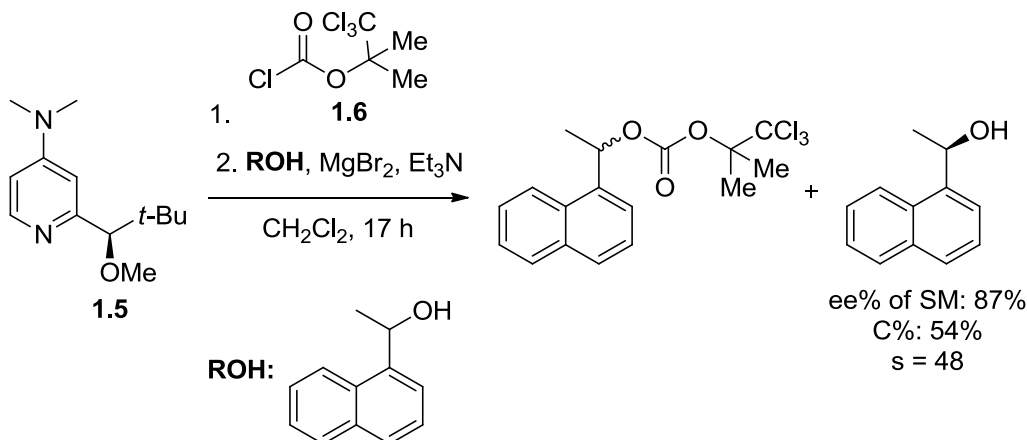
The first example of a useful selectivity factor for an organocatalyzed enantioselective acylation was reported by the Vedejs group.³⁸ In this reaction, a chiral phosphine (**1.1**) efficiently catalyzed the acylation of one enantiomer (Scheme 1.6) of the racemic mixture of acyclic secondary alcohol **1.2** using *m*-chlorobenzoic anhydride as the acyl source. This class of catalyst was later modified to give the more efficient catalyst **1.3**. This catalyst was very effective at achieving high levels of enantioselectivity with sterically hindered alcohols. Phosphine catalyst **1.3** can achieve selectivity factors in the 370-390 range at considerably shorter reactions times than **1.1** (Scheme 1.6). This high value of *s*, as pointed out by the authors, has a high amount of potential error.³⁹ In fact, a *s* > 50 should be viewed as an estimate of what the real selectivity factor is.^{39, 40} Despite this, it is still common in the literature to report selectivity factors well over 50.



Scheme 1.6 Kinetic resolution of secondary alcohols as described by the Vedejs group.

Shortly after the phosphine catalyst **1.1** was introduced, the same group developed the chiral 4-dimethylaminopyridine (DMAP) based catalyst (**1.5**) which afforded a $s \leq 48$ for a series of acyclic secondary alcohols with chloroformate **1.6** as the acyl source.⁴¹ Also reported was that the achiral Lewis acids ZnCl_2 or MgBr_2 and a nitrogenous base such as Et_3N was necessary (Scheme 1.7). This result represented the first application of a chiral DMAP catalyst in the kinetic resolution of secondary alcohols. Due to the high level of nucleophilicity of DMAP, this is noteworthy. Because of the nucleophilicity of DMAP and the encouraging levels of selectivity achieved by the Vedejs group, there has been extensive research into the synthesis of novel chiral DMAP based catalysts and their use as chiral catalysts in kinetic resolutions.^{37, 42} However, this system required

preformation of the active acylation complex, therefore, the system required stoichiometric amounts of **1.5**.



Scheme 1.7 The kinetic resolution of secondary aryl carbinols with the chiral DMAP based catalyst **1.5**.

At around the same time as the Vedejs group's report, Fu and co-workers reported the synthesis of a series of ferrocene containing planar chiral DMAP catalysts. This family of catalysts was shown to achieve excellent selectivity factors and in some cases results as high as a $s = 107$ (Figure 1.7),^{46,47} and unlike the system described in Scheme 1.7, the catalyst developed by Fu required only catalytic quantities of their chiral DMAP catalysts. In the example shown in Figure 1.6, the recovered alcohol (**1.8**) is an important intermediate in the synthesis of epothilone A⁴⁸ and the reaction was found to be successful when performed on the gram scale. These catalysts have been used with many different classes of substrates and have achieved useful selectivity factors for a majority of these systems.³⁷

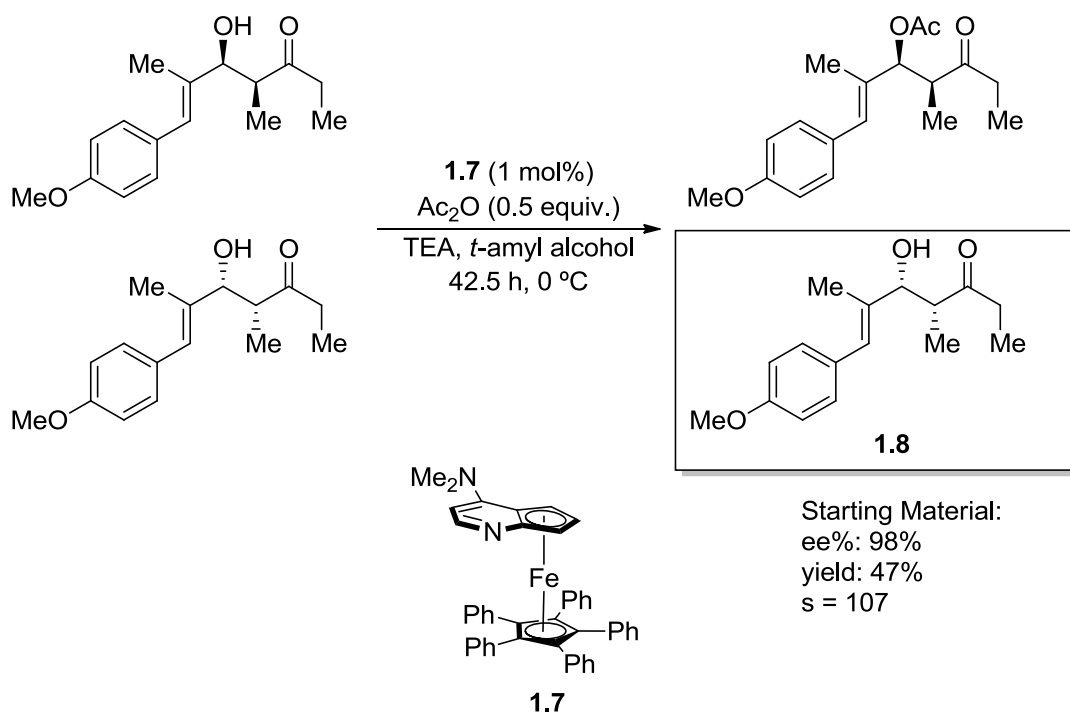


Figure 1.6 The planar chiral ferrocene catalysts developed by the Fu group and their application as a acyl transfer catalyst.

Due to the high selectivity and efficiency that can be achieved by enzymes, there has been an effort to use small peptides to mimic the active sites of enzymes for enantioselective acylation. This biomimetic approach to catalyst design has led to another major class of organocatalysts, the peptide based or imidazole based catalysts. This class, first reported by Miller and co-workers⁴⁹ contained multiple intramolecular hydrogen bonds to form a rigid chiral cavity with the right amount of rigidity. Then a histidine or modified histidine acts as a nucleophilic catalyst for the activation of an acyl source. Therefore, the nucleophilic center behaves as a modified chiral imidazole or N-methylimidazole, which are common nucleophilic activators for this type of reaction, and activates the acyl group in a chiral environment.

Miller's group,⁵⁰ discovered that the polypeptides **1.9-1.11** were selective as catalysts in the activation of acetic anhydride in the kinetic resolution via acylation of

chiral alcohol **1.13** (Figure 1.7). In particular, catalyst **1.9** had a high selectivity and was shown by NMR and x-ray crystallographic analysis to possess a β -hairpin secondary structure. Catalyst **1.9** was tested against **1.10**, which did not possess a secondary structure, was less structurally rigid than **1.9**, and gave a selectivity factor that was considerably lower. The importance of the rigidity of the catalyst structure was also tested by incorporating a butyl linker in catalyst **1.11** which would have a more conformationally defined macrocyclic structure. The considerable decrease in the selectivity of catalyst **1.11** strongly suggests that the catalyst must also retain some flexibility for optimal selectivity. The small molecule **1.12** was used as a control and was found to afford only racemic product ($s = 1$), suggesting that the chiral environment generated by the catalyst plays a more important role than the point chirality of a specific peptide.

In a range of studies,⁵¹ the octapeptide **1.9** was observed to give superior results to almost all of the catalysts screened. The proposed mechanistic pathway⁵² (Figure 1.8), involves the N-methylimidazole moiety activating the anhydride via nucleophilic acyl substitution. Then the chiral alcohol is stabilized through a secondary interaction, most likely hydrogen bonding or π - π stacking that orients the alcohol into position to the correct stereoelectronic configuration to attack the activated carbonyl. It is presumably this interaction that allows for transfer of chirality from the polypeptide's secondary structure to alcohol. Once, the alcohol has been oriented into position through interaction with the peptide backbone, the alcohol is then activated by the conjugate base of the anhydride via general base catalysis to attack the acylated N-methylimidazole.

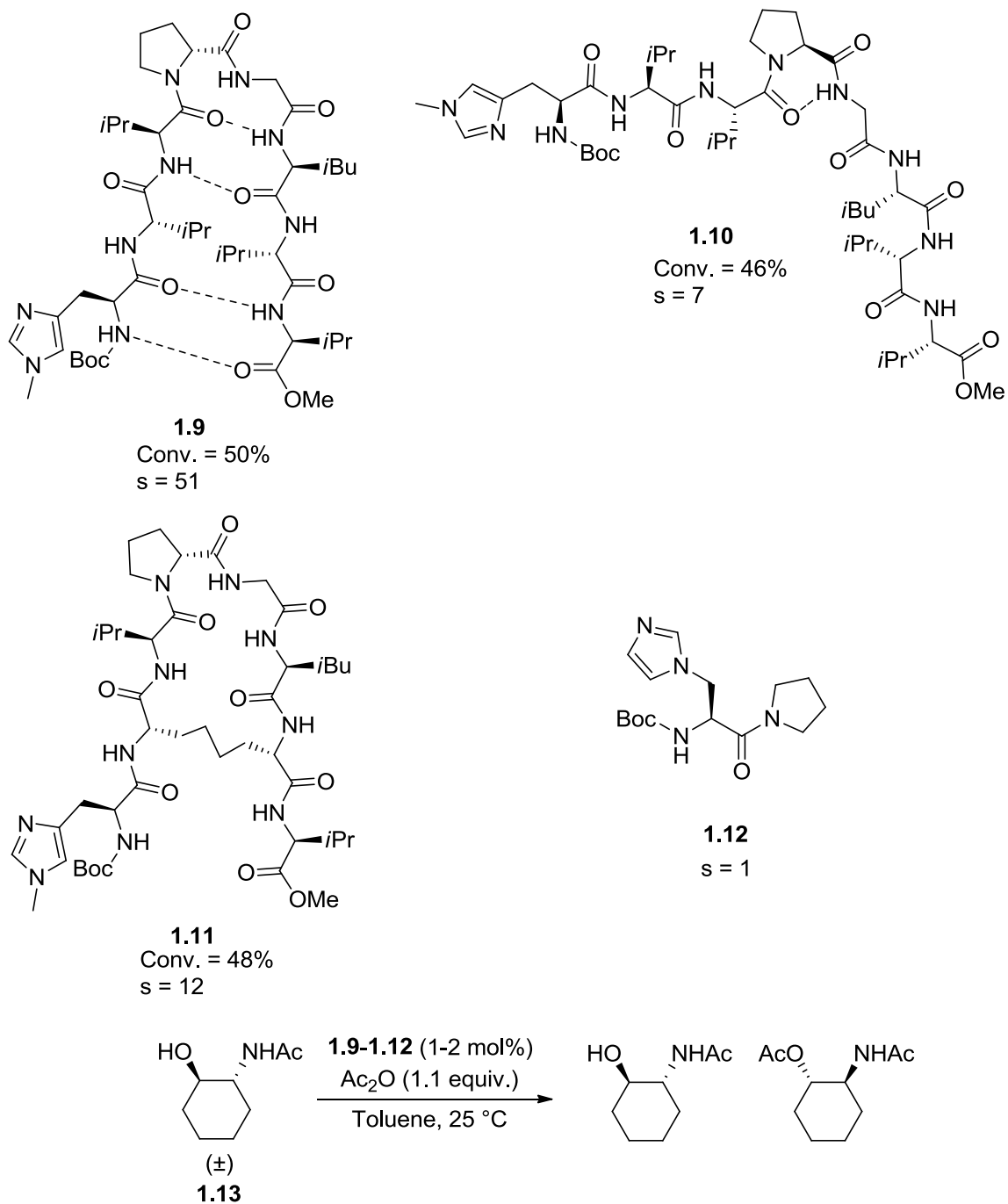


Figure 1.7 Peptide based catalysts screened in the enantioselective acylation of **1.13**.

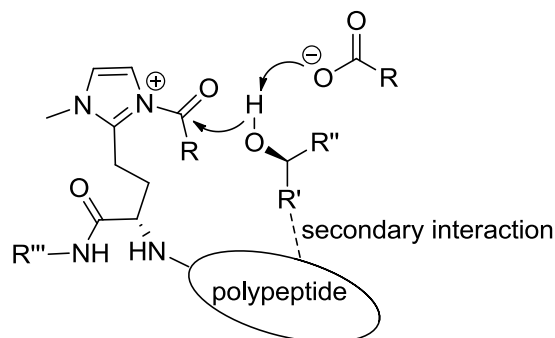
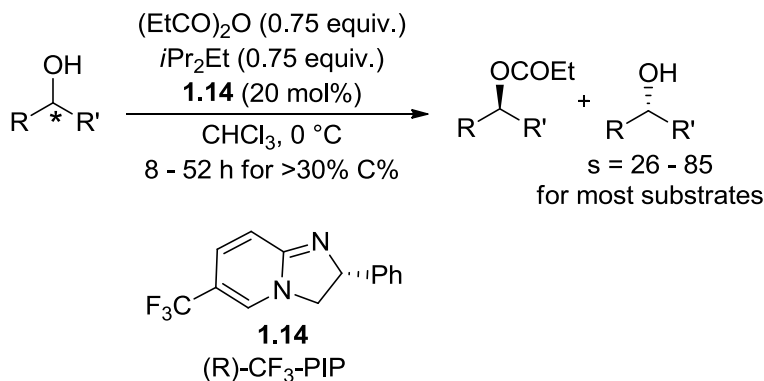


Figure 1.8 Proposed mechanism for the kinetic resolution of secondary alcohols with the peptide based catalysts developed by the Miller group.

The final classes of chiral acylating organocatalysts that will be discussed are the amidine and isothioureia based catalysts,⁵³ whose first application in the field of acylation based kinetic resolution was reported by the Birman group.⁵⁴ Their initial catalyst (*R*)-CF₃-PIP (**1.14**) achieved a high level of selectivity for several substrates (Scheme 1.8).



Scheme 1.8 Enantioselective acylation with the chiral amidine catalyst **1.14**.

It was reported that the system has the ability to resolve a number of substrates except cyclic alcohols, and alcohols that lack aromatic rings. The mechanism that was purposed also attempts to explain why the catalyst needs a substrate with a π -system (Figure 1.9). In their explanation, upon covalent attachment of the catalyst to the acyl group, the subsequent cationic charge that forms on the aryl substituent of the catalyst

allows for a favorable cation- π and π - π stacking interaction with the π -system of the substrate. This attractive interaction results in a preference for the (*R*)-alcohol due to steric repulsion of the non-aryl substituent in the (*S*)-alcohol. In a subsequent study,⁵⁵ calculations were performed on the (*R*)-CF₃-PIP acyl complex and 1-phenyl ethanol in the proposed transition state. The assumption that the cation- π interaction was a significant stabilizing influence on the conformation was supported by computational studies. Between the two diastereomeric transition states, they calculated a $\Delta\Delta G_{\text{rel}} = 5.7$ kcal/mol (B3LYP/6-31G*). The (*R*) enantiomer was predicted to be the faster reacting enantiomer. The energy difference in the diastereomeric transition states that incorporate the (*R*) and (*S*) conformation was $\Delta\Delta G_{\text{rel}} = 1.6$ kcal/mol (B3LYP/6-31G*) when corrected for solvent effects. This value is in agreement with the 1.5 kcal/mol that can be calculated for a selectivity factor of 12 from the kinetic resolution of 1-phenylethanol.

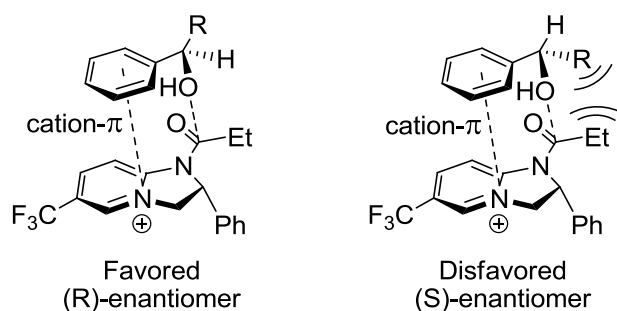


Figure 1.9 Proposed transition state for the enantioselective acylation by **1.14**

Based on the assumption that extension of the π -system enhance selectivity factor, the (*R*)-CF₃-PIP catalyst went through several generations of development (Figure 1.10). During the exploration for more selective catalysts, the Birman group moved beyond the

amidine based catalysts and found greater success with the isothiourea based catalysts.⁵⁶⁻

⁵⁸ These catalysts have achieved some of the best results to date for the acylation of secondary alcohols with a variety of different substrates to date.⁵⁹

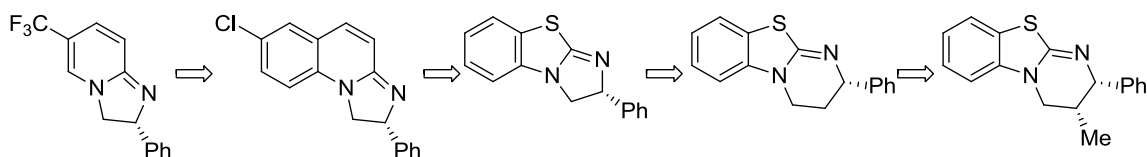


Figure 1.10 The evolution of the amidine and isothiourea catalysts developed by the Birman group.

An extension of this work was reported by the Deng and Fossey groups in which a variation of the (*R*)-CF₃-PIP catalyst was combined with a ferrocene based planar chiral catalyst **1.15** (Figure 1.11).⁶⁰ The new system gave an incredibly high selectivity factor (a reported *s* = 1892) with only 2 mol% of catalyst. This represents, to the best of our knowledge, the highest selectivity factor for the organocatalyzed kinetic resolution of secondary alcohols. However, it is worth noting again that a value this high should be viewed as an estimate.

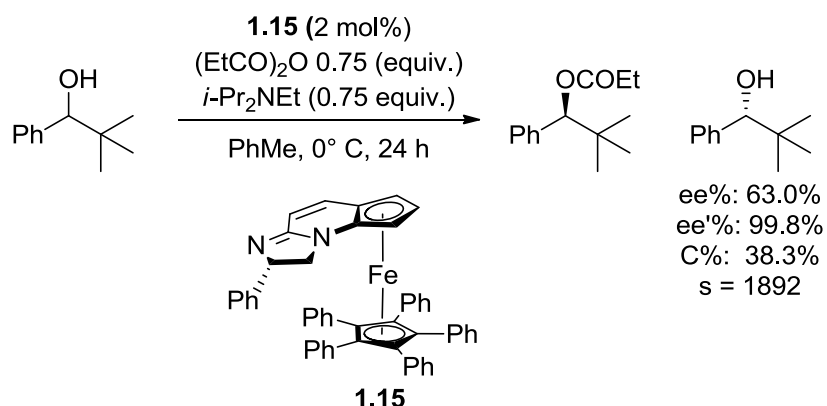


Figure 1.11 Kinetic resolution of secondary alcohols via **1.15**

1.4 Conclusions

Due to the importance of chiral building blocks in the development of pharmacologically active compounds, kinetic resolutions have become an important tool for generating chirally pure. Although kinetic resolutions have been known for a long time, there remains a need for developing new methodologies to meet the demand for chiral molecules. Among the types of kinetic resolutions, much interest in organocatalyzed kinetic resolutions have been shown, due to their potential for lower toxicity compared to transition metal catalysts, greater substrate tolerance, and lower costs when compared to enzymatic kinetic resolutions. The substrate class of particular interest to us was secondary alcohols. While enantioselective acylation has been extensively studied there has been very few examples of enantioselective silylation for the resolution of chiral alcohols which is the primary focus of this thesis.

In the following chapters, the investigations undertaken by the Wiskur lab toward the development of the organocatalyzed enantioselective silylation of secondary alcohols will be discussed. A detailed examination of the catalysts, silyl sources, and reaction conditions tested will be presented as well as investigations into the substrate scope. Then, investigations into the mechanism of the enantioselective silylation will be presented. In particular, ^1H - ^{29}Si gHMQC NMR studies and ^{29}Si solid-state NMR data used in determining the structure (or nature) of the silylating species is will be discussed. Finally, preliminary investigations into the transfer of chirality will be discussed as well the origin of the transfer of chirality.

1.5 References

1. Collins, A. N.; Sheldrake, G. N.; Crosby, J. E., *Chirality in Industry: The Commercial Manufacture and Applications of Optically Active Compounds*. Wiley-VCH: New York, 1992.
2. Collins, A. N.; Sheldrake, G. N.; Crosby, J. E., *Chirality in Industry II: Developments in the Commercial Manufacture and Applications of Optically Active Compounds*. Wiley-VCH: New York, 1998.
3. FDA,
<http://www.fda.gov/drugs/GuidanceComplianceRegulatoryInformation/Guidances/ucm122883.htm> (accessed on April 9, 2012).
4. Olbe, L.; Carlsson, E.; Lindberg, P., A proton-pump inhibitor expedition: the case histories of omeprazole and esomeprazole. *Nat Rev Drug Discov* **2003**, *2*, 132-139.
5. Harvey, A. L., Natural products in drug discovery. *Drug Discovery Today* **2008**, *13*, 894-901.
6. Shai, Y.; Oren, Z., Diastereomers of Cytolysins, a Novel Class of Potent Antibacterial Peptides. *J. Biol. Chem.* **1996**, *271*, 7305-7308.
7. Kaminski, H. M.; Feix, J. B., Effects of D-Lysine Substitutions on the Activity and Selectivity of Antimicrobial Peptide CM15. *Polymers* **2011**, *3*, 2088-2106.
8. Oren, Z.; Hong, J.; Shai, Y., A comparative study on the structure and function of a cytolytic α -helical peptide and its antimicrobial β -sheet diastereomer. *Eur. J. Biochem.* **1999**, *259*, 360-369.
9. Martínez-Rodríguez, S.; Martínez-Gómez, A. I.; Rodríguez-Vico, F.; Clemente-Jiménez, J. M.; Las Heras-Vázquez, F. J., Natural Occurrence and Industrial Applications of d-Amino Acids: An Overview. *Chem. Biodiversity* **2010**, *7*, 1531-1548.
10. Wani, M. C.; Taylor, H. L.; Wall, M. E.; Coggon, P.; McPhail, A. T., Plant antitumor agents. VI. Isolation and structure of taxol, a novel antileukemic and antitumor agent from *Taxus brevifolia*. *J. Amer. Chem. Soc.* **1971**, *93*, 2325-2327.
11. Patel, R. N., Tour de Paclitaxel: Biocatalysis for Semisynthesis. *Annu. Rev. Microbiol.* **1998**, *52*, 361-395.
12. Ottaggio, L.; Bestoso, F.; Armirotti, A.; Balbi, A.; Damonte, G.; Mazzei, M.; Sancandi, M.; Miele, M., Taxanes from Shells and Leaves of *Corylus avellana*. *J. Nat. Prod.* **2007**, *71*, 58-60.
13. Pellissier, H. I. n., Asymmetric organocatalysis. *Tetrahedron* **2007**, *63*, 9267-9331.
14. Jacobsen, E. N., Pfaltz, A.; Yamamoto, H. (Eds.), *Comprehensive Asymmetric Catalysis*. Springer: New York, 1999; Vol. i-iii.
15. Jacobsen, E. N. Pfaltz, A.; Yamamoto, H. (Eds.), *Comprehensive Asymmetric Catalysis Supplement*. Springer: New York, 2004; Vol. 1-2.

16. Katsuki, T.; Sharpless, K. B., The first practical method for asymmetric epoxidation. *J. Amer. Chem. Soc.* **1980**, *102*, 5974-5976.
17. Finn, M. G.; Sharpless, K. B., Mechanism of asymmetric epoxidation. 2. Catalyst structure. *J. Am. Chem. Soc.* **1991**, *113*, 113-126.
18. Katsuki, T.; Martin, V., Asymmetric Epoxidation of Allylic Alcohols: the Katsuki–Sharpless Epoxidation Reaction. In *Organic Reactions*, John Wiley & Sons, Inc.: 2004.
19. Noyori, R.; Ohkuma, T.; Kitamura, M.; Takaya, H.; Sayo, N.; Kumobayashi, H.; Akutagawa, S., Asymmetric hydrogenation of beta-keto carboxylic esters. A practical, purely chemical access to beta-hydroxy esters in high enantiomeric purity. *J. Am. Chem. Soc.* **1987**, *109*, 5856-5858
20. Ager, D. J.; Laneman, S. A., Reductions of 1,3-dicarbonyl systems with ruthenium-biarylphosphine catalysts. *Tetrahedron: Asymmetry* **1997**, *8*, 3327-3355.
21. Noyori, R.; Ohta, M.; Hsiao, Y.; Kitamura, M.; Ohta, T.; Takaya, H., Asymmetric synthesis of isoquinoline alkaloids by homogeneous catalysis. *J. Am. Chem. Soc.* **1986**, *108*, 7117-7119.
22. Chi, Y.; Tang, W.; Zhang, X., Rhodium-Catalyzed Asymmetric Hydrogenation. In *Modern Rhodium-Catalyzed Organic Reactions*, Wiley-VCH Verlag GmbH & Co. KGaA: 2005; pp 1-31.
23. Knowles, W. S.; Sabacky, M. J., Catalytic asymmetric hydrogenation employing a soluble, optically active, rhodium complex. *Chem. Comm.* **1968**, *22*, 1445-1446.
24. Knowles, W. S., Asymmetric hydrogenation. *Acc. of Chem. Res.* **1983**, *16*, 106-112.
25. Knowles, W. S., Asymmetric Hydrogenations (Nobel Lecture 2001). *Adv. Synt. & Catal.* **2003**, *345*, 3-13.
26. Giacalone, F.; Gruttadauria, M.; Agrigento, P.; Noto, R., Low-loading asymmetric organocatalysis. *Chem. Soc. Rev.* **2012**, *41*, 2406-2447.
27. Collet, A., Resolution of Racemates: Did You Say “Classical”? *Angew. Chem. Int. Ed.* **1998**, *37*, 3239-3241.
28. Dalmolen, J.; Tiemersma-Wegman, T. D.; Nieuwenhuijzen, J. W.; van der Sluis, M.; van Echten, E.; Vries, T. R.; Kaptein, B.; Broxterman, Q. B.; Kellogg, R. M., The Dutch Resolution Variant of the Classical Resolution of Racemates by Formation of Diastereomeric Salts: Family Behaviour in Nucleation Inhibition. *Chem. Eur. J.* **2005**, *11*, 5619-5624.
29. Kagan, H. B.; Fiaud, J. C., Kinetic Resolution. In *Topics in Stereochemistry*, John Wiley & Sons, Inc.: 1988; pp 249-330.
30. Kagan, H. B., Various aspects of the reaction of a chiral catalyst or reagent with a racemic or enantiopure substrate. *Tetrahedron* **2001**, *57*, 2449-2468.
31. Keith, J. M.; Larrow, J. F.; Jacobsen, E. N., Practical Considerations in Kinetic Resolution Reactions. *Adv. Synth. Catal.* **2001**, *343*, 5-26.

32. Vedejs, E.; Jure, M., Efficiency in Nonenzymatic Kinetic Resolution. *Angew. Chem. Int. Ed.* **2005**, *44*, 3974-4001.
33. Anslyn, E. V.; Dougherty, D. A., *Modern Physical Organic Chemistry*. University Science Books: Sausalito, California, 2006.
34. Liu, H.-L.; Anthonsen, T., Enantiopure building blocks for chiral drugs from racemic mixtures of secondary alcohols by combination of lipase catalysis and Mitsunobu esterification. *Chirality* **2002**, *14*, 25-27.
35. Pellissier, H., Catalytic Non-Enzymatic Kinetic Resolution. *Adv. Synth. Catal.* **2011**, *353*, 1613-1666.
36. Spivey, A.; Arseniyadis, S.; List, B., Amine, Alcohol and Phosphine Catalysts for Acyl Transfer Reactions Asymmetric Organocatalysis. In Springer Berlin / Heidelberg: 2009; Vol. 291, 233-280.
37. Müller, C. E.; Schreiner, P. R., Organocatalytic Enantioselective Acyl Transfer onto Racemic as well as meso Alcohols, Amines, and Thiols. *Angew. Chem. Int. Ed.* **2011**, *50*, 6012-6042.
38. Vedejs, E.; Daugulis, O.; Diver, S. T., Enantioselective Acylations Catalyzed by Chiral Phosphines. *J. Org. Chem.* **1996**, *61*, 430-431.
39. Vedejs, E.; Daugulis, O., A Highly Enantioselective Phosphabicyclooctane Catalyst for the Kinetic Resolution of Benzylic Alcohols. *J. Am. Chem. Soc.* **2003**, *125*, 4166-4173.
40. Klare, H. F. T.; Oestreich, M., Chiral Recognition with Silicon-Stereogenic Silanes: Remarkable Selectivity Factors in the Kinetic Resolution of Donor-Functionalized Alcohols. *Angew. Chem. Int. Ed.* **2007**, *46*, 9335-9338.
41. Vedejs, E.; Chen, X., Kinetic Resolution of Secondary Alcohols. Enantioselective Acylation Mediated by a Chiral (Dimethylamino)pyridine Derivative. *J. Am. Chem. Soc.* **1996**, *118*, 1809-1810.
42. Wurz, R. P., Chiral Dialkylaminopyridine Catalysts in Asymmetric Synthesis. *Chem. Rev.* **2007**, *107*, 5570-5595.
43. Ruble, J. C.; Tweddell, J.; Fu, G. C., Kinetic Resolution of Arylalkylcarbinols Catalyzed by a Planar-Chiral Derivative of DMAP: A New Benchmark for Nonenzymatic Acylation. *J. Org. Chem.* **1998**, *63*, 2794-2795.
44. Tao, B.; Ruble, J. C.; Hoic, D. A.; Fu, G. C., Nonenzymatic Kinetic Resolution of Propargylic Alcohols by a Planar Chiral DMAP Derivative: Crystallographic Characterization of the Acylated Catalyst. *J. Am. Chem. Soc.* **1999**, *121*, 5091-5092.
45. Ruble, J. C.; Latham, H. A.; Fu, G. C., Effective Kinetic Resolution of Secondary Alcohols with a Planar Chiral Analogue of 4-(Dimethylamino)pyridine. Use of the Fe(C₅Ph₅) Group in Asymmetric Catalysis. *J. Am. Chem. Soc.* **1997**, *119*, 1492-1493.
46. Fu, G. C., Enantioselective Nucleophilic Catalysis with Planar-Chiral • Heterocycles. *Acc. Chem. Res.* **2000**, *33*, 412-420.

47. Fu, G. C., Asymmetric Catalysis with Planar-Chiral • Derivatives of 4-(Dimethylamino)pyridine. *Acc. Chem. Res.* **2004**, *37*, 542-547.
48. Sinha, S. C.; Barbas, C. F.; Lerner, R. A., The antibody catalysis route to the total synthesis of epothilones. *Proc. Natl. Acad. Sci. USA* **1998**, *95*, 14603-14608.
49. Miller, S. J.; Copeland, G. T.; Papaioannou, N.; Horstmann, T. E.; Ruel, E. M., Kinetic Resolution of Alcohols Catalyzed by Tripeptides Containing the N-Alkylimidazole Substructure. *J. Am. Chem. Soc.* **1998**, *120*, 1629-1630.
50. Jarvo, E. R.; Copeland, G. T.; Papaioannou, N.; Bonitatebus, P. J.; Miller, S. J., A Biomimetic Approach to Asymmetric Acyl Transfer Catalysis. *J. Am. Chem. Soc.* **1999**, *121*, 11638-11643.
51. Davie, E. A. C.; Mennen, S. M.; Xu, Y.; Miller, S. J., Asymmetric Catalysis Mediated by Synthetic Peptides. *Chem. Rev.* **2007**, *107*, 5759-5812.
52. Formaggio, F.; Barazza, A.; Bertocco, A.; Toniolo, C.; Broxterman, Q. B.; Kaptein, B.; Brasola, E.; Pengo, P.; Pasquato, L.; Scrimin, P., Role of Secondary Structure in the Asymmetric Acylation Reaction Catalyzed by Peptides Based on Chiral Tetrasubstituted Amino Acids. *J. Org. Chem.* **2004**, *69*, 3849-3856.
53. Taylor, J. E.; Bull, S. D.; Williams, J. M. J., Amidines, isothioureas, and guanidines as nucleophilic catalysts. *Chem. Soc. Rev.* **2012**, *41*, 2109-2121.
54. Birman, V. B.; Uffman, E. W.; Jiang, H.; Li, X.; Kilbane, C. J., 2,3-Dihydroimidazo[1,2-a]pyridines: A New Class of Enantioselective Acyl Transfer Catalysts and Their Use in Kinetic Resolution of Alcohols. *J. Am. Chem. Soc.* **2004**, *126*, 12226-12227.
55. Li, X.; Liu, P.; Houk, K. N.; Birman, V. B., Origin of Enantioselectivity in CF₃-PIP-Catalyzed Kinetic Resolution of Secondary Benzylic Alcohols. *J. Am. Chem. Soc.* **2008**, *130*, 13836-13837.
56. Birman, V. B.; Li, X., Benztetramisole: A Remarkably Enantioselective Acyl Transfer Catalyst. *Org. Lett.* **2006**, *8*, 1351-1354.
57. Birman, V. B.; Li, X., Homobenzotetramisole: An Effective Catalyst for Kinetic Resolution of Aryl-Cycloalkanols. *Org. Lett.* **2008**, *10*, 1115-1118.
58. Zhang, Y.; Birman, V. B., Effects of Methyl Substituents on the Activity and Enantioselectivity of Homobenzotetramisole-Based Catalysts in the Kinetic Resolution of Alcohols. *Adv. Synth. Catal.* **2009**, *351*, 2525-2529.
59. Li, X.; Jiang, H.; Uffman, E. W.; Guo, L.; Zhang, Y.; Yang, X.; Birman, V. B., Kinetic Resolution of Secondary Alcohols Using Amidine-Based Catalysts. *J. Org. Chem.* **2012**, *77*, 1722-1737.
60. Hu, B.; Meng, M.; Wang, Z.; Du, W.; Fossey, J. S.; Hu, X.; Deng, W.-P., A Highly Selective Ferrocene-Based Planar Chiral PIP (Fc-PIP) Acyl Transfer Catalyst for the Kinetic Resolution of Alcohols. *J. Am. Chem. Soc.* **2010**, *132*, 17041-17044.

Chapter 2. Kinetic resolution of secondary alcohols by enantioselective silylation

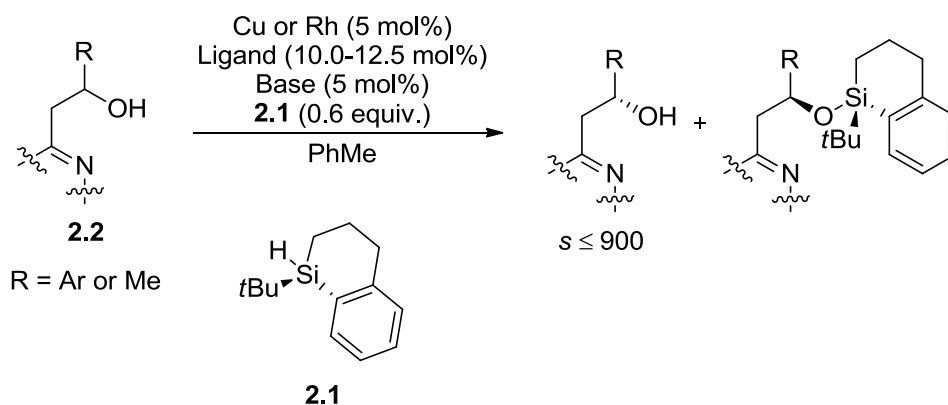
2.1 Introduction

In the last ten years, the field of kinetic resolution of alcohols via enantioselective silylation has become an area of active research.¹ The major advantages from this methodology are the ease of separation of the resulting silyl ether from the enriched starting material and the synthetic usefulness of the silyl ether products themselves.² These factors provided an impetus for the development of new methodologies to achieve enantiomerically enriched monofunctional secondary alcohols with selectivity factors of at least 10, while using catalytic quantities of catalyst.

Both transition metal catalyzed kinetic resolution methodologies and organocatalyzed techniques have been reported to perform resolutions via enantioselective silylation reactions. Although modest to high selectivity factors can be achieved using either approach, most of the reported methodologies show major limitations on either reaction conditions or substrate scope. Reported herein is an overview of all of the reported enantioselective silylation methodologies and the work done towards development of the isothioureia based enantioselective silylation system reported by the Wiskur group.³

2.2 Transition metal catalyzed kinetic resolutions by enantioselective silylation

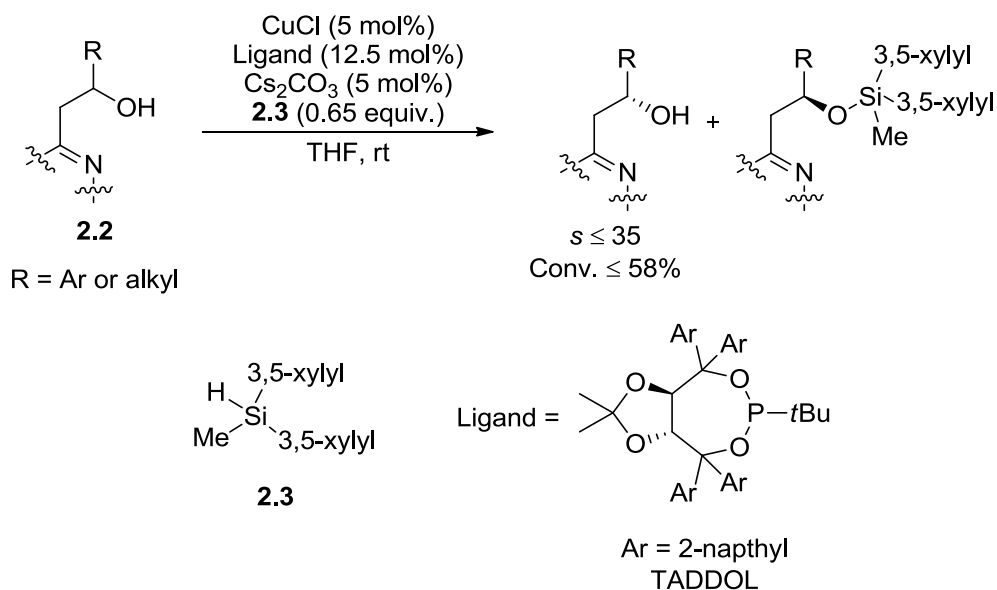
The transition metal catalyzed enantioselective silylation reactions were found to be successful when relatively stable Cu(I) or Rh(I) were used as catalysts and moisture and oxygen stable silanes were used as the silicon source. This mild and very effective methodology, developed by the Oestreich group,⁴ achieved very high selectivity factors for the enantioselective Si-O coupling reaction of alcohols to generate enantiomerically enriched alcohols and silyl ethers through a dehydrogenative coupling (Scheme 2.1). The Oestreich group has reported some of the highest selectivity factors ever achieved for any silylation-based kinetic resolution organocatalyzed kinetic resolution.⁵ The major drawback of this methodology is the relatively limited substrate scope which, and must possess a nitrogenous donor (specifically γ relative to the alcohol) facilitate for 2-point binding of the substrate to the catalyst. Furthermore, a stoichiometric quantity of chiral silane (**2.1**) is needed for the kinetic resolution process.



Scheme 2.1 The general reaction conditions for the enantioselective oxidative silane coupling reaction developed by the Oestreich group.

The silylation-based kinetic resolution via dehydrogenative coupling was later expanded to include achiral silanes and chiral monodentate ligands.⁶ In this system, copper (I) chloride with a chiral TADDOL ligand was able to enantioselectively silylate

secondary alcohols with a selectivity factor of up to 35 (Scheme 2.2). Although this procedure utilizes an achiral bis-3,5-xylyl silane (**2.3**), the substrate still needs to contain a nitrogen donor atom.



Scheme 2.2 The enantioselective silane dehydrogenative coupling conditions utilizing achiral silanes and chiral ligands as reported by the Oestreich group.

Based on experimental studies of chiral copper-based reducing agents⁷ and computational studies, the Oestreich group has proposed a mechanism for the chiral silane reaction.⁸ Upon addition of the chiral alcohol **2.2** to the metal center and concomitant removal of dihydrogen, two diastereomeric chiral metal complexes form. A chiral silane then interacts preferentially with one of the diastereomeric complexes which is the enantioselective step (**2.4**). Finally, displacement of the attached alcohol gives the enantiomerically enriched secondary alcohol and silyl ether (Figure 2.1). In order to be catalytic, many of the early steps need to be reversible to allow release of the slower reacting enantiomers. If chiral ligands are used, then the catalytic metal complex creates

a chiral environment that selectively binds and activates one enantiomer of the alcohol for silylation.

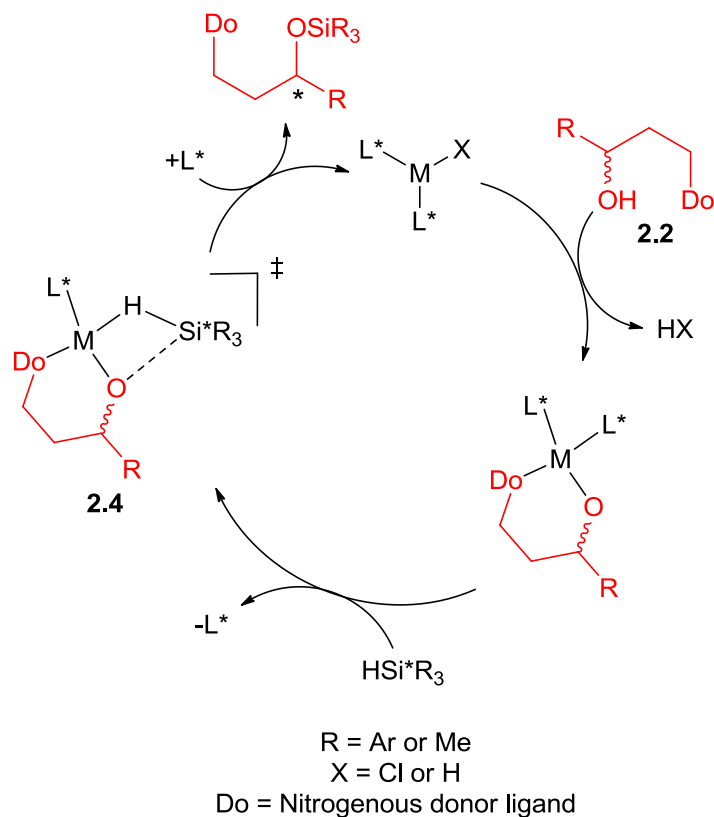
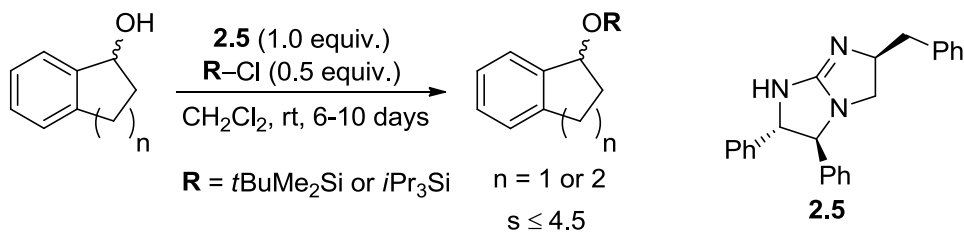


Figure 2.1 Catalytic pathway for the enantioselective Si-O coupling proposed by the Oestreich group.

2.3 Organocatalyzed Enantioselective Silylation

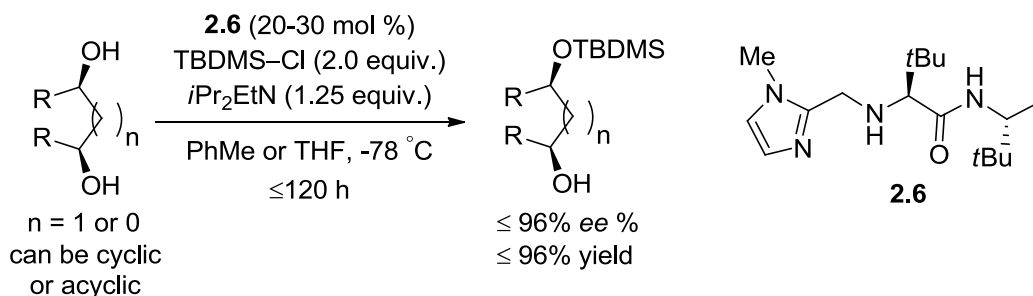
The other type of catalyst that has been successfully employed in the silylation based kinetic resolution of secondary alcohols are organocatalysts. The first enantioselective silylation-based kinetic resolution was reported by the Ishikawa group.⁹ In this report, the Ishikawa group developed novel guanidines as asymmetric catalysts for the enantioselective silylation of cyclic monofunctional secondary alcohols with either *tert*butyldimethylsilyl chloride (TBDMS-Cl) or triisopropylsilyl chloride (TIPS-Cl)

(Scheme 2.3). Although this was a seminal report in its field, there were several disadvantages in this technique. First, the highest selectivity factor was less than the synthetically useful benchmark of 10. Also, the need for stoichiometric quantities of chiral catalyst **2.5** and the six to ten day reaction time are major disadvantages of this methodology. However, this report garnered much interest and instituted a new approach to the preparation of enantiomerically enriched secondary alcohols using organocatalysts.



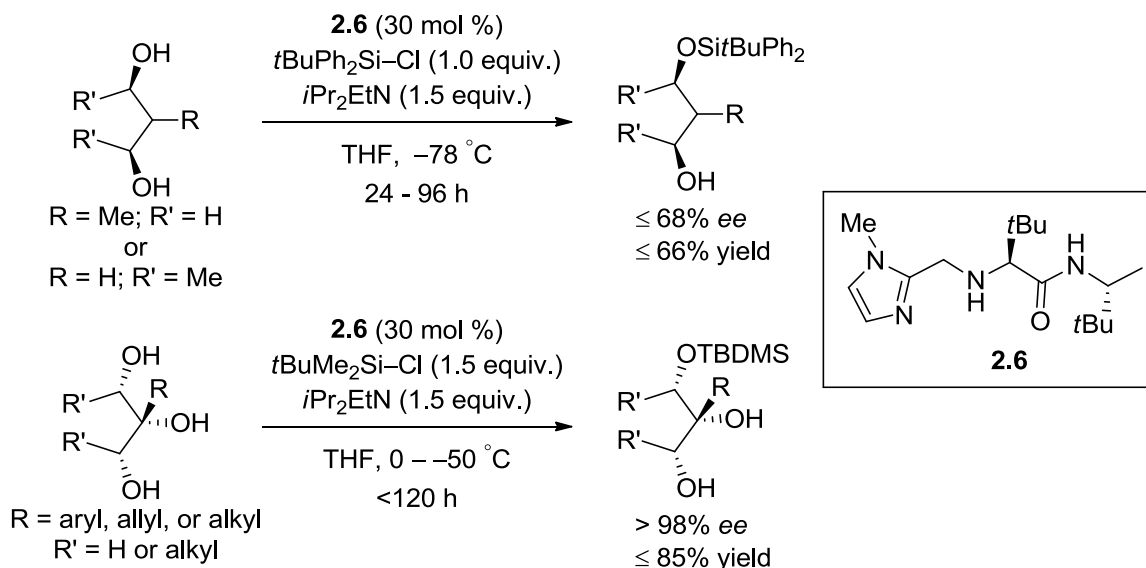
Scheme 2.3 The chiral guanidine based methodology that was reported by the Ishikawa group.

Inspired by these results, the Hoveyda and Snapper groups applied a different approach to the enantioselective silylation problem. Using the imidazole-based catalyst **2.6**, that is reminiscent of Miller's peptide-based acylation catalyst,¹⁰ the Hoveyda and Snapper groups have developed very selective desymmetrization¹¹ and kinetic resolution routes for the preparation of enantioselective syn-1,2 and 1,3-diols.^{11,12} For the desymmetrization of meso diols, catalyst **2.6** was the most selective for both cyclic and acyclic substrates. Catalyst **2.6** enantioselectively mono-silylated syn-1,2 and 1,3-diols with *ee*'s of up to 96% with high yields. However, the reactions required up to 5 days (Scheme 2.4). This silylation methodology could utilize Et₃SiCl and TIPS-Cl although with lower yields and enantioselectivity.



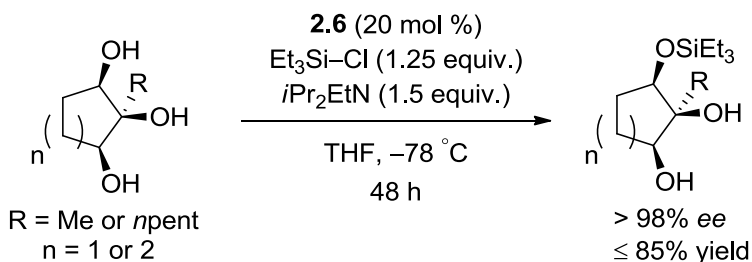
Scheme 2.4 Enantioselective desymmetrization of meso 1,2 and 1,3-syn diols with the amino acid-based catalyst **2.6**

The desymmetrization methodology has also been utilized in the desymmetrization of syn-1,2,3-triols including the synthesis of a key chiral intermediate used in the synthesis of Cleroindicins D, F, and C. Catalyst **2.6** was found to be effective for the enantioselective silylation of a series of cyclic and acyclic meso 1,2,3-triols. Based on the catalyst's difficulty in resolving 1,3-diols and success with 1,2,3-triols, it is believed that the substrate scope must possess a 1,2-vicinal diol. When the enantioselective silylation methodology was applied to 1,2,3-triols, the optimal reaction conditions were very similar to the desymmetrization of meso syn-1,2-diols (Scheme 2.5). The reaction tolerated higher temperatures however, on average, lower yields were reported. This reaction was also effective in the resolution of both primary and secondary alcohols.



Scheme 2.5 Enantioselective silylation of 1,2,3-syn triols with catalyst **2.6**.

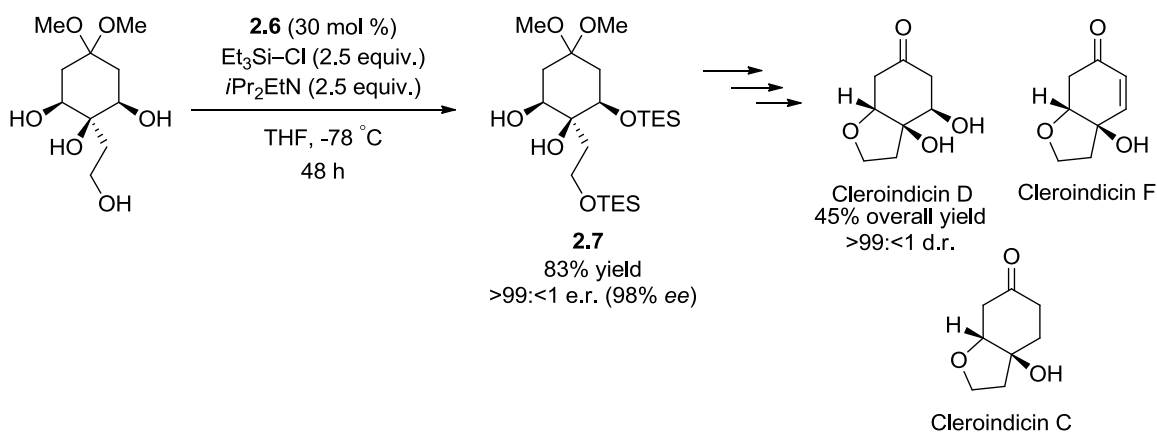
Cyclic 1,2,3-triols were also reported to be resolved and a silyl chloride of lesser steric bulk (Et₃SiCl instead of *t*BuMe₂SiCl) was needed to achieve maximum efficiency. Interestingly, the resulting silyl ether was preferentially formed enriched in the opposite stereochemistry then then product with the acyclic 1,2,3-triols reported earlier (Scheme 2.6). For the enantioselective silylation of 1,2,3-triols, < 2% *bissilylated* product was formed (¹H NMR).



Scheme 2.6 Enantioselective silylation of cyclic 1,2,3-triol with **2.6** as catalyst

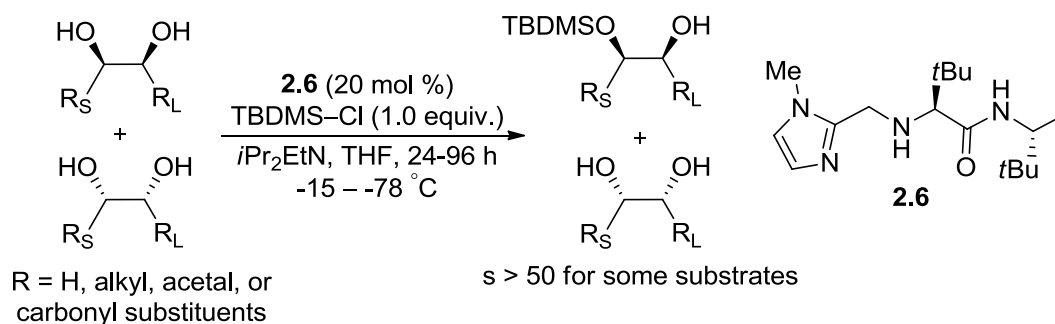
This enantioselective silylation methodology was also applied in the production of a key chiral intermediate (**2.7**) in the total synthesis of Cleroindicin D, F, and C.¹³ In

THF at -78°C using $\text{Et}_3\text{Si}-\text{Cl}$ as the silyl source, **2.7** was synthesized in good yields and good enantiomeric purity. With **2.7** in hand, the authors synthesized the D, F, and C forms of Cleroindicin. Reportedly the D form was isolated with 45% overall yield (5 steps) and practically a single diastereomer was isolated (Scheme 2.7).



Scheme 2.7 The application of the Hoveyda-Snapper enantioselective silylation methodology in the synthesis of Cleroindicin D, F, and C.

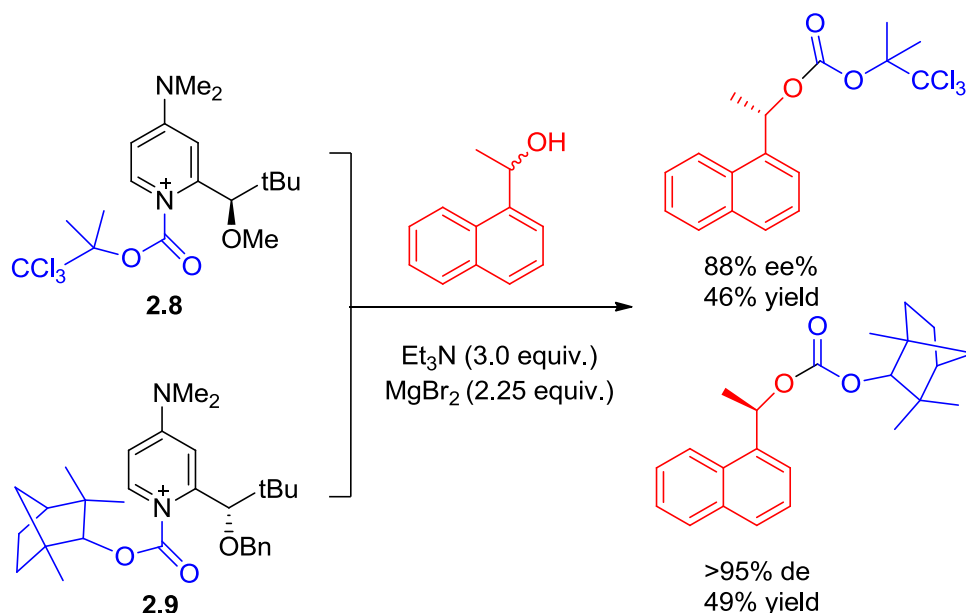
This enantioselective silylation methodology reported by the Hoveyda and Snapper groups was then applied in the kinetic resolution of chiral alcohols. For chiral acyclic syn-1,2-diols, the catalyst **2.6** was found to achieve a $s > 50$ in the installation of the TBDMS group in the presence of $i\text{Pr}_2\text{EtN}$, in THF after 96 h. The most selective substrates had smaller substituent (R_S) equal H and the larger substituent (R_L) equal acetal or bulky alkyl group (*isopropyl*, *cyclohexyl*, or *tertbutyl*). This methodology represents the highest level of selectivity achieved for an organocatalyzed enantioselective silylation-based kinetic resolution.



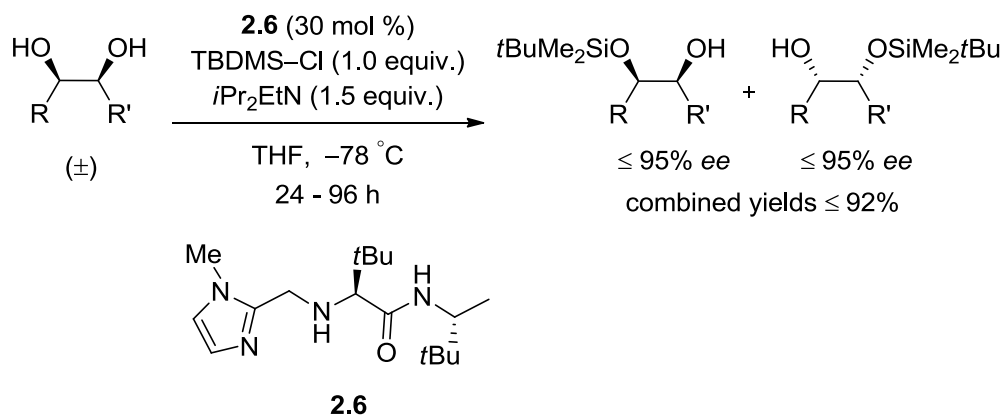
Scheme 2.8 The kinetic resolution of syn-1,2-diols developed by the Hoveyda and Snapper groups using imidazole-based catalyst **2.6**.

Recently, Hoveyda and Snapper's silylation methodology has been applied to the regiodivergent reactions of racemic mixtures (RRRM).¹⁴ RRRM reactions are similar to kinetic resolutions where a racemic mixture is enantioselectively reacted. However, in a RRRM, both enantiomers are consumed to give two separable products with high enantiomeric purity. A RRRM resembles a parallel kinetic resolution, but RRRM reactions use only a single reagent.¹⁵ In a RRRM, a chiral molecule with multiple stereocenters reacts with both enantiomers of a chiral compound to form products that can be separated. For an example of a parallel kinetic resolution, the seminal report of a parallel kinetic resolution was reported by the Vedejs group¹⁶ in which a racemic mixture of secondary alcohols were reacted with a pair of chiral DMAP derivatives (**2.8** and **2.9**). In this case the chiral DMAP salt **2.8** preferentially reacted with the *S* enantiomer of the secondary alcohol while **2.9** showed preference for the *R* enantiomer. The corresponding carbonate products were isolated with high *ee* (or *de*) and high yields (95% combined yield) (Scheme 2.9). In the reported RRRM by Hoveyda and Snapper, cyclohex-3-ene-1,2-diol was enantioselectively silylated by **2.6** to give a mixture of products that can be isolated with high yields and high enantiomeric excess.

Parallel Kinetic Resolution



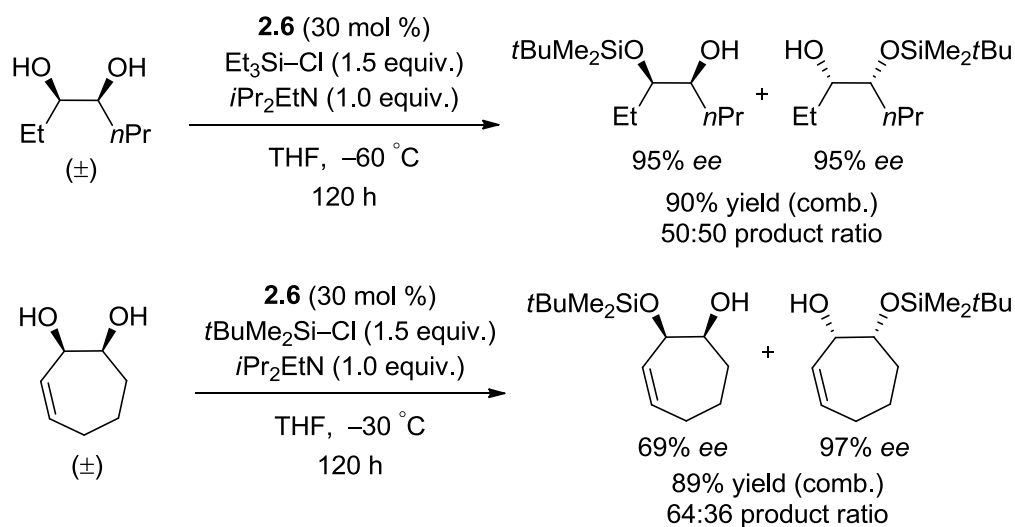
Regiodivergent Reaction on a Racemic Mixture (RRRM)



Scheme 2.9 The first reported parallel kinetic resolution (top) and the RRRM reported by the Hoveyda and Snapper groups (bottom).

The key (and challenge) to achieving such high levels of enantioselectivity for both parallel kinetic resolutions and RRRMs is to find conditions and reagents in which both enantiomers react at the same rate. If the rate of reaction between the enantiomers deviates from 1:1, a decrease in enantioselectivity is observed. This is believed to be due to the increase of the relative rate of the undesired enantiomer leading to an increase in

the relative concentration of the slower enantiomer, which will then compete with the faster enantiomer for the chiral reagent and result in lower ee's. This phenomenon was observed by Hoveyda and Snapper while screening substrates with their enantioselective silylation methodology as shown in Scheme 2.10. As shown in the bottom example, when the product ratio deviates from a 50:50 ratio, a decrease in the enantioselectivity was observed.



Scheme 2.10 Two substrates reported by Hoveyda and Snapper that gave different product ratios and the effects upon enantiomeric excess.

The mechanism for this reaction is believed to be through a pre-organization of the diol through hydrogen bonding to **2.6**. It is believed that the sterics of the peptide backbone of the catalyst would force the preferential binding of the diol so that the smaller substituent of the substrate would be positioned close to the nucleophilic center of the catalyst (**Figure 2.2**). Then the TBDMS-Cl is bound to the catalyst by the nucleophilic, *N*-methylimidazole based moiety of the catalyst to form the activated pentavalent silicon intermediate. The activated silyl chloride is formed close to the diol,

allowing for one of the alcohols to easily attack the silicon, resulting in enantioselective silylation of the alcohol.^{11, 12}

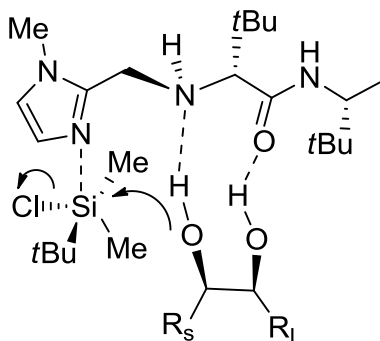
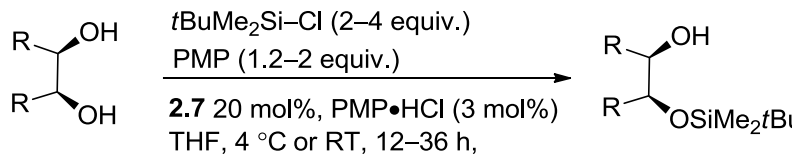
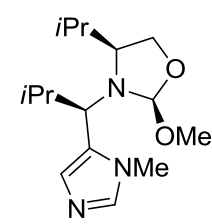
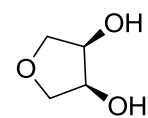
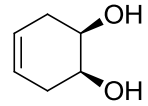
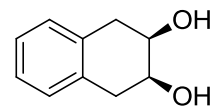
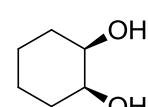
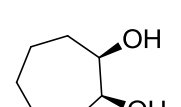
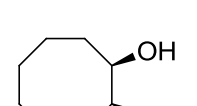
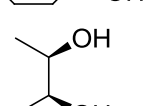


Figure 2.2 The proposed transition state for the enantioselective silylation of 1,2-syn diols by the bifunctional catalyst, **2.6**.

In a similar approach of enantioselective silylation, the Tan group has applied their reversible covalent bonding approach to bifunctional catalyst development¹⁷ to the enantioselective silylation of secondary alcohols.^{17, 18} In this work, the Tan group reported modest to great yields with good enantioselectivity on a number of cyclic meso-diols as well as 2,3-butane-diol using the amino acid derived catalyst **2.7** (Table 2.1).

Table 2.1 The substrate scope reported for the enantioselective silylation of meso diols with catalyst **2.7**.

		 2.7	
Entry	Substrate	Yield (%)	ee (%)
1		79	89
2		87	90
3		88	95
4		86	92
5		82	90
6		93	86
7		78	90

Their catalyst is believed to behave in a similar fashion to the Hoveyda and Snapper catalyst, except the Tan group imidazole based catalyst utilizes a reversible covalent bonding approach in an attempt to increase the rigidity of the catalyst-substrate binding complex when compared to a hydrogen bonding based complex. The proposed mechanism is shown in Figure 2.3. The reaction is believed to begin when the cyclic syn-

1,2-diol displaces a molecule of methanol from the hemiacetal moiety of the catalyst (**2.7**). The resulting covalently bound intermediate containing the meso diol (Figure 2.3, structure **A**) is then silylated stereoselectively thereby desymmetrizing the cyclic diol. Once stereoselectively bound, the contiguous alcohol is then free to be silylated. This methodology is reported to work for Et_3SiCl , $t\text{BuMe}_2\text{SiCl}$, $t\text{BuPh}_2\text{SiCl}$, and Ph_2MeSiCl as the silyl chloride source.

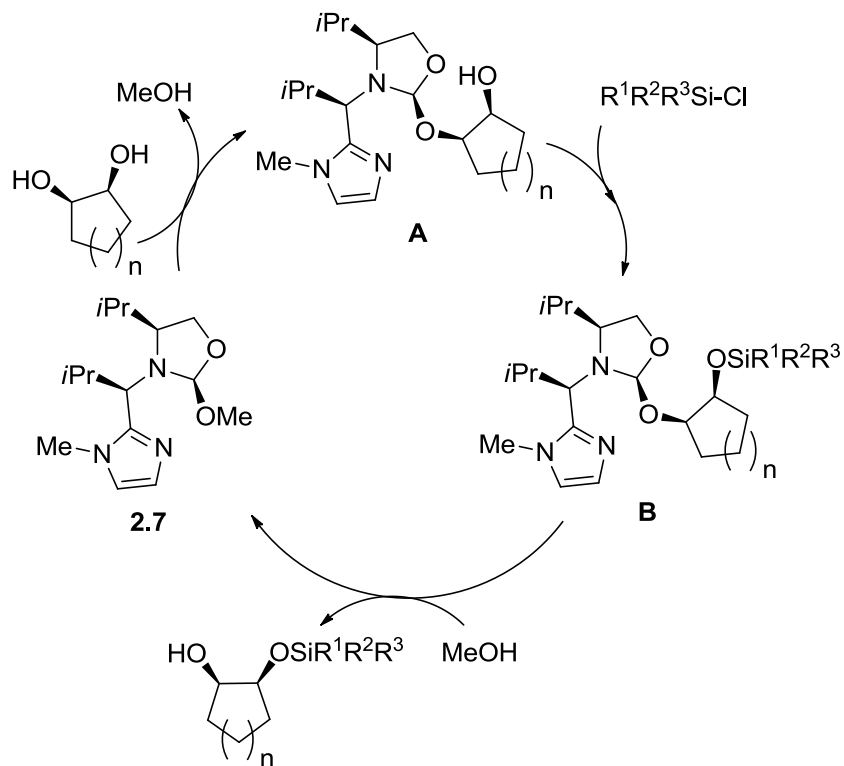
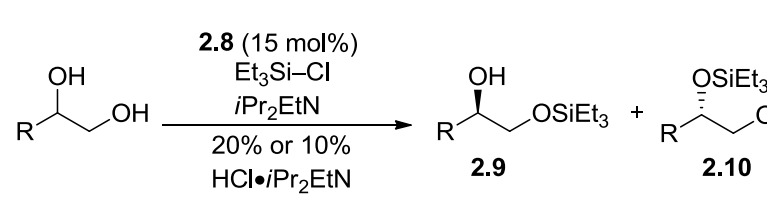


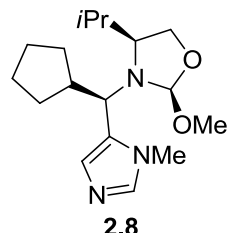
Figure 2.3 The proposed catalytic cycle for the desymmetrization of cyclic syn-1,2-diols using the bifunctional catalyst **2.7** with $\text{Et}_3\text{Si-Cl}$.

When this system is applied to a substrate containing both primary and secondary alcohols a RRRM occurs.¹⁹ The product ratio between silylation of the primary and secondary alcohols proved to be more difficult to control than in the methodology reported by the Hoveyda and Snapper groups (Table 2.2, entry 2).¹⁴ This is presumably due to the higher reactivity of the primary alcohol relative to the secondary alcohol.

Thereby **2.9** and the undesired enantiomer of **2.9** forms first then **2.10** is formed. Due to the potential for large deviations from the desired 50:50 ratio, to isolate **2.10** with high enantiopurity, adding less Et₃Si–Cl allowed for **2.9** to be isolated with high enantiopurity (entry 1a and 1b).

Table 2.2 Reaction conditions and substrate screening of the RRRM silylation reported by the Tan group





2.8

Entry	R	Et ₃ Si–Cl equiv.	<i>i</i> Pr ₂ EtN equiv.	product ratio (2.9:2.10)	ee (2.9)	ee (2.10)
1a	cyclohexyl	1.3	1.3	52:48	81 %	97 %
1b		0.6	0.7	47% (2.9)	92 %	NR
2	H ₂ C=CH	1.2	1.2	53:37	57 %	81%

An interesting methodology for the enantioselective silylation of secondary alcohols was reported by the Wiskur group. In this report,²⁰ a Mukiyama aldol reaction is performed through the addition of a silyl ketene acetal to an aldehyde in the presence of a chiral cinchona alkaloid salt. Even though the β-hydroxy ester was not generated in an enantiomerically enriched form, the protected intermediate was found to be enriched (**Figure 2.4**). This suggests that the reaction proceeded through a step wise mechanism and that the chirality generating step is not the aldol step but rather the silylation step.

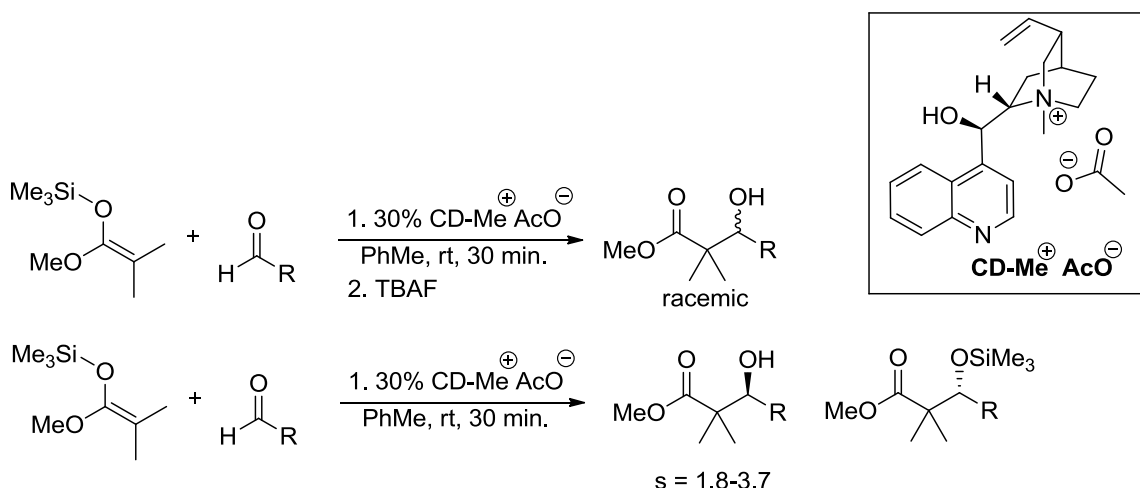


Figure 2.4 Initial findings of the Wiskur group which suggest that the silylation step was the enantiomerically enriching step.

What is particularly noteworthy is that the enantiomeric excess shows a dependence upon conversion. This strongly suggests that the reaction is not an asymmetric reaction, but rather a kinetic resolution. Because the isolated β -hydroxy ester was found to be racemic when treated with TBAF, this suggests that the silylation step is the enantiomerically enriching step. Also, since the initial step starts with an achiral substrate, the product of the carbon-carbon bond forming step should not show a dependence of enantiomeric excess on conversion. This also implies that the reaction proceeds through a step-wise mechanism. To encompass these findings, the Wiskur group proposes that the formation of the β -alkoxy intermediate is first generated in a racemic fashion, which forms a diastereomeric salt with the chiral quaternary ammonium. This alkoxy now promotes the next Mukaiyama aldol reaction, becoming silylated with the silicon from the second equivalent of silyl ketene acetal. One of the diastereomeric salts react faster in this reaction over the other resulting in a kinetic resolution. As the new product forms the diastereomeric salt is regenerated (Figure 2.5). Unfortunately, this reaction failed to achieve high selectivity factors ($s \leq 3.7$), but by

presenting a situation where the selectivity determining step is not the carbon-carbon bond forming step, but rather the silylation step, opens another approach to performing a Mukiyama aldol reaction in which enantiomerically enriched products are desired.

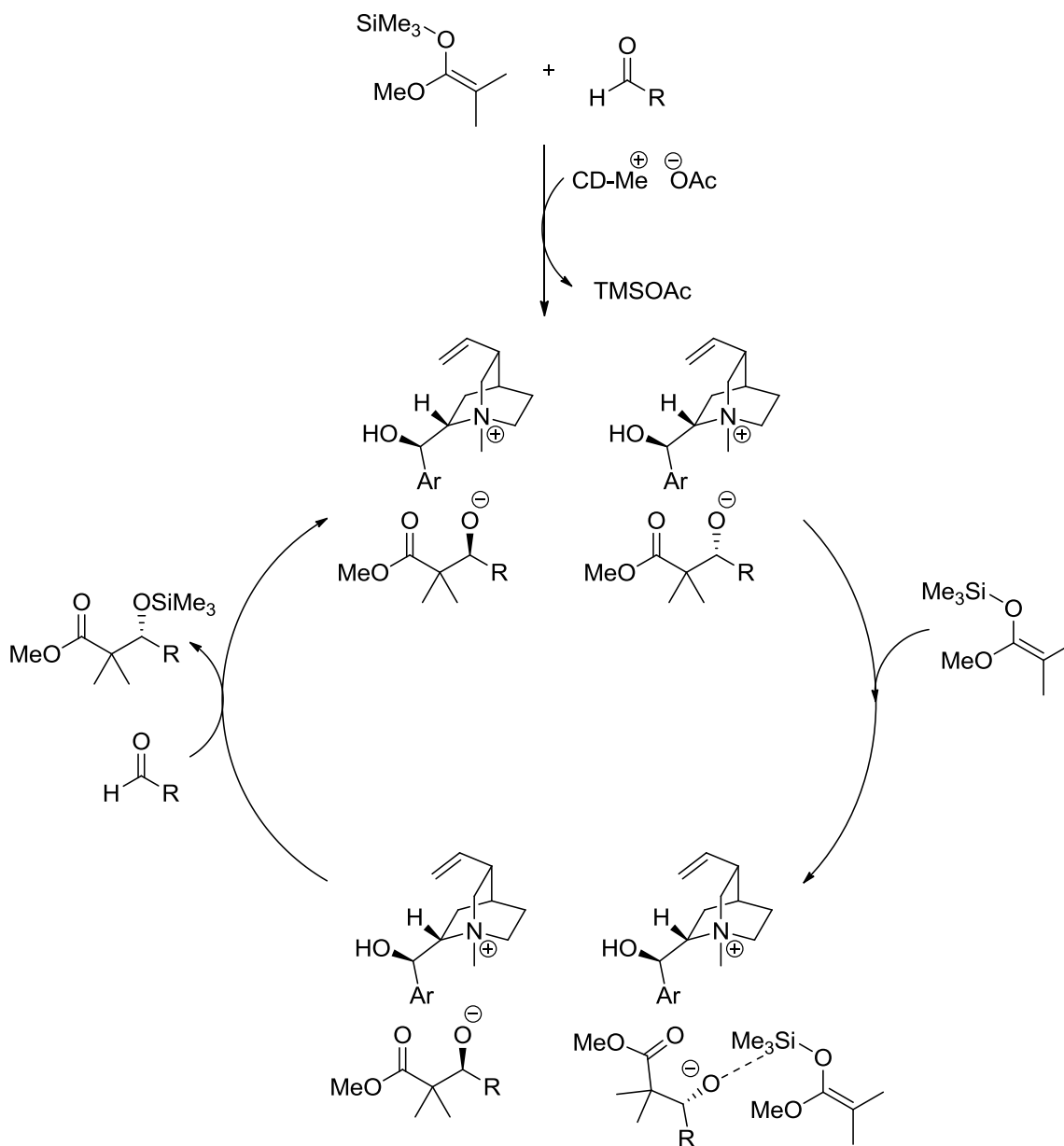
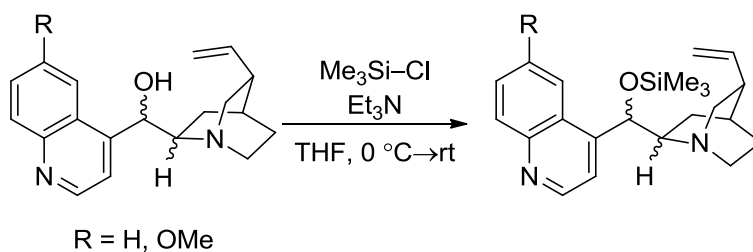


Figure 2.5 The mechanism proposed by the Wiskur group for the generation of enantiomerically enriched trimethylsilyl protected β -hydroxy esters from the Mukiyama aldol reaction catalyzed by a quaternary cinchona alkaloid salt.

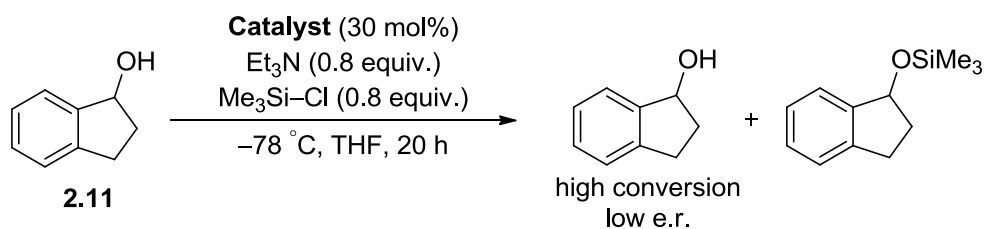
2.4 Identifying a selective catalyst for the enantioselective silylation of secondary alcohols

Although there have been several reported methods for the enantioselective silylation of secondary alcohols, the only report in which a selectivity factor greater than 2 for monofunctional secondary alcohols was obtained was by the Ishikawa group.⁹ However, this silylation technique suffers from stoichiometric catalyst loading, long reaction times and low selectivity. Due to the paucity of efficient techniques for the silylation of monofunctional secondary alcohols, the Wiskur group decided to investigate new methodologies to fill this salient gap in the literature.

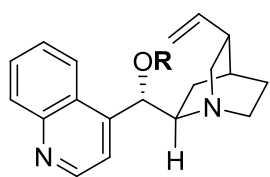
To begin our explorations into discovering a new silylation methodology, the cinchona alkaloids were first explored as catalysts. They were selected due to their well-established precedence of catalyzing enantioselective reactions.²¹ However, because the catalyst itself possesses a free alcohol, the catalyst itself was silylated to mitigate any competitive silylation that may occur. Therefore, the alcohol was protected as the trimethylsilyl ether (Scheme 2.11). To measure the selectivity factor, the equations described by Kagan and Fiaud were used.²² With several silylated cinchona alkaloids in hand, the enantioselective silylation of 1-indanol (**2.11**) was performed with Et₃N used as the base and Me₃SiCl in the presence of 4 Å molecular sieves (it was observed that using activated molecular sieves gave better reproducibility, presumably due to eliminating any adventitious water that may be present). When the cinchona alkaloids were used as catalysts in THF at -78 °C with Me₃SiCl, the reaction generated high conversion of silylated indanol, but the recovered starting material had a low e.r. (Scheme 2.12).



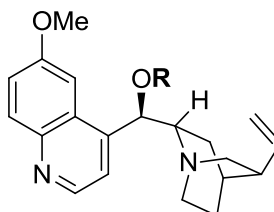
Scheme 2.11 Synthesis of Me_3Si- derived cinchona alkaloids.



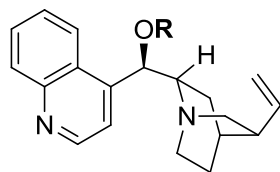
Catalysts



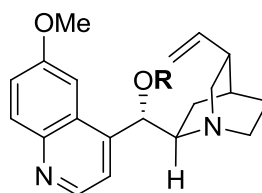
$R = H$; Cinchonine (CN)
 $R = Me_3Si-$ (CN-TMS)



$R = H$; Quinine (QN)
 $R = Me_3Si-$ (QN-TMS)



$R = H$; Cinchonidine (CD)
 $R = Me_3Si-$ (CD-TMS)

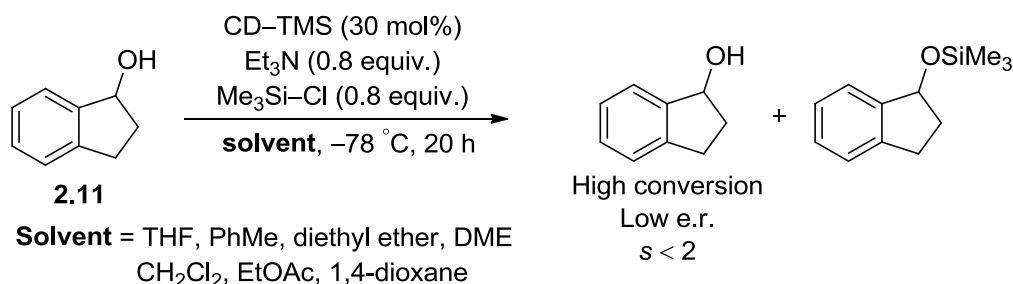


$R = H$; Quinidine (QD)
 $R = Me_3Si-$ (QD-TMS)

Scheme 2.12 Initial catalyst screening for the enantioselective silylation of **2.11** with the trimethylsilyl derivatized cinchona alkaloids.

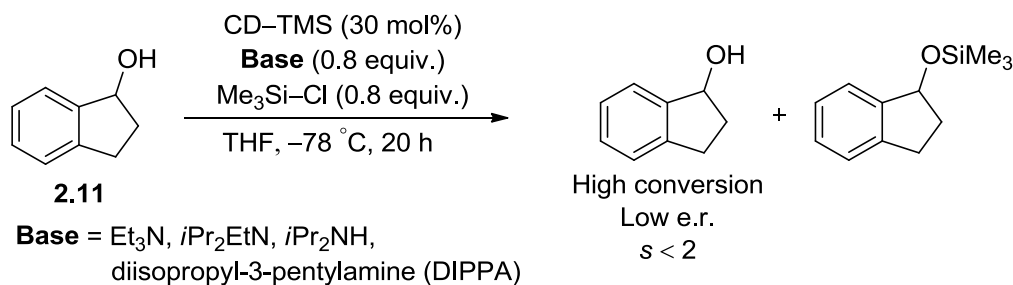
Due to the high conversion but low enantiomeric excess, it was decided to modify reaction conditions to try to improve the enantiomeric ratio. The first condition that was altered was the solvent. In this study, the catalyst CD-TMS was used to screen the enantioselective silylation of **2.11**. Solvents of different polarities were screened

(Scheme 2.12) in the presence of **2.11**, Et₃N, and Me₃SiCl. It was observed that the solvent had little effect on the enantioselective silylation of **2.11** with the chosen reaction conditions. The same issue of high conversion with low enantioselectivity kept the selectivity factors below 2.



Scheme 2.13 Testing the solvent effect on e.r. in the enantioselective silylation of **2.11**

Although solvent seemed to play a minor role in determining the e.r. for the enantioselective silylation of **2.11**, it was then decided to determine if altering the base played any role. To test this effect, CD-TMS, Me₃SiCl and a series of bases were reacted in THF at -78 °C. Sterically hindered secondary and tertiary bases were used but no major changes in the selectivity factors were observed.

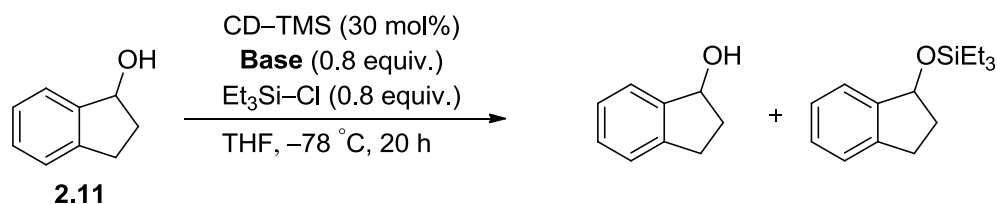


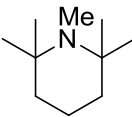
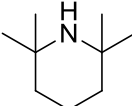
Scheme 2.14 Screening bases for the enantioselective silylation of **2.11** with CD-TMS and Me₃SiCl

Although conversion was achieved for the enantioselective silylation of **2.11** with Me₃SiCl, low selectivity factors were achieved when screening reaction conditions for

this reaction; it was thereby decided to screen the slightly more bulky Et₃SiCl. The effect of the base upon selectivity factor was then tested. Screening hindered and unhindered secondary and tertiary bases with Et₃SiCl gave significantly higher selectivity factors than with Me₃SiCl. Although Et₃N (Table 2.3, Entry 1) still gave a selectivity factor of less than 2, *i*Pr₂EtN gave the best result thus far with a selectivity factor of 4.0 (Entry 2). When the secondary base *i*Pr₂NH was screened (Entry 3), there was little enantiomeric enrichment and the same was also observed for the more sterically hindered base, diisopropyl-3-pentylamine (*i*Pr₂NCH(CH₂CH₃)₂) (Entry 4). The sterically demanding bases 2,2,5,5-tetramethyl piperidine and the tertiary base 1,2,2,5,5-pentamethyl piperidine gave modest improvements then what was observed thus far (Entry 5 and 6), but the selectivity factor was inferior to *i*Pr₂EtN. Despite these improved results, the benchmark of *s* = 10 remained elusive.

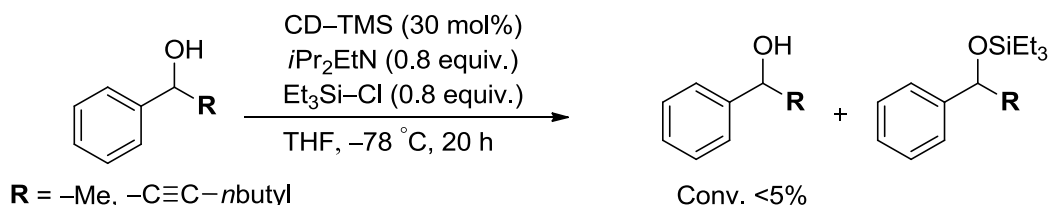
Table 2.3 Testing bases for the enantioselective silylation of **2.11** with CD-TMS and Et₃Si-Cl.



Entry	Base	Conversion (%) ^a	e.r. ^b	s ^c
1	Et ₃ N	81%	75:25	1.9
2	<i>i</i> Pr ₂ EtN	62%	80.5:19.5	4.0
3	<i>i</i> Pr ₂ NH	84%	54:46	1.1
4	DIPPA	80%	53:47	1.1
5		62%	81:19	2.8
6		69%	69.5:30.5	2.0

^a Conversion was calculated by GC with an internal standard. ^b The e.r. listed is of the recovered starting material ^c s was calculated from the equations provided in ref 22.

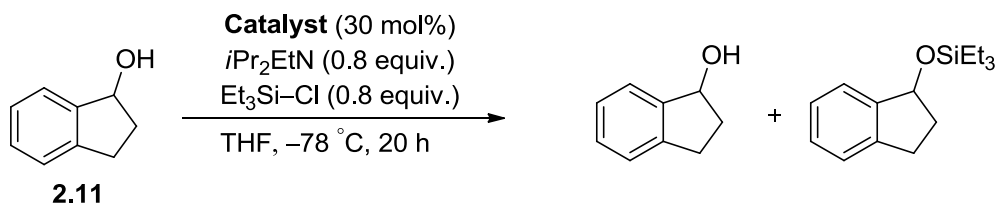
To see if an improvement in selectivity factor can be achieved by switching from cyclic to acyclic secondary alcohols, 1-phenyl ethanol and 1-phenyl-hept-2-yn-1-ol were tested with the improved reaction conditions from Table 2.3, Entry 2. However both substrates were found to show no conversion (Scheme 2.15). Perhaps this can be due to the increased relative steric bulk caused by the increased bond angle of the chiral carbinol center and the ability for the phenyl ring to freely rotate. The bicyclic secondary alcohols contain a phenyl ring that is locked from freely rotating. Therefore, it would appear that the reactive silicon intermediate is very sensitive to the steric environment near the chiral alcohol.



Scheme 2.15 Testing acyclic alcohols with the improved reactions conditions in Table 2.3, Entry 2.

With the inability to improve the selectivity factor into an efficient range by altering the base and solvent, other catalysts were then screened. Due to the catalytic activity of tertiary amines in the enantioselective silylation of secondary alcohols with Et_3SiCl , several amine catalysts were chosen to be screened for their catalytic activity. Among the catalysts tested was the chiral tertiary amine Brucine (Table 2.4, Entry 2) which showed inferior selectivity to that of CD-TMS. Also, the chiral tertiary amine (S)-nicotine (Entry 3) was found to asymmetrically catalyze the enantioselective silylation of **2.11** although with lower enantioselectivity. Interestingly, the *N*-heterocyclic carbene (Entry 4) was found to catalyze the reaction, although this catalyst was not chiral and therefore no ee was generated. However, this does show that chiral *N*-heterocyclic carbenes may be a viable catalyst for the enantioselective silylation of secondary alcohols. It was also discovered that the HCl salt of (-)-tetramisole and the free based version, **2.12** (Entry 5 and 6 respectively), were effective at catalyzing the enantioselective silylation of secondary alcohols and also generating enantiomeric excess. However, when attempts at activating the protonated form of (-)-tetramisole by deprotonating the isothioureia in situ a selectivity factor of only 2.2 was achieved. The previous deprotonated isothioureia catalyst (**2.12**) was found to achieve a selectivity factor as high as 4.1. Due to this promising result, it was then decided to optimize the reaction conditions for the enantioselective silylation of **2.11** with the isothioureia catalyst **2.12**.

Table 2.4 Testing various catalysts for the enantioselective silylation of **2.11** with Et₃Si-Cl



Entry	Catalyst	Conversion (%) ^a	e.r. ^b	s ^c
1	CD-TMS	62%	80.5:19.5	4.0
2		47%	64.5:35.5	2.6
3		84%	56.5:43.5	1.7
4 ^d		40%	—	—
5 ^e		82%	81:19	2.2
6 ^f		50%	72.8:27.2	4.1

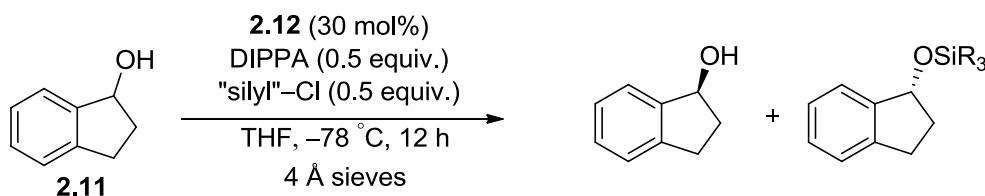
^a Conversion was calculated from the e.r. of the product and recovered starting material. ^b e.r. was calculated by HPLC on a chiral stationary phase. ^c Selectivity factor was calculated from e.r. of the starting material and product²² ^d 1.1 equiv. *i*Pr₂EtN ^e 1.1 equiv. *i*Pr₂EtN. ^f 0.5 equiv. DIPPA and Et₃Si-Cl.

2.5 Optimizing reaction conditions for the enantioselective silylation of secondary alcohols with (-)-tetramisole (**2.12**).

(-)-Tetramisole (**2.12**) was first identified as a nucleophilic asymmetric catalyst by the Birman group for the asymmetric acylation of secondary alcohols.²³ This catalyst and other isothioureas and amidine based catalysts were found to be very effective at achieving very high selectivity factors for a number of difficult substrates for acylation based kinetic resolutions.²⁴ In an unrelated report, the Kim group found that the bicyclic amidine base 1,8-diazabicyclo[5.4.0]undec-7-ene (DBU) was a very effective catalyst for the silylation of alcohols. This was even true for the bulky silyl protecting group *t*BuMe₂SiCl.²⁵ This gave us an impetus for investigating the reaction conditions for the enantioselective silylation of **2.11** with (-)-tetramisole (**2.12**).

To begin our study, **2.11** was silylated with a series of silyl protecting groups with **2.12** as the catalyst and using DIPPA as the base (Table 2.5). The alkyl silyl chloride Et₃SiCl gave comparable results to that of the cinchona alkaloid series (Entry 1). When phenyl substituents were introduced, there was a noticeable trend of increased enantioselectivity (Entries 2-4) culminating with a selectivity factor of 8.6 for Ph₃SiCl. When the bulk of the silyl chloride was increased in the cases of *t*BuMe₂SiCl and *i*Pr₃SiCl (Entry 5 and 6 respectively) there was no observable conversion by ¹H NMR. Presumably, either the size of the silyl chlorides were too large to allow for the formation of the active silylating species, or the resulting active silylating species was too large to allow for alcoholysis.

Table 2.5 The effect of different silyl substituents on the enantioselective silylation of **2.11** with **2.12**.



Entry	"silyl" ($\text{R}_3\text{Si}-\text{Cl}$)	Conversion (%) ^a	e.r. ^b	s ^c
1	$\text{Et}_3\text{Si}-\text{Cl}$	50%	73:27	4.1
2	$\text{Me}_2\text{PhSi}-\text{Cl}$	51.9%	72:28	3.4
3	$\text{Ph}_2\text{MeSi}-\text{Cl}$	52.8%	77:22	5.2
4 ^d	$\text{Ph}_3\text{Si}-\text{Cl}$	60%	92:8	8.6
5	$t\text{BuMe}_2\text{Si}-\text{Cl}$	<5% ^e	—	—
6	$i\text{Pr}_3\text{Si}-\text{Cl}$	<5% ^e	—	—

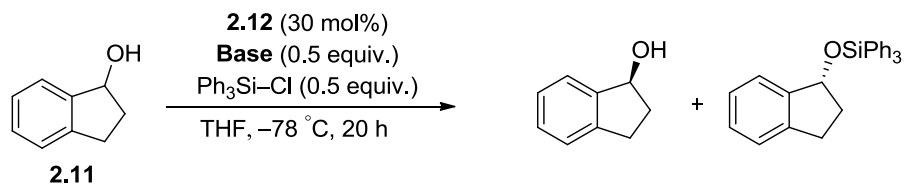
^a Conversion was calculated from the e.r. of the product and recovered starting material. ^b e.r. was calculated by HPLC on a chiral stationary phase.

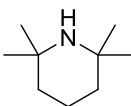
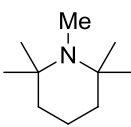
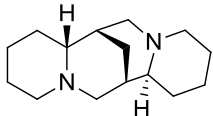
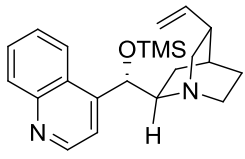
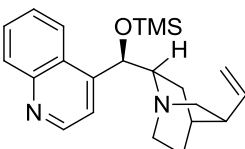
^c Selectivity factor was determined from e.r. of the starting material and product (see ref 22) ^d 0.6 equiv. DIPPA and $\text{Ph}_3\text{Si}-\text{Cl}$. ^e As observed by $^1\text{H-NMR}$.

To further optimize the reaction conditions, the base was changed to determine what effect the base may have. When testing the effect of the base upon selectivity factor for the enantioselective silylation of **2.11** with **2.12**, bases which possess nucleophilic character were avoided to prevent competitive pathways that would result in racemic silylation. Therefore, the bases chosen were sterically congested. The least sterically hindered of the bases, Et_3N (Table 2.6, Entry 1) was found to be inferior to the more sterically hindered bases $i\text{Pr}_2\text{EtN}$ and DIPPA (Entry 2 and 3 respectively). When the

concentration was reduced by half, there was a noticeable drop in the selectivity factor to 5.1 (Entry 4). The secondary amine 2,2,6,6-tetramethylpiperidine and the tertiary analog 1,2,2,6,6-pentamethylpiperidine (Entry 5 and 6 respectively) showed comparable levels of selectivity however these results were still inferior to the branched alkyl bases DIPPA and *i*Pr₂EtN. When the chiral base (–)-sparteine was used (Entry 7), a substantial drop in selectivity was observed. The previous catalysts CN-TMS and CD-TMS (Entry 8 and 9 respectively) were also employed as base/co-catalysts for the enantioselective silylation of **2.11** and also gave lower selectivity factors than Entry 2 or 3. Although DIPPA and *i*Pr₂EtN were found to give practically identical selectivity factors for **2.11**, when other substrates were used, it was observed that DIPPA gave consistently higher selectivity factors. Therefore, DIPPA was chosen as the base for further screenings.

Table 2.6 The effect of base upon the selectivity factor for the enantioselective silylation of **2.11** with **2.12**.

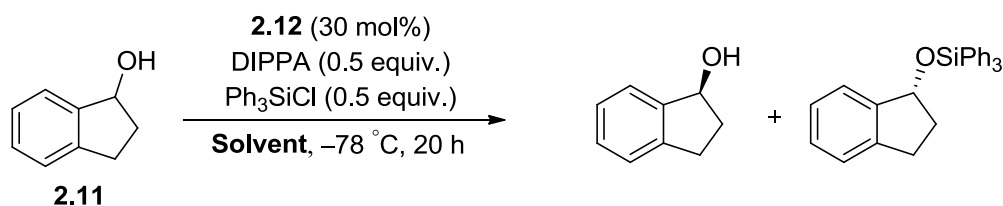


Entry	Base	Conversion (%) ^a	e.r. ^b	s ^c
1	Et ₃ N	34%	67:33	6.8
2	<i>i</i> Pr ₂ EtN	47%	65:35	8.4
3	DIPPA	59%	92:8	8.6
4 ^d	DIPPA	25%	60:40	5.1
5		43%	74:26	7.0
6		46%	75:25	6.6
7		45%	74:26	6.3
8		40%	69:31	6.1
9		41%	73:27	7.1

^a Conversion was calculated from the e.r. of the product and recovered starting material. ^b e.r. of recovered starting material was calculated by HPLC on a chiral stationary phase. ^c Selectivity factor was determined from e.r. of the starting material and product²² ^d Reaction was performed at a concentration of 0.15 M (half the normal concentration) with respect to **2.11**

To further optimize the reaction conditions, a series of solvents of different polarities were tested in the enantioselective silylation reaction. When the solvent was changed from THF to diethyl ether (Table 2.7, entry 2), there was no observable conversion. What may be occurring is the precipitation of the reactive silylating intermediate between the catalyst and the Ph_3SiCl . When CH_2Cl_2 was used as the solvent (Entry 3) the selectivity factor fell to 2.8, and when toluene was the solvent (Entry 4), there was a small decrease in the selectivity factor compared to THF. When the coordinating solvent DME was used (Entry 5), a noticeable decrease in selectivity to 4.7 was observed. Interestingly, when DMF was the solvent only a small decrease of selectivity was observed (Entry 6). This is mainly notable because DMF is known to catalyze the silylation of secondary alcohols.^{26, 27} This suggests that **2.11** has a higher catalytic activity than DMF and that the reaction is probably proceeding to completion well before the full 20 h of reaction time.

Table 2.7 Testing the solvent effect on the enantioselective silylation of **2.11**.

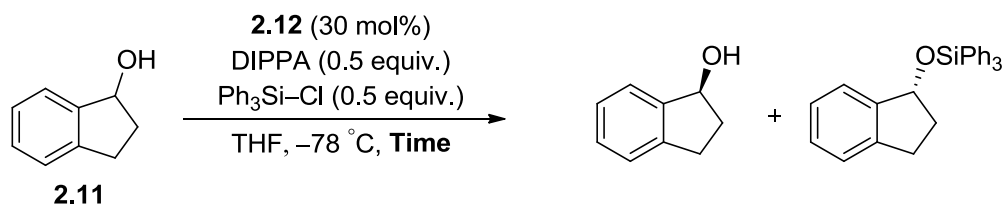


Entry	Solvent	Conversion (%) ^a	e.r. ^b	s ^c
1 ^d	THF	59%	92:8	8.6
2	Diethyl ether	<5%	-	-
3	CH ₂ Cl ₂	48%	66:34	2.8
4	PhMe	47%	70:30	3.7
5 ^e	DME	43%	70:30	4.7
6 ^e	DMF	37%	64:36	6.6

^a Conversion was calculated from the e.r. of the product and recovered starting material. ^b e.r. was calculated by HPLC on a chiral stationary phase. ^c Selectivity factor was determined from e.r. of the starting material and product (see ref 22). ^d Reaction was performed with (0.6 equiv) DIPPA and (0.6 equiv.) Ph₃SiCl. ^e Reaction run at -40 °C

Upon observing the result of performing the enantioselective silylation reaction in DMF (Table 2.7, entry 6), the reaction was analyzed at different time intervals to determine the optimal reaction time. It was observed that running the reaction with the optimized conditions caused the enantioselective silylation of **2.11** to go to completion between 30 minutes and 1 hour (Table 2.8). This represents a vast improvement over the reported reaction times of other enantioselective silylation methodologies.^{1, 5, 6, 9, 12}

Table 2.8 Determining the length of the reaction for the enantioselective silylation of **2.11** with **2.12**.



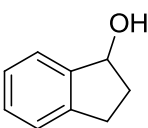
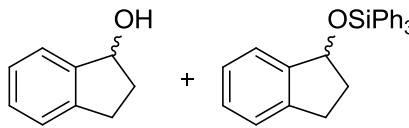
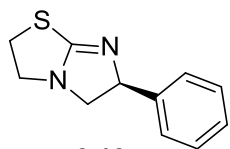
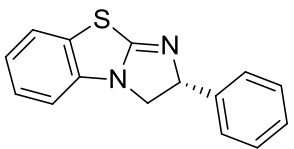
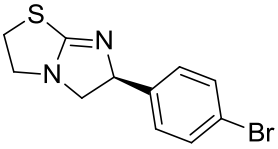
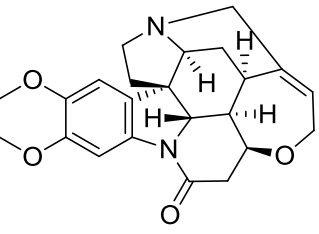
Entry	Time	Conversion (%) ^a	e.r. ^b	s ^c
1	10 min	38%	71:29	8.0
2	30 min	44.5%	77:23	8.2
3	1 h	45.4%	77:23	8.4
4	2 h	45.4%	77:22	8.4

^a Conversion was calculated from the e.r. of the product and recovered starting material. ^b e.r. was calculated by HPLC on a chiral stationary phase. ^c Selectivity factor was determined from e.r. of the starting material and product (see ref 22)

While investigating asymmetric acylation reactions it was observed by the Birman group that the benzo- derivatives of their isothioureia catalysts were more selective in most cases.²⁴ It was therefore decided to use benztetramisole and some other derivatives of **2.12** as the catalyst for the enantioselective silylation of **2.11**. Unfortunately, the selectivity factor observed for benztetramisole was found to be inferior to **2.12** (Entry 1). The para-bromo derivative of (–)-tetramisole (Entry 3) was also tested as catalyst and interestingly, the selectivity was also inferior to that seen for **2.12**. The optimized reaction conditions were also tried with the tertiary amine catalysts previously tested. CD-TMS and brucine (Entry 4 and 5) and these catalysts gave far inferior results. Without a catalyst present, the reaction was found to only go to 8%

completion even after 45 h. In subsequent studies it was also discovered that the catalyst loading can be lowered to 25 mol % without decreasing the selectivity factor. It is also noteworthy that although the selectivity factor for **2.11** was less than the desired selectivity factor of 10, a selectivity factor of 8.6 is, to the best of our knowledge, the highest selectivity factor achieved for an organocatalyzed kinetic resolution of **2.11**. With these optimal conditions, it was then decided to move forward to test the substrate scope with the optimal reaction conditions discovered thus far using 25 mol % of **2.12**.

Table 2.9 Testing other nucleophilic catalysts with the optimized conditions developed for the enantioselective silylation of 1-indanol (**2.11**).

<div style="display: flex; align-items: center; justify-content: center;"> <div style="text-align: center;">  <p>2.11</p> </div> <div style="margin: 0 20px; text-align: center;"> <p>Catalyst (30 mol%)</p> <p><i>i</i>Pr₂EtN (0.5 equiv.)</p> <p>Ph₃Si-Cl (0.5 equiv.)</p> <p>THF, -78 °C, 21-22 h,</p> <p>4 Å sieves</p> </div> <div style="text-align: center;">  </div> </div>				
Entry	Time	Conversion (%) ^a	e.r. ^b	<i>s</i> ^c
1 ^d		59%	92:8	8.6
2		48%	62:38	3.5
3		44%	73:27	6.2
4	CD-TMS	14% ^e	—	1.0
5		47%	59:41	1.8
6 ^e	None	8% ^f	—	—

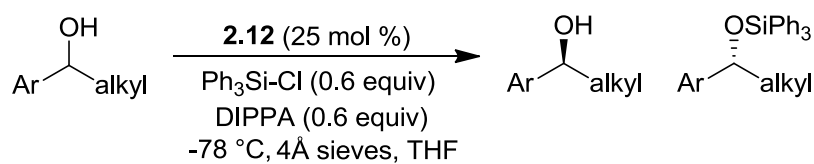
^a Conversion was calculated from the e.r. of the product and recovered starting material. ^b e.r. was calculated by HPLC on a chiral stationary phase. ^c Selectivity factor was determined from e.r. of the starting material and product (see ref 22). ^d 0.6 equiv. of *i*Pr₂EtN and Ph₃Si-Cl ^e Reaction was left to react for 45 h. ^f As determined by ¹H-NMR.

2.6 Determining the substrate scope for the enantioselective silylation of secondary alcohols with **2.12**

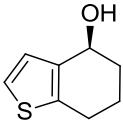
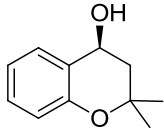
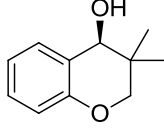
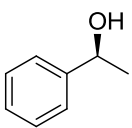
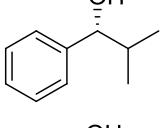
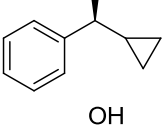
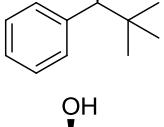
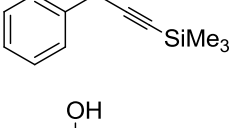
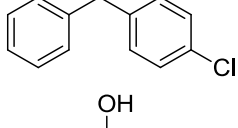
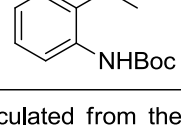
With the optimal catalyst and reaction conditions determined for the enantioselective silylation of monofunctional secondary alcohols, the substrate scope was then tested to determine any steric and electronic effects that may influence the selectivity factor (Table 2.10). First, the effect of the alkyl ring size was tested (Entry 2 and 3). In the case of tetralol (entry 2) the ring was increased from a 5 to a 6 membered ring, and there was an improvement in the selectivity factor to 14. However, when the ring size was increased to 7 in the case of benzosuberol (entry 3), there was a drop in the selectivity factor to 4.9, which is lower than even 1-indanol. The tricyclic substrate 1-acenaphthenol (entry 4) was also found to be inferior to **2.11** giving comparable selectivity to that of benzosuberol. When the alkyl ring was substituted with oxygen in the case of 4-chromanol (entry 5) a selectivity factor of 22 was observed. When the heteroatom was sulfur in the case of thiochromanol (entry 6) the highest selectivity factors to date were reported with a selectivity factor of 25. When the tetralol core possessed a methoxy substituent on the 7-position, (entry 7a) the selectivity factor remained basically unchanged relative to tetralol. When substituted with a fluorine on the 7-position (entry 7b) the selectivity dropped slightly to 11. This suggests that the electron density of the aryl ring plays a minor role in determining the selectivity factor of the enantioselective silylation. When the tetralol core was substituted with a 6-methoxy substituent (entry 8), the reaction did not readily undergo deprotection with TBAF. When TBAF was used for removal of the triphenylsilyl group, all that was recovered was the dehydrated elimination product of the starting material (Figure 2.6). This result is

presumably due to the donating effect of the methoxy group located in the para position to the benzylic carbon. Therefore, it appears that a stabilized benzylic position (through π -donation) can more readily undergo elimination. Further screening of electronic effects of a thiophene derivative in place of the phenyl substitute has (Entry 9) gave a selectivity factor close to that of tetralol.

Table 2.10 Testing the substrate scope with the optimized reaction conditions for enantioselective silylation with **2.12**.



Entry	sec-alcohol	t (hr)	conv (%) ^a	er of recovered alcohol	s ^b
1 ^c		1	59	92:8	8.5
2		8	52	89:11	14
3		12	59	82:18	4.9
4		8	56	80:20	4.8
5		14	53	94:6	22
6		8	52	94:6	25
7		a. 14 b. 12	a. 55 b. 55	93: 7 90:10	16 11
	a. R = -OMe b. R = -F				
8 ^d		14	56 ^e	89:11	9.2^f

9		15	56	93.5:6.5	14
10		8	53	91:9	15
11		24	<5 ^c	—	—
12		25	41	63:37	2.8
13		46	29	63:37	5.7
14		4	34	55.9:44.1	1.9
15		48	<5 ^c	—	—
16		6	40	64.1:35.9	3.3
17		15	51 ^c	—	1.0
18		38	40	63:37	2.7

^a Conversion was calculated from the e.r. of the product and recovered starting material. ^b Selectivity factor was determined from e.r. of the starting material and product (see ref 22). ^c As determined by NMR ^d 0.6 equivalents of *i*Pr₂EtN and Ph₃Si-Cl ^e Conv. was calculated from recovered starting material. ^f Selectivity factor was calculated from e.r. of the starting material and the conv. calculated from the recovered starting material.

To test the effect of sterics on the selectivity of the reaction, a dimethyl substitution was made to 4-chroman-2-ol at the 2 and 3 positions (Entry 10 and 11 respectively). When the dimethyl substituents were in the 2 position, there was a diminishment in the stereoselectivity of the reaction. When the steric bulk was in the 3-position, the reaction failed to convert at all. Therefore the reaction seems to be sensitive to steric bulk, especially near the carbinol center.

When acyclic substrates were tested, the results were less selective (Entries 12-17). The substrate 1-Phenylethanol (Entry 12) was found to be barely selective at all while the more sterically hindered 2-methyl-1-phenylpropan-1-ol was more selective (Entry 13). Interestingly, the faster reacting enantiomer was the *S* enantiomer, which is the opposite of what was observed for all of the previous substrates. This interesting result is contrary to the initial assumption that the alkyl substituent would be the larger substituent, because increasing the bulk of the alkyl substituent should not reverse the enantioselectivity of the reaction. Unfortunately, when the alkyl substituent was further increased in bulk, the system was presumably too bulky and no observable product was formed, even after 48 h (Entry 14). When compared to **2.11**, which takes roughly 30 minutes to complete, the slower reaction time of 1-phenylethanol lends further evidence to the steric sensitivity of this system. The trimethylsilyl substituted propargylic alcohol (Entry 15) shown gave nearly identical selectivity to that of Entry 12. To test if this new methodology was also capable of differentiating solely based upon electronic effects, the differentially substituted diphenylmethanol (4-chlorophenyl)phenylmethanol (Entry 16) was subjected to the reaction conditions but unfortunately the reaction was completely unselective, although there was a good level of conversion. Due to the paucity of

techniques that can tolerate amine functionalities, Entry 17 was screened as well and although the system was capable of giving acceptable levels of conversion, the reaction showed identical selectivity to 1-phenylethanol.

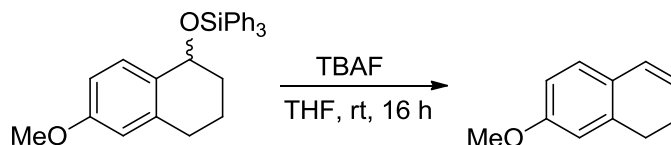


Figure 2.6 The product observed from the deprotection of ((6-methoxy-1,2,3,4-tetrahydronaphthalen-1-yl)oxy)triphenylsilane.

Due to the result observed from the deprotection of 6-methoxy tetralol, it would therefore also seem logical to expect such an effect from 4-chromanol and potentially thiochromanol (Entry 5 and 6 respectively). However, it has been noted that there appears to be a relatively small ortho stabilizing effect in the cases of 4-chromanol and thiochromanol. In a study done by the O'Donoghue group in which the rates of hydrolysis of 4-chromanol and thiochromanol were studied,²⁸ it was observed that the rates for these heterocyclic compounds were greatly diminished than when a methoxy group was placed para to the benzylic alcohol. They suggest that the reason for this lack of benzylic carbocation stabilizing ability was due to a stereochemically disfavored conjugation of the endocyclic heteroatom with the benzylic cation.

2.7 Conclusion

Described heretofore are the developments in the active field of enantioselective silylation with an in depth discussion of the contributions by the Wiskur group on their (-)-tetramisole catalyzed methodology. In an effort to improve upon the seminal work

done by the Ishikawa group with monofunctional secondary alcohols,⁹ the Wiskur group has tested a number of catalysts and reaction conditions in an attempt to achieve a synthetically useful selectivity factor ($s \geq 10$). Although comparable results to the report by the Ishikawa group were observed for the enantioselective silylation of 1-indanol (**2.11**) with the trimethylsilyl derivatized cinchonidine catalyst, further optimization gave better results. Through extensive testing of reaction conditions and catalysts, the optimal conditions were described. With the optimal reaction conditions, the Wiskur group reports³ achieving for the substrate **2.11** a selectivity factor of 8.6 with the reaction taking place in less than one hour with only 25 mol% of catalyst. This is an improvement over the only other report of an enantioselective silylation for **2.11** in which a selectivity factor of 4.5 was achieved, but only after 6-10 days with a stoichiometric catalyst loading. When this new methodology was expanded to other substrates, it was discovered that 1-thiochromanol (**Table 2.10**, Entry 6) gave the highest selectivity factor ($s = 25$). The system also shows sensitivity to sterics and when the β -branching was equivalent to a tertiary butyl in size, the reaction failed to give any conversion. Also observed was a small electronic effect and that the system failed to achieve any usable selectivity with acyclic benzylic secondary alcohols. Although the generation of chiral materials is one of the objectives of this research, another major goal is to help in the understanding of the origin of enantioselectivity in these silylation reactions. This topic was also pursued and will be discussed in the subsequent chapter.

In addition to mechanistic investigations, further expanding the substrate scope to include substrates that other reported methodologies are not selective for would increase this methodologies utility. Substrates such as tertiary alcohols, for example, would place

this enantioselective silylation methodology among only a few organocatalyzed methodologies that are known to resolve this difficult class of functional group.²⁹⁻³¹ Also, substrates that have biological significance would also be beneficial, such as alcohol containing compounds that possess amines, such as amino alcohols. These amino containing compounds are of particular interest due to their prevalence in manufactured chemical compounds such as pharmaceuticals and agrochemicals.³² Other substrates of particular interest would be hydroxy lactones and hydroxy lactams, particularly β -lactams, as these are ubiquitous functional groups found in nature. The β -lactam functionality is particularly interesting as since amides have been known to catalyze the silylation of alcohols these substrates should lower the selectivity of the silylation based kinetic resolution. However, although they are by definition a lactam, due to the orthogonality of the nitrogen and carbonyl orbitals,³³ the nucleophilicity of the amide functionality is diminished. Therefore, hydroxy lactams may lend themselves to resolution by enantioselective silylation and thereby obtainment of enantiomerically enriched lactams.

2.8 Experimental

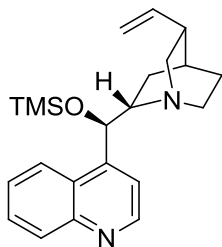
All reactions were carried out under a dry N₂ atmosphere in oven-dried glassware. Dry dichloromethane (CH₂Cl₂), tetrahydrofuran (THF), *N,N*-dimethylformamide (DMF), toluene (PhMe), diethyl ether, and dimethoxyethane (DME), were obtained by passing the previously degassed solvents through activated alumina columns. Triethylamine (Et₃N) was distilled over CaH₂ prior to use. Pyrrolidine was distilled over KOH prior to

use. All chemicals were purchased from major suppliers such as Alfa Aesar, Sigma-Aldrich, TCI, or Acros. Unless otherwise stated all reagents were used as received without further purification. *N*-Butyllithium in hexanes was obtained from Sigma-Aldrich and the concentration was determined from titration with *N*-benzylbenzamide.³⁴ Molecular sieves were activated by heating to 170 °C for at least 48 hours prior to use. ¹H NMR spectra were recorded on a Varian Mercury/VX (400MHz). Chemical shifts are reported in ppm with either TMS (0.00 ppm for ¹H and ¹³C) or CDCl₃ as the internal standard (CDCl₃: δ 7.26 and 77.0 ppm for ¹H and ¹³C respectively). Data are reported as follows: chemical shift, multiplicity (s = singlet, d = doublet, t = triplet, q = quartet, dd = doublet of doublet, dt = doublet of triplets, dsep = doublet of septet, m = multiplet, br = broad, ur = unresolved multiplet) and coupling constants (Hz). ¹³C NMR spectra were recorded on a Varian Mercury/VX (100 MHz) with complete proton decoupling. Reactions were monitored by thin layer chromatography (TLC) using EMD chemicals 60F silica gel plates. Flash column chromatography was performed over silica gel (32-63 μm). High resolution mass spectrometry (HRMS) was performed by the mass spectrometry facility at the University of South Carolina. IR data were obtained on a Perkin Elmer Spectrum 100 FT-IR ATR spectrophotometer, ν_{max} in cm⁻¹. All enantiomeric ratios were determined by HPLC on an Agilent 1200 series using the chiral stationary phases Daicel Chiralcel AD-H, OJ-H, or OD-H (4.6 × 250 mm × 5 μm) columns, and monitored by DAD (Diode Array Detector) in comparison with authentic racemic materials. Melting points (mp) were taken with a Laboratory Devices Mel-Temp and were uncorrected. Optical rotations were obtained using a JASCO P-1010 polarimeter.

Preparation of the catalysts (-)-tetramisole (**2.12**) and (-)-*p*-Bromotetramisole

(-)-Tetramisole HCl (200 mg, 0.83 mmol) or (-)-*p*-Bromotetramisole oxalate (147 mg, 0.394 mmol) was added to a 4-dram vial. The vial was then charged with 2 mL diethyl ether and the suspension was then treated with 4 M NaOH and shaken until the solid dissolved. The aqueous phase was then extracted with diethyl ether (4 x 3 mL). The ethereal layer was then dried over anhydrous Na₂SO₄, filtered, then evaporated to dryness to afford the white solids **2.12** (167 mg, 0.82 mmol, Yield 98%) or (-)-*p*-Bromotetramisole oxalate (91 mg, 0.32 mmol, Yield 82 %).

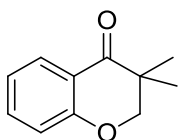
Synthesis of CD-TMS³⁵



Compound **6** was synthesized in a similar procedure to the published method.³⁵ To an oven dried 50 mL RBF fitted with a Teflon coated stir bar was added cinchonidine (1.0 g, 3.40 mmol). The flask was then charged with 20 mL THF and treated with Et₃N (0.59 mL, 4.24 mmol) and stirred at 0 °C. To the heterogeneous mixture was added TMS-Cl (0.60 mL, 4.73 mmol) and the reaction was stirred for 21 h while warming to room temperature. The reaction was then filtered and rinsed with diethyl ether. The filtrate was concentrated and purified via column chromatography (9:1 MeOH (NH₃ sat.) in ethyl acetate followed by 4:1 MeOH (NH₃ sat.) in ethyl acetate) to yield product **6** as a white solid (1.01g, 2.75 mmol, Yield 81%).

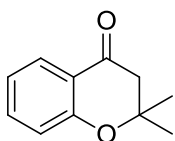
¹H NMR (400 MHz, CDCl₃) δ ppm 8.86 (d, *J* = 4 Hz, 1 H), 8.13-8.09 (m, 2 H), 7.69 (dt, *J* = 7.5, 1.0 Hz, 1 H), 7.57 (dt, *J* = 7.5, 1.0 Hz, 1 H), 7.48 (br, 1H), 5.72-5.63 (m, 2 Hz), 4.90 (d, *J* = 17.0 Hz, 1 H), 4.85 (d, *J* = 10.0 Hz, 1 H), 3.40 (ur, 1 H), 3.06 (t, *J* = 12.5 Hz, 1 H), 2.98 (ur, 1 H), 2.68-2.56 (m, 2 H), 2.22 (ur, 1 H), 1.77-1.65 (m, 3 H), 1.51-1.44 (m, 2 H), 0.01 (s, 9H). **¹³C NMR** (101 MHz, CDCl₃) δ ppm 150.0, 149.2, 148.1, 141.9, 130.2, 128.7, 126.4, 125.2, 123.1 (br), 118.3 (br), 114.0, 72.6 (br), 61.2, 57.1, 42.87, 39.9, 27.8, 27.4, 20.3 (br), 0.03.

Synthesis of 3,3-dimethylchromanone³⁶



A 50 mL RBF fitted with a Teflon coated stir bar and containing potassium *tert*-butoxide (475 mg, 4.23 mmol), was charged with 16 mL THF and stirred vigorously at -78 °C. A solution of 4-chromanone (0.3 mL, 1.61 mmol), and iodomethane (0.74 mL, 11.9 mmol) in 2.2 mL THF was then added in three portions to the cooled solution and left to react for 2 h. Then a solution of additional potassium *tert*-butoxide (177 mg, 1.57 mmol) in 2 mL THF was added to the orange reaction mixture and the reaction was allowed to warm to room temperature and stir for 19 h. at which time a white precipitant appeared and the reaction turned clear yellow. The reaction mixture was then filtered through celite and concentrated down. The crude oil was purified via column chromatography (silica gel, 1:1 hexanes: CH₂Cl₂ to 100% CH₂Cl₂) yielding a pale yellow oil (252 mg, 1.43 mmol, Yield 89 %). **¹H NMR** (400 MHz, CDCl₃) δ ppm 7.88 (dd, *J* = 8.0, 1.5 Hz, 1 H), 7.43 (dt, *J* = 7.5, 1.5 Hz, 1 H), 6.99, (t, *J* = 6.0 Hz, 1 H), 6.93 (d, *J* = 8.0 Hz, 1 H), 4.12 (s, 2 H), 1.18 (s, 6 H). **¹³C NMR** (101 MHz, CDCl₃) δ ppm 197.1, 161.0, 135.4, 127.6, 121.3, 119.4, 117.5, 76.5, 41.5, 20.3.

Synthesis of 2,2-dimethylchroman-4-one³⁷



To a 100 mL 3-neck flask containing 2-hydroxyacetophenone (3.96 mL, 32.9 mmol), a Teflon coated stir bar, and 4 Å MS was charged 30 mL PhMe. The solution was then treated with acetone (6.04 mL, 82.3 mmol) followed by the addition of pyrrolidine (3.17 mL, 38.2 mmol) over 10 minutes. The reaction was stirred at room temperature for 4 h during which time the reaction turned a deep purple. It was then stirred at reflux for 20 h. The reaction was cooled to room temperature and washed with 4 N HCl (40 mL). The organic layer was then washed with 2 N NaOH (40 mL) followed by water (30 mL). The organic layer was dried over Na₂SO₄, filtered and concentrated to give a brown oil which solidified upon standing. The solid was rinsed with cold absolute ethanol then dried under vacuum to yield a yellow solid (1.35 g, 7.7 mmol, Yield 23%).

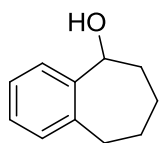
¹H NMR (400 MHz, CDCl₃) δ ppm 7.85 (d, *J* = 7.5 Hz, 1 H), 7.46 (t, *J* = 8.0 Hz, 1 H), 6.97 (t, *J* = 7.5 Hz, 1 H), 6.92 (d, 8.0 Hz, 1 H), 2.72 (s, 2 H), 1.46 (s, 6 H). ¹³C NMR (101 MHz, CDCl₃) δ ppm 192.5, 159.9, 136.1, 126.4, 120.6, 120.1, 118.2, 79.1, 48.8, 26.5.

General procedure for the reduction of ketones (GP1)

To a 4-dram vial fitted with a Teflon coated stir-bar was added the ketone and absolute ethanol to a concentration of 1 M. The solution was treated with NaBH₄ and stirred at room temperature overnight. The reaction mixture was then quenched with 3 mL H₂O, then 3 mL brine, and extracted with EtOAc (4 x 3 mL). The organic layers were combined, dried over Na₂SO₄, filtered, and then evaporated to dryness. The resulting

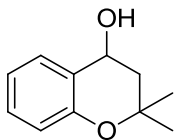
residue was usually pure enough that filtration through a plug of silica gel was all that was required. This was done by dissolving the crude in 2 mL diethyl ether and pushed through a plug of silica gel. The silica gel was then rinsed once more with 2 mL diethyl ether to give the desired alcohol. If further purification was necessary, column chromatography (silica gel, CH₂Cl₂ followed by 2% MeOH in CH₂Cl₂) was performed without filtering through silica gel first.

Preparation of *rac*-benzosuberol³⁸



According to **GP1**, benzosuberone (500 μ L, 3.34 mmol) was treated with NaBH₄ (126 mg, 3.34 mmol) giving a white solid (529 mg, 3.26 mmol, Yield 98%). ¹H NMR (400 MHz, CDCl₃) δ ppm 7.44 (d, J = 4 Hz, 1 H), 7.23-7.13 (m, 2 H), 7.10 (d, J = 4.0 Hz, 1 H), 4.94 (d, J = 4.0 Hz, 1 H), 2.92 (dd, J = 14.0, 5.5 Hz, 1 H), 2.72 (ddd, 14.4, 10.0, 1.5 Hz, 1 H), 2.07-1.93 (m, 2 H), 1.85-1.75 (m, 4 H), 1.49-1.45 (m, 1 H). ¹³C NMR (101 MHz, CDCl₃) δ ppm 144.2, 140.7, 129.4, 126.9, 126.0, 124.5, 73.9, 36.5, 35.7, 27.7, 27.5.

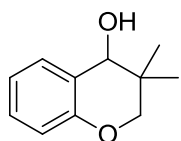
Preparation of *rac*-2,2-dimethylchroman-4-ol³⁹



According to **GP1**, 2,2-dimethylchroman-4-one (257 mg, 1.46 mmol) was reacted with NaBH₄ (110 mg, 2.92 mmol) giving a pale yellow liquid (238.2 mg, 1.34 mmol, Yield 92%). ¹H NMR (400 MHz, CDCl₃) δ ppm 7.44 (d, J = 9.0 Hz, 1H), 7.17 (dt, J = 7.5, 1.5 Hz, 1 H), 6.91 (dt, J = 7.0, 1.0 Hz, 1 H), 6.78 (d, J = 9.0 Hz, 1 H), 4.83 (dd, J = 8.5, 6.0 Hz, 1 H), 2.15 (dd, J = 19.5, 7.0 Hz, 1 H), 1.84 (dd, J =

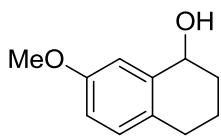
22.5, 5 Hz, 1 H), 1.43 (s, 3 H), 1.30 (s, 3 H). **¹³C NMR** (101 MHz, CDCl₃) δ ppm 153.1, 129.2, 127.5, 124.2, 120.2, 117.1, 75.2, 63.6, 42.6, 28.9, 25.9.

Preparation of *rac*-3,3-dimethylchroman-4-ol



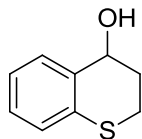
According to **GP1**, 3,3-dimethylchroman-4-one (214 mg, 1.21 mmol) was reacted with NaBH₄ (104 mg, 2.76 mmol), giving a white solid (163 mg, 0.92 mmol, Yield 76%). **mp range** = 66-67 °C **¹H NMR** (400 MHz, CDCl₃) δ ppm 7.28 (dd, *J* = 7.5, 1.0 Hz, 1 H), 7.17 (t, *J* = 7.5 Hz, 1 H), 6.90 (dt, 7.0, 1.0 Hz, 1 H), 6.80 (dd, 8.0, 0.5 Hz, 1 H), 4.18 (s, 1 H), 3.92 (d, *J* = 10.5 Hz, 1 H), 3.71 (dd, *J* = 10.5, 1.0 Hz, 1 H), 2.08 (br, 1 H), 1.00 (s, 3 H), 0.92 (s, 3 H). **¹³C NMR** (101 MHz, CDCl₃) δ ppm 153.4, 129.7, 129.3, 123.9, 120.6, 116.3, 72.1, 71.5, 33.2, 22.4, 19.3. **HRMS** (ESI) (M⁺) Calculated for (C₁₁H₁₄O₂⁺): 178.0988 Observed: 178.0994. **IR** (neat, cm⁻¹): 3195 (br), 2965, 1610, 1584, 1487, 1226, 1038, 1019, 753.

Preparation of *rac*-7-methoxytetralol⁴⁰



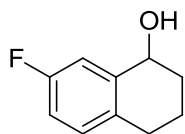
According to **GP1**, 7-methoxytetralone (300 mg, 1.70 mmol) was reacted with NaBH₄ (129 mg, 3.4 mmol), to yield a clear colorless oil (303 mg, 1.70 mmol, Yield >99%). **¹H NMR** (400 MHz, CDCl₃) δ ppm 7.00 (d, *J* = 8.0 Hz, 1 H) 6.97 (d, *J* = 3.0 Hz, 1 H), 6.76 (dd, *J* = 8.0, 2.5 Hz, 1 H), 4.71 (*J* = 4.5 Hz, 1 H), 3.78 (s, 3 H), 2.77- 2.70 (m, 1 H), 2.67-2.60 (m, 1 H), 2.04- 1.80 (m, 3 H), 1.77-1.70 (m, 1 H). **¹³C NMR** (101 MHz, CDCl₃) δ ppm 157.8, 139.7, 129.8, 129.0, 114.2, 112.5, 68.4, 55.2, 32.3, 28.3, 19.1.

Preparation of *rac*-thiochroman-4-ol⁴¹



According to **GP1**, thiochroman-4-one (500 mg, 3.0 mmol), was treated with NaBH₄ (115 mg, 3.0 mmol) to yield a pale yellow solid (498 mg, 3.0 mmol, Yield 98%). ¹H NMR (400 MHz, CDCl₃) δ ppm 7.31 (d, *J* = 9.0 Hz, 1 H), 7.14-7.12 (m, 2 H), 7.08-7.04 (m, 1 H), 4.79 (br, 1 H), 3.14 (dt, *J* = 27.0, 12.5, 3.0 Hz 1 H), 2.88-2.83 (m, 1 H), 2.37-2.31 (m, 1 H), 2.08-2.00 (m, 1 H), 1.92 (br, 1 H). ¹³C NMR (101 MHz, CDCl₃) δ ppm 134.5, 133.1, 130.3, 128.4, 126.7, 124.2, 66.4, 29.9, 21.4.

Preparation of *rac*-7-Fluorotetralol



According to **GP1**, 7-fluorotetralone (500 mg, 3.05 mmol) was reacted with NaBH₄ (230 mg, 6.09 mmol), to yield a clear colorless oil (506 mg, 3.05 mmol, Yield >99%). ¹H NMR (400 MHz, CDCl₃) δ ppm 7.14 (d, *J* = 9.5, 1 H) 7.04 (dd, *J* = 14.0, 5.5 Hz, 1 H), 6.88 (dt, *J* = 8.4, 2.8 Hz, 1 H), 4.72 (t, *J* = 4.5 Hz), 2.76-2.73 (m, 1 H), 2.71-2.67 (m, 1 H), 2.02-1.75 (m, 5 H). ¹³C NMR (101 MHz, CDCl₃) δ ppm 162.4-160.0 (d, *J* = 241.3 Hz), 140.7, 132.4, 114.6, 114.4, 68.1, 32.2, 28.4, 19.1. HRMS (ESI) (M⁺) Calculated for (C₁₀H₁₁FO⁺): 166.0788 Observed: 166.0789 IR (neat, cm⁻¹): 3316 (br), 2937, 1677, 1613, 1492, 1247, 1222, 873, 806

General procedure for the gas chromatographic method for determining conversion from the silylation based kinetic resolution of secondary alcohols.

To an oven dried 1 dram vial with activated 4 Å molecular sieves (20-25 mg) was fitted an oven dried Teflon coated stir bar. To the vial was added 1-indanol (30 mg, 0.22 mmol), 4-bromobiphenyl (10.5mg, 0.45 mmol) and catalyst (25.5 mg, 0.125 mmol) then

quickly sealed under dry N₂. The vial was then charged with 1.6 mL THF to generate a 0.3 M solution and the solution was treated with base (0.3 mmol) and cooled to -78 °C in a crycool apparatus for about 30 minutes. The cooled solution was then treated with a 1.19 M solution of silyl chloride in the reaction solvent and left to react for the specified amount of time at -78 °C. The reaction was then quenched with 250 µL MeOH and poured into a 4-dram vial containing 1.5 mL sat. aqueous NH₄Cl and extracted with diethyl ether (3 x 5 mL), the ethereal layer was then dried over sodium sulfate. After filtration and removal of solvent, the residue was analyzed by gas chromatography and conversion was calculated based on the area of the 4-bromobiphenyl to the unreacted starting material. Then the residue was purified by silica gel chromatography (1:1 hexanes:CH₂Cl₂ followed by 2% MeOH in CH₂Cl₂) and the unreacted alcohol was then analyzed by HPLC with a chiral stationary phase.

General procedure for the silylation based kinetic resolution of secondary alcohols and desilylation of the isolated products.

To an oven dried 1 dram vial with activated 4 Å molecular sieves (20-25 mg) was fitted an oven dried Teflon coated stir bar. To the vial was added the racemic substrate (0.5 mmol) and catalyst (25.5 mg, 0.125 mmol) then quickly sealed under dry N₂. The vial was then charged with 1.6 mL THF to generate a 0.3 M solution and the solution was treated with base (0.3 mmol) and cooled to -78 °C in a crycool apparatus for about 30 minutes. The cooled solution was then treated with a 0.357 M solution of silyl chloride in the reaction solvent and left to react for the specified amount of time at -78 °C. The reaction was then quenched with 250 µL MeOH and poured into a 4-dram vial containing

1.5 mL sat. aqueous NH_4Cl and extracted with diethyl ether (3 x 5 mL), the ethereal layer was then dried over sodium sulfate. After filtration and removal of solvent, the residue was purified by silica gel chromatography (1:1 hexanes: CH_2Cl_2 followed by 2% MeOH in CH_2Cl_2). The unreacted alcohol was then analyzed by HPLC with a chiral stationary phase.

The purified silyl ether was dissolved in 3 mL THF and fitted with a Teflon coated stir bar. The solution was treated with 1.6 mL TBAF (1 M in THF) and stirred at ambient temperature for 10 h. The reaction was quenched with brine and extracted with diethyl ether (3 x 3 mL) and dried over silica gel. After filtration and removal of solvent, the crude was purified by silica gel chromatography (CH_2Cl_2 to 2% MeOH in CH_2Cl_2).

The absolute stereochemistry for **Table 2.10**, Entry 7b was ascertained by comparing the observed specific rotation to the listed literature reference. The absolute configurations of the remaining enantioenriched alcohols were assigned by comparison to literature references. By using the same separation technique (same HPLC chiral column and separation conditions) the configuration was assigned by comparison with the known retention times and order of elution

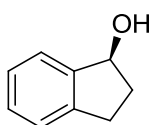


Table 2.10, Entry 1: Recovered starting material: 30 mg, 44% ^1H NMR (400 MHz, CDCl_3) δ ppm 7.41 (d, $J = 4$ Hz, 1 H), 7.27-7.23 (m, 3 H), 5.23

(t, 6.0 Hz, 1 H), 3.05-3.02 (m, 1 H), 2.86-2.80 (m, 1 H), 2.51-2.46 (m, 1 H), 1.97-1.91 (m, 2 H). ^{13}C NMR (101 MHz, CDCl_3) δ ppm 144.9, 143.3, 128.3, 126.7, 124.9, 124.1, 76.4, 35.9, 29.7.

The HPLC separation conditions and subsequent stereochemical assignment was determined from the literature:⁴² Chiralpak OD-H column, 4% *i*PrOH in hexane, flow rate: 0.5 mL/min, 25 °C; t_R 23.1 min for (*S*)-enantiomer (major) and t_R 27.0 min for (*R*)-enantiomer (minor). (er = 92:8)

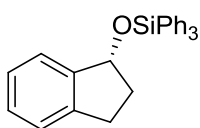
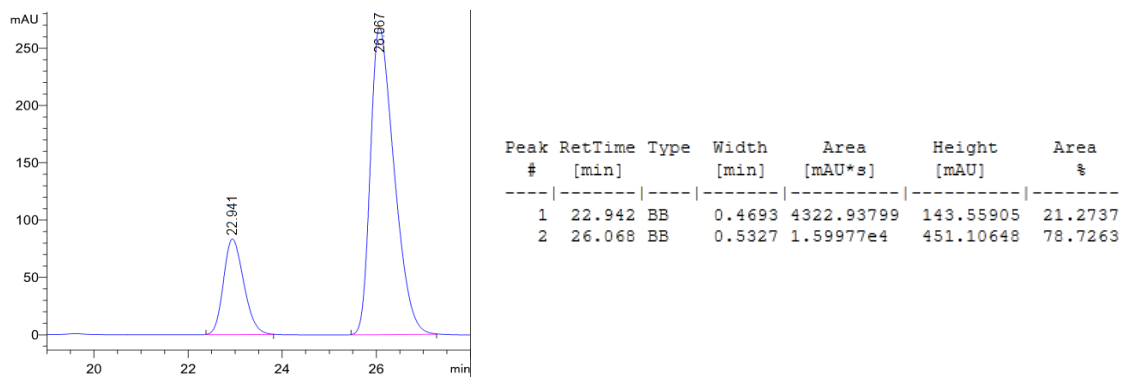


Table 2.10, Entry 1: Major product: 99 mg, 50%, white solid. **mp** range = 63-64 °C. ^1H NMR (400 MHz, CDCl_3) δ ppm 7.60 (d, J = 12.0 Hz, 6 H), 7.34-7.25 (m, 9 H), 7.08-7.02 (m, 4 H), 5.36 (t, 6.0 Hz, 1 H), 2.92-2.85 (m, 1 H), 2.61-2.53 (m, 1 H), 2.19-2.11 (m, 1 H), 2.01-1.92 (m, 1 H). ^{13}C NMR (101 MHz, CDCl_3) δ ppm 145.0, 142.8, 135.5, 134.6, 130.0, 127.8, 127.7, 126.3, 124.6, 124.4, 77.4, 36.2, 29.7. **Optical Rotation** $[\alpha]^{25}_D = + 27.2$ (c = 0.98, CHCl_3) **HRMS** (ESI) (M^+) Calculated for ($\text{C}_{27}\text{H}_{24}\text{SiO}^+$): 392.1591 Observed: 392.1587. **IR** (neat, cm^{-1}): 3068, 2933, 1960, 1890, 1824, 1589, 1477, 1427, 1113, 1070, 985, 737, 707.

HPLC data is of the desilylated and purified alcohol product using the same HPLC conditions as the recovered starting material. (er = 21:79)



Kinetic Resolution Data for Table 2.10, Entry 1

#	er _{SM}	er _{Pr} ^a	C %	s	SAVG
1	87:13	89:11	56.4	7.6	8.6
2	92:8	79:21	59.6	9.5	
3 ^b	81:19	21:79	52.1	6.8	

a) er_{Pr} % is of the deprotected and purified product b) Run 3 was done on a 1.5 g scale

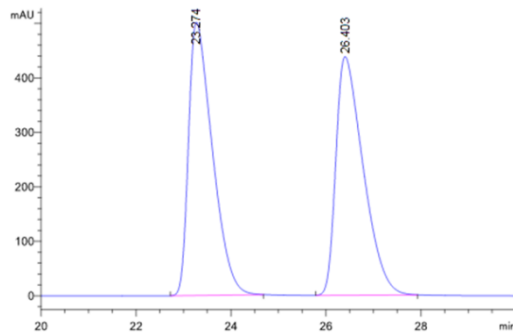
Procedure for the large scale silylation based kinetic resolution of 1-indanol (Table 2.10, Entry 1).

To an oven dried 250 mL round bottom flask with activated 4 Å molecular sieves (200-250 mg) was fitted an oven dried Teflon coated stir bar. To the flask was added 1-indanol (1.5 g, 11.2 mmol) and catalyst (571 mg, 2.79 mmol) then quickly sealed under dry N₂. The vial was then charged with 37 mL THF and the solution was treated with

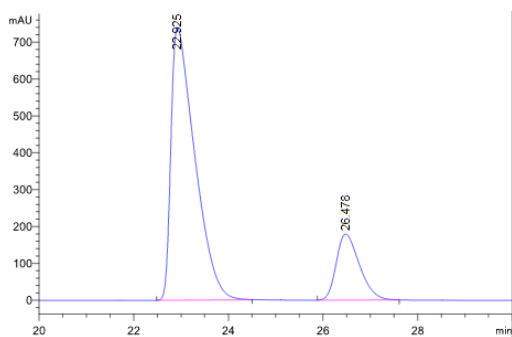
N,N-diisopropyl-3-pentylamine (1.2 mL, 6.71 mmol) and cooled to -78 °C in a crycool apparatus for about 45 minutes. The cooled solution was then treated with a 0.357 M solution of Ph_3SiCl in THF (18.8 mL, 6.7 mmol) and left to react for 2 h at -78 °C. The reaction was then quenched with 5.5 mL MeOH and treated with 23 mL sat. aqueous NH_4Cl and extracted with diethyl ether (3 x 20 mL), the ethereal layer was then dried over silica gel. After filtration and removal of solvent, the residue was purified by silica gel chromatography (1:1 hexanes: CH_2Cl_2 followed by 2% MeOH in CH_2Cl_2) yielding a pale yellow oil (2.26g, 52%) and unreacted starting material as a white solid (0.677 g, 45%). The unreacted alcohol was then analyzed by HPLC with a chiral stationary phase.

In a 4-dram vial, purified silyl ether (76.0 mg, 0.2 mmol) was dissolved in 3 mL THF and fitted with a Teflon coated stir bar. The solution was treated with 1.6 mL TBAF (1 M in THF) and stirred at ambient temperature for 10 h. The reaction was quenched with brine and extracted with diethyl ether (3 x 3 mL) and dried over silica gel. After filtration and removal of solvent, the crude was purified by silica gel chromatography (CH_2Cl_2 to 2% MeOH in CH_2Cl_2) to yield a white solid (11.1 mg, 43%).

The HPLC separation conditions and subsequent stereochemical assignment for recovered starting material of the gram scale reaction of 1-indanol was determined from the literature:⁸ Chiralpak OD-H column, 4% *i*PrOH in hexane, flow rate: 0.5 mL/min, 25 °C; t_R 22.9 min for (*S*)-enantiomer (major) and t_R 26.5 min for (*R*)-enantiomer (minor). (er = 81:19)

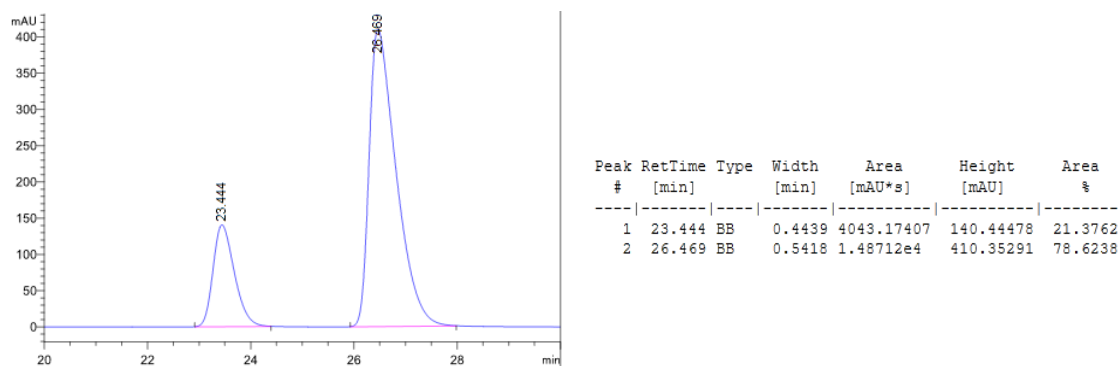


Peak #	RetTime [min]	Type	Width [min]	Area [mAU*s]	Height [mAU]	Area %
1	23.274	BB	0.5267	1.74915e4	501.78116	49.9410
2	26.403	BB	0.6058	1.75329e4	438.16910	50.0590



Peak #	RetTime [min]	Type	Width [min]	Area [mAU*s]	Height [mAU]	Area %
1	22.925	BB	0.5208	2.58431e4	739.41748	80.8848
2	26.478	BB	0.5234	6107.41162	179.31850	19.1152

HPLC data is of the desilylated and purified alcohol product from the gram scale reaction of 1-indanol (**Table 2.10**, entry 1) using the same HPLC conditions as the recovered starting material. (er = 21:79)



er _{SM} %	er _{Pr} % ^a	C %	s
81:19	21:79	52.1	6.8

a) er_{Pr} % is of the deprotected and purified product

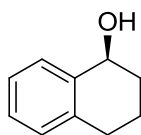
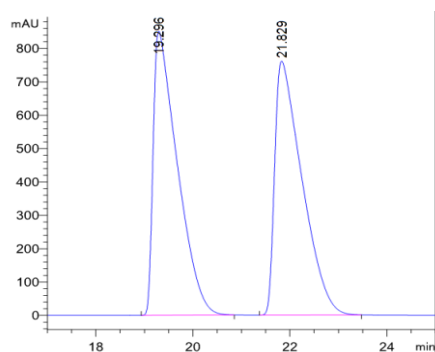


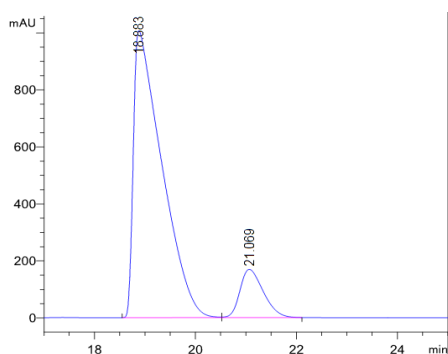
Table 2.10, Entry 2: Recovered starting material: 35 mg, 48% ¹H NMR

(400 MHz, CDCl₃) δ ppm 7.44-7.23 (m, 1 H), 7.21-7.18 (m, 2 H), 7.12-7.09 (m, 1 H), 4.78 (t, 5.0 Hz, 1 H), 2.87-2.70 (m, 2 H), 2.02-1.74 (m, 5 H). ¹³C NMR (101 MHz, CDCl₃) δ ppm 138.7, 128.9, 128.6, 127.5, 126.1, 68.1, 32.2, 29.1, 19.8.

The HPLC separation conditions and subsequent stereochemical assignment was determined from the literature:⁴¹ Chiralpak OD-H column, 4% *i*PrOH in hexane, flow rate: 0.5 mL/min, 25 °C; *t*_R 18.8 min for (*S*)-enantiomer (major) and *t*_R 21.0 min for (*R*)-enantiomer (minor). (er = 88:12)



Peak #	RetTime [min]	Type	Width [min]	Area [mAU*s]	Height [mAU]	Area %
1	19.296	BB	0.4952	2.94094e4	851.04730	49.7115
2	21.829	BB	0.5680	2.97507e4	761.12689	50.2885



Peak #	RetTime [min]	Type	Width [min]	Area [mAU*s]	Height [mAU]	Area %
1	18.883	BB	0.5621	3.93688e4	1006.97498	87.8345
2	21.069	BB	0.4996	5452.78271	169.38046	12.1655

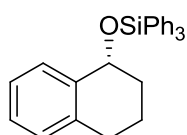
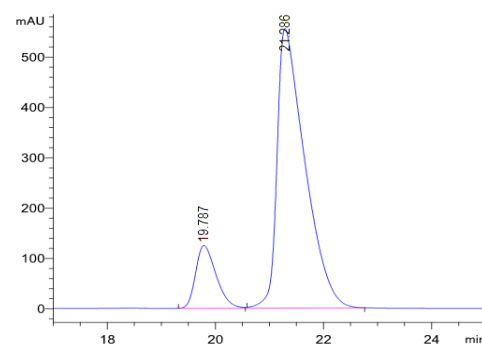


Table 2.10, Entry 2: Major product: 106 mg, 52%, white solid. **mp**

range = 74-75 °C. **¹H NMR** (400 MHz, CDCl₃) δ ppm 7.72 (d, *J* = 4.0

Hz, 6 H), 7.50-7.41 (m, 9 H), 7.34 (d, *J* = 8.0 Hz, 1 H), 7.22-7.11 (m, 3 H), 5.04 (t, 6.0 Hz, 1 H), 2.93-2.86 (m, 1 H), 2.77-2.69 (m, 1H), 2.15-2.09 (m, 1 H), 2.01-1.88 (m, 2 H), 1.76- 1.70 (m, 1 H). **¹³C NMR** (101 MHz, CDCl₃) δ ppm 138.9, 137.0, 135.5, 134.8, 129.9, 128.7, 128.6, 127.7, 127.0, 125.6, 70.2, 32.5, 29.0, 19.1. **Optical Rotation** [α]²⁵_D = + 15.3 (*c* = 1.00, CHCl₃) **HRMS** (ESI) (M⁺) Calculated for (C₂₈H₂₆SiO⁺): 406.1747 Observed: 406.1747. **IR** (neat, cm⁻¹): 3066, 2998, 1963, 1892, 1827, 1775, 1588, 1427, 1350, 1113, 1062, 1010, 984, 736, 697.

HPLC data is of the desilylated and purified alcohol product using the same HPLC conditions as the recovered starting material. (er = 14:86)



Peak #	RetTime [min]	Type	Width [min]	Area [mAU*s]	Height [mAU]	Area %
1	19.787	BB	0.4023	3279.99658	124.95020	14.1871
2	21.286	BB	0.5235	1.98396e4	555.75330	85.8129

Kinetic Resolution Data for Table 2.10, Entry 2

#	er _{SM} %	er _{Pr} % ^a	C %	s	SAVG
1	88:12	85:15	51.7	13	14
2	89:11	86:14	52.2	14	

a) er_{Pr} % is of the deprotected and purified product

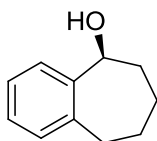


Table 2.10, Entry 3: Recovered starting material: 33 mg, 40%. ¹H NMR

(400 MHz, CDCl₃) δ ppm 7.44 (d, *J* = 4 Hz, 1 H), 7.23-7.13 (m, 2 H), 7.10 (d, *J* = 4.0 Hz, 1 H), 4.94 (d, *J* = 4.0 Hz, 1 H), 2.92 (dd, *J* = 14.0, 5.5 Hz, 1 H), 2.72 (ddd, 14.4, 10.0, 1.5 Hz, 1 H), 2.07-1.93 (m, 2 H), 1.85-1.75 (m, 4 H), 1.49-1.45 (m, 1 H). ¹³C NMR (101 MHz, CDCl₃) δ ppm 144.2, 140.7, 129.4, 126.9, 126.0, 124.5, 73.9, 36.5, 35.7, 27.7, 27.5.

The HPLC separation conditions and subsequent stereochemical assignment was determined from the literature:⁴³ Chiralpak OD-H column, 4% *i*PrOH in hexane, flow

rate: 0.5 mL/min, 25 °C; t_R 21.1 min for (*R*)-enantiomer (minor) and t_R 24.3 min for (*S*)-enantiomer (major). (er = 19:81)

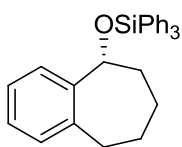


Table 2.10, Entry 3: Major product: 114 mg, 54%, clear colorless oil.

^1H NMR (400 MHz, CDCl_3) δ ppm 7.59 (d, J = 4.0 Hz, 6 H), 7.45-7.40 (m, 10 H), 7.14-7.05 (m, 3 H), 5.05 (t, 4.5 Hz, 1 H), 3.01 (ur, 1 H), 2.59

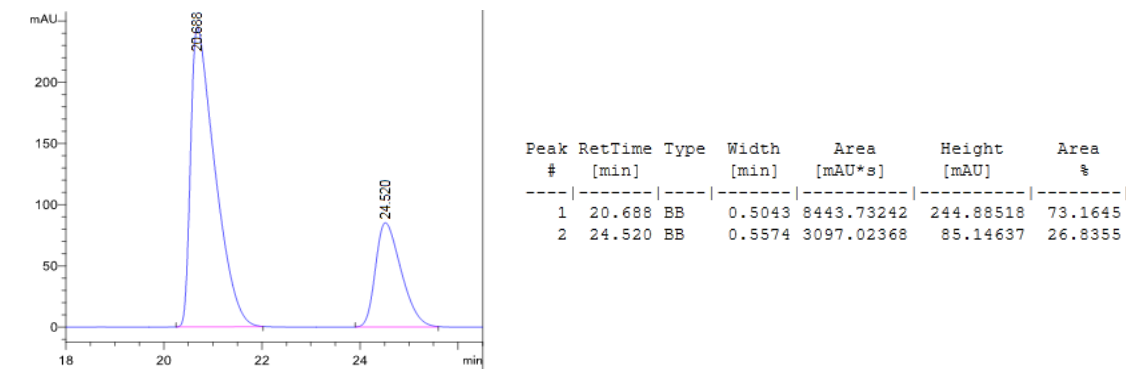
(dt, J = 11.0, 1.5 Hz, 1 H), 2.00 (br, 1 H), 1.78 (d, J = 5.0 Hz, 2 H), 1.64-1.52 (m, 3 H).

^{13}C NMR (101 MHz, CDCl_3) δ ppm 144.0, 135.4, 135.1, 134.6, 129.8, 129.2, 127.7, 126.7, 125.7, 75.8, 36.9, 35.7, 27.7, 27.2. **Optical Rotation** $[\alpha]^{25}_D$ = + 17.5 (c = 0.88,

CHCl_3) **HRMS** (ESI) (M^+) Calculated for $(\text{C}_{29}\text{H}_{28}\text{SiO}^+)$: 420.1904 Observed: 420.1895.

IR (neat, cm^{-1}): 3068, 2924, 1959, 1890, 1824, 1589, 1444, 1427, 1113, 1057, 1010, 871, 739, 696.

HPLC data is of the desilylated and purified product using the same HPLC conditions as the recovered starting material. (er = 73:27)



Kinetic Resolution Data for Table 2.10, Entry 3

#	er _{SM} %	er _{Pr} % ^a	C %	s	S _{AVG}
1	81:19	73.2:26.9	57.1	4.9	4.9
2	82:18	72.6:27.5	58.8	4.9	

a) er_{Pr} % is of the deprotected and purified product

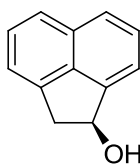


Table 2.10, Entry 4 :Recovered starting material: 37 mg, 44% ¹H NMR

(400 MHz, CDCl₃) δ ppm 7.76 (d, 6.5 Hz), 7.66 (d, 7.5 Hz, 1 H), 7.51-7.48 (m, 3 H), 7.31(d, *J* = 6.5 Hz, 1 H), 5.73 (d, *J* = 6.0 Hz, 1 H), 3.81 (dd, *J* =

17.5, 6.5 Hz, 1 H) 3.25 (d, *J* = 15.0 Hz), 2.06 (br, 1 H). ¹³C NMR (101 MHz, CDCl₃) δ ppm 145.6, 141.5, 137.1, 131.1, 128.2, 128.0, 124.9, 122.7, 120.3, 119.8, 74.3, 41.8.

The HPLC separation conditions and subsequent stereochemical assignment was determined from the literature:⁴⁴ Chiralpak OD-H column, 3% *i*PrOH in hexane, flow rate: 1.5 mL/min, 25 °C; *t*_R 20.4 min for (*S*)-enantiomer (major) and *t*_R 24.9 min for (*R*)-enantiomer (minor). (er = 75:25)

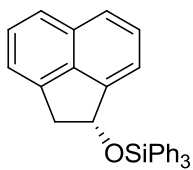
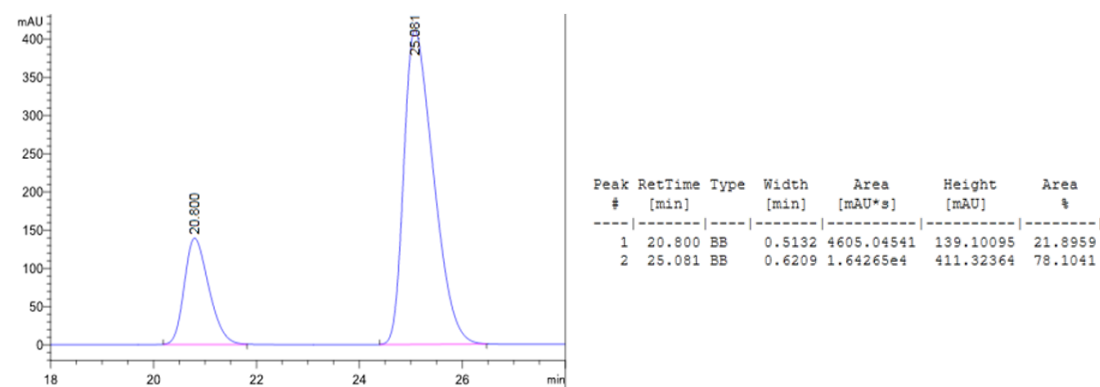


Table 2.10, Entry 4: Major product: 121 mg, 56%, white solid. **mp** range = 101-102 °C. **¹H NMR** (400 MHz, CDCl₃) δ ppm 7.65 (d, *J* = 6.0 Hz, 6 H), 7.71 (d, *J* = 8.0 Hz, 1 H), 7.63 (d, *J* = 8.0 Hz, 1 H), 7.51-7.42 (m, 11 H), 7.25-7.18 (m, 2 H), 6.01 (dd, *J* = 7.0, 3.0 Hz, 1 H), 3.60 (dd, *J* = 17.0, 7.0 Hz), 3.63 (d, 17.5 Hz). **¹³C NMR** (101 MHz, CDCl₃) δ ppm 145.6, 141.6, 137.2, 135.5, 134.3, 131.0, 130.1, 127.9, 124.3, 122.5, 120.5, 119.2, 75.3, 41.9. **Optical Rotation** [α]_D²⁵ = + 8.5 (*c* = .90, CHCl₃) **HRMS** (ESI) (M⁺) Calculated for (C₃₀H₂₄SiO⁺): 428.1591 Observed: 428.1590. **IR** (neat, cm⁻¹): 3068, 2915, 1959, 1891, 1823, 1567, 1483, 1427, 1114, 1062, 931, 781, 738, 696.

HPLC data is of the desilylated and purified product using the same HPLC conditions as the recovered starting material. (er = 22:78)



Kinetic Resolution Data for Table 2.10, Entry 4

#	er _{SM} %	er _{Pr} % ^a	C %	s	s _{AVG}
1	76:25	78:21	47.6	5.1	5.1
2	80:20	74:26	56.0	5.0	

a) er_{Pr} % is of the deprotected and purified product

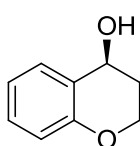


Table 2.10, Entry 5: Recovered starting material: 34 mg, 46 % ¹H NMR (400 MHz, CDCl₃) δ ppm 7.30 (d, *J* = 8.0 Hz, 1 H), 7.20 (dt, *J* = 5.0, 1.5 Hz, 1 H), 6.92 (dt, *J* = 7.0, 1.0 Hz, 1 H), 6.84 (d, *J* = 9.5 Hz, 1 H), 4.76, (t, *J* = 3.5 Hz, 1 H) 4.26-4.23 (m, 2 H), 2.11-1.99 (m, 3 H). ¹³C NMR (101 MHz, CDCl₃) δ ppm 154.5, 129.6, 124.2, 120.5, 117.0, 63.1, 61.8, 30.7.

The HPLC separation conditions and subsequent stereochemical assignment was determined from the literature:⁴⁵ Chiralpak OD-H column, 2% *i*PrOH in hexane, flow rate: 1.3 mL/min, 25 °C; *t*_R 20.1 min for (*S*)-enantiomer (major) and *t*_R 26.1 min for (*R*)-enantiomer (minor). (er = 95:5)

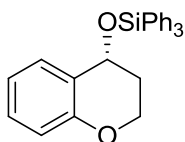
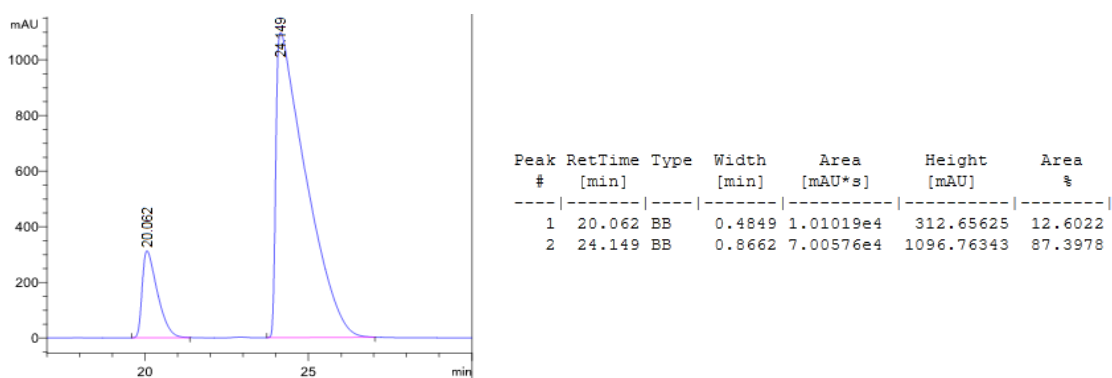


Table 2.10, Entry 5: Major product: 102 mg, 50%, white solid. **mp** range = 108-109 °C. ¹H NMR (400 MHz, CDCl₃) δ ppm 7.55 (d, *J* = 8.0 Hz, 6 H), 7.54-7.27 (m, 9 H), 7.04 (dt, *J* = 8.0, 1.5 Hz 1H), 6.88 (d, *J* = 6.0 Hz, 1 H), 6.71-6.65 (m, 2 H), 4.86 (t, *J* = 4.0 Hz. 1 H), 4.34 (dt, 20.0, 4.0, 3.0 Hz, 1 H), 4.10-4.08 (m, 1 H), 1.90-1.84 (m, 2 H).). ¹³C NMR (101 MHz, CDCl₃) δ ppm 154.4,

135.5, 134.3, 130.0, 129.9, 129.2, 127.9, 124.1, 119.9, 116.6, 64.9, 62.1, 31.4. **Optical Rotation** $[\alpha]_D^{25} = + 43.8$ ($c = 1.0$, CHCl_3) **HRMS** (ESI) (M^+) Calculated for ($\text{C}_{27}\text{H}_{24}\text{O}_2\text{Si}^+$): 408.1540 Observed: 408.1535. **IR** (neat, cm^{-1}): 3067, 2953, 1906, 1825, 1582, 1488, 1428, 1114, 1007, 931, 739, 707.

HPLC data is of the desilylated and purified product using the same HPLC conditions as the recovered starting material. (er = 13:87)



Kinetic Resolution Data for Table 2.10, Entry 5

#	er _{SM} %	er _{Pr} % ^a	C %	s	S _{AVG}
1	95:5	87:13	54.6	21	22
2	94:6	89:11	53.1	22	

a) er_{Pr} % is of the deprotected and purified product

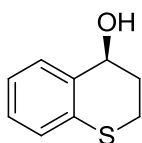


Table 2, Entry 6: Recovered starting material: 36 mg, 43 % ¹H NMR (400 MHz, CDCl_3) δ ppm 7.31 (d, $J = 9.0$ Hz, 1 H), 7.14-7.12 (m, 2 H), 7.08-7.04 (m, 1 H), 4.79 (br, 1 H), 3.14 (dt, $J = 27.0, 12.5, 3.0$ Hz 1 H), 2.88-2.83 (m, 1 H), 2.37-

2.31 (m, 1 H), 2.08-2.00 (m, 1 H), 1.92 (br, 1 H). ^{13}C NMR (101 MHz, CDCl_3) δ ppm 134.5, 133.1, 130.3, 128.4, 126.7, 124.2, 66.4, 29.9, 21.4.

The HPLC separation conditions and subsequent stereochemical assignment was determined from the literature.⁴² Chiralpak OD-H column, 5% *i*PrOH in hexane, flow rate: 0.6 mL/min, 25 °C; t_R 22.6 min for (*S*)-enantiomer (major) and t_R 29.1 min for (*R*)-enantiomer (minor). (er = 94:6)

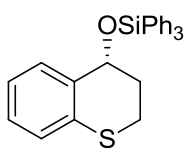
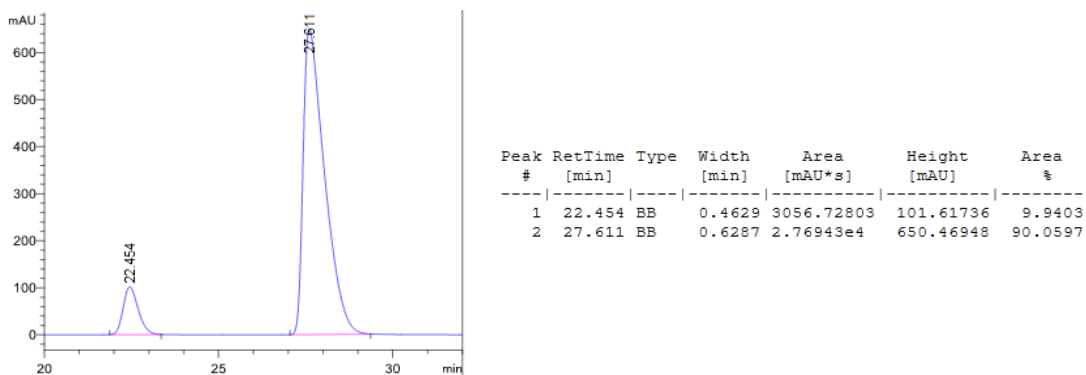


Table 2.10, Entry 6: Major product: 97 mg, 46%, faint yellow solid. **mp** range = 105-106 °C. ^1H NMR (400 MHz, CDCl_3) δ ppm 7.64 (d, J = 6.5 Hz, 6 H), 7.48-7.37 (m, 9 H), 7.13-7.12 (m, 2 H), 6.99 (d, J = 7.0 Hz, 1 H), 6.93-6.89 (m, 1 H), 4.96 (dd, J = 8.0, 3.0 Hz, 1 H), 3.53 (dt, J = 27.0, 12.0, 3.0 Hz, 1 H), 2.86-2.81 (m, 1 H), 2.26-2.21 (m, 1 H), 1.98-1.95 (m, 1 H). ^{13}C NMR (101 MHz, CDCl_3) δ ppm 135.4, 134.7, 134.3, 133.2, 130.1, 130.0, 127.9, 127.8, 126.4, 123.6, 68.3, 30.6, 21.8. **Optical Rotation** $[\alpha]^{25}_D$ = +70.0 (c = 0.91, CHCl_3) **HRMS** (ESI) (M^+) Calculated for ($\text{C}_{27}\text{H}_{24}\text{OSSi}^+$): 424.1312 Observed: 424.1314. **IR** (neat, cm^{-1}): 3067, 2916, 1961, 1891, 1827, 1588, 1473, 1427, 1114, 1040, 971, 741, 696.

HPLC data is of the desilylated and purified product using the same HPLC conditions as the recovered starting material. (er = 10:90)



Kinetic Resolution Data for Table 2.10, Entry 6

#	er _{SM} %	er _{Pr} % ^a	C %	s	SAVG
1	94:6	90:10	52.1	26	25
2	93:7	90:10	51.5	24	

a) er_{Pr}% is of the deprotected and purified product

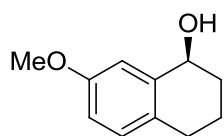


Table 2.10, Entry 7a: Recovered starting material: 40 mg, 45%. ¹H

NMR (400 MHz, CDCl₃) δ ppm 7.00 (d, *J* = 8.0 Hz, 1 H) 6.97 (d, *J* = 3.0 Hz, 1 H), 6.76 (dd, *J* = 8.0, 2.5 Hz, 1 H), 4.71 (*J* = 4.5 Hz, 1 H), 3.78 (s, 3 H), 2.77-2.70 (m, 1 H), 2.67-2.60 (m, 1 H), 2.04- 1.80 (m, 3 H), 1.77-1.70 (m, 1 H). ¹³C **NMR** (101 MHz, CDCl₃) δ ppm 157.8, 139.7, 129.8, 129.0, 114.2, 112.5, 68.4, 55.2, 32.3, 28.3, 19.1.

The HPLC separation conditions and subsequent stereochemical assignment was determined from the literature:^{40, 42} Chiralpak OD-H column, 4% *i*PrOH in hexane, flow

rate: 0.5 mL/min, 25 °C; t_R 50.1 min for (*S*)-enantiomer (major) and t_R 56.5 min for (*R*)-enantiomer (minor). (er = 93:7)

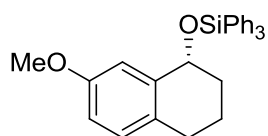


Table 2.10, Entry 7a: Major product: 120 mg, 55%, white solid.

mp range = 69-70 °C. **¹H NMR** (400 MHz, CDCl₃) δ ppm 7.68

(d, J = 8.0, 6 H), 7.44-7.34 (m, 9 H), 6.94 (d, J = 8.0, 1 H), 6.80 (d, J = 2 Hz, 1 H), 6.71

(dd, J = 8.0, 2.5 Hz, 2 H) 4.95 (t, J = 4.5 Hz, 1 H), 3.54 (s, 3 H), 2.75-2.69 (m, 1 H),

2.62-2.56 (m, 1 H), 2.03-2.00 (m, 1 H), 1.91-1.86 (m, 2 H), 1.64-1.61 (m, 1 H). **¹³C NMR**

(101 MHz, CDCl₃) δ ppm 157.5 139.9, 135.5, 134.7, 129.9, 129.6, 129.0, 127.8, 114.6,

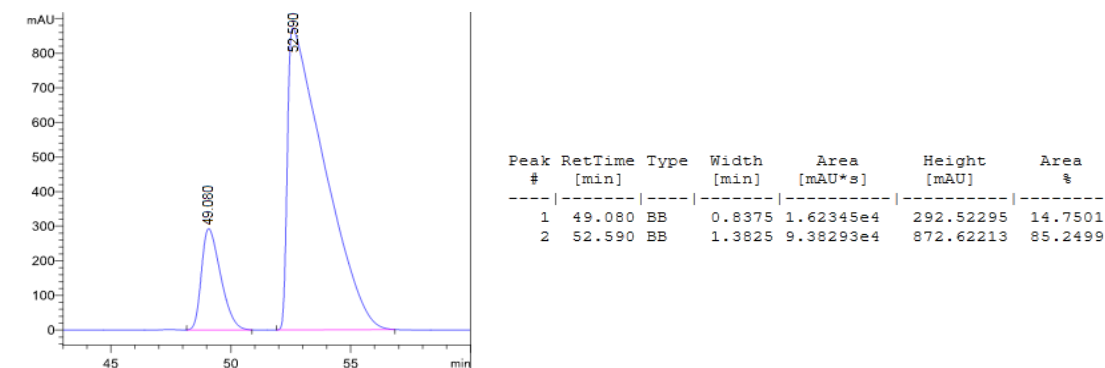
111.9, 70.5, 55.0, 32.6, 28.2, 19.6. **Optical Rotation** $[\alpha]^{25}_D$ = + 11.7 (c = 1.05, CHCl₃).

HRMS (ESI) (M^+) Calculated for (C₂₉H₂₈O₂Si⁺): 436.1853 Observed: 436.1866. **IR**

(neat, cm⁻¹): 3065, 2949, 1960, 1907, 1826, 1612, 1503, 1427, 1252, 1113, 1062, 991,

825, 743, 697.

HPLC data is of the desilylated and purified product using the same HPLC conditions as the recovered starting material. (er = 15:85)



Kinetic Resolution Data for Table 2.10, Entry 7a

#	er _{SM} %	er _{Pr} % ^a	C %	s	s _{AVG}
1	93:7	85:15	54.9	16	16
2	92:8	86:14	53.8	15	

a) er_{Pr}% is of the deprotected and purified product

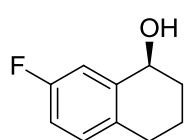


Table 2.10, Entry 7b: Recovered starting material: 35 mg, 42 %. ¹H NMR (400 MHz, CDCl₃) δ ppm 7.14 (d, *J* = 9.5, 1 H) 7.04 (dd, *J* = 14.0, 5.5 Hz, 1 H), 6.88 (dt, *J* = 8.4, 2.8 Hz, 1 H), 4.72 (t, *J* = 4.5 Hz), 2.76-2.73 (m, 1 H), 2.71-2.67 (m, 1 H), 2.02-1.75 (m, 5 H). ¹³C NMR (101 MHz, CDCl₃) δ ppm 162.4-160.0 (d, *J* = 241.3 Hz), 140.7, 132.4, 114.6, 114.4, 68.1, 32.2, 28.4, 19.1. **Optical Rotation** [α]²⁵_D = + 28.0 (*c* = 1.05, CHCl₃), Lit:¹² [α]²⁴_D = -36.9 (*c* = 1.01, CHCl₃), 98% ee (*R*)-7-fluoro-1-tetralol.⁴⁶ **HRMS** (ESI) (*M*⁺) Calculated for (C₁₀H₁₁FO⁺): 166.0788 Observed: 166.0789 **IR** (neat, cm⁻¹): 3316 (br), 2937, 1677, 1613, 1492, 1247, 1222, 873, 806

The stereochemical assignment was determined relative to the published optical rotation value.⁴⁶ Chiralpak AD-H column, 4% *i*PrOH in hexane, flow rate: 0.5 mL/min, 25 °C; *t*_R 23.9 min for (*S*)-enantiomer (major) and *t*_R 27.1 min for (*R*)-enantiomer (minor). (er = 90:10)

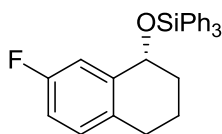
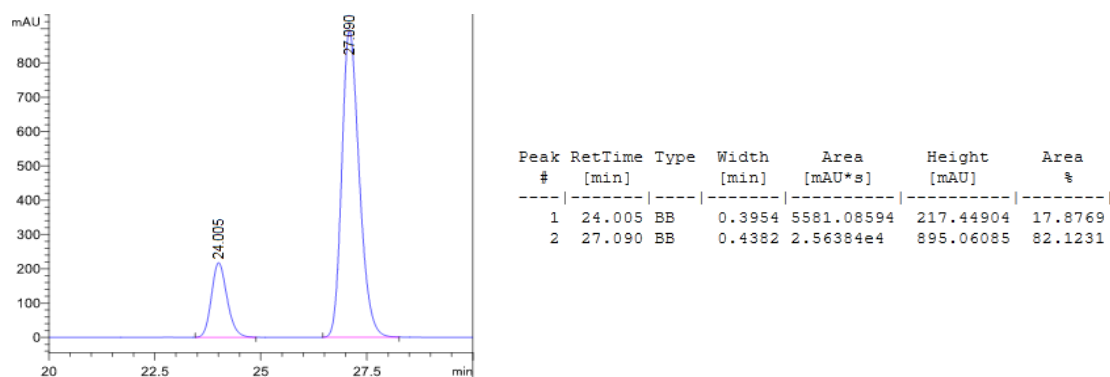


Table 2.10, Entry 7b: Major product: 109 mg, 51%, white solid. **mp** range = 102-103 °C. ¹H NMR (400 MHz, CDCl₃) δ ppm 7.66 (d, *J* =

6.0 Hz, 6 H), 7.46-7.36 (m, 9 H), 7.01-6.93 (m, 9 H), 6.83 (dt, $J = 8.0, 5.5$ Hz, 1 H), 4.90 (t, $J = 6.0$ Hz, 1 H), 2.80-2.57 (m, 1 H), 2.64-2.57 (m, 1 H), 2.04-1.97 (m, 1 H), 1.88-1.83 (m, 2 H), 1.68-1.60 (m, 1H). ^{13}C NMR (101 MHz, CDCl_3) 162.2-159.8 (d, $J = 243.2$ Hz), 141.0, 135.5, 134.4, 132.4, 130.1-130.0, 129.9, 127.8, 114.7-114.0 (m, 2 C), 70.0, 32.2, 28.2, 13.9. **Optical Rotation** $[\alpha]^{25}_{\text{D}} = +14.4$ ($c = 0.99$, CHCl_3). **HRMS** (ESI) (M+) Calculated for $(\text{C}_{28}\text{H}_{25}\text{FOSi}^+)$: 424.1653 Observed: 424.1657. **IR** (neat, cm^{-1}): 3066, 2936, 1897, 1827, 1775, 1589, 1497, 1427, 1246, 1113, 1062, 993, 821, 696.

HPLC data is of the desilylated and purified product using the same HPLC conditions as the recovered starting material. (er = 18:82)



Kinetic Resolution Data for Table 2.10, Entry 7b

#	er _{SM} %	er _{Pr} % ^a	C %	s	SAVG
1	87:13	84:16	52.2	11	11
2	90:10	82:18	55.3	11	

a) er_{Pr}% is of the deprotected and purified product

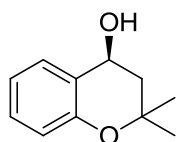


Table 2.10, Entry 10: Recovered starting material: 42 mg, 47% ^1H NMR

(400 MHz, CDCl_3) δ ppm 7.44 (d, $J = 9.0$ Hz, 1H), 7.17 (dt, $J = 7.5, 1.5$ Hz, 1 H), 6.91 (dt, $J = 7.0, 1.0$ Hz, 1 H), 6.78 (d, $J = 9.0$ Hz, 1 H), 4.83 (dd, $J = 8.5, 6.0$ Hz, 1 H), 2.15 (dd, $J = 19.5, 7.0$ Hz, 1 H), 1.84 (dd, $J = 22.5, 5$ Hz, 1 H), 1.43 (s, 3 H), 1.30 (s, 3 H). ^{13}C NMR (101 MHz, CDCl_3) δ ppm 153.1, 129.2, 127.5, 124.2, 120.2, 117.1, 75.2, 63.6, 42.6, 28.9, 25.9.

The HPLC separation conditions and subsequent stereochemical assignment was determined from the literature:³⁹ Chiralpak AD-H column, 4% *i*PrOH in hexane, flow rate: 0.3 mL/min, 25 °C; t_R 39.4 min for (*S*)-enantiomer (major) and t_R 42.0 min for (*R*)-enantiomer (minor). (er = 91:9)

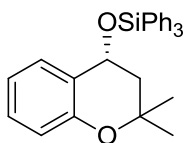


Table 2.10, Entry 10: Major product: 112 mg, 51 %, white solid. **mp**

range = 118-119 °C. ^1H NMR (400 MHz, CDCl_3) δ ppm 7.69 (d, $J = 9.5$ Hz, 6 H), 7.46-7.32 (m, 10 H), 7.13 (dt, $J = 8.0, 2.0$ Hz, 1 H), 6.83, (dt, $J = 7.5, 1.0$ Hz, 1H), 6.75, (d, $J = 9.0$, 1 H), 5.0 (dd, $J = 8.0, 6.0$, Hz, 1 H), 1.98 (dd, $J = 21.5, 5.0$ Hz, 1 H), 1.86 (dd, $J = 19.0, 5.0$ Hz, 1 H), 1.39 (s, 3 H), 1.27 (s, 3 H). ^{13}C NMR (101 MHz, CDCl_3) δ ppm 153.2, 135.5, 134.3, 130.1, 128.7, 128.1, 127.9, 124.2, 119.8, 116.9, 75.0, 65.2, 42.2, 28.8, 26.3. **Optical Rotation** $[\alpha]^{25}_D = + 16.6$ ($c = 0.94$, CHCl_3). **HRMS** (ESI) (M^+) Calculated for ($\text{C}_{29}\text{H}_{28}\text{O}_2\text{Si}^+$): 436.1853; Found: 436.1857. **IR** (neat, cm^{-1}): 3067, 2924, 1961, 1889, 1823, 1579, 1428, 1116, 1081, 852, 743, 697.

HPLC data is of the desilylated and purified product using the same HPLC conditions as the recovered starting material. (er = 13:87)

Kinetic Resolution Data for Table 2.10, Entry 10

#	er _{SM} %	er _{Pr} % ^a	C %	s	s _{AVG}
1	90:10	86:14	52.5	15	16
2	91:9	87:13	52.5	16	

a) er_{Pr}% is of the deprotected and purified product

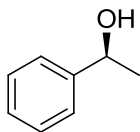


Table 2.10, Entry 12: Recovered starting material: 13 mg, 22%. ¹H NMR (400 MHz, CDCl₃) δ ppm 7.39-7.33 (m, 4 H), 7.29-7.25 (m, 1 H), 4.90 (q, *J* = 6.0 Hz), 1.89 (br, 1 H), 1.50 (d, 6.0 Hz). ¹³C NMR (101 MHz, CDCl₃) δ ppm 145.7, 128.5, 127.4, 125.3, 70.4, 25.1.

The HPLC separation conditions and subsequent stereochemical assignment was determined from the literature:³⁹ Chiralpak AD-H column, 4% *i*PrOH in hexane, flow rate: 1.0 mL/min, 25 °C; *t*_R 11.3 min for (*R*)-enantiomer (minor) and *t*_R 13.7 min for (*S*)-enantiomer (major). (er = 39:61)

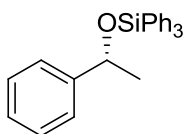


Table 2.10, Entry 12: Major product: 76 mg, 40%, clear colorless oil. ¹H NMR (400 MHz, CDCl₃) δ ppm 7.66 (d, *J* = 6.0 Hz, 6 H), 7.48-7.25

(m, 14 H), 5.11 (q, $J = 6.0$ Hz, 1 H), 1.49 (d, 6.0 Hz, 3 H). **^{13}C NMR** (101 MHz, CDCl_3) δ ppm 145.9, 135.4, 134.5, 129.8, 128.0, 127.7, 126.8, 125.4, 71.9, 26.8. **Optical Rotation** $[\alpha]^{25}_{\text{D}} = + 8.1$ ($c = 1.00$, CHCl_3). **HRMS** (ESI) (M^+) Calculated for ($\text{C}_{26}\text{H}_{24}\text{OSi}^+$): 380.1591 Observed: 380.1592. **IR** (neat, cm^{-1}): 3068, 2973, 1958, 1893, 1825, 1585, 1428, 1114, 1083, 958, 795, 694.

HPLC data is of the desilylated and purified product using the same HPLC conditions as the recovered starting material. (er = 68:32)

Kinetic Resolution Data for Table 2.10, Entry 12

#	er _{SM} %	er _{Pr} % ^a	C %	s	s _{AVG}
1	61:39	70:30	35.9	2.8	2.8
2	63:37	68:32	40.9	2.7	

a) er_{Pr}% is of the deprotected and purified product

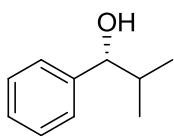


Table 2.10, Entry 13: 31 mg, 41 %Recovered starting material: **^1H NMR** (400 MHz, CDCl_3) δ ppm 7.35-7.24 (m, 5 H), 4.36 (dd, $J = 6.5$, 2.0 Hz, 1 H), 1.95 (dsep, $J = 6.5$, 1.0 Hz, 1 H) 1.86 (d, $J = 2.0$ Hz, 1 H), 1.00 (dd, $J = 6.5$, 1.0 Hz, 3 H), 0.79 (dd, $J = 7.0$, 1.0 Hz, 3 H). **^{13}C NMR** (101 MHz, CDCl_3) δ ppm 143.6, 128.1, 127.3, 126.5, 80.0, 35.2, 18.9, 18.2.

The HPLC separation conditions and subsequent stereochemical assignment was determined from the literature:⁴⁷ Chiralpak AD-H column, 2% *i*PrOH in hexane, flow

rate: 0.5 mL/min, 25 °C; t_R 28.3 min for (*R*)-enantiomer (major) and t_R 20.5 min for (*S*)-enantiomer (minor). (er = 63:37)

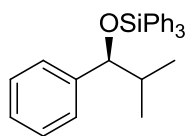


Table 2.10, Entry 13: Major product: 43 mg, 21%, clear colorless oil.

^1H NMR (400 MHz, CDCl_3) δ ppm 7.50 (dd, $J = 4.0, 1.0$ Hz, 6 H), 7.49-7.33 (m, 3 H), 7.29-7.25 (m, 6 H), 7.17 (s, 5 H), 4.53 (d, 6.0 Hz, 1 H), **^{13}C NMR** (101 MHz, CDCl_3) δ ppm 142.7, 135.5, 134.5, 129.7, 127.6, 127.5, 127.2, 126.8, 81.3, 36.1, 18.7, 18.3. **Optical Rotation** $[\alpha]_D^{25} = -18.9$ ($c = 1.00$, CHCl_3) **IR** (neat, cm^{-1}): 3068, 2959, 1961, 1887, 1824, 1428, 1115, 1053, 736, 695. **HRMS** (CI) (M-H) Calculated for ($\text{C}_{28}\text{H}_{28}\text{OSi}$): 407.1837 Observed: 407.1826

HPLC data is of the desilylated and purified product using the same HPLC conditions as the recovered starting material. (er = 20:80)

Kinetic Resolution Data for Table 2.10, Entry 13

#	er _{SM} %	er _{Pr} % ^a	C %	s	s _{AVG}
1	63:37	82:18	29.3	5.9	5.6
2	63:37	80:20	29.3	5.3	

a) er_{Pr}% is of the deprotected and purified product

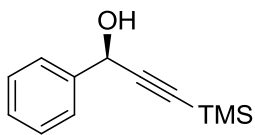


Table 2.10, Entry 15: clear colorless oil. **^1H NMR** (400 MHz,

CDCl_3) δ ppm 7.55 (d, $J = 8.0$ Hz, 2 H), 7.42-7.31 (m, 3 H), 5.46 (d, $J = 8.0$ Hz, 1 H), 5.30 (s, 1 H), 0.21 (s, 9 H).

The HPLC separation conditions and subsequent stereochemical assignment was determined from the literature:⁴⁸ Chiralpak OD-H column, 6% *i*PrOH in hexane, flow rate: 0.5 mL/min, 25 °C; t_R 13.5 min for (*R*)-enantiomer (major) and t_R 12.2 min for (*S*)-enantiomer (minor). (er = 64:36)

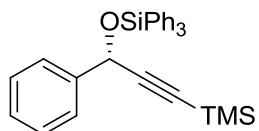


Table 2.10, Entry 15 clear colorless oil. ¹H NMR (400 MHz, CDCl₃) δ ppm 7.70-7.64 (m, 8 H), 7.51-7.25 (m, 12 H), 5.59 (s, 1 H), 0.10 (s, 9 H).

Upon deprotection, the substrate was converted to 1-phenyl-3-(trimethylsilyl)prop-2-yn-1-ol. The HPLC separation conditions were as followed Chiralpak OJ-H column, 6% *i*PrOH in hexane, flow rate: 0.5 mL/min, 25 °C; t_R 23.5 min for (*R*)-enantiomer (minor) and t_R 32.5 min for (*R*)-enantiomer (major). (er = 70:30)

General procedure for the screening of silyl sources and catalysts for enantioselective silylation

To an oven dried 1 dram vial with activated 4 Å molecular sieves (20-25 mg) was fitted an oven dried Teflon coated stir bar. To the vial was added 1-indanol (30.0 mg, 0.22 mmol) and catalyst (13.5 mg, 0.066 mmol) then quickly sealed under dry N₂. The vial was then charged with 1.0 mL THF to generate a 0.3 M solution and the solution was treated with either diisopropylethyl amine or *N,N*-diisopropyl-3-pentylamine (0.11 mmol) and cooled to -78 °C in a crycool apparatus for about 30 minutes. The cooled solution

was then treated with a 0.298 M solution of Ph_3SiCl in THF (0.370 mL, 0.11 mmol) and left to react for the specified amount of time. The reaction was then quenched with 200 μL MeOH and poured into a 4-dram vial containing 1.0 mL sat. aqueous NH_4Cl and extracted with diethyl ether (3 x 5 mL) and the ethereal layer was then dried over silica gel. After filtration and removal of solvent, the residue was purified by silica gel chromatography (1:1 hexanes: CH_2Cl_2 followed by 2% MeOH in CH_2Cl_2). The unreacted alcohol was then analyzed by HPLC with a chiral stationary phase.

The purified silyl ether was then dissolved in 3 mL THF and fitted with a Teflon coated stir bar. The solution was treated with 1.0 mL TBAF (1 M in THF) and stirred at ambient temperature for 10 h. The reaction was then quenched with brine and extracted with diethyl ether (3 x 3 mL) and dried over silica gel. After filtration and removal of solvent, the crude was purified by silica gel chromatography (CH_2Cl_2 to 2% MeOH in CH_2Cl_2).

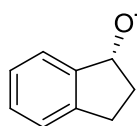


Table 2.5, Entry 1: Major product: 24 mg, 43%, clear colorless oil. ^1H NMR (400 MHz, CDCl_3) δ ppm 7.35-7.34 (m, 1 H), 7.24-7.21 (m, 3H), 5.27 (t, J = 6.5 Hz, 1 H), 2.99-2.97 (m, 1H), 2.80-2.76 (m, 1 H), 2.49-2.41 (m, 1 H), 1.97-1.92 (m, 1 H), 1.06-1.02 (m, J = 16.0, 8.0 Hz, 9 H), 0.72 (q, 8.0 Hz, 6 H), ^{13}C NMR (101 MHz, CDCl_3) δ ppm 145.5, 142.5, 127.6, 126.4, 124.6, 124.0, 76.3, 36.5, 29.6, 6.8, 4.9. **Optical Rotation** $[\alpha]_{\text{D}}^{25} = +0.5$ (c = 1.91, CHCl_3). **HRMS** (ESI) (M^+) Calculated for ($\text{C}_{15}\text{H}_{24}\text{OSi}^+$): 248.1591 Observed: 248.1596 **IR** (neat, cm^{-1}): 2954, 2876, 1607, 1459, 1108, 1074, 846, 738.

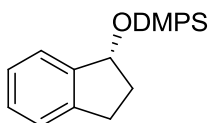


Table 2.5, Entry 2: Major product: 27 mg, 44%, clear colorless oil. ^1H

NMR (400 MHz, CDCl_3) δ ppm 7.70-7.67 (m, 2 H), 7.44-7.41 (m, 3 H), 7.29-7.26 (m, 1 H), 7.22-7.21 (m, 3 H), 5.27 (dt, $J = 6.5, 1.0$ Hz, 1 H), 3.05- 2.97 (m, 1H), 2.76-2.72 (m, 1 H), 2.35-2.33 (m, 1 H), 2.00-1.94 (m, 1 H), 0.50 (s, 6H). ^{13}C **NMR** (101 MHz, CDCl_3) δ ppm 145.0, 142.6, 138.1, 133.5, 129.6, 127.8, 127.7, 126.4, 124.6, 124.1, 76.6, 36.1, 29.7, -1.0. **Optical Rotation** $[\alpha]^{25}_{\text{D}} = + 17.3$ ($c = 0.58$, CHCl_3). **HRMS** (ESI) (M^+) Calculated for ($\text{C}_{17}\text{H}_{20}\text{OSi}^+$): 268.1278 Observed: 268.1285. **IR** (neat, cm^{-1}): 3069, 2958, 1887, 1590, 1477, 1427, 1250, 1114, 1070, 985, 870, 782, 737, 697

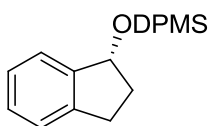


Table 2.5, Entry 3: Major product:⁴⁹ 36 mg, 54 %, clear colorless oil.

^1H **NMR** (400 MHz, CDCl_3) δ ppm 7.71-7.67 (m, 4 H), 7.46-7.38 (m, 6 H), 7.28 (d, $J = 4$ Hz, 1 H), 7.23-7.19 (m, 3 H), 5.38 (t, $J = 6.0$ Hz, 1 H), 3.05-2.98 (m, 1H), 2.78-2.70 (m, 1 H), 2.37-2.29 (m, 1 H), 2.10-2.00 (m, 1 H), 0.77 (s, 3H). ^{13}C **NMR** (101 MHz, CDCl_3) δ ppm 145.0, 142.7, 136.4, 134.4, 129.8, 127.8, 127.7, 126.4, 124.6, 124.2, 77.3, 36.2, 29.7, -2.1. **Optical Rotation** $[\alpha]^{25}_{\text{D}} = + 10.0$ ($c = 2.93$, CHCl_3) **HRMS** (ESI) (M^+) Calculated for ($\text{C}_{26}\text{H}_{24}\text{OSi}^+$): 330.1434 Observed: 330.1428 **IR** (neat, cm^{-1}): 3069, 2959, 1955, 1885, 1820, 1428, 1252, 1109, 1068, 861, 788, 721, 696.

2.9 References

1. Weickgenannt, A.; Mewald, M.; Oestreich, M., Asymmetric Si-O coupling of alcohols. *Organic & Biomolecular Chemistry* **2010**, 8, 1497-1504.
2. Greene, T. W.; Wuts, P. G. M., *Protective Groups in Organic Synthesis*. 3rd ed.; John Wiley & Sons: New York, 1999.
3. Sheppard, C. I.; Taylor, J. L.; Wiskur, S. L., Silylation-Based Kinetic Resolution of Monofunctional Secondary Alcohols. *Org. Lett.* **2011**, 13, 3794-3797.

4. Rendler, S.; Auer, G.; Oestreich, M., Kinetic Resolution of Chiral Secondary Alcohols by Dehydrogenative Coupling with Recyclable Silicon-Stereogenic Silanes. *Angew. Chem. Int. Ed.* **2005**, *44*, (46), 7620-7624.
5. Klare, H. F. T.; Oestreich, M., Chiral Recognition with Silicon-Stereogenic Silanes: Remarkable Selectivity Factors in the Kinetic Resolution of Donor-Functionalized Alcohols. *Angew. Chem. Int. Ed.* **2007**, *46*, 9335- 9338.
6. Weickgenannt, A.; Mewald, M.; Muesmann, T. W. T.; Oestreich, M., Catalytic Asymmetric Si-O Coupling of Simple Achiral Silanes and Chiral Donor-Functionalized Alcohols. *Ang. Chem. Int. Ed.* **2010**, *49*, 2223-2226.
7. Rendler, S.; Oestreich, M., Polishing a Diamond in the Rough: “Cu-H” Catalysis with Silanes. *Angew. Chem. Int. Ed.* **2007**, *46*, 498-504.
8. Rendler, S.; Plefka, O.; Karatas, B.; Auer, G.; Fröhlich, R.; Mück-Lichtenfeld, C.; Grimme, S.; Oestreich, M., Stereoselective Alcohol Silylation by Dehydrogenative Si–O Coupling: Scope, Limitations, and Mechanism of the Cu–H-Catalyzed Non-Enzymatic Kinetic Resolution with Silicon-Stereogenic Silanes. *Chem. Eur. J.* **2008**, *14*, 11512-11528.
9. Isobe, T.; Fukuda, K.; Araki, Y.; Ishikawa, T., Modified guanidines as chiral superbases: the first example of asymmetric silylation of secondary alcohols. *Chem. Comm.* **2001**, 243-244.
10. Jarvo, E. R.; Copeland, G. T.; Papaioannou, N.; Bonitatebus, P. J.; Miller, S. J., A Biomimetic Approach to Asymmetric Acyl Transfer Catalysis. *J. Am. Chem. Soc.* **1999**, *121*, 11638-11643.
11. Zhao, Y.; Rodrigo, J.; Hoveyda, A. H.; Snapper, M. L., Enantioselective silyl protection of alcohols catalysed by an amino-acid-based small molecule. *Nature* **2006**, *443*, 67-70.
12. Zhao, Y.; Mitra, A. W.; Hoveyda, A. H.; Snapper, M. L., Kinetic Resolution of 1,2-Diols through Highly Site- and Enantioselective Catalytic Silylation. *Angew. Chem. Int. Ed.* **2007**, *46*, 8471-8474.
13. You, Z.; Hoveyda, A. H.; Snapper, M. L., Catalytic Enantioselective Silylation of Acyclic and Cyclic Triols: Application to Total Syntheses of Cleroindicans D, F, and C. *Angew. Chem. Int. Ed.* **2009**, *48*, 547-550.
14. Rodrigo, J. M.; Zhao, Y.; Hoveyda, A. H.; Snapper, M. L., Regiodivergent Reactions through Catalytic Enantioselective Silylation of Chiral Diols. Synthesis of Sapinofuranone A. *Org. Lett.* **2011**, *13*, 3778-3781.
15. Vedejs, E.; Jure, M., Efficiency in Nonenzymatic Kinetic Resolution. *Angew. Chem. Int. Ed.* **2005**, *44*, 3974-4001.
16. Vedejs, E.; Chen, X., Parallel Kinetic Resolution. *J. Am. Chem. Soc.* **1997**, *119*, 2584- 2585.

17. Tan, K. L.; Sun, X.; Worthy, A. D., Scaffolding Catalysis: Expanding the Repertoire of Bifunctional Catalysts. *Synlett* **2012**, 2012, 321-325.
18. Sun, X.; Worthy, A. D.; Tan, K. L., Scaffolding Catalysts: Highly Enantioselective Desymmetrization Reactions. *Angew. Chem. Int. Ed.* **2011**, 50, 8167-8171.
19. Worthy, A. D.; Sun, X.; Tan, K. L., Site-Selective Catalysis: Toward a Regiodivergent Resolution of 1,2-Diols. *J. Am. Chem. Soc.* **2012**, 134, 7321-7324.
20. Patel, S. G.; Wiskur, S. L., Mechanistic investigations of the Mukaiyama aldol reaction as a two part enantioselective reaction. *Tet. Lett.* **2009**, 50, 1164-1166.
21. Song, C. E., *Cinchona Alkaloids in Synthesis & Catalysis*. Wiley-VCH Verlag GmbH & Co.: Weinheim, Germany, 2009.
22. Kagan, H. B.; Fiaud, J. C., Kinetic Resolution. In *Topics in Stereochemistry*, John Wiley & Sons, Inc.: 1988; pp 249-330.
23. Birman, V. B.; Li, X., Benzotetramisole: A Remarkably Enantioselective Acyl Transfer Catalyst. *Org. Lett.* **2006**, 8, 1351-1354.
24. Li, X.; Jiang, H.; Uffman, E. W.; Guo, L.; Zhang, Y.; Yang, X.; Birman, V. B., Kinetic Resolution of Secondary Alcohols Using Amidine-Based Catalysts. *J. Org. Chem.* **2012**, 77, 1722-1737.
25. Kim, S.; Chang, H., 1,8-Diazabicyclo[5.4.0]undec-7-ene. An Effective and Selective Catalyst for the *t*-Butyldimethylsilylation of Alcohols. *Bull. Chem. Soc. Jpn.* **1985**, 58, 3669-3670.
26. Corriu, R. J. P.; Dabosi, G.; Martineau, M., Macanisme de l'hydrolyse des chlorosilanes, catalysée par un nucleophile: etude cinetique et mise en evidence d'un intermediaire hexacoordonne. *J. Organomet. Chem.* **1978**, 150, 27-38.
27. Bassindale, A. R.; Stout, T., The interaction of electrophilic silanes (Me_3SiX , $\text{X} = \text{ClO}_4, \text{I}, \text{CF}_3\text{SO}_3, \text{Br}, \text{Cl}$) with nucleophiles. The nature of silylation mixtures in solution. *Tet. Lett.* **1985**, 26, 3403-3406.
28. Fujio, M.; Keeffe, J. R.; More O'Ferrall, R. A.; O'Donoghue, A. C., Unexpectedly Small Ortho-Oxygen Substituent Effects on Stabilities of Benzylic Carbocations. *J. Am. Chem. Soc.* **2004**, 126, 9982-9992.
29. Jarvo, E. R.; Evans, C. A.; Copeland, G. T.; Miller, S. J., Fluorescence-Based Screening of Asymmetric Acylation Catalysts through Parallel Enantiomer Analysis. Identification of a Catalyst for Tertiary Alcohol Resolution. *J. Org. Chem.* **2001**, 66, 5522-5527.
30. Angione, M. C.; Miller, S. J., Dihedral angle restriction within a peptide-based tertiary alcohol kinetic resolution catalyst. *Tetrahedron* **2006**, 62, 5254-5261.

31. Karatas, B.; Rendler, S.; Frohlich, R.; Oestreich, M., Kinetic resolution of donor-functionalised tertiary alcohols by Cu-H-catalysed stereoselective silylation using a strained silicon-stereogenic silane. *Org. Biomol. Chem.* **2008**, *6*, 1435-1440.
32. Breuer, M.; Ditrich, K.; Habicher, T.; Hauer, B.; Keßeler, M.; Stürmer, R.; Zelinski, T., Industrial Methods for the Production of Optically Active Intermediates. *Angew. Chem. Int. Ed.* **2004**, *43*, 788-824.
33. Nicolaou, K. C.; Sorensen, E. K., Classics in Total Synthesis. VCH Publishers: New York, 1996; pp 41-53.
34. Burchat, A. F.; Chong, J. M.; Nielsen, N., Titration of alkyllithiums with a simple reagent to a blue endpoint. *J. Organomet. Chem.* **1997**, *542*, 281-283.
35. Lindholm, A.; Maki-Arvela, P.; Toukoniitty, E.; Pakkanen, T. A.; Hirvi, J. T.; Salmi, T.; Murzin, D. Y.; Sjoholm, R.; Leino, R., Hydrosilylation of cinchonidine and 9-O-TMS-cinchonidine with triethoxysilane: application of 11-(triethoxysilyl)-10,11-dihydrocinchonidine as a chiral modifier in the enantioselective hydrogenation of 1-phenylpropane-1,2-dione. *J. Chem. Soc., Perkin Trans. I* **2002**, *23*, 2605-2612.
36. Yamashita, A.; Norton, E. B.; Hanna, C.; Shim, J.; Salaski, E. J.; Zhou, D.; Mansour, T. S., Synthesis of 3,3-Dimethyl-4-chromanones: Improved Procedures Without Ring Opening. *Synth. Commun.* **2006**, *36*, 465 - 472.
37. Breschi, M. C.; Calderone, V.; Martelli, A.; Minutolo, F.; Rapposelli, S.; Testai, L.; Tonelli, F.; Balsamo, A., New Benzopyran-Based Openers of the Mitochondrial ATP-Sensitive Potassium Channel with Potent Anti-Ischemic Properties. *J. Med. Chem.* **2006**, *49*, 7600-7602.
38. Bonvallet, P. A.; Todd, E. M.; Kim, Y. S.; McMahon, R. J., Access to the Naphthylcarbene Rearrangement Manifold via Isomeric Benzodiazocycloheptatrienes. *J. Org. Chem.* **2002**, *67*, 9031-9042.
39. Yamada, T.; Nagata, T.; Sugi, K. D.; Yoroazu, K.; Ikeno, T.; Ohtsuka, Y.; Miyazaki, D.; Mukaiyama, T., Enantioselective Borohydride Reduction Catalyzed by Optically Active Cobalt Complexes. *Chem. Eur. J.* **2003**, *9*, 4485-4509.
40. Inagaki, T.; Ito, A.; Ito, J.-i.; Nishiyama, H., Asymmetric Iron-Catalyzed Hydrosilane Reduction of Ketones: Effect of Zinc Metal upon the Absolute Configuration. *Angew. Chem. Int. Ed.* **2010**, *49*, 9384-9387.
41. Mao, J.; Guo, J., Chiral amino amides for the ruthenium(II)-catalyzed asymmetric transfer hydrogenation reaction of ketones in water. *Chirality* **2010**, *22*, 173-181.
42. Zeror, S.; Collin, J.; Fiaud, J.-C.; Zouioueche, L. A., Evaluation of Ligands for Ketone Reduction by Asymmetric Hydride Transfer in Water by Multi-Substrate Screening. *Adv. Synth. Catal.* **2008**, *350*, (1), 197-204.

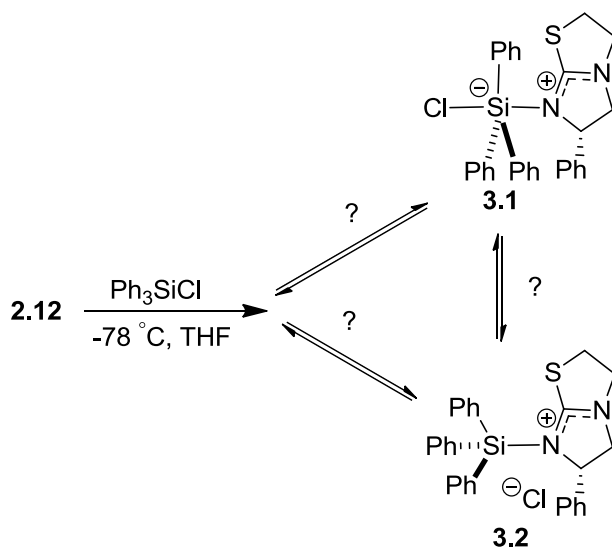
43. Nolin, K. A.; Ahn, R. W.; Kobayashi, Y.; Kennedy-Smith, J. J.; Toste, F. D., Enantioselective Reduction of Ketones and Imines Catalyzed by (CN-Box)ReV–Oxo Complexes. *Chem. Eur. J.* **2010**, *16*, 9555-9562.
44. Bouzemi, N.; Aribi-Zouioueche, L.; Fiaud, J.-C., Combined lipase-catalyzed resolution/Mitsunobu esterification for the production of enantiomerically enriched arylalkyl carbinols. *Tetrahedron: Asymmetry* **2006**, *17*, 797-800.
45. Zeror, S.; Collin, J.; Fiaud, J.-C.; Zouioueche, L. A., A recyclable multi-substrates catalytic system for enantioselective reduction of ketones in water. *J. Mol. Catal. A: Chem.* **2006**, *256*, 85-89.
46. Ohkuma, T.; Hattori, T.; Ooka, H.; Inoue, T.; Noyori, R., BINAP/1,4-Diamine-Ruthenium(II) Complexes for Efficient Asymmetric Hydrogenation of 1-Tetralones and Analogues. *Org. Lett.* **2004**, *6*, 2681-2683.
47. Glynn, D.; Shannon, J.; Woodward, S., On the Scope of Trimethylaluminium-Promoted 1,2-Additions of ArZnX Reagents to Aldehydes. *Chem. Eur. J.* **2010**, *16*, 1053-1060.
48. Yang, F.; Xi, P.; Yang, L.; Lan, J.; Xie, R.; You, J., Facile, Mild, and Highly Enantioselective Alkynylzinc Addition to Aromatic Aldehydes by BINOL/N-Methylimidazole Dual Catalysis. *J. Org. Chem.* **2007**, *72*, 5457-5460.
49. Chang, S.-Y.; Jiaang, W.-T.; Cherng, C.-D.; Tang, K.-H.; Huang, C.-H.; Tsai, Y.-M., The Scope and Limitations of Intramolecular Radical Cyclizations of Acylsilanes with Alkyl, Aryl, and Vinyl Radicals. *J. Org. Chem.* **1997**, *62*, 9089-9098.

Chapter 3. Mechanistic investigations into the enantioselective silylation of secondary alcohols with Ph_3SiCl by Levamisole (**2.12**)

3.1 Introduction

The use of enantioselective silylation has begun to be explored in the preparation of enantiomerically pure alcohols. Although there now exists several different methodologies that have been reported to perform the activation of silylchlorides towards enantioselective silylation,¹⁻⁵ no formal mechanistic study has been reported thus far. In a recent report from the Wiskur group,³ the isothioureia based catalyst (-)-tetramisole (**2.12**, Figure 3.1), was found to be the most successful of the catalysts tested for the kinetic resolution^{6, 7} of monofunctional secondary alcohols via enantioselective silylation. Isothioureia containing catalysts and similar amidine containing catalysts have been employed in a number of Lewis base activated asymmetric reactions⁸ and have garnered much interest as catalysts due to their superior nucleophilic properties in enantioselective acylation.⁹ Therefore, to gain a better understanding of the enantioselective silylation that was reported by the Wiskur group, and to gain more insight into reaction mechanisms catalyzed by isothioureia based compounds, work has begun to be performed by the Wiskur group to understand the enantioselective silylation of secondary alcohols by **2.12** in the presence of Ph_3SiCl .

To begin to answer the question of what the reactive silylating species is, an understanding of the coordination state of silicon must first be known. Once the structure of the silylating species is determined, the second question of how the activated silylating species leads to the enantioselective discrimination of the substrate can begin to be approached. The putative intermediate for a Lewis base activated enantioselective silylation would conceivably involve a direct coordination between (-)-tetramisole and Ph_3SiCl (Scheme 3.1) in a tetravalent intermediate. However, determining the structure of the reactive silylating species is complicated by the relative ease that silicon expands its coordination number to form extracoordinate species. Furthermore, although there has been much work done in the field of mechanistic organosilicon chemistry; it remains difficult to predict the valency of the resulting silicon–catalyst complex. A silicon species with hypercoordination such as **3.1** is commonly invoked to explain nucleophilic substitution at silicon¹³⁻¹⁹ but a tetravalent species (**3.2**) must also be considered as a potential intermediate.^{17, 20-22} Also, the possibility of an equilibrium between **3.1** and **3.2** is also a possibility.



Scheme 3.1 Potential pentavalent and tetravalent intermediates (**3.1** and **3.2** respectively)

The ability to form a hypervalent species is believed to be due to silicon's ability to form three center four electron (3c-4e) bonds.²³ A 3c-4e bond occurs when three atomic centers contribute an orbital (and four electrons) and form a bonding interaction. Specifically for silicon, the 3c-4e bonds are a result of the ligands binding to the non-bonding molecular orbital at silicon. These three atomic centers arrange in a linear conformation with two electrons residing in a bonding orbital while the other two electrons reside in a non-bonding orbital (Figure 3.3).²⁴ This has the practical structural implication that the more electronegative ligand will take the axial position at the silicon.^{13, 25} Also, because the bonding interaction is in the weaker non-bonding orbital, the apical positions possess longer bonds than the equatorial ligands.¹³ In the case of an even higher coordinate intermediate such as a hexavalent silicon, there is believed to be three 3c-4e bonds that allow for 6 bonds at silicon all of equal average lengths (i.e. axial and equatorial bonds are indistinguishable). Although there are many examples of penta-

and hexavalent intermediates in organosilicon chemistry, the possibility for a tetravalent (substitution like) intermediate at silicon is also possible.²⁰

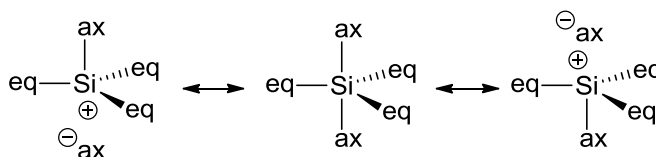


Figure 3.3 A valence bond visualization of a 3c-4e bond between silicon and its axial ligands in a pentavalent silicon species.

3.2 Determining the valency of the reactive silylating intermediate by NMR analysis

To elucidate the level of coordination of a reactive silicon intermediate, ²⁹Si-NMR analysis has become one of the most diagnostic techniques available for detecting hypervalent silicon intermediates. ²⁹Si-NMR is well suited for detecting extracoordinate silicon species due to the large characteristic upfield shift for hypervalent silicon species, whereas tetravalent species show a much less significant shift.^{21, 26, 27} However, it has been noted that the temperature, concentration, and substituents²⁶ as well as potential bond lengths and bond angles²⁸ must also be taken into consideration when interpreting any shifts that occur in the ²⁹Si-NMR spectrum. It is noteworthy though that solvent seems to have only a small effect on δ_{Si} resonances in most cases.²⁹⁻³¹

First, in an attempt to synthesize the intermediate, a 1 M solution of Ph₃SiCl in anhydrous THF was added to 1.0 equiv. of **2.12**. It was observed that within seconds, a very moisture sensitive white precipitant formed. Although such a sparingly soluble product can be considered to be an indication of an ionic silicon compound,^{32, 33} neutral hypervalent silicon compounds have also been known to show poor solubility.³⁴ When

the solid was added to CD_2Cl_2 , the product was found to be soluble enough to obtain ^1H and ^{29}Si NMR data.

3.2.1 ^1H -NMR analysis of the **2.12** / $\text{Ph}_3\text{Si-Cl}$ complex

When compared to (-)-tetramisole (Figure 3.4, spectrum (a)), the bicyclic ring protons of the resulting (-)-tetramisole / Ph_3SiCl complex (Figure 3.4, spectrum (b)) were shifted noticeably downfield. This suggests that the compound which forms involves a coordinating interaction between (-)-tetramisole and a Lewis acidic species, such as Ph_3SiCl . Also, the integration of the aromatic region of the ^1H -NMR spectrum for the complex (-)-tetramisole/ Ph_3SiCl reveals additional protons that may correspond to the aromatic protons of a bound Ph_3SiCl . Also, there was no evidence for the presence of unreacted **2.12** or Ph_3SiCl which suggests stoichiometric conversion.

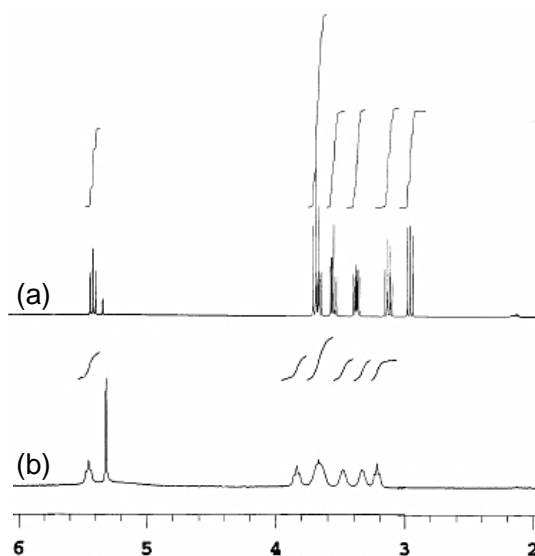


Figure 3.4 A comparison of the bicyclic ring protons in CD_2Cl_2 of (a) **2.12** and (b) the isolated solid that forms from the addition of **2.12** and Ph_3SiCl .

Further proof that the precipitant contains a species with a direct interaction between (-)-tetramisole and Ph_3SiCl was provided by a 1D nOe-Difference experiment (Figure 3.5). In this experiment, it was observed that when the methine proton of **2.12** (Figure 3.5, proton H_b) was irradiated, a positive nOe resulted between the methine proton of **2.12** and the ortho ring protons (H_a) of Ph_3SiCl . This confirms quite conclusively that a CD_2Cl_2 soluble **2.12**/ Ph_3SiCl complex is present in the precipitant. Also, the presence of a positive nOe supports the claim that the ortho protons on Ph_3SiCl are near the methine proton on **2.12**. When the same procedure was followed to form the **2.12**/ Ph_3SiCl complex directly in CD_2Cl_2 , there is no proof of coordination by either ^1H NMR or by nOe-difference study, thus indicating the important role that solvent plays in the formation of any potential adduct. For all subsequent solution based NMR studies, the complexes were first formed in THF, evaporated and then dissolved in CD_2Cl_2 .

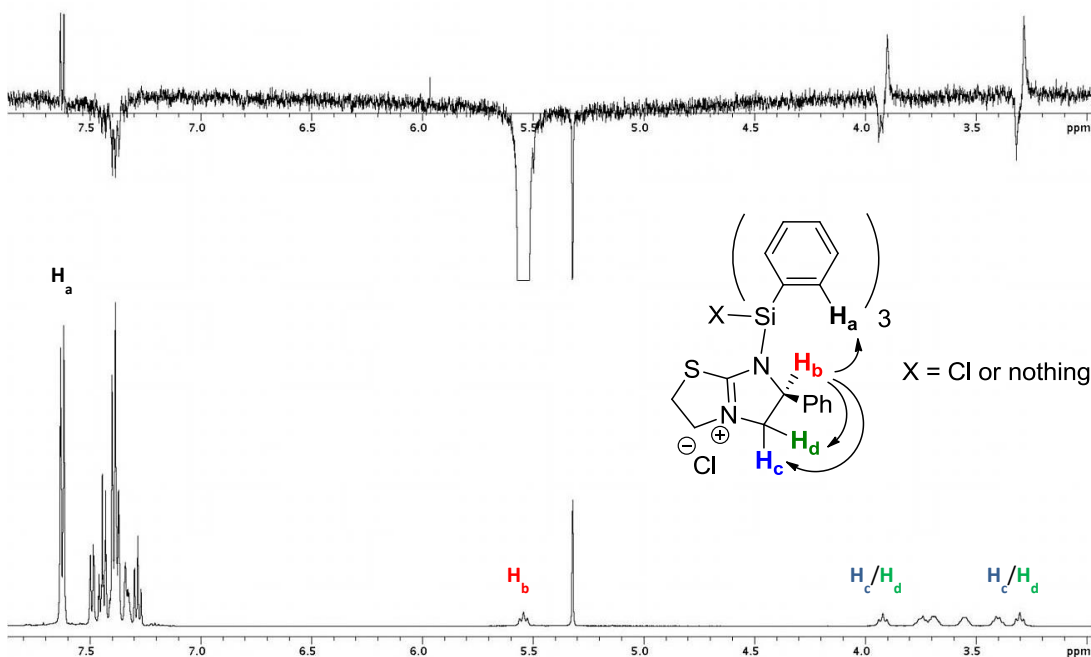


Figure 3.5 nOe-difference spectrum of the isolated solid from the addition of **2.12** to Ph_3SiCl in THF and the observed nOe correlations.

3.2.2 Magic Angle Spinning-²⁹Si-Solid State Nuclear Magnetic Resonance of the 2.12/Ph₃SiCl complex

To directly determine if the resulting adduct of **2.12** and Ph₃SiCl contains a hypervalent or tetravalent silicon species, direct analysis of the solid by Magic Angle Spinning-²⁹Si-Solid State Nuclear Magnetic Resonance (MAS-²⁹Si-SSNMR) was performed. If a pentavalent silicon species precipitates upon complexation of **2.12** to Ph₃SiCl, a significant upfield shift is expected relative to the unassociated Ph₃SiCl (2.5 ppm) just as is expected from solution state ²⁹Si-NMR.³⁵ However, what was observed was a single sharp peak at -16.6 ppm. This represents an overall upfield shift of less than 20 ppm. When compared to a recent report by the Wagler group in which an isothioureia moiety was found to give the pentavalent silicon species **3.3** (Figure 3.6).³⁶ There was an overall upfield shift of >60 ppm (δ ²⁹Si) relative to Me₃SiCl (CDCl₃, δ ²⁹Si = +31.0 ppm³⁷). Therefore, due to the smaller upfield shift observed for the **2.12**/Ph₃SiCl complex, it suggests that the isolated species is not hypervalent silicon but most likely a tetracoordinate species like that of **3.2**.

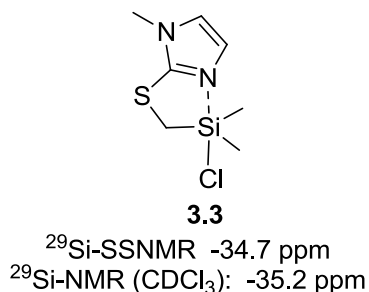


Figure 3.6 ²⁹Si-SSNMR and ²⁹Si-NMR resonances for the known pentavalent isothioureia/silylchloride (**3.3**)

Due to the high moisture sensitivity of **2.12**, the complex was compared to the two most likely hydrolysis products that would form from any adventitious water that may be present, triphenylsilanol (Ph₃SiOH) and hexaphenyldisiloxane (HPDS) (Table

3.1). The MAS-²⁹Si-SSNMR spectrum of Ph₃SiOH is known to give a complicated multiplet when analyzed near room temperature (Figure 3.7). This splitting pattern is attributed to the hydrogen bonding network that results as the compound crystallizes.³⁸ To prevent this, Ph₃SiOH was rapidly precipitated by dissolving in hot hexanes then cooling quickly to -78 °C. When prepared in this fashion, only a single broad peak centered around -11 ppm was observed (Table 3.1). The other potential product resulting from hydrolysis is the condensation product, hexaphenyldisiloxane (HPDS). Analysis of the disiloxane only showed a single peak at -18.5 ppm. Although the difference in the resonances for these compounds is smaller than the resolution, HPDS is readily soluble in both THF and CD₂Cl₂ so this excludes any sizeable portion of the resulting **2.12**/Ph₃SiCl adduct from being the condensation hydrolysis product HPDS.

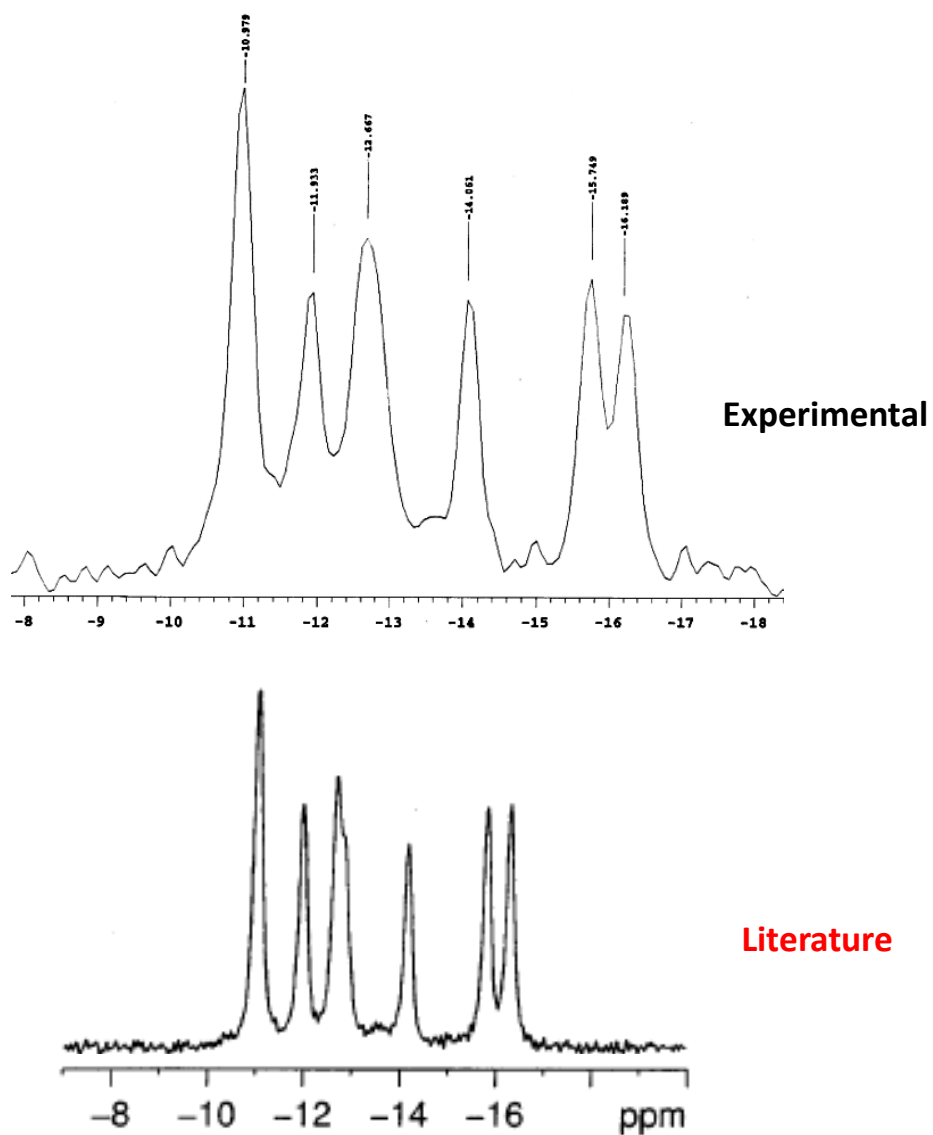


Figure 3.7 The obtained and literature³⁸ MAS- ^{29}Si -SSNMR spectra of Ph_3SiOH .

Table 3.1 Solid State MAS-²⁹Si-SSNMR analysis of **2.12**/Ph₃SiCl and hydrolysis products

Entry	Silicon source	δ ²⁹ Si (ppm)
1	2.12 /Ph ₃ SiCl	-16.6
2	Ph ₃ SiCl	2.5
3	Ph ₃ SiOH	-11.0
4	HPDS	-18.5

3.2.3 ¹H-²⁹Si gradient heteronuclear multiple quantum coherence spectroscopy analysis of the **2.12**/Ph₃SiCl complex.

To attempt to observe whether a hypervalent species like **3.1** or a tetracoordinate silicon species such as **3.2** is present in solution, or if an equilibrium between the two coordination states is occurring, the 2D NMR analysis technique, ¹H-²⁹Si gHSQC was performed on the adduct. The sequence was modified by using delays optimized to the multiple bond coupling constants for silicon. By setting up the sequence this way, ¹H nuclei that are 2-3 bonds away from ²⁹Si nuclei will show a correlation instead of just ¹H nuclei directly attached to ²⁹Si nuclei. Furthermore, by using this modified gHSQC method, as opposed to the traditional multiple bond correlation experiment, HMBC³⁹, greater resolution can be achieved due to the phase sensitivity of the HSQC method and the same data can be obtained. The other advantage of using this technique is that since this technique directly observes the ¹H nucleus instead of the ²⁹Si, the sensitivity is based off of the natural abundance of the ¹H nucleus (>99%) instead of ²⁹Si (ca. 5%).⁴⁰

The heteronuclear correlation technique HSQC was performed in order to detect the presence of a hypervalent silicon species, which can be inferred by a significant and characteristic upfield shift in the δ ²⁹Si resonance. Some reported examples of

pentavalent silicon compounds detected by ^{29}Si are Ph_3SiH_2 (**3.4**) which was shown to give a ^{29}Si resonance at -74 ppm, while Ph_5Si (**3.5**) and Ph_3SiF_2 (**3.6**) gave resonances at -103 and -111 ppm respectively⁴¹⁻⁴³, all of which showed significant upfield shifts relative to Ph_3SiCl (1.9 ppm)⁴⁴ (Figure 3.8). Furthermore, use of the NMR technique ^1H - ^{29}Si gHSQC, will allow for determination of which ^1H signals are correlated to the corresponding ^{29}Si resonance, which will aid in distinguishing different ^{29}Si containing species that may be present in solution. Being able to correlate ^1H resonances to ^{29}Si resonances can prove useful in identifying hydrolyzed silicon side products. Also, to further simulate the conditions of the enantioselective silylation that is occurring in Scheme 3.1, all analysis were performed at -78 °C. Apart from the lower temperature simulating the reaction conditions, lower temperatures allow for the most favorable condition to observe a hypervalent species.^{45, 46}

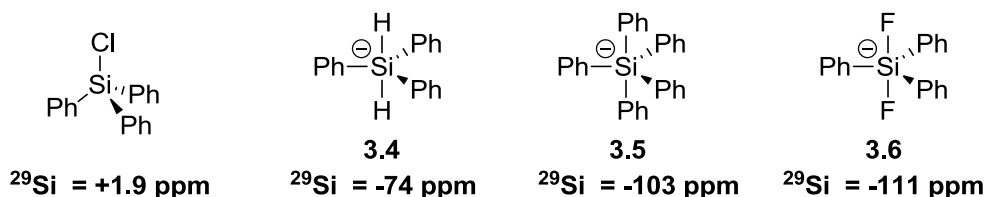


Figure 3.8 Reported ^{29}Si resonances for Ph_3SiCl ⁴⁴ and some hypervalent silicon containing compounds of the formula Ph_3SiX_2 .⁴¹⁻⁴³

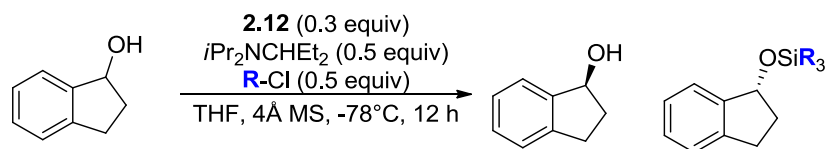
To perform the ^1H - ^{29}Si gHSQC analysis of the **2.12** activated silyl chlorides, as well as the potential side products, all spectra were referenced to Me_4Si in both the ^{29}Si and ^1H spectra. Reported in Table 3.2 are the observed ^{29}Si spectra and the corresponding ^1H resonances. In most cases there are multiple ^1H resonances that correspond to multiple ^1H correlations to the listed ^{29}Si signal. These represent long distance (4 bond correlation) between meta protons on the aryl groups or 3 bond correlation of protons on

alkyl ligands attached to silicon. The error associated with the ^{29}Si spectra is approximately ± 1.5 ppm.

^1H - ^{29}Si gHSQC analysis of the **2.12**/ Ph_3SiCl complex shows a similar magnitude upfield shift from Ph_3SiCl (Table 3.2, Entry 1) as was observed in the ^{29}Si -SSNMR. The silanol derivative gives a δ ^{29}Si resonance (Table 3.2, Entry 5) close to the signal seen for **2.12**/ Ph_3SiCl , the corresponding ^1H signal is >0.4 ppm upfield than for **2.12**/ Ph_3SiCl which is much greater than the resolution for the ^1H spectrum. This strongly suggests that the observed δ ^{29}Si resonance corresponds to a unique species. When compared to the disiloxane side product (Table 3.2, Entry 6), the δ ^{29}Si resonance is significantly different. To test whether an equilibrium between tetra- and pentavalent species is present, 3.0 equivalents of **2.12** was added (Entry 2). What was observed was an upfield shift that was practically identical to when 1.0 equivalent was used. This suggests that there is no equilibrium between different coordination states at silicon. The complex was also analyzed at 20°C to see if there was a shift downfield when compared to Entry 1. The reason a downfield shift would be expected is due to the preference for pentavalent silicon formation at lower temperatures.^{45, 46} When analyzed at 20°C , there is a negligible shift upfield. This further supports that there is neither an equilibrium between tetra- and pentavalent silicon species nor is the resonance observed at -11 ppm (δ ^{29}Si) a pentavalent species. Therefore, because there was no significant upfield shift in the δ ^{29}Si signal, on a magnitude expected for pentacoordinate silicon species, this supports the hypothesis that the active silylating agent in the (-)-tetramisole catalyzed enantioselective silylation reaction is the tetracoordinate silicon salt **3.2**.

It was previously reported by the Wiskur group,³ that several different alkyl and aryl containing silylchlorides besides Ph₃SiCl were found to afford enantioenriched secondary alcohols when catalyzed by **2.12**, albeit with lower selectivity factors (Scheme 3.2). To determine if these other silylchlorides (Table 3.2, Entries 8, 12, 16, and 20) show similar results when analyzed by the same ¹H-²⁹Si gHSQC NMR technique, a series of **2.12**/silylchloride complexes were prepared. It was observed that all of the **2.12**/silylchloride complexes showed upfield shifts of < 25 ppm compared to the free silyl chloride, suggesting the observed species are tetravalent. Also, in all cases, the **2.12**/silylchloride complexes showed similar upfield shifts in their ²⁹Si resonances to that of their corresponding silanol compounds (Entries 1 and 5, 7 and 9, 11 and 13, 15 and 17, 19 and 21). However, the corresponding ¹H resonances are in all cases significantly different. There even appears to be formation of a *t*BuMe₂Si-**2.12** complex (Table 3.2, Entry 19). The potential formation of a **2.12** activated complex is noteworthy because no conversion was observed for the enantioselective silylation based kinetic resolution of 1-indanol when *t*BuMe₂Si-Cl was the silyl source (Scheme 3.2, Entry 5). This suggested that there may not have been formation of a reactive silylating intermediate, or that a reactive intermediate did form, but the complex was so sterically hindered that the overall rate of the kinetic resolution decreased significantly, that almost no conversion was observed. It was also observed that as the phenyl groups were replaced with alkyl groups, (Table 3.2, Entries 7, 11, 15, 19), the δ ²⁹Si signal for all **2.12**/silylchloride complexes showed an increase in deshielding compared to their corresponding silylchloride. For the **2.12**/Et₃Si-Cl sample (Table 3.2, Entry 15), three ²⁹Si resonance were observed. The first at 9.6 ppm, appears to be hexaethyldisiloxane (Entry 18). The

^{29}Si resonances at 14 ppm would correspond to an upfield shift of approximately 23 ppm while the other correlation would correspond to an upfield shift of about 33 ppm. With the greatest potential upfield shift of approximately 30 ppm, both of these resonances do not strongly support a pentavalent silicon species. It is not clear which of the two correlations would be a tetravalent silicon species or what the other correlation is. However, it is clear that all of the **2.12**/silyl chloride complexes show an upfield shift in the ^{29}Si resonances relative to the corresponding silyl chloride. This trend is in accordance with literature values.⁴⁷ Therefore, the data presented thus far fails to support the hypothesis of a pentavalent (**3.1**) type intermediate for any of the **2.12**/silyl chloride substrates.



Entry	R-	conv (%) ^b	<i>s</i> ^b
1	Et ₃ Si-	48	4.0
2	Me ₂ PhSi-	50	3.4
3	Ph ₂ MeSi-	46	5.2
4 ^c	Ph ₃ Si-	59	8.5
5 ^d	<i>t</i> BuMe ₂ Si-	<5	--

^a For reaction conditions, see ref 3. ^b Conversion and selectivity factor were calculated from the ee (starting material) and ee (product). ^c The reaction was run with 0.6 equiv. Ph₃Si-Cl and *i*Pr₂EtN and 25 mol% **2.12**. ^d Conversion for this entry was determined via recovered starting material after 48 h.

Scheme 3.2 Enantioselective silylation of (±)-1-indanol with **2.12** and various silyl chlorides

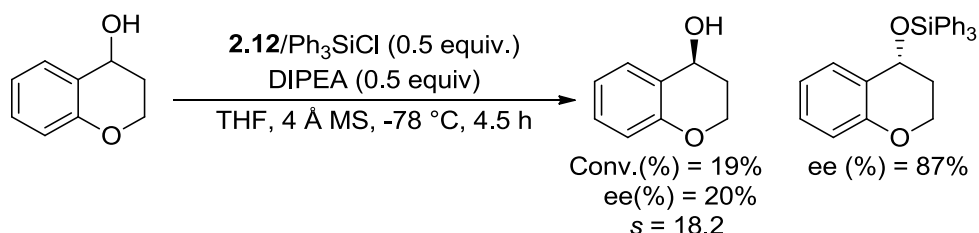
Table 3.2 ^1H - ^{29}Si gHSQC NMR analysis at -78°C of several **2.12**/silylchloride complexes and their potential hydrolysis products

Entry	$\text{R}_1\text{R}_2\text{R}_3\text{Si-X}$	δ_{Si} (ppm)	δ_{H} (ppm)
1	$\text{Ph}_3\text{Si-2.12}$	-11.3	7.61;7.45
2	$\text{Ph}_3\text{Si-2.12}^{\text{a}}$	-11.0 -19.2	7.60 7.52
3	$\text{Ph}_3\text{Si-2.12}^{\text{b}}$	-13.9 -18.8	7.61 7.50
4	$\text{Ph}_3\text{Si-Cl}$	+1.9	7.64
5	$\text{Ph}_3\text{Si-OH}$	-13.4	7.20
6	$\text{Ph}_3\text{Si-O-SiPh}_3$	-20.1	7.53
7	$\text{Ph}_2\text{MeSi-2.12}$	-1.2 -10.2	7.69;7.47 7.57
8	$\text{Ph}_2\text{MeSi-Cl}$	+10.5	7.63;0.97
9	$\text{Ph}_2\text{MeSi-OH}$	-4.2	7.33;0.20
10	$\text{Ph}_2\text{MeSi-O-SiPh}_2\text{Me}$	-10.2	7.58;0.62
11	$\text{PhMe}_2\text{Si-2.12}$	-1.0 +10.6	7.59;0.36 7.61;7.49
12	$\text{PhMe}_2\text{Si-Cl}$	+20.8	7.64;0.71
13	$\text{PhMe}_2\text{Si-OH}$	+5.6	7.47;0.19
14	$\text{PhMe}_2\text{Si-O-SiPhMe}_2$	-0.8	7.59;0.35
15	$\text{Et}_3\text{Si-2.12}$	+9.6 +14.2 +24.3	0.91;0.50 0.84;0.40 0.90;0.50
16	$\text{Et}_3\text{Si-Cl}$	+37.3	1.00;0.81
17	$\text{Et}_3\text{Si-OH}$	+19.4	0.93;0.53
18	$\text{Et}_3\text{Si-O-SiEt}_3$	+9.0	0.91;0.50
19	$t\text{BuMe}_2\text{Si-2.12}$	+14.1	0.79;-0.12
20	$t\text{BuMe}_2\text{Si-Cl}$	+37.3	0.97;0.38
21	$t\text{BuMe}_2\text{Si-OH}$	+18.8	0.89;0.00
22	$t\text{BuMe}_2\text{Si-O-SiMe}_2t\text{Bu}$	+9.5	0.86;0.07

^a 3.0 equiv. of **2.12** ^b Analysis was performed at 20°C

Despite the data presented thus far, it is still unknown if the isolated silyl species is the reactive silylating species. To determine if the **2.12**/ Ph_3SiCl complex was capable

of silylating an alcohol, a kinetic resolution of 4-chromanol with the **2.12**/ Ph_3SiCl complex used directly as a chiral silyl reagent was performed. It was observed that the selectivity factor for the enantioselective silylation of 4-chromanol was slightly higher than when the complex was formed in situ with a substoichiometric amount of catalyst. However, it appears that the conversion for this reaction was considerably lower after 4.5 h then when formed in situ and no silanol or disiloxane products were observed. When $\text{Ph}_3\text{Si-OH}$ and HPDS were used as the silyl source, there was no observable conversion after even 16 h (< 5%).



Scheme 3.3 The kinetic resolution of (±)-4-chromanol with the **2.12**/ Ph_3SiCl complex as a chiral reagent.

In order to test if altering the electronics of the aryl rings of the silylchloride has any effect on silicon's coordination number, the electron withdrawing ($p\text{BrC}_6\text{H}_4$) $_3\text{SiCl}$ ($\sigma_p = 0.26$)⁴⁸ and electron donating ($p\text{H}_3\text{COC}_6\text{H}_4$) $_3\text{SiCl}$ ($\sigma_p = -0.12$)⁴⁸ derivatives of Ph_3SiCl were synthesized. In addition to electronics, sterics were increased to determine if an increase in steric bulk will prevent complex formation. For this reason ($pt\text{BuC}_6\text{H}_4$) $_3\text{SiCl}$ was also synthesized and all three of these derivatives were reacted with **2.12** then prepared in the same fashion as for Table 3.2 then analyzed by ^1H - ^{29}Si -gHSQC NMR.⁴⁹

The **2.12**/ $(pt\text{BuC}_6\text{H}_4)_3\text{SiCl}$ complex (Table 3.2, Entry 1) was observed to give two silicon correlations, one at -16 ppm and another at -11 ppm. Both of these correlations appear to be unique in both δ ^{29}Si and ^1H spectra and represent a maximum upfield shift

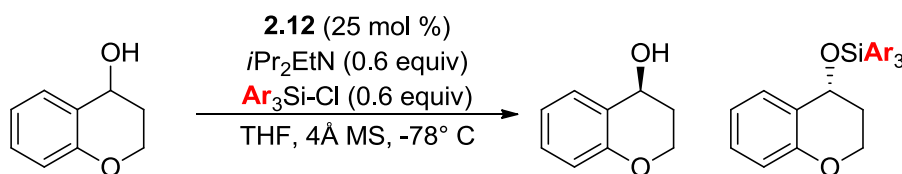
of approximately 17 ppm. When the electron donating *p*-methoxy substituted Ar_3SiCl was reacted with **2.12** two δ ^{29}Si resonances were observed (Entry 5). There appeared to be some hydrolysis as the resonances that was observed at -19.2 ppm (^{29}Si) and 7.42 ppm (^1H) corresponds to one of the correlations observed for the disiloxane derivative -19.3 ppm (^{29}Si) and 7.44 ppm (^1H) (Entry 8). The other correlation at -10.7 ppm (^{29}Si) and 7.55 ppm (^1H) represent a unique correlation with an upfield shift of approximately 11 ppm when compared to the silylchloride (Entry 6). Interestingly, the disiloxane was found to give three unique correlations (Entry 8) none of which correspond to either the silylchloride (Entry 6) or the silanol (Entry 7). Further NMR analysis of the disiloxane will be necessary to determine the structure of the other silicon containing species. ^1H - ^{29}Si -gHSQC analysis of the **2.12**/ $(p\text{BrAr})_3\text{SiCl}$ complex (Entry 9) also revealed two silicon containing species present. The resonance at -17 ppm (^{29}Si) and 7.28 ppm (^1H) corresponds very closely to the disiloxane condensation product (Entry 12). The resonance at -10.9 ppm (^{29}Si) and 7.59 ppm (^1H) appears to be a unique resonance that corresponds to an upfield shift of approximately 11 ppm. Interestingly, no resonance was observed for the ^1H - ^{29}Si -gHSQC analysis of $(p\text{BrAr})_3\text{SiOH}$ (Entry 11). This may be because the bond frequency differed significantly to the delay frequency (which was optimized for 10 Hz). When analyzed by direct observe, one dimensional ^{29}Si NMR (1D- ^{29}Si NMR), a single silicon species at -12.1 ppm was observed. In all cases the **2.12**/silylchloride complexes show unique silicon species that are shifted upfield from 11-17 ppm relative to their respective silylchlorides. Therefore, since the upfield shift is not of a similar magnitude to what is commonly observed for pentavalent silicon species the data fails to support the presence of a hypervalent silicon species.

Table 3.3 ^1H - ^{29}Si gHSQC NMR analysis of Ar_3SiCl with electron donating, electron withdrawing, and *pt*Bu- substituents at -78°C in CD_2Cl_2 .

Entry	$\text{R}_1\text{R}_2\text{R}_3\text{Si-X}$	^{29}Si Shift (ppm)	^1H Shift (ppm)
1	$(\text{ptBuAr})_3\text{Si-2.12}$	-16.4	7.61
		-11.2	7.51
2	$(\text{ptBuAr})_3\text{Si-Cl}$	+1.1	7.56
3	$(\text{ptBuAr})_3\text{Si-OH}$	-14.5	7.14
4	$(\text{ptBuAr})_3\text{Si-O-Si}(\text{ptBuAr})_3$	-19.9	7.50;7.37
5	$(\text{pH}_3\text{COAr})_3\text{Si-2.12}$	-10.7	7.55
		-19.2	7.42
6	$(\text{pH}_3\text{COAr})_3\text{Si-Cl}$	+1.2	7.55
7	$(\text{pH}_3\text{COAr})_3\text{Si-OH}$	-13.1	7.12
8	$(\text{pH}_3\text{COAr})_3\text{Si-O-Si}(\text{pH}_3\text{COAr})_3$	-20.1	7.45
		-19.3	7.44
		-10.3	7.41
9	$(\text{pBrAr})_3\text{Si-2.12}$	-17.4	7.28
		-10.9	7.59
10	$(\text{pBrAr})_3\text{Si-Cl}$	+1.3	7.64;7.49
11 ^a	$(\text{pBrAr})_3\text{Si-OH}$	-12.1	—
12	$(\text{pBrAr})_3\text{Si-O-Si}(\text{pBrAr})_3$	-17.7	7.28

^a δ ^{29}Si signal was determined by 1D- ^{29}Si NMR

When used in the kinetic resolution of 4-chromanol,⁵⁰ all three silylchloride species were capable of enantioselectively silylating the chiral secondary alcohol (Table 3.4). The more sterically hindered $(\text{ptBuC}_6\text{H}_4)_3\text{SiCl}$ (Entry 2) showed superior selectivity to Ph_3SiCl (Entry 1) although the reaction was slower than all of the other triarylsilyl chlorides that were tested, presumably due to greater steric congestion around the silicon center. Both the electron donating and the electron withdrawing substituents (Entry 3 and 4 respectively) showed comparable selectivity factors, although both were less selective than Ph_3SiCl (Entry 1).

Table 3.4 Enantioselective silylation of (±)-4-chromanol with **2.12**^a

Entry	Ar	time (h) ^b	conv (%) ^c	s ^c
1	Ph	15	58	15
2	<i>p</i> tBuC ₆ H ₄	48	37	26
3	<i>p</i> CH ₃ OC ₆ H ₄	40	47	10
4	<i>p</i> BrC ₆ H ₄	48	45	12

^a A 0.3 M solution of (±)-4-chromanol (0.50 mmol) was subjected to the reaction conditions.³ ^b Reaction time was not optimized.

^c Conversion and selectivity factor was calculated from the ee of the starting material and ee of the deprotected product.⁷

The isothiurea catalysts Homotetramisole (**3.7**)^{51, 52} and benzotetramisole (**3.8**)⁵³ have been shown to be very effective acylation catalysts for the enantioselective acylation of secondary alcohols. These isothiurea compounds have also been shown to be superior enantioselective catalysts to **2.12** for enantioselective acylation.^{51, 53} To see if a similar upfield shift to that seen for the **2.12**/silylchloride complexes analyzed thus far, these catalysts were also reacted with Ph₃SiCl and analyzed by ¹H-²⁹Si gHSQC NMR to determine if a tetravalent species forms. In addition to **3.7** and **3.8**, the Lewis basic compounds N-methylimidazole (**3.9**) and HMPA (**3.10**) were also reacted with Ph₃SiCl. In an attempt to force a pentavalent species, tetrabutylammonium chloride (**3.11**) was reacted with Ph₃SiCl.

When **3.4** was reacted with Ph₃SiCl, three resonances were observed by ¹H-²⁹Si gHSQC (Table 3.5, Entry 1). The resonance furthest downfield at 1.5 ppm (²⁹Si) and 7.64 ppm (¹H) most likely is unreacted Ph₃SiCl (Entry 6). The resonance furthest upfield

at -17.5 ppm (^{29}Si) and 7.55 ppm (^1H) is within error of the peak location of hexaphenyldisiloxane (Entry 8). The resonance at -4.9 ppm (^{29}Si) and 7.58 ppm (^1H) does not correlate to hydrolysis side products and shows a lesser upfield shift relative to the **2.12**/ Ph_3SiCl complex (Table 3.2, Entry 1), but this can still correspond to a reactive tetravalent Ph_3SiCl complex. When Ph_3SiCl was allowed to react with benzotetramisole (**3.8**), three resonances were observed (Table 3.5, Entry 2). Once again there appeared to be unreacted Ph_3SiCl at 2.4 ppm (^{29}Si) and 7.60 ppm (^1H), and what may be hexaphenyldisiloxane at -16.8 ppm (^{29}Si) and 7.53 ppm (^1H), although the silicon resonance is more than ± 3.0 ppm and may correspond to new silicon species. The resonance at -10.4 ppm (^{29}Si) and 7.66 ppm (^1H) does correspond to a new silicon species that is nearly identical in magnitude to the **2.12**/ Ph_3SiCl complex. The achiral Lewis base N-methylimidazole (**3.9**) and other N-substituted Lewis bases have been known to form both tetravalent⁵⁴ and hypervalent silicon complexes with several different silylchlorides.^{54, 55} When **3.9** was added to Ph_3SiCl , the only peak that was observed was a single resonance at -19.0 ppm (^{29}Si) and 7.50 ppm (^1H) which again may indicate a tetravalent silicon species (Entry 3). The question of whether Hexamethylphosphoramide (HMPA, **3.10**) forms a tetravalent or pentavalent species with Ph_3SiCl has been studied before by the Corriu group. It was reported that when **3.10** is reacted with Ph_3SiCl in hexanes, a white solid precipitates from solution.⁵⁶ To determine whether or not the resulting precipitant is a tetravalent or pentavalent silicon species, the Corriu group performed conductivity studies on the **3.12**/ Ph_3SiCl compound in CH_2Cl_2 to determine whether the product was a hypervalent species or an ionic compound. The measured conductivity was less than what would be anticipated for an ionic (tetravalent) species.

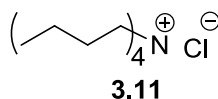
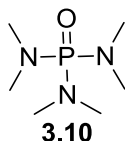
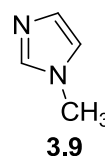
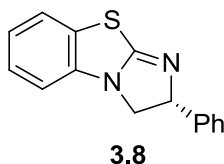
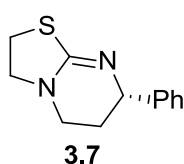
This led the authors to conclude that the species which was formed was a hypervalent silicon complex and not ionic in nature.⁵⁶ However, in a later study by the Bassindale group it was shown that compounds with relatively small upfield shifts (suggesting a tetravalent silicon species) can give low conductivity measurements (which would suggest a hypervalent silicon species). To explain these potentially contradictory results, the authors suggest that in solvents of low ionizing potential, such as CH₂Cl₂, an ionic compound would give a lower conductivity measurement due to a tight ion pairing.³⁷ Therefore, ¹H-²⁹Si gHSQC NMR analysis of the **3.12**/Ph₃SiCl complex was performed to determine whether the conclusions drawn by the conductivity results done by the Corriu group can be supported by NMR, or if what was observed was a tight ion pairing of a tetravalent intermediate, the **3.12**/Ph₃SiCl complex was formed and analyzed. When analyzed by ¹H-²⁹Si gHSQC NMR, there were two ²⁹Si resonances (Entry 4), one at -7.4 ppm (²⁹Si) and 7.61 ppm (¹H) and another at -18.1 ppm (²⁹Si) and 7.63 ppm (¹H). Neither of these results correspond strongly to either Ph₃SiCl or hydrolysis products (Entries 6-8). However, neither of these silicon species show significant upfield shifts to be indicative of pentavalent silicon formation. When tetrabutylammonium chloride (**3.11**, Entry 5) was added to Ph₃SiCl, the resulting signal was shifted upfield to -17.4 ppm (²⁹Si) and 7.71 ppm (¹H). It is unclear if this value represents a dichloro- substituted pentavalent silicon compounds since the Ph₃SiH₂ (**3.4**) and Ph₃SiF₂ (**3.6**) species are reported to give ²⁹Si resonances at -74 ppm⁴¹ and -111 ppm⁴³ respectively. Also, due to the presence of an unreacted Ph₃SiCl in the ²⁹Si NMR spectrum represented by the resonance at 1.9 ppm (²⁹Si) and 7.65 ppm (¹H), the possibility of a fast equilibrium between a penta- and tetravalent species can be ruled out as only a single, averaged peak

would be observed if a rapid equilibrium was present. Most this suggests that what is being observed is a more complicated silicon species that is in solution.

From the ^1H - ^{29}Si gHSQC NMR studies, it was observed that none of the nucleophiles studied or any of the silylchlorides analyzed gave results that would indicate pentavalent silicon formation. By altering the sterics and electronics of the Ar_3SiCl , there was no evidence that any of these derivatives formed a pentavalent species with all of the potential complexes being shifted upfield no more than 20 ppm. Nucleophiles that have been reported to be more nucleophilic than **2.12** such as homotetramisole (**3.7**)⁵⁷ were found to only give a new silicon species that was shift about 7 ppm upfield from Ph_3SiCl suggests that more nucleophilic isothioureas may not be capable of forming a pentavalent silicon species. The same was also observed for the less nucleophilic catalyst **3.9**⁵⁷ which only gave a single ^{29}Si resonance that was shifted approximately 21 ppm upfield from Ph_3SiCl .

Table 3.5. ^1H - ^{29}Si gHSQC NMR analysis at -78°C of complexes formed with different nucleophiles

Entry	Silicon species	$\delta^{29}\text{Si}$ (ppm)	$\delta^1\text{H}$ (ppm)
1	Ph_3Si - 3.7	+1.5 -4.9 -17.5	7.64 7.58 7.55
2	Ph_3Si - 3.8	+2.4 -10.4 -16.8	7.60 7.66 7.53
3	Ph_3Si - 3.9	-19.0	7.50
4	Ph_3Si - 3.10	-7.4 -18.1	7.61 7.63
5	Ph_3Si - 3.11	+1.9 -17.4	7.65 7.71
6	Ph_3Si -Cl	+1.9	7.64
7	Ph_3Si -OH	-13.4	7.20
8	Ph_3Si -O-SiPh ₃	-20.1	7.53



3.2.4 Conclusion

The results reported herein represent our initial probe into the mechanism of the enantioselective silylation using the Lewis base catalyst (-)-tetramisole (**2.12**). It was observed that upon addition of (-)-tetramisole to Ph_3SiCl a moisture sensitive solid precipitates. Upon analysis of this solid by solid state MAS- ^{29}Si -NMR, the upfield shift of the ^{29}Si resonance strongly suggests that the solid is a tetravalent salt. In solution, a nOe-difference analysis shows a positive nOe between the ortho aryl protons of Ph_3SiCl

and the methine protons of (-)-tetramisole. These nOe-difference results combined with the large difference between the ortho aryl protons of the **2.12**/ Ph_3SiCl complex and the potential hydrolysis products, $\text{Ph}_3\text{Si-OH}$ and hexaphenyldisiloxane (HPDS), observed by ^1H - ^{29}Si gHSQC NMR indicate that a tetravalent silicon species is present in solution as well. Therefore, the data presented leads us to suggest that the active silylating reagent for the enantioselective silylation reaction is an ionic tetravalent silicon species. When used as a stoichiometric chiral reagent, the **2.12**/ Ph_3SiCl complex was found to catalyze the kinetic resolution of (\pm)-4-chromanol with a slightly enhanced selectivity factor, but with lower conversion. When the electronics and steric environment of the aryl substituents on silicon were altered by synthesizing triarylsilyl chlorides with electron donating, electron withdrawing, and *pt*Bu groups, a similar upfield shift was observed for all of the subsequent complexes when compared to the **2.12**/ Ph_3SiCl complex. When tested in the kinetic resolution of (\pm)-4-chromanol via enantioselective silylation by (-)-tetramisole, the more sterically demanding (*pt*Bu C_6H_4) $_3\text{SiCl}$ showed superior selectivity when compared to Ph_3SiCl , but gave a diminished conversion. Both (*p*Br C_6H_4) $_3\text{SiCl}$ and (*p*H $_3\text{COC}_6\text{H}_4$) $_3\text{SiCl}$ reacted faster than the (*pt*Bu C_6H_4) $_3\text{SiCl}$, but gave similar but slightly lower selectivity factors than even Ph_3SiCl . These findings suggest that the electronics of the aryl groups attached to silicon play a minor role in influencing the selectivity factor of the enantioselective silylation reaction. However, it appears that increasing the sterics of the substituents attached to the aryl groups located at silicon will greatly enhance the selectivity factor, but will slow the rate of the kinetic resolution down considerably. Furthermore, we have shown that other isothioureas and Lewis bases give chemical shifts comparable to a tetravalent silicon compounds with Ph_3SiCl . Although there appears to

be no chemical shifts in the far upfield region that is typical of hypervalent silicon species, the existence of such a species below the limits of detection by ^{29}Si NMR remains a possibility.

3.3 Determining the existence of a single propeller conformation of silyl ethers by circular dichroism

With the NMR studies suggesting that the reactive silyl intermediate is a tetravalent species, studies could then be performed to answer the question of how the transfer of chirality can occur (Figure 3.2). To get enantiodiscrimination, the incoming alcohol would seemingly need to be near the chiral environment that is part of the silyl species during alcoholysis. However, since the silyl transfer would most likely proceed via a Walden inversion similar to an $\text{S}_{\text{N}}2$ type mechanism, the most direct means by which to accomplish this would be if the aromatic rings attached to silicon were arranged in a chiral fashion (Figure 3.9). This could be possible if the aromatic rings were arranged in a “screw propeller” type of conformation. The main requirement for this type of configuration being the possession of a central atom with at least two radiating aryl rings twisted to form part of a helical surface. Furthermore, the aryl rings must be twisted in the same direction, therefore the propeller would be chiral.^{58, 59}

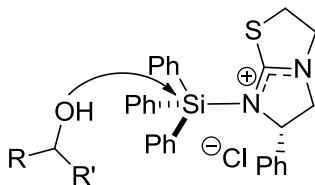


Figure 3.9 Presumed nucleophilic attack of the chiral alcohol.

The potential for a rigid propeller arrangement of the phenyl rings of Ph_3SiCl would be impossible as the aromatic rings attached to silicon have been found to undergo a rapid interconversion between propeller conformations due to a low barrier of inversion (Figure 3.9).⁶⁰ The racemization mechanism for triaryl methane species⁶¹ should apply to Ph_3SiCl , however, due to the bond length of silicon, the inversion barrier should be even lower in energy than the corresponding carbon analog. For example, it has been observed that the ring rotation barrier of Mes_3CH ($\text{C-Mes} = 1.55 \text{ \AA}^{62}$) is approximately 20 kcal. When the central carbon atom is replaced with a tin atom, the bond length from the central atom to the mesityl groups is elongated ($\text{Sn-Mes} = 2.14 \text{ \AA}^{63}$) and the calculated ring rotation barrier is lowered to 5-7 kcal. It is assumed that a similar trend would occur when comparing Ph_3CCl ($\text{C-Ph} = 1.55 \text{ \AA}^{60}$) to Ph_3SiCl ($\text{Si-Ph} = 1.86 \text{ \AA}^{60}$).

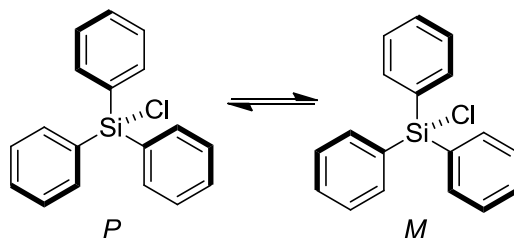


Figure 3.10 Ph_3SiCl undergoes a rapid interconversion between helical propeller conformations.

Despite the rapid interconversion between the helical propeller arrangements of the trityl group, it has been shown that by attaching a chiral ligand to the central carbon atom, the resulting diastereomers will assume a single helical conformation (Figure 3.11).^{64, 65} Therefore, when **2.12** is attached to Ph_3SiCl , this may cause the propeller arrangement to lock into a single conformation. This may also explain how **2.12** can cause the enantioselective silylation of racemic alcohols, since the alcohol will have to pass through the chiral arrangement of the aryl groups (Figure 3.12). Presented will be

the initial studies into the potential to cause a preference for a single helical arrangement around Ph_3SiCl by attaching chiral ligands. Due to the helical conformation of such a molecule, the compound would therefore lend itself well to study by circular dichroism (CD) spectroscopy. CD measures to what degree a compound absorbs circularly polarized light. In particular, if the chiral compound is arranged in a helical conformation, there will be the appearance of a Cotton effect (which occurs when a chiral center is near a chromophore and is observed at a wavelength near the compound's λ_{max}) which would allow for easy confirmation of such a chiral arrangement.

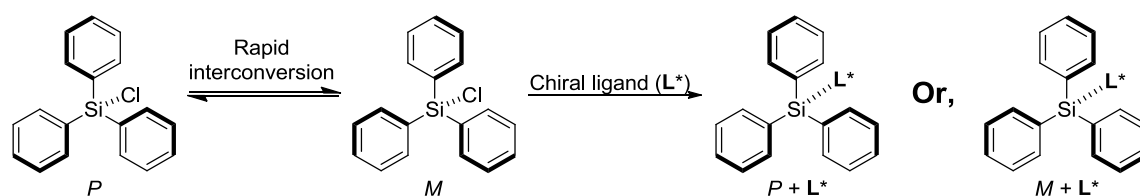


Figure 3.11 By attaching a chiral ligand to Ph_3SiCl , it may be possible to get a single helical arrangement of the phenyl groups.

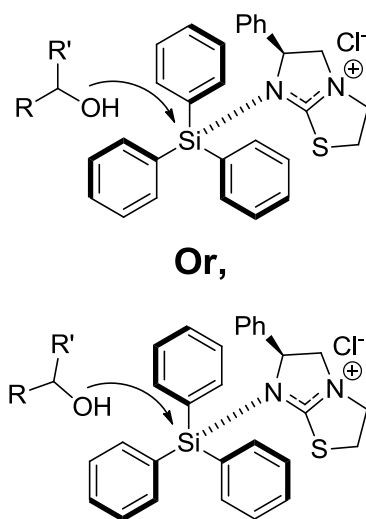


Figure 3.12 The proposed origin of enantiodiscrimination for the enantioselective silylation of secondary alcohols with **2.12** and Ph_3SiCl .

The concept of using a chiral ligand attached to the center atom of a propeller to force a single conformation of the aryl rings has been tested before. This concept was investigated by the Gawronski group in which a series of chiral alcohols were derivatized with a trityl ether protecting group.⁶⁴ The resulting overall helicity was then analyzed by CD spectroscopy and compared to calculated results. One conclusion from this study was that the steric environment surrounding the chiral center of the resulting ether can affect the direction of the attached aryl groups. It was calculated that only two of the three aryl rings were arranged in a helical propeller while the third ring intersected the central plane of the propeller (for some examples see Figure 3.13). This effect was observed even when the difference of steric bulk between the substituents was as small as (S)-2-butanol (**3.12**). The opposite configuration of the aryl groups was observed when the stereocenter was changed from S to R as in **3.13**. Interestingly, the opposite effect was observed when (R)-endo-borneol was derivatized (**3.14**). The observed result suggested that the aryl rings were in the conformation that would be consistent with an S alcohol. This is explained by a long distant steric effect caused by the gem-dimethyl substituents on the bridge (C7) carbon.

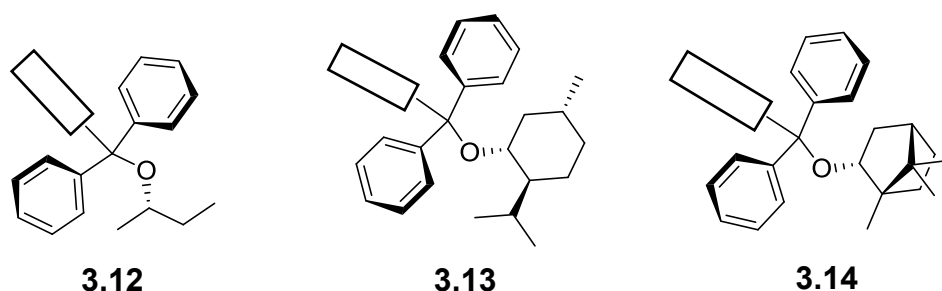


Figure 3.13 Three representative chiral trityl ethers and the reported aryl configuration⁶⁴

Although the work described by the Gawronski group lays the foundation for the possibility that catalyst **2.12** could force a similar enantioselective effect in Ph_3SiCl , the

elongated Si–aryl bond relative to that of the trityl analog may prove to be too long for **2.12** to have much effect on the helicity of Ph_3SiCl . To test whether or not a chiral molecule could affect the aryl conformation of Ph_3SiCl , analogous compounds to those studied by the Gawronski group were prepared (Figure 3.14). Among the derivatized compounds tested were the (R)–(L)–menthol (**3.15**), (S)-endo-borneol (**3.16**), and (S) and (R)-4-chromanol (**3.17** and **3.18** respectively).

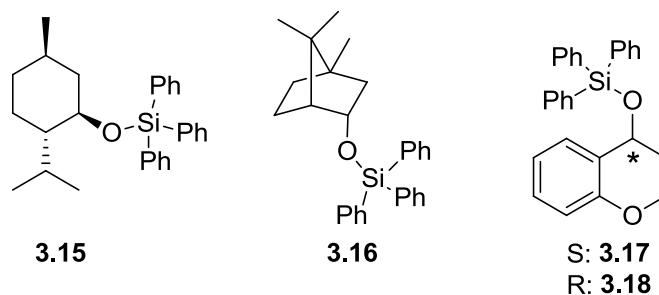


Figure 3.14 Ph_3Si - derivatized silyl ether compounds analyzed via CD spectroscopy.

Once compounds **3.15-3.18** were prepared, the compounds were dissolved in either a 1% or 10% pentane in cyclohexane solution. Because all of the studied compounds showed CD absorbance in short wavelengths, this specific solution was chosen due to the low UV absorbance of cyclohexane. However, due to the low solubility of the compounds in cyclohexane, pentane was added to aid in the dissolving of the compound. Once dissolved to a final concentration of approximately 8.0×10^{-5} M, the samples were analyzed in a 1 mm path length, strain free, quartz cell. The concentration was chosen to give the maximum absorbance without reaching a high tension (HT) voltage >600. Once high tension voltage reaches >600 the detector becomes saturated and false signals can occur.⁶⁶ The choice of cuvette was made to minimize UV absorbance while a 1 mm pathlength was chosen so a higher concentration of sample can

be used to maximize any observed Cotton effect while minimizing HT voltage. All reported spectra was processed by using 15 point Savitzky-Golay smoothing.⁶⁷

Compound **3.15** was shown to give a positive then a negative Cotton effect (recognizable by a positive peak at the longer wavelengths which then crosses the zero rotation axis to give a negative peak at a short wavelength) (Figure 3.15). This CD pattern is similar to what was observed for trityl ether compounds with an (R) configuration at the chiral center of the alcohol. Noteworthy is that the most prominent peaks of the CD spectrum are blue shifted relative to the corresponding trityl ether. This could be due to the lesser angle of the pitch axis of the propeller, itself a result of the longer C–Si bond.

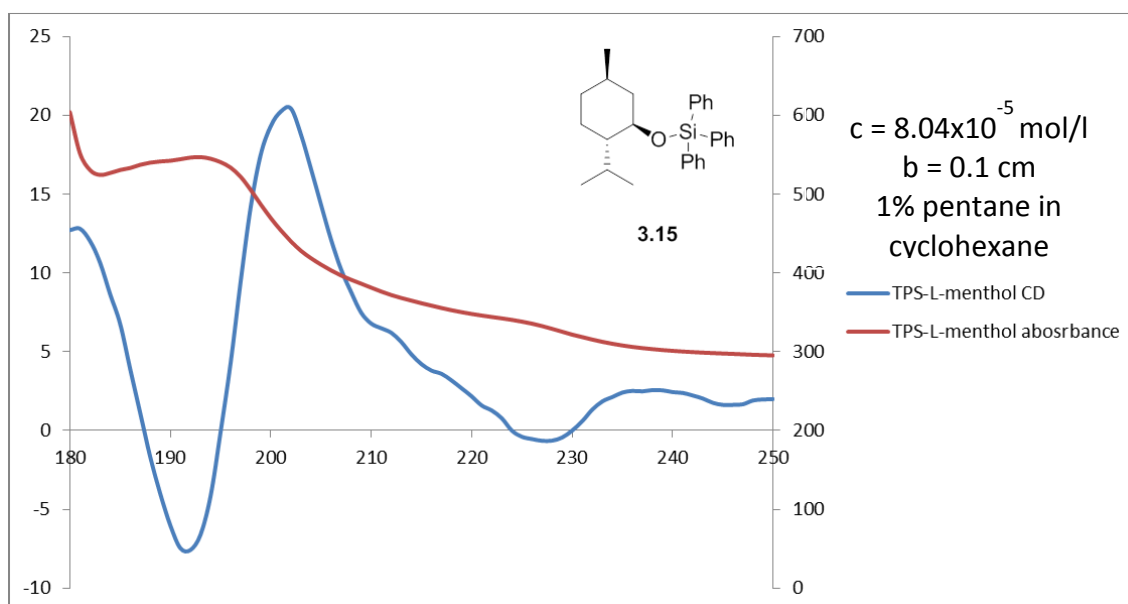


Figure 3.15 The acquired CD spectrum of **3.15** showing a Cotton effect.

When the (S)-endo-borneol silyl ether (**3.16**) was analyzed (Figure 3.16), a similar cotton effect was observed was a negative Cotton effect. Which is a similar Cotton effect to was observed by the Gawronski group. The observed Cotton effect for **3.16**, was smaller in magnitude than **3.15**. This could be due to the smaller pitch axis of the

triphenylsilyl ether as a result of the longer Si–C bond.⁶⁸ However, the Cotton effect was also blue shifted to what was observed by the Gawronski for analogous trityl ether compound.⁶⁴

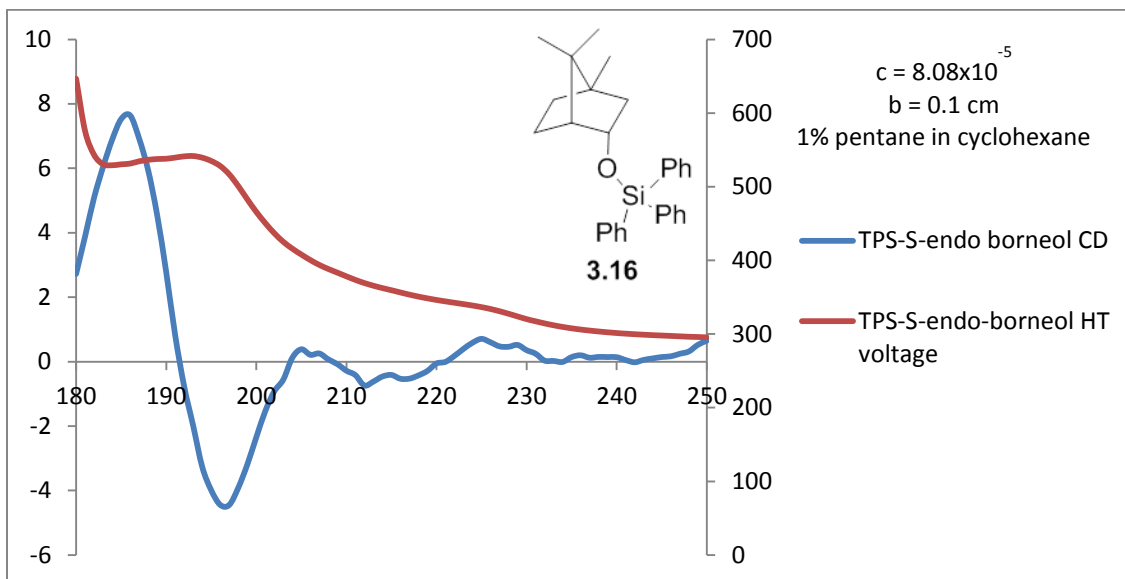


Figure 3.16 The acquired CD spectrum of **3.16**

One of the substrates which gave the best selectivity factor when subjected to the enantioselective silylation reaction, 4-chromanol, was silylated with Ph_3SiCl . Then both the silylated and unsilylated alcohol was analyzed by CD spectroscopy (Figure 3.17). It was observed that the triphenylsilyl ether of (S) and (R) chromanol were found to give Cotton effects. However, all of the compounds presented thus far do not possess chromophores, therefore the unsilylated compounds of the previous silyl ethers cannot have a Cotton effect. The unsilylated alcohol, 4-chromanol, however does possess a chromophore and due to the chiral center's proximity to the chromophore, (R)-4-chromanol was found to cause a Cotton effect. When the silylated and unsilylated material was analyzed, both compounds caused a Cotton effect. Therefore, the CD

analysis of 4-chromanol alone does not confirm a single helical arrangement of the silyl ether aromatic groups.

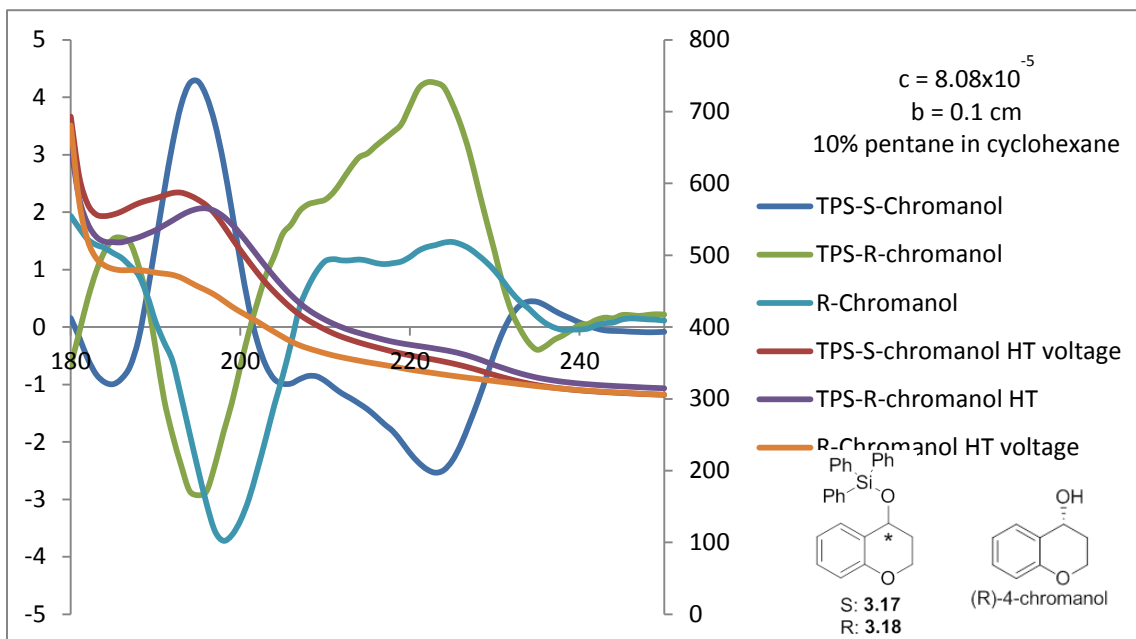


Figure 3.17 The acquired CD spectrum of **3.17** & **3.18**.

3.4 Studying the propeller conformation of silylether compounds in the solid state

To gain further insight into whether or not a single helical conformation can be locked by **2.12**, the triphenylsilyl ether compounds were analyzed by single crystal x-ray analysis. When (S)-endo-borneol (**3.16**) was crystallized, it was observed that two crystals crystallized from solution and these crystals were found to be chemically identical but conformationally distinct. It was found that these two crystals were the two helical conformations of the Ph_3Si moiety of the silyl ether (Figure 3.18). This information combined with the CD results suggest that **3.16** may exist as a single diastereomer in solution, but in the solid state both forms are similar in energy and crystallize to the same extent. There is also the possibility that a ratio of the two

propellers can be found in solution but one is strongly favored and this unequal ratio causes the observed Cotton effect.

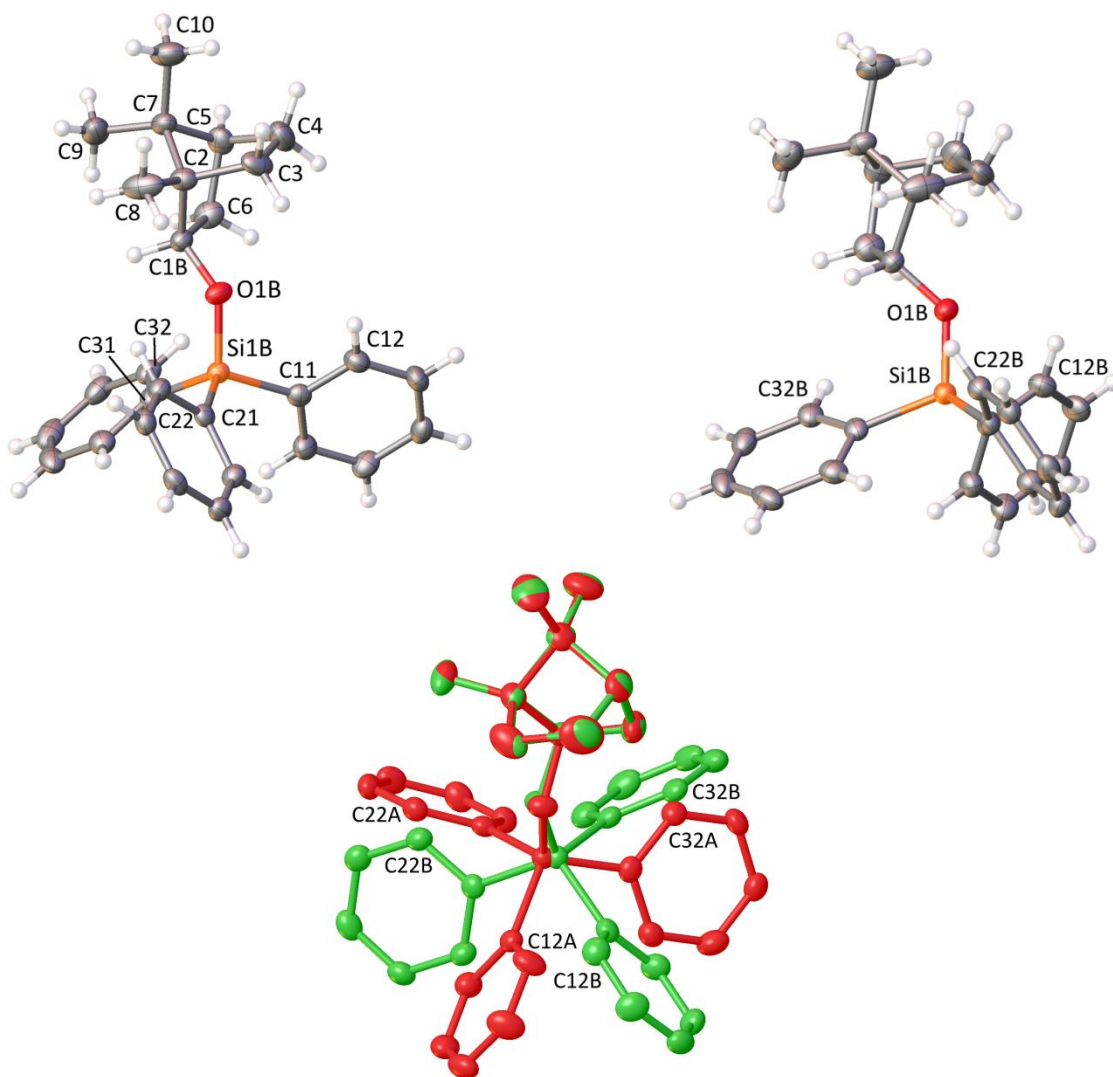


Figure 3.18 The two crystal structures isolated from **3.16** showing both potential helical conformations of the silyl ether group.

Also studied by single crystal diffraction was the triphenylsilyl ether of (S) and (R)-chromanol (**3.17** and **3.18** respectively). However, when **3.17** and **3.18** were synthesized individually and crystals grown of these compounds a different behavior was observed than that of **3.16**. For the 4-chromanol derivatives, only a single crystal was found in both cases, not two distinct crystals such as for **3.16**. Therefore, only a single

diastereomer of the triphenylsilyl ether of (S) and (R) 4-chromanol forms in the solid state. More importantly, the silyl ethers were in a propeller conformation and **3.17** and **3.18** were found to be of opposite helicity (Figure 3.19).

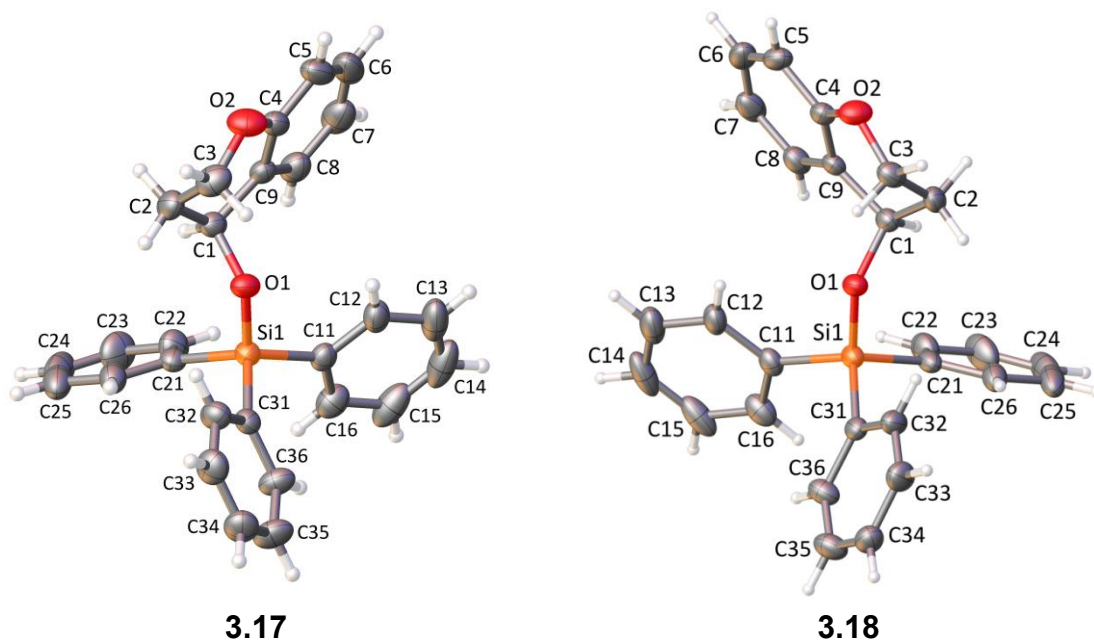


Figure 3.19 The only crystal structures obtained from **3.17** and **3.18**

Future work will include the formation of **2.12**/silylchloride complexes for study by CD. Attempts at analyzing the **2.12**/ Ph_3SiCl complex were unsuccessful due to poor solubility in pentane:cyclohexane solutions. Due to the reproducible occurrence of a small upfield shift in the ^{29}Si resonance (therefore indicating that all silylchloride complexes studied thus far form tetravalent silicon complexes), forming more soluble **2.12**/silylchloride complexes may be a viable option to determine whether or not a Cotton effect is present. Alternatively, using an Ar_3SiCl derivative (such as naphthyl containing silylchlorides) which would absorb at a longer wavelength than Ph_3SiCl would allow for the use of more polar solvents with slightly higher UV cut off (such as acetonitrile) could be used.

3.5 Conclusion

To better understand the mechanism of the enantioselective silylation that was described by the Wiskur group,³ ^1H and ^{29}Si -NMR as well as preliminary circular dichroism (CD) studies were performed. The NMR studies were performed on an intermediate which precipitated out of solution upon the addition of (-)-tetramisole (**2.12**) to Ph_3SiCl in THF. ^1H NMR analysis (in CD_2Cl_2) of the solid when compared to **2.12** showed a slight but significant downfield shift of the bicyclic ring protons of **2.12**. This suggests that **2.12** was coordinated to a slightly Lewis acidic compound, and integration of the protons and their location downfield suggests that the protons are aryl protons. This is what would be expected if the isolated intermediate would be Ph_3SiCl directly coordinated to **2.12**. The intermediate itself was then isolated and added as a stoichiometric silylating reagent to perform a kinetic resolution of racemic 4-chromanol. The resulting selectivity factor was comparable to what was observed when the silylating intermediate was formed in situ, while the hydrolysis products ($\text{Ph}_3\text{Si-OH}$ and hexaphenyldisiloxane) gave little conversion. This suggests that the isolated intermediate was the reactive silylating species and further analysis of this compound could give better insight into the mechanism of the enantioselective silylating reagent. Furthermore, an nOe was observed between the methine proton on **2.12** and what would be the ortho aryl protons on an attached Ph_3SiCl .

With what is believed to be the reactive silylating intermediate isolated, the next question of what the coordination state of silicon was investigated next. The most direct method to determine what the valency of silicon is in the isolated intermediate species is by ^{29}Si -NMR analysis. This is because of the significant upfield shift of silicon

resonances for penta and hexavalent silicon species relative to tetravalent silicon species.^{21, 26, 27} However, what was observed was only a slight upfield shift in the ppm of **2.12**/Ph₃SiCl intermediate from the ppm of Ph₃SiCl (+2.5 ppm for Ph₃SiCl to -11.3 ppm for the **2.12**/Ph₃SiCl complex). This suggests that the isolated intermediate was a tetravalent silicon species. When compared to Ph₃Si–OH and hexaphenyldisiloxane, the ²⁹Si resonances were fairly similar to the isolated species, however, when analyzed by ¹H-²⁹Si gHSQC NMR techniques, the ¹H-NMR resonances were significantly different so as to exclude the potential hydrolysis side products from being the measured silicon resonance for the **2.12**/Ph₃SiCl complex. It was also observed that by increasing the concentration of **2.12** in solution, there was no observable change in the ²⁹Si-resonance; this suggests that there is no equilibrium present between the tetra- and pentavalent species. When other aryl silylchlorides were synthesized and treated with **2.12** similar shifts were also observed suggesting that a tetravalent species was also present in their observed resonances as well.

²⁹Si-Magic angle spinning solid state nmr (²⁹Si SSNMR) was also performed on the isolated solid and this gave similar results to what was observed from the condensed state, ²⁹Si gHSQC NMR analysis. The isolated compound was significantly different from the hydrolysis compounds and unreacted Ph₃SiCl to suggest that in the solid state what was observed was not the precipitation of a hydrolysis product or protonated **2.12**. The solid state results in combination with the condensed state studies fail to disprove the tetravalent silicon hypothesis while no clear evidence of a pentavalent species was observed.

With a clearer mechanistic picture of the silylating species, work on determining how the transfer of chirality occurs was then initiated. Initial studies were performed by testing the hypothesis that the aryl rings were assuming a screw propeller like conformation which was locked into a single chiral conformation by attachment of **2.12**. This is believed to cause a chiral environment in which the attacking chiral alcohol must pass through in order to perform the subsequent alcoholysis of the silylating intermediate. To test this hypothesis, a series of chiral silyl ethers were analyzed by circular dichroism (CD) spectroscopy in which the C–O bond of the silyl ether was a chiral center. These results were then compared to a similar study in which chiral trityl ethers were synthesized and the potential propeller conformations were analyzed by CD spectroscopy.⁶⁴ The observed results suggest that although the C(sp²)–Si bond was in fact longer than the analogous trityl ether compounds, there was still enough influence by the chiral center to give a similar effect to the previous study on trityl ethers. Direct analysis of the **2.12**/Ph₃SiCl intermediate has been elusive due to the insolubility of the complex in the solvents needed to get accurate measurements in the short wavelengths the observed Cotton effect occur. These results are preliminary and further studies such as attempting to analyze chiral amines influence on the helicity of the triphenylsilyl ether as well as the direct analysis of the **2.12**/Ph₃SiCl complex by CD.

3.6 Experimental

All reactions were carried out under a dry N₂ or Ar atmosphere in oven-dried glassware and all NMR experiments were performed with oven-dried NMR tubes. Dry tetrahydrofuran (THF) and hexanes were obtained by passing the previously degassed

solvents through activated alumina columns into a flask containing activated 4Å molecular sieves. Triphenylsilyl chloride was recrystallized from dry, hot hexanes. Diphenylmethylsilyl chloride (DPMS-Cl), dimethylphenyl silyl chloride (DMPS-Cl), triethylsilyl chloride (TES-Cl), and *tert*Butyldimethylsilyl chloride (TBDMS-Cl) were distilled prior to use. CD₂Cl₂ was dried over 4Å MS, then distilled to a Schlenk tube containing 4Å MS. Triethylamine (Et₃N) and hexamethylphosphoramide (HMPA) were stirred over CaH₂ then distilled prior to use. *N*-methylimidazole (NMI) was stirred over Na metal for 3 hours prior to distillation. All chemicals were purchased from major suppliers such as Alfa Aesar, Sigma-Aldrich, TCI, or Acros. Unless otherwise stated all reagents were used as received without further purification. 4Å Molecular sieves (4Å MS) were activated by heating and storage at 170 °C for at least 48 hours prior to use. ¹H NMR spectra were recorded on a Varian Mercury/VX (400 and 500MHz). Chemical shifts are reported in ppm with either TMS (0.00 ppm for ¹H and ¹³C), CD₂Cl₂ (CD₂Cl₂: δ 5.32 and 53.8 ppm for ¹H and ¹³C respectively), or CDCl₃ as the internal standard (CDCl₃: δ 7.26 and 77.0 ppm for ¹H and ¹³C respectively). Data are reported as follows: chemical shift, multiplicity (s = singlet, d = doublet, t = triplet, q = quartet, dd = doublet of doublet, dt = doublet of triplets, dsep = doublet of septet, m = multiplet, br = broad, ur = unresolved multiplet) and coupling constants (Hz). ¹³C NMR spectra were recorded on a Varian Mercury/VX (100 MHz) with complete proton decoupling. Reactions were monitored by thin layer chromatography (TLC) using EMD chemicals 60F silica gel plates. Flash column chromatography was performed on silica gel (32-63 μm). High resolution mass spectrometry (**HRMS**) was performed by the mass spectrometry facility at the University of South Carolina. **IR** data were obtained on a Perkin Elmer Spectrum

100 FT-IR ATR spectrophotometer, ν_{max} in cm^{-1} . All enantiomeric ratios were determined by **HPLC** on an Agilent 1200 series using the chiral stationary phases Daicel Chiralcel AD-H, OJ-H, or OD-H ($4.6 \times 250 \text{ mm} \times 5 \text{ }\mu\text{m}$) columns, and monitored by DAD (Diode Array Detector) in comparison with authentic racemic materials. Melting points (**mp**) were taken with a Laboratory Devices Mel-Temp and were uncorrected. **Optical rotations** were obtained using a JASCO P-1010 polarimeter.

General procedure for the formation of Lewis base/ $R^1R^2R^3\text{Si-Cl}$ complex and ^{29}Si -NMR samples

In an inert N_2 atmosphere glovebox, to an oven dried 4-dram vial fitted with an oven-dried Teflon coated stir was added Lewis base (25.0 mg). The vial was then charged with 1 mL dry THF and to the solution was added $R^1R^2R^3\text{Si-Cl}$ (1.0 equiv.). In most cases, almost instantly, a white precipitant formed. The reaction was then stirred vigorously for ca. 10 minutes and evacuated to dryness. The vial was then charged with 1 mL of freshly distilled CD_2Cl_2 . 0.9 mL of the heterogeneous solution was then transferred to an oven-dried NMR tube, capped, sealed with parafilm and placed in a desiccator. Due to the poor solubility of the complexes in CD_2Cl_2 , just prior to analysis, the NMR sample was centrifuged.

All NMR samples were prepared in a glovebox using oven dried glassware and freshly distilled deuterated solvents. Upon preparation of samples, they were placed in a desiccator until ready to be analyzed.

General Procedure for the preparation of Ar₃Si–OH

To a 4 dram vial fitted with a stir bar was added Ar₃Si–Cl (2–3 mmol). The vial was then charged with THF (2 mL) then DI water (4 mL), except for (*p*BuAr)₃Si–Cl which was dissolved in THF then diethyl ether was added until the suspension became homogenous. The reaction was left to stir for 24 hours. After this time, the reaction was then extracted with EtOAc (3x, 3 mL). The extracts were then filtered through a pad of silica gel. The filtrate was then evaporated to dryness and purified by flash column chromatography (CH₂Cl₂ to 2% MeOH in CH₂Cl₂).

Et₃Si–OH: 147.6 mg (54%); Also isolated was (Et₃Si)₂–O: 67.2 mg (26%)

*t*BuMe₂Si–OH: 206.1 mg (48%)

Ph₂MeSi–OH: 194.0 mg (81%); Also isolated was (Ph₂MeSi)₂–O: 15.9 mg (6%)

MePh₂Si–OH: 13.2 mg (5%); Also isolated was (PhMe₂Si)₂–O: 185.1 mg (78%)

(*p-t*BuAr)₃Si–OH: 57 mg (48%)

General Procedure for the preparation of (Ar₃Si)₂–O

Under a N₂ atmosphere was added silanol (0.2-0.4 mmol) and silyl chloride (1.1 equiv.) to an oven-dried 4-dram vial fitted with a stir bar. To the vial was then charged 2 mL dry THF. The solution was then treated with DIPEA (1.0 equiv.) then *N*-methylimidazole (1.0 equiv.) and the reaction was left to stir for 24 h. The reaction was then quenched with 3 mL of 1 M HCl, then 1 mL of NaHCO₃, then 1 mL brine. The product was then taken up in diethyl ether (3x, 1 mL). The ethereal layer was then dried over sodium sulfate, filtered, and evaporated to dryness. The crude was then purified by flash column

chromatography (silica gel, CH₂Cl₂; except for [(p-*t*BuAr)₃Si]₂-O in which the mobile phase used was 4:1 hexanes: CH₂Cl₂ to 1:1 hexanes: CH₂Cl₂) to give the desired disiloxane.

(*t*BuMe₂Si)₂-O: 3.4 mg (3%)

(Ph₂MeSi)₂-O: 67.7 mg (53%)

[(p-*t*BuAr)₃Si]₂-O: 8.2 mg (15%)

General procedure for the silylation based kinetic resolution of secondary alcohols using the Ph₃SiCl/2.12 complex and desilylation of the isolated products.

In an inert N₂ atmosphere in a glovebox an oven dried 1 dram vial with activated 4 Å molecular sieves (20-25 mg) was fitted an oven dried Teflon coated stir bar. To the vial was added **2.12** (51.1 mg, 0.25 mmol) and freshly recrystallized Ph₃SiCl (73.7 mg, 0.25 mmol). The vial was then charged with 1.67 mL anhydrous THF. The solution was stirred vigorously for 5 minutes, during which time a thick white precipitant formed. Then vial was then taped close, fitted with a septum and taped again. The solvent was then removed under vacuum. The vial was then cooled to -78 °C and the vial was then charged with 43.5 µL of DIPEA then treated with 1 mL of a 0.5 M solution of 4-chromanol. The reaction was then stirred vigorously for 4.5 h at -78 °C. The reaction was then quenched with 1 mL MeOH and poured into a 4-dram vial containing 1.0 mL sat. aqueous NH₄Cl and extracted with diethyl ether (3 x 5 mL), the ethereal layer was then pushed through a pad of silica gel. The filtrate was then evaporated to dryness and

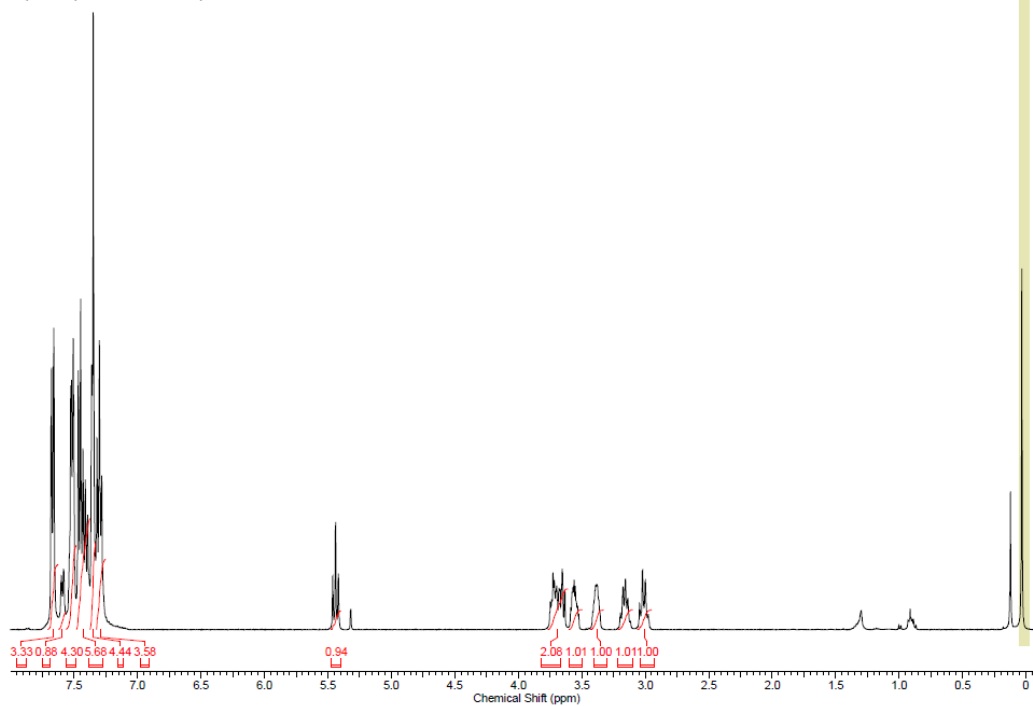
purified by silica gel chromatography (4:1 hexanes:CH₂Cl₂ followed by 2% MeOH in CH₂Cl₂). The unreacted alcohol was then analyzed by HPLC with a chiral stationary phase.

The purified silyl ether was dissolved in 3 mL THF and fitted with a Teflon coated stir bar. The solution was treated with 1.6 mL TBAF (1 M in THF) and stirred at ambient temperature for 10 h. The reaction was quenched with brine and extracted with diethyl ether (3 x 3 mL) and dried over silica gel. After filtration and removal of solvent, the crude was purified by silica gel chromatography (1:1 hexanes: H₂Cl₂ to 5% MeOH in CH₂Cl₂).

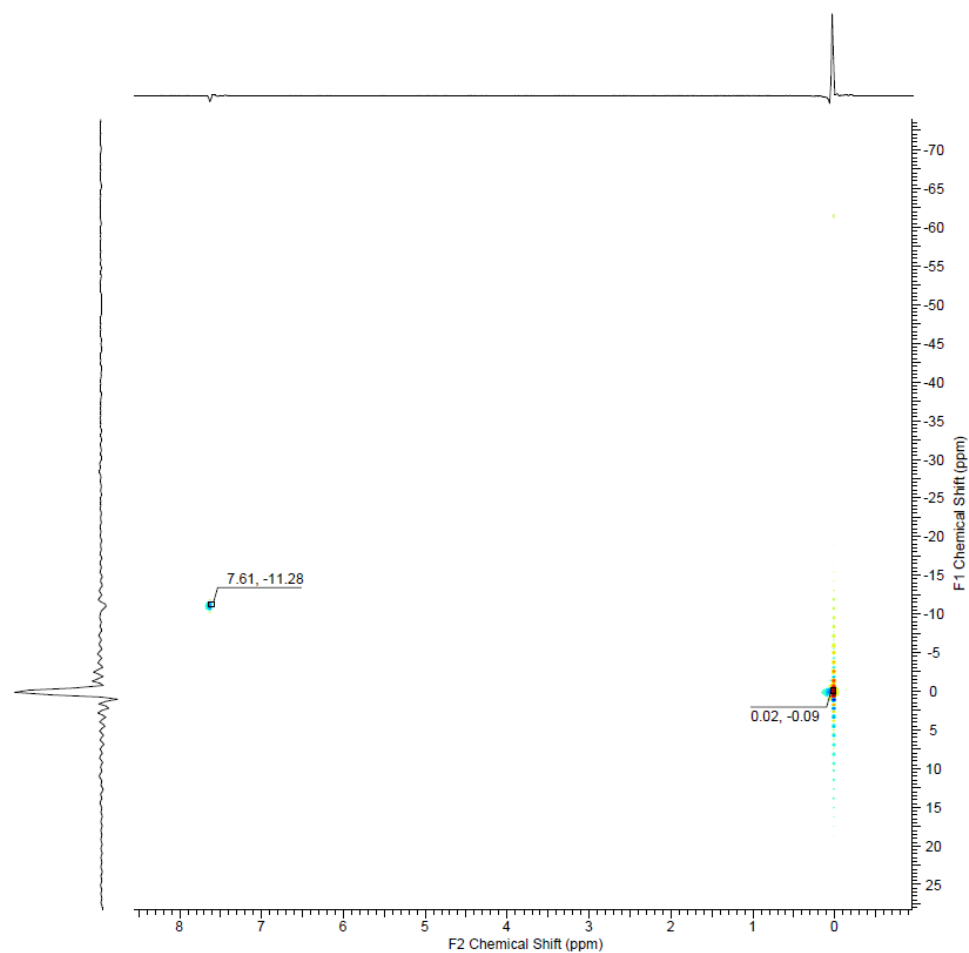
Spectral data

2.12/Ph₃SiCl, -78 °C:

¹H NMR (400 MHz, DICHLOROMETHANE-*d*₂) δ ppm 3.01 (q, *J*=9.33 Hz, 1 H) 3.10 - 3.22 (m, 1 H) 3.33 - 3.43 (m, 1 H) 3.50 - 3.60 (m, 1 H) 3.61 - 3.77 (m, 2 H) 5.44 (t, *J*=8.87 Hz, 1 H) 7.30 (t, *J*=7.41 Hz, 4 H) 7.33 - 7.37 (m, 5 H) 7.37 - 7.48 (m, 7 H) 7.48 - 7.56 (m, 5 H) 7.59 (d, *J*=7.50 Hz, 1 H) 7.67 (d, *J*=6.77 Hz, 1 H)

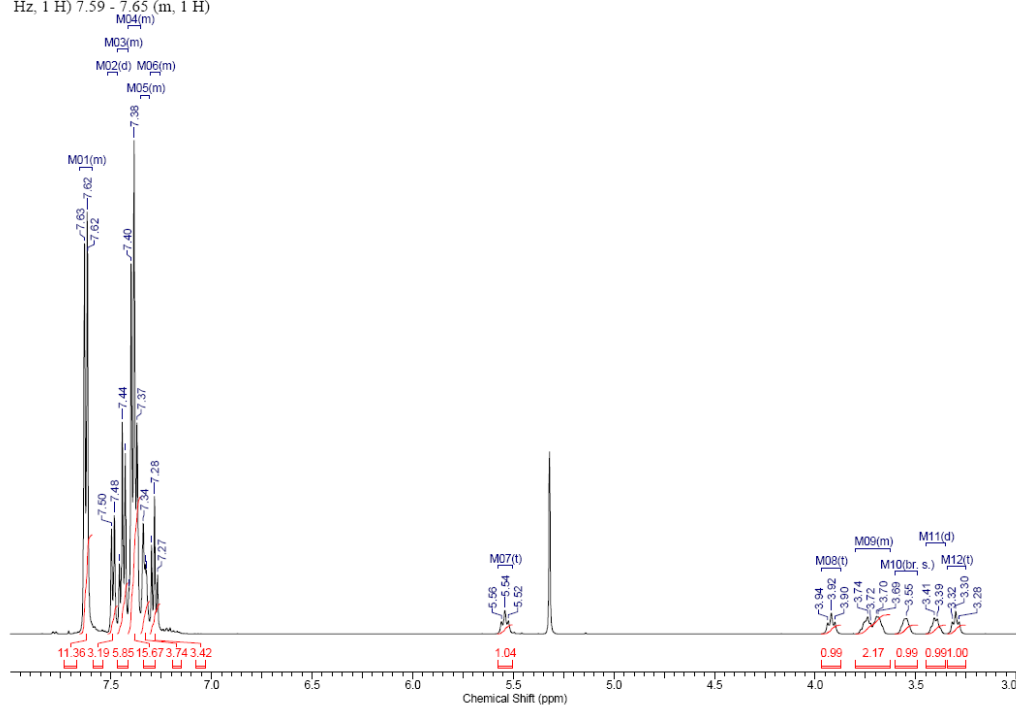


^1H - ^{29}Si gHSQC NMR

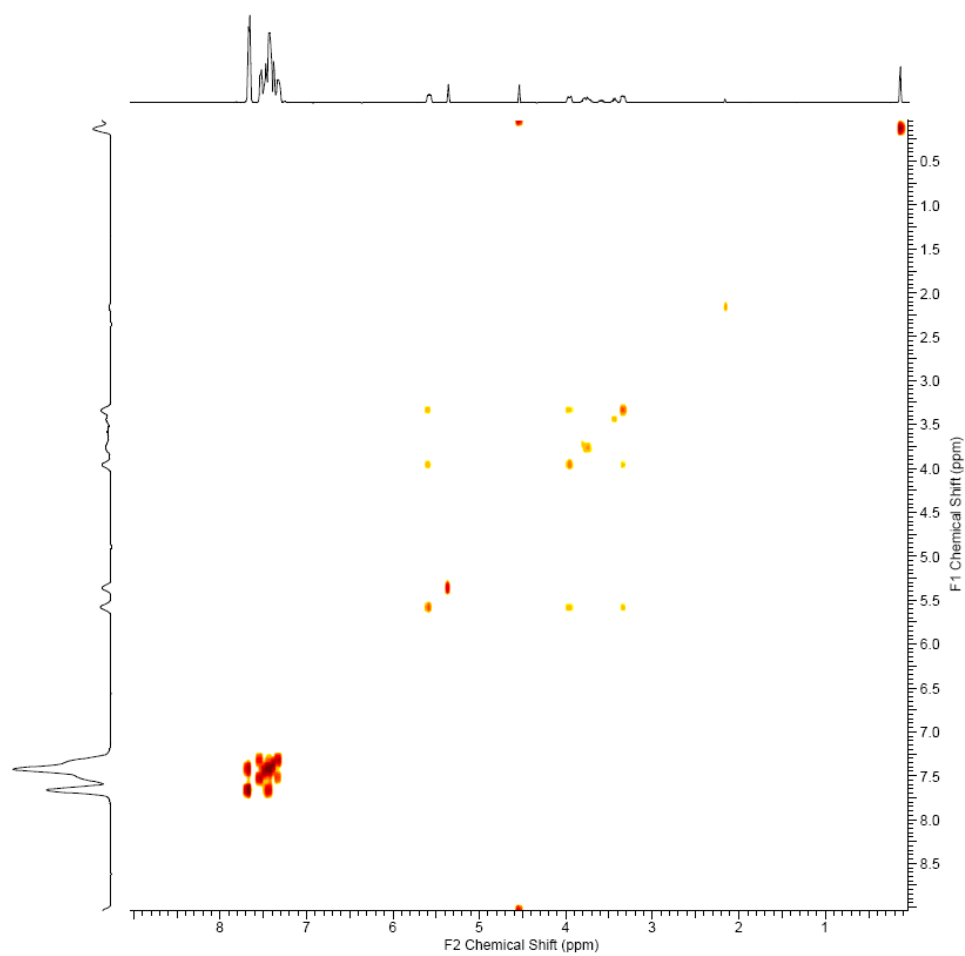


2.12/Ph₃SiCl, 20 °C:

¹H NMR (500 MHz, DICHLOROMETHANE-*d*₂) δ ppm 3.30 (t, *J*=8.43 Hz, 1 H) 3.40 (d, *J*=7.57 Hz, 1 H) 3.55 (br. s., 1 H) 3.63 - 3.80 (m, 2 H) 3.92 (t, *J*=9.04 Hz, 1 H) 5.54 (t, *J*=8.55 Hz, 1 H) 7.26 - 7.31 (m, 1 H) 7.31 - 7.35 (m, 1 H) 7.35 - 7.41 (m, 3 H) 7.42 - 7.47 (m, 1 H) 7.49 (d, *J*=6.84 Hz, 1 H) 7.59 - 7.65 (m, 1 H)

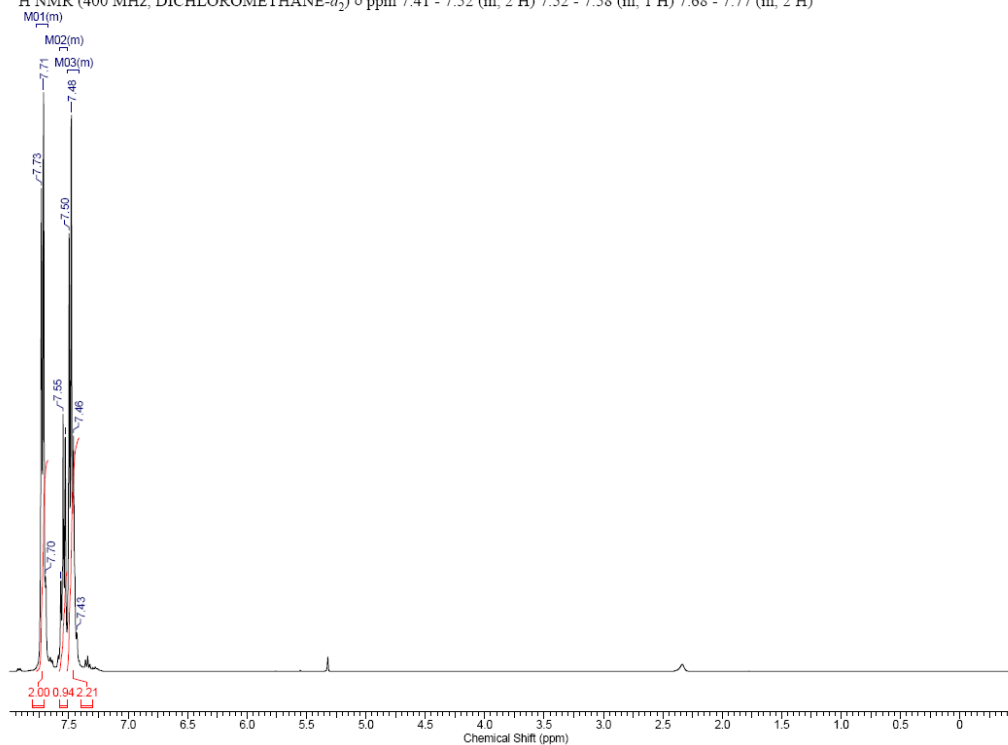


COSY

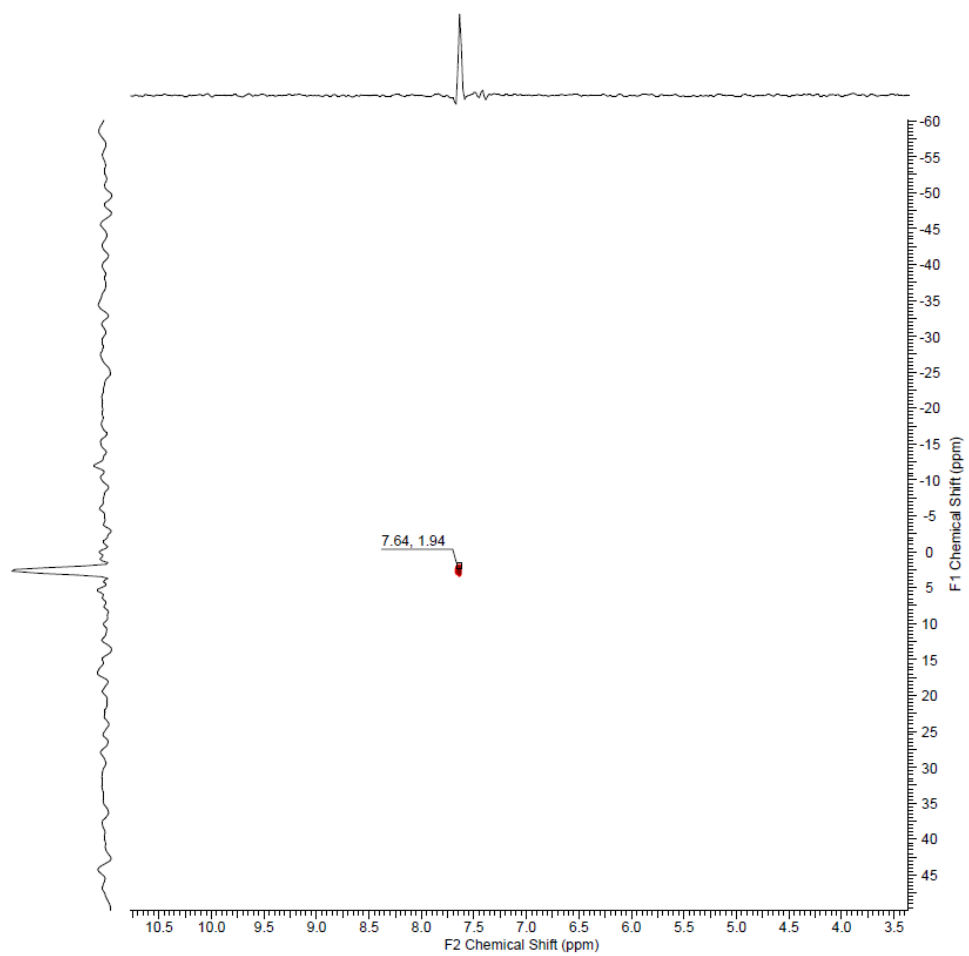


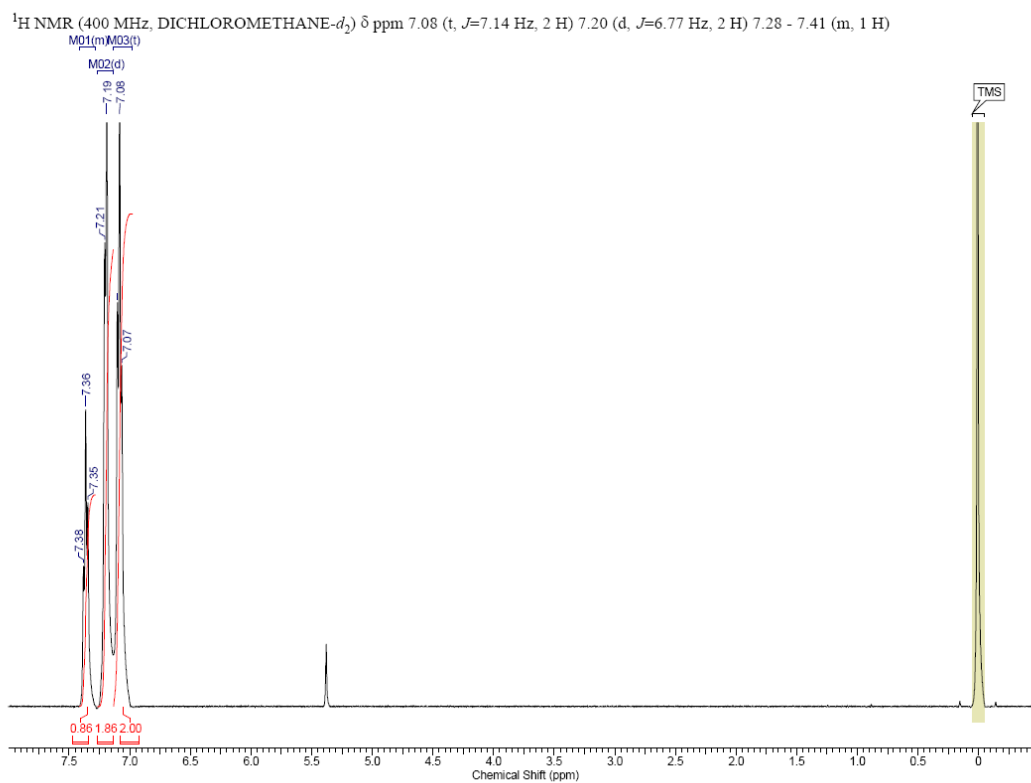
Ph_3SiCl

^1H NMR (400 MHz, $\text{DICHLOROMETHANE-}d_2$) δ ppm 7.41 - 7.52 (m, 2 H) 7.52 - 7.58 (m, 1 H) 7.68 - 7.77 (m, 2 H)

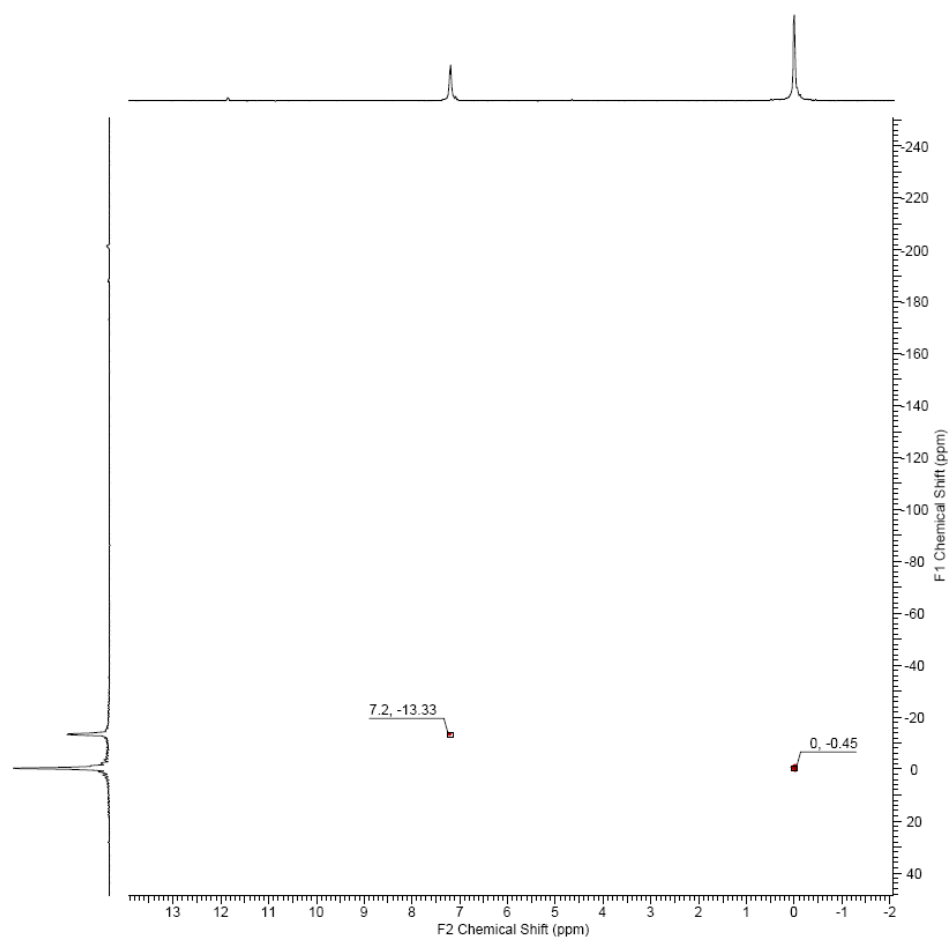


^1H - ^{29}Si gHSQC NMR



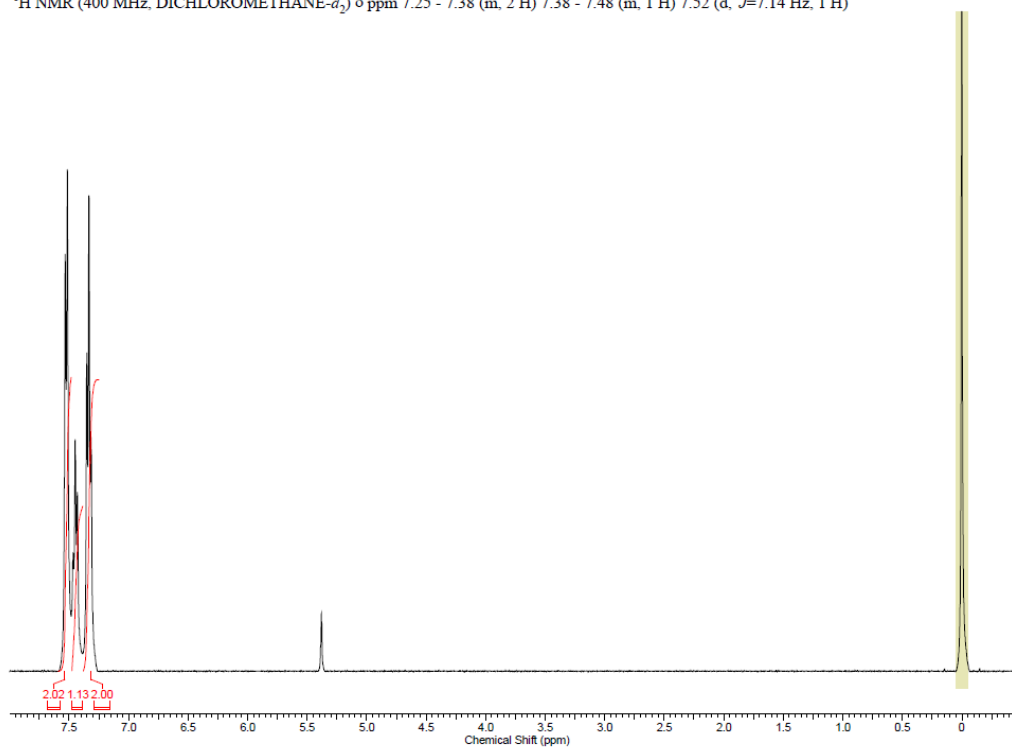


^1H - ^{29}Si gHSQC NMR

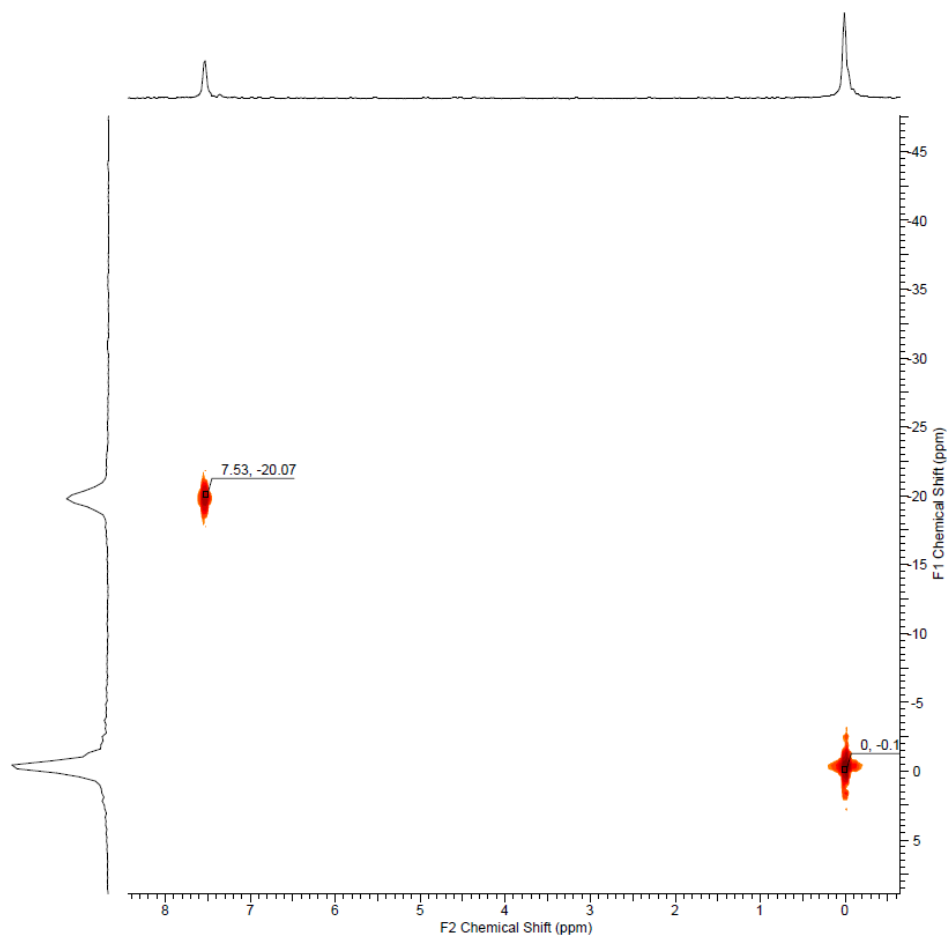


HPDS

^1H NMR (400 MHz, DICHLOROMETHANE- d_2) δ ppm 7.25 - 7.38 (m, 2 H) 7.38 - 7.48 (m, 1 H) 7.52 (d, $J=7.14$ Hz, 1 H)

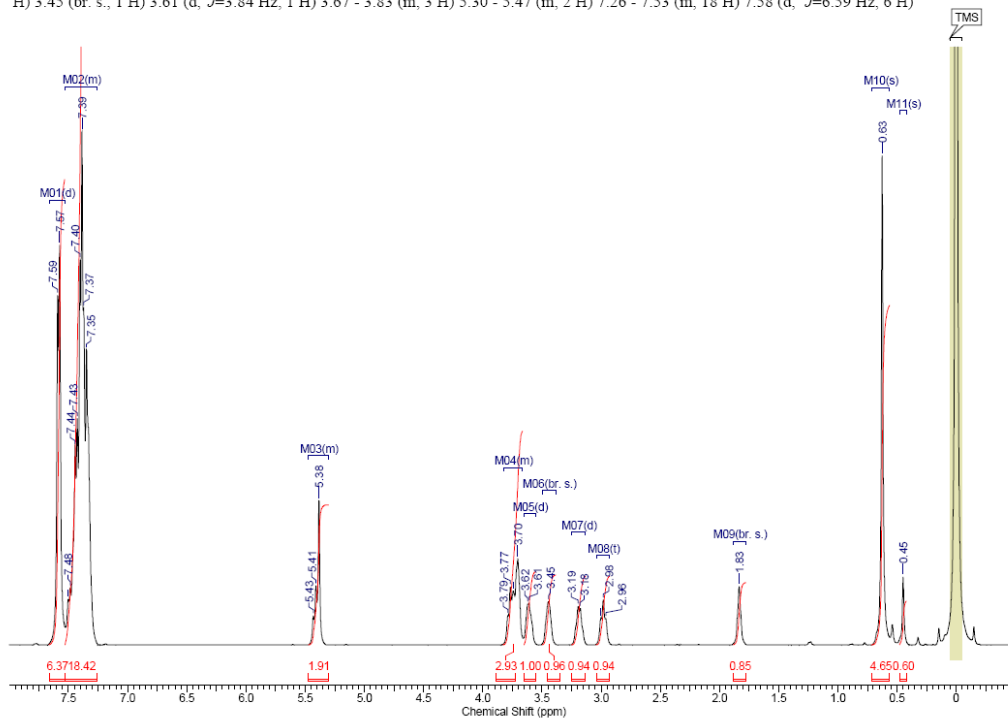


^1H - ^{29}Si gHSQC NMR

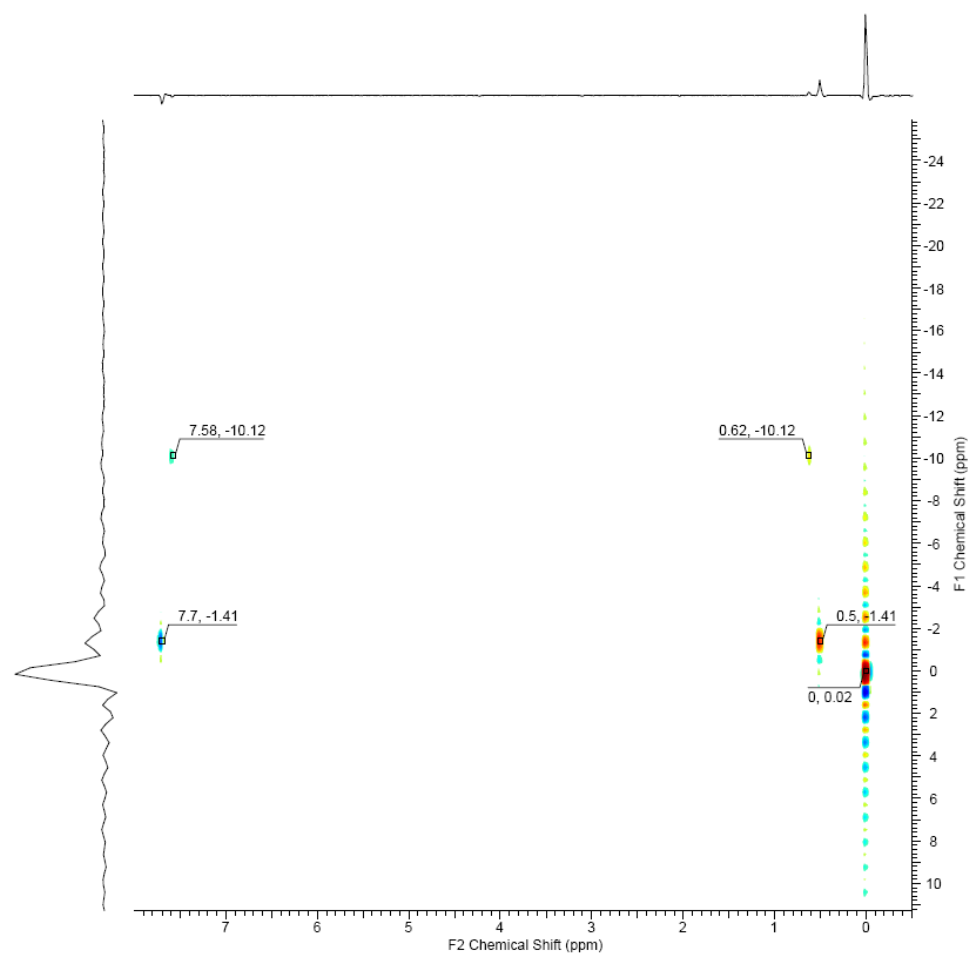


2.12/Ph₂MeSiCl

¹H NMR (400 MHz, DICHLOROMETHANE-*d*₂) δ ppm 0.45 (s, 1 H) 0.63 (s, 5 H) 1.83 (br. s., 1 H) 2.98 (t, *J*=8.23 Hz, 1 H) 3.19 (d, *J*=6.95 Hz, 1 H) 3.45 (br. s., 1 H) 3.61 (d, *J*=3.84 Hz, 1 H) 3.67 - 3.83 (m, 3 H) 5.30 - 5.47 (m, 2 H) 7.26 - 7.53 (m, 18 H) 7.58 (d, *J*=6.59 Hz, 6 H)

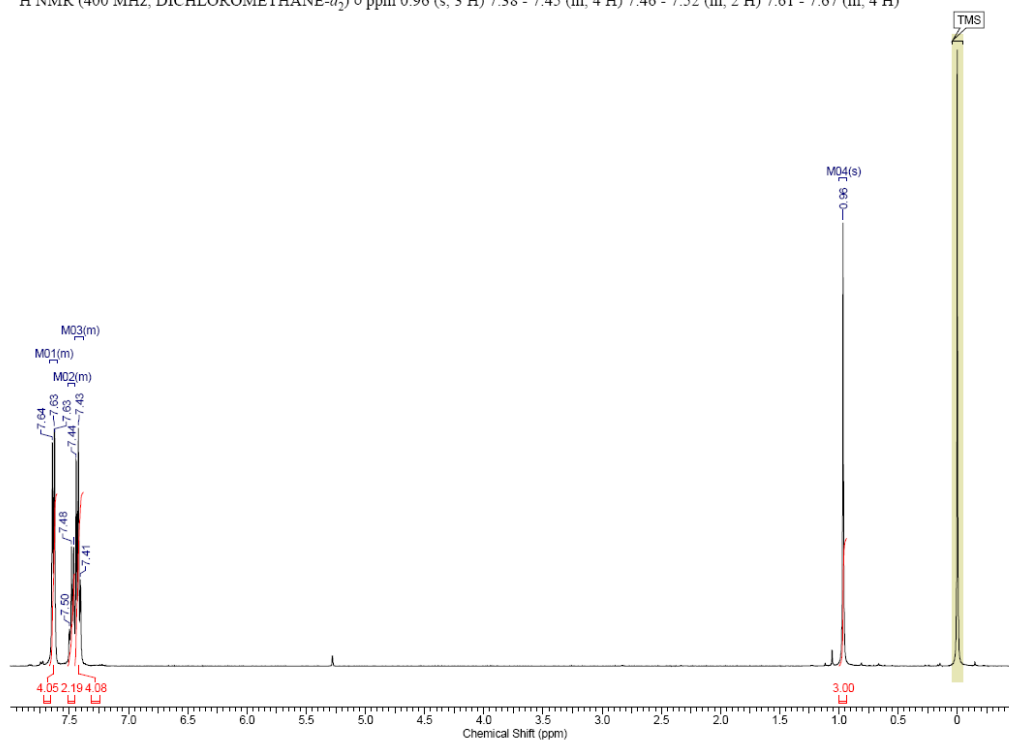


^1H - ^{29}Si gHSQC NMR

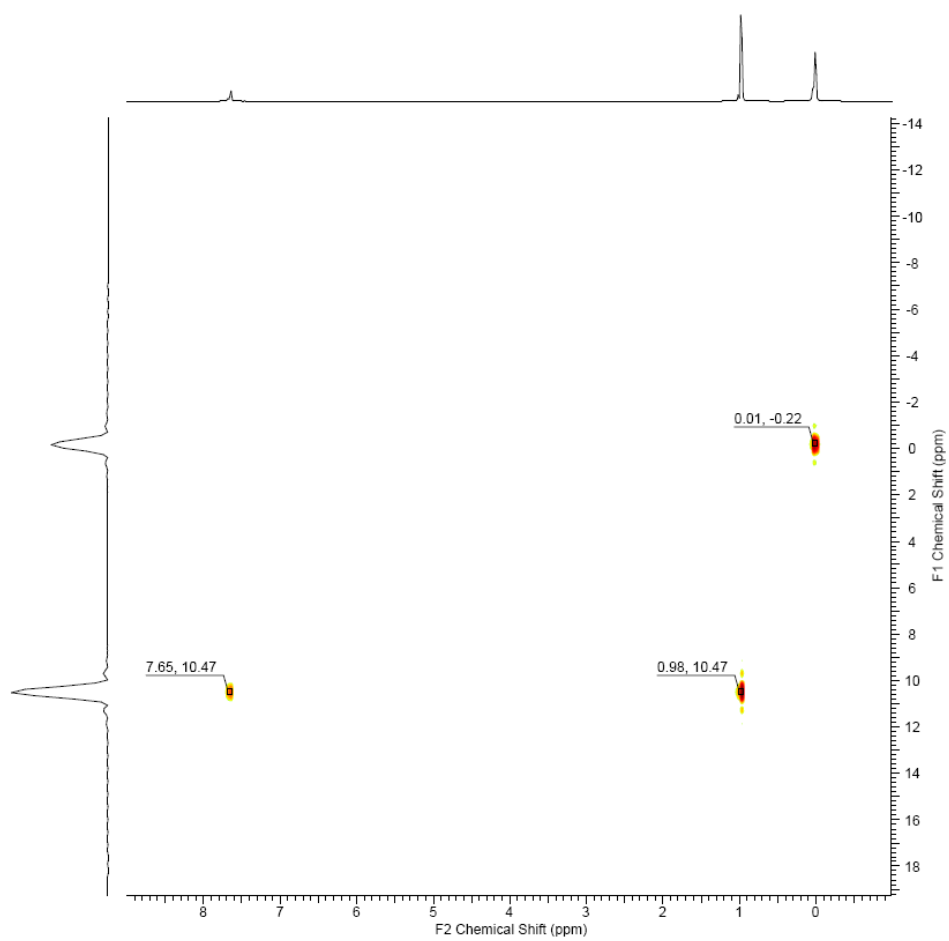


Ph₂MeSiCl

¹H NMR (400 MHz, DICHLOROMETHANE-*d*₂) δ ppm 0.96 (s, 3 H) 7.38 - 7.45 (m, 4 H) 7.46 - 7.52 (m, 2 H) 7.61 - 7.67 (m, 4 H)

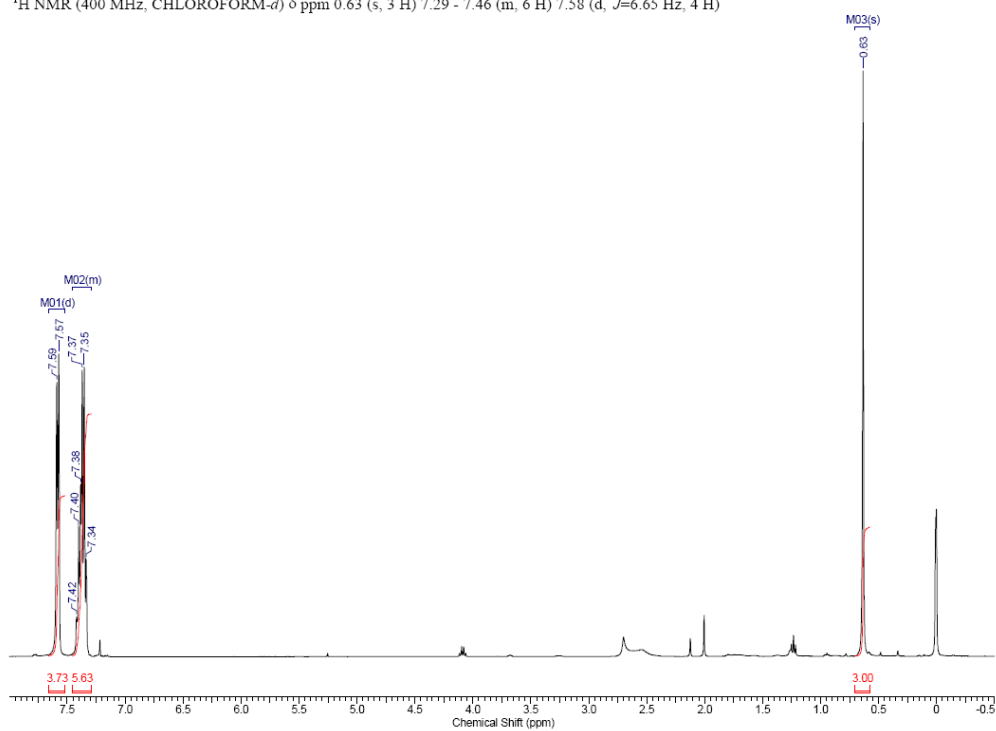


^1H - ^{29}Si gHSQC NMR

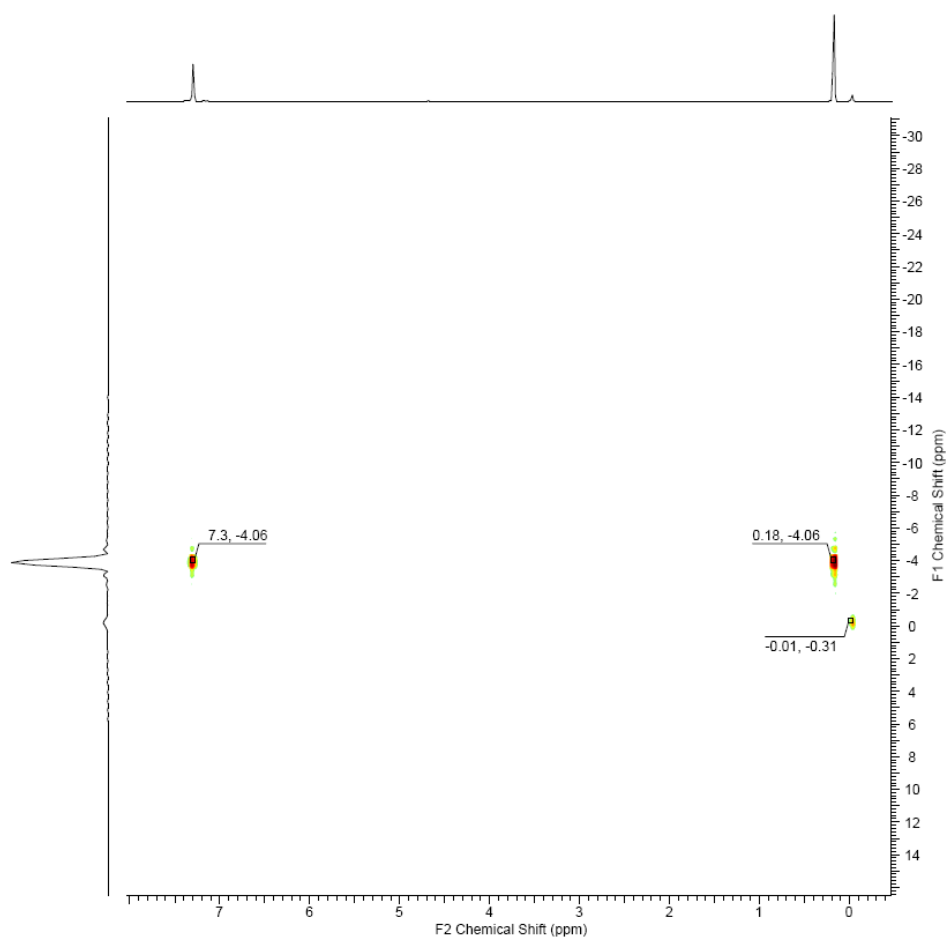


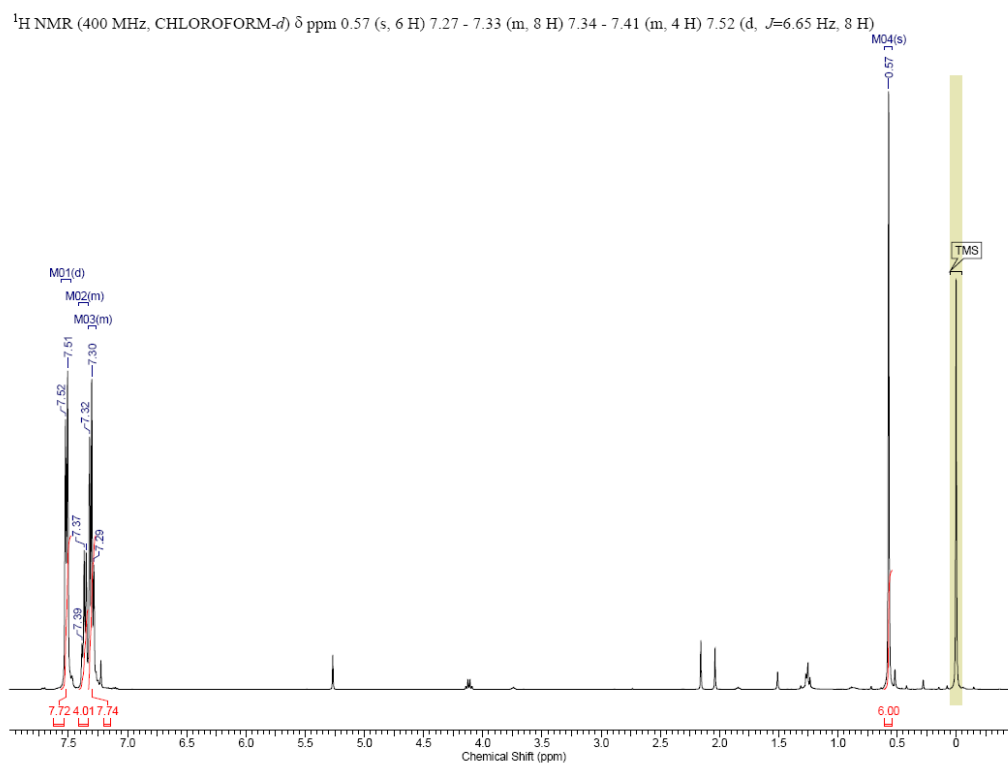
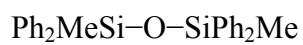
Ph₂MeSiOH

¹H NMR (400 MHz, CHLOROFORM-*d*) δ ppm 0.63 (s, 3 H) 7.29 - 7.46 (m, 6 H) 7.58 (d, *J*=6.65 Hz, 4 H)

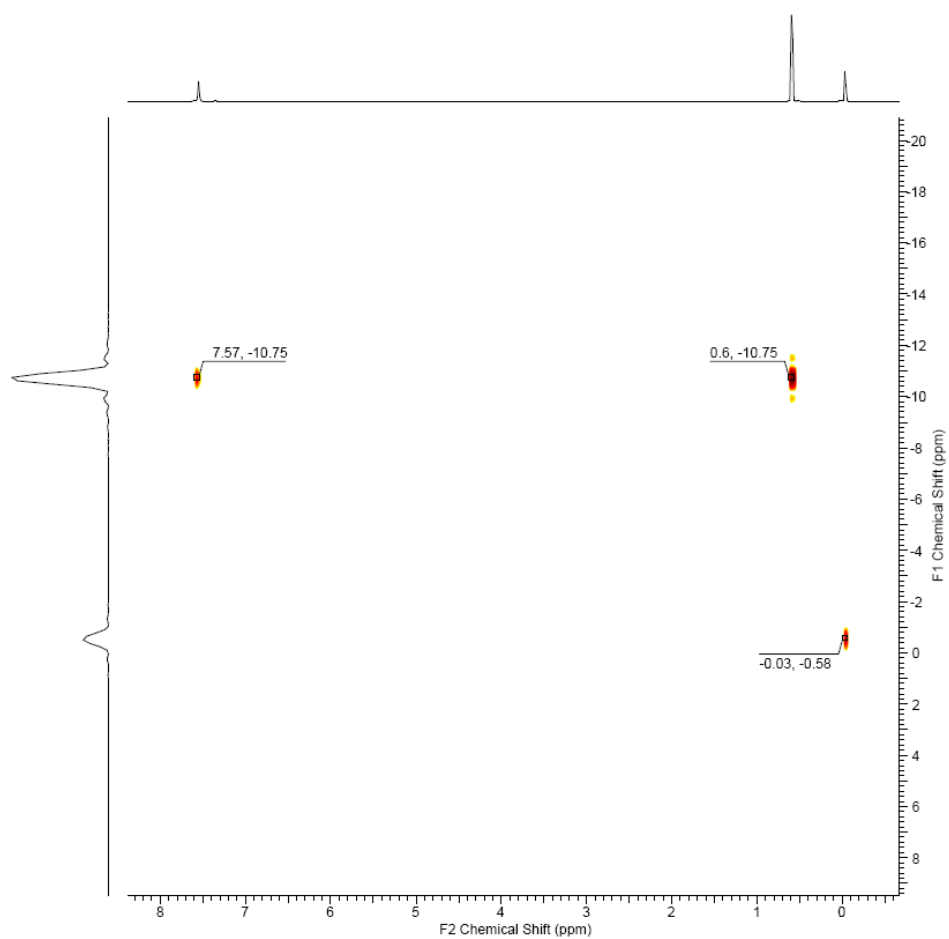


^1H - ^{29}Si gHSQC NMR



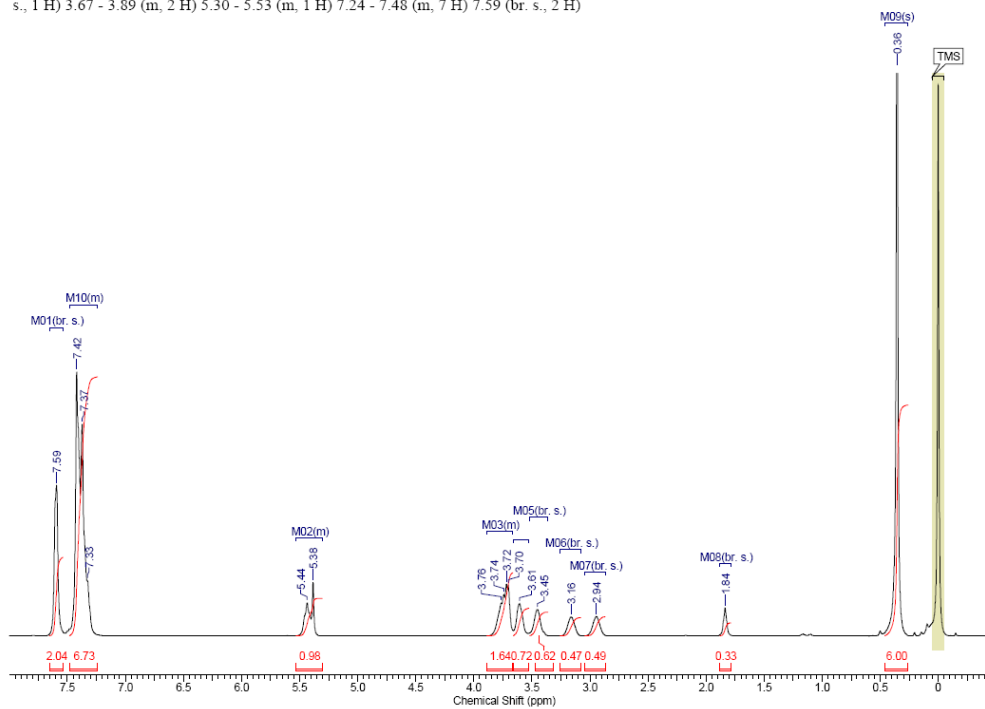


^1H - ^{29}Si gHSQC NMR

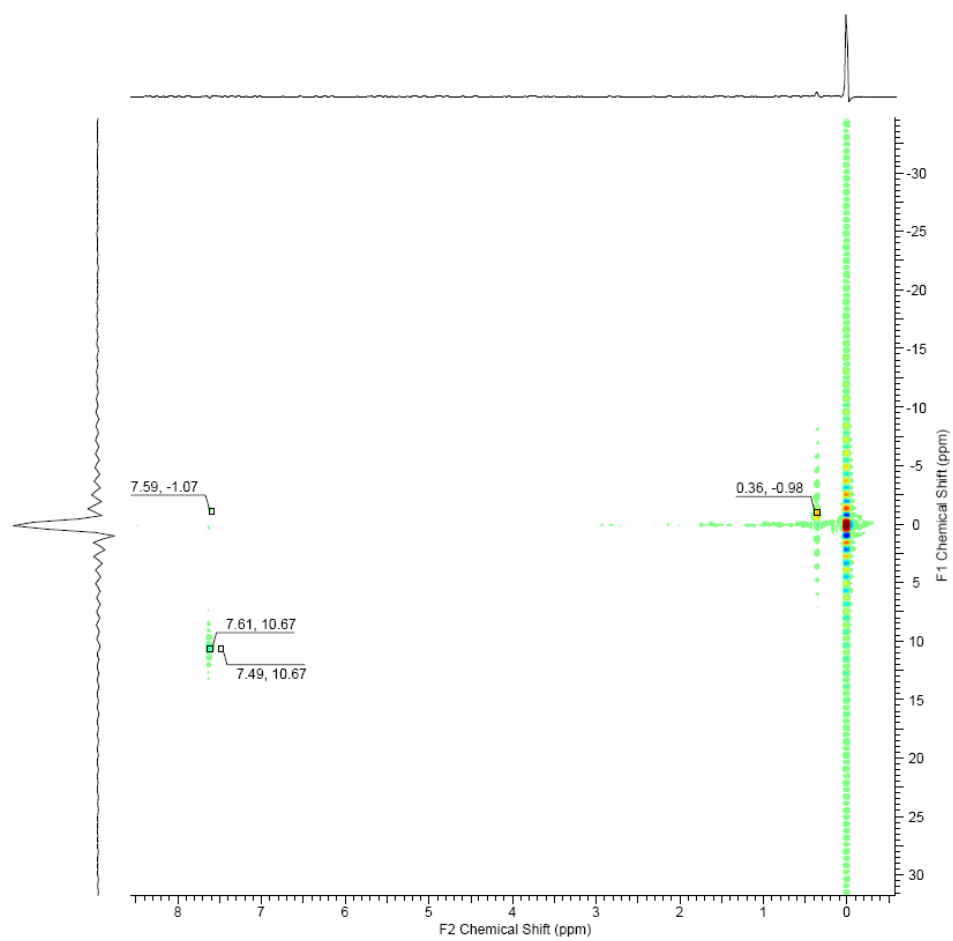


2.12/PhMe₂SiCl

¹H NMR (400 MHz, DICHLOROMETHANE-*d*₂) δ ppm 0.36 (s, 6 H) 1.84 (br. s., 1 H) 2.94 (br. s., 1 H) 3.16 (br. s., 1 H) 3.45 (br. s., 1 H) 3.61 (br. s., 1 H) 3.67 - 3.89 (m, 2 H) 5.30 - 5.53 (m, 1 H) 7.24 - 7.48 (m, 7 H) 7.59 (br. s., 2 H)

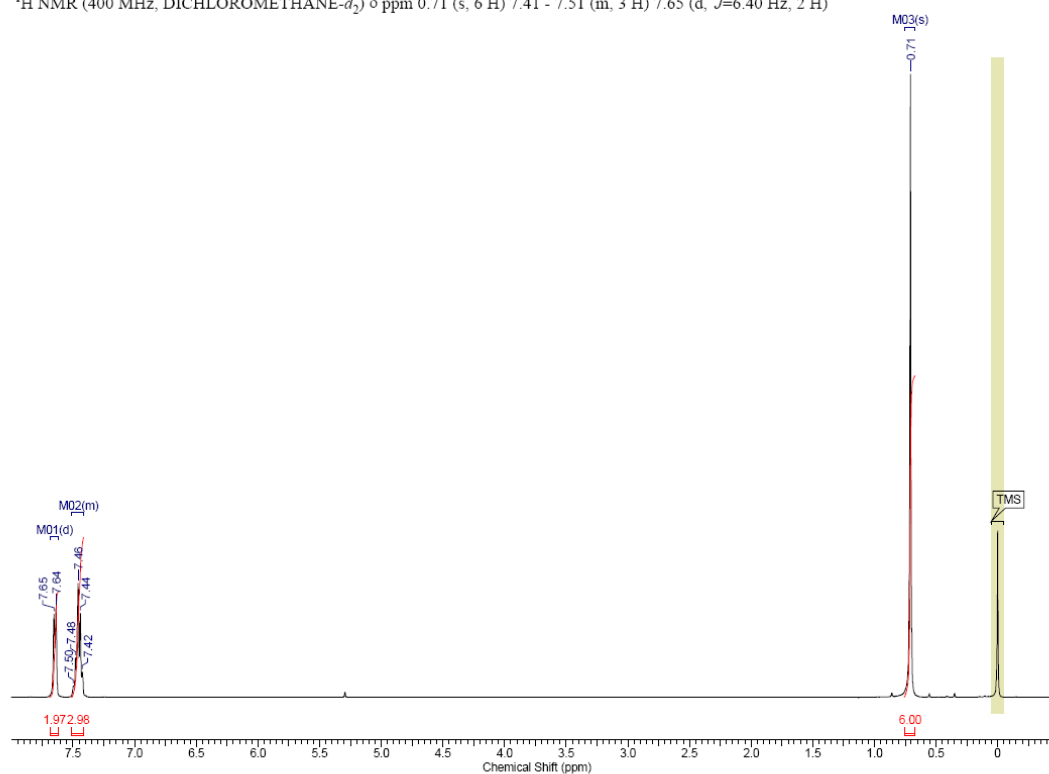


^1H - ^{29}Si gHSQC NMR

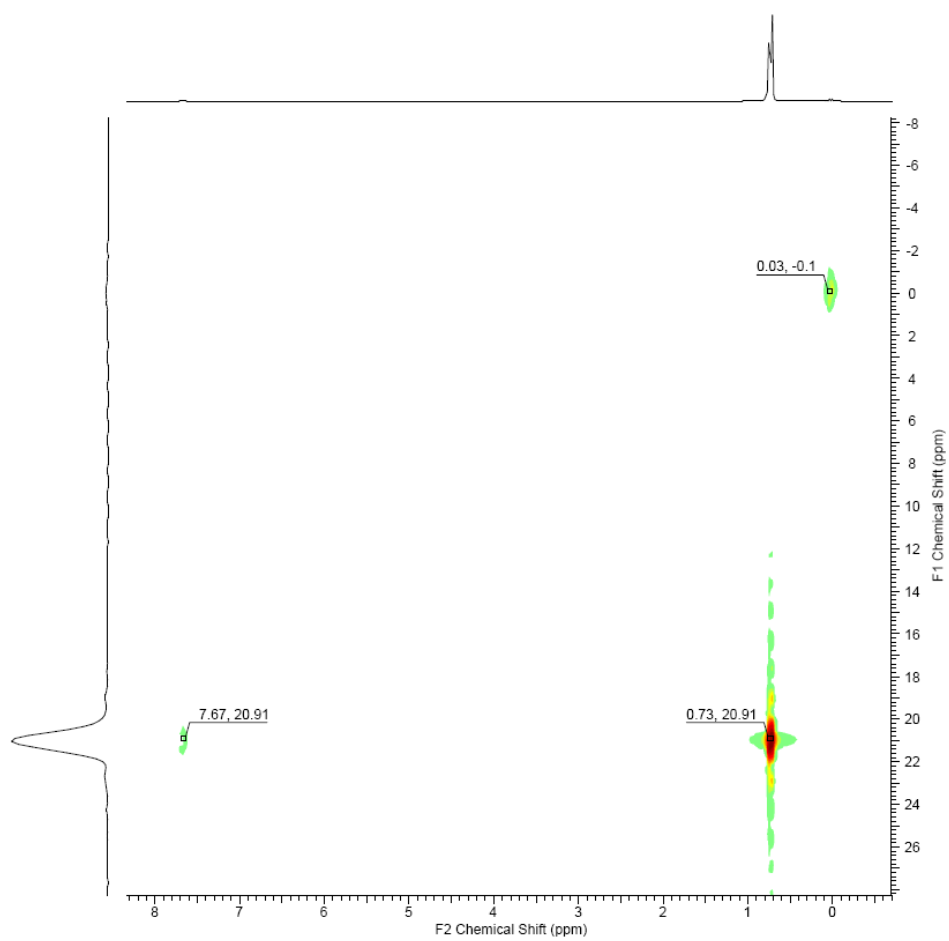


PhMe₂SiCl

¹H NMR (400 MHz, DICHLOROMETHANE-*d*₂) δ ppm 0.71 (s, 6 H) 7.41 - 7.51 (m, 3 H) 7.65 (d, *J*=6.40 Hz, 2 H)

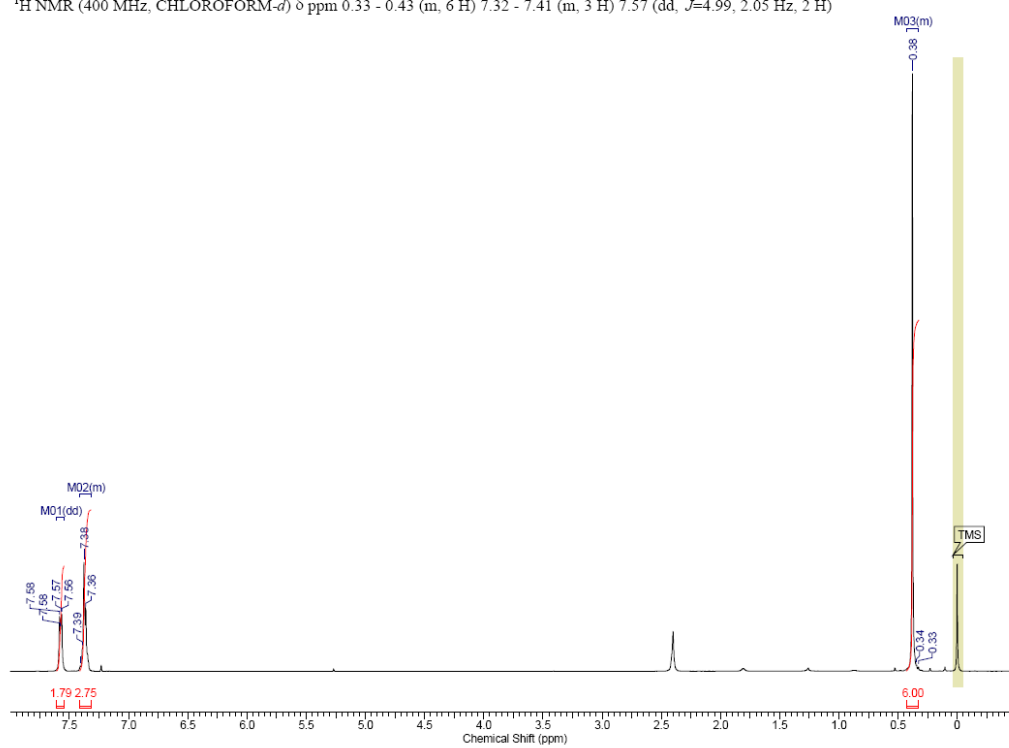


^1H - ^{29}Si gHSQC NMR

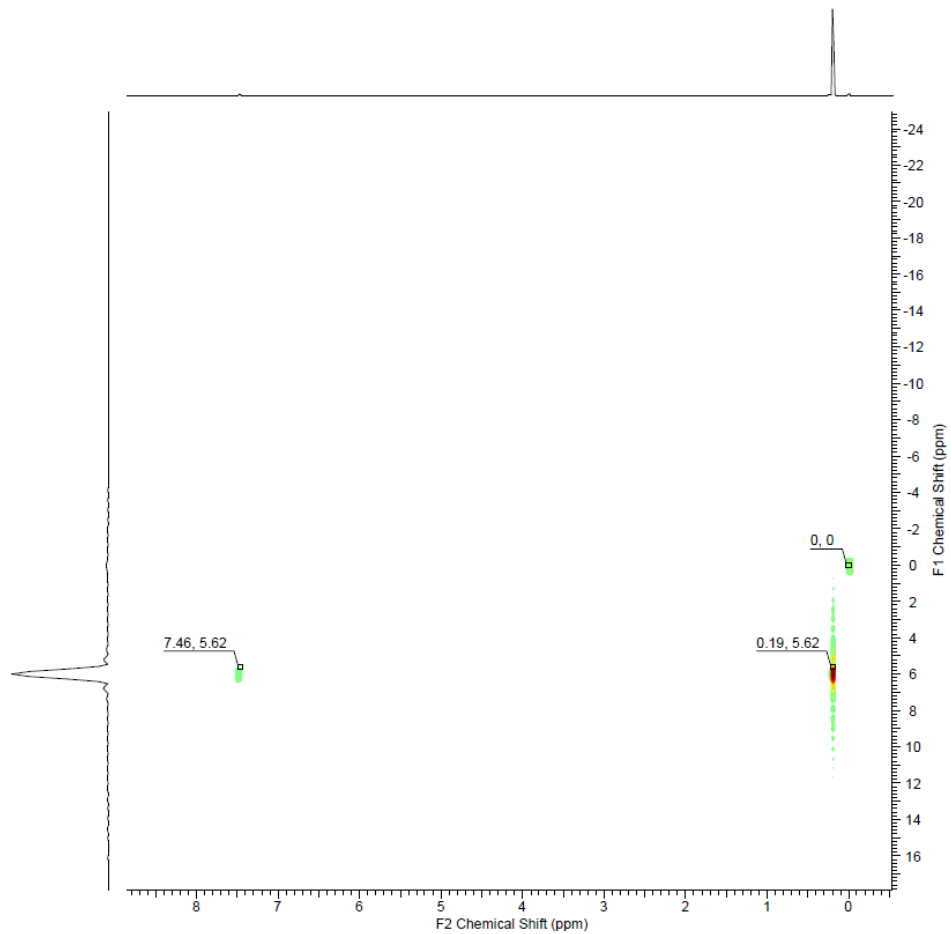


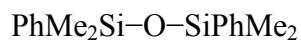
PhMe₂SiOH

¹H NMR (400 MHz, CHLOROFORM-*d*) δ ppm 0.33 - 0.43 (m, 6 H) 7.32 - 7.41 (m, 3 H) 7.57 (dd, *J*=4.99, 2.05 Hz, 2 H)

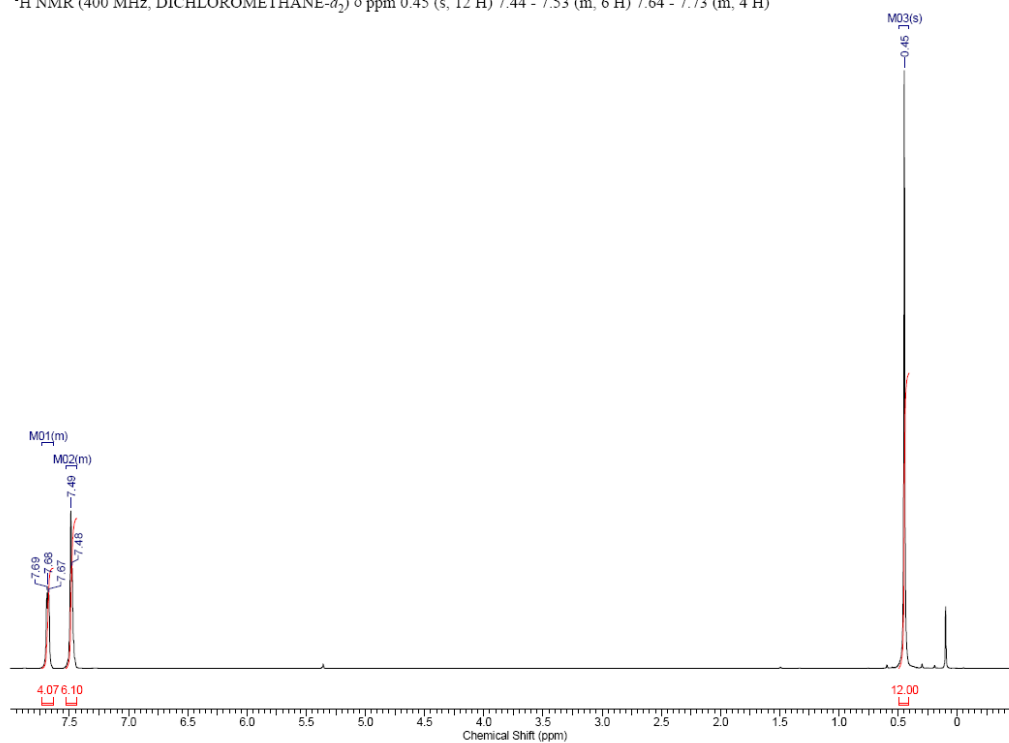


^1H - ^{29}Si gHSQC NMR

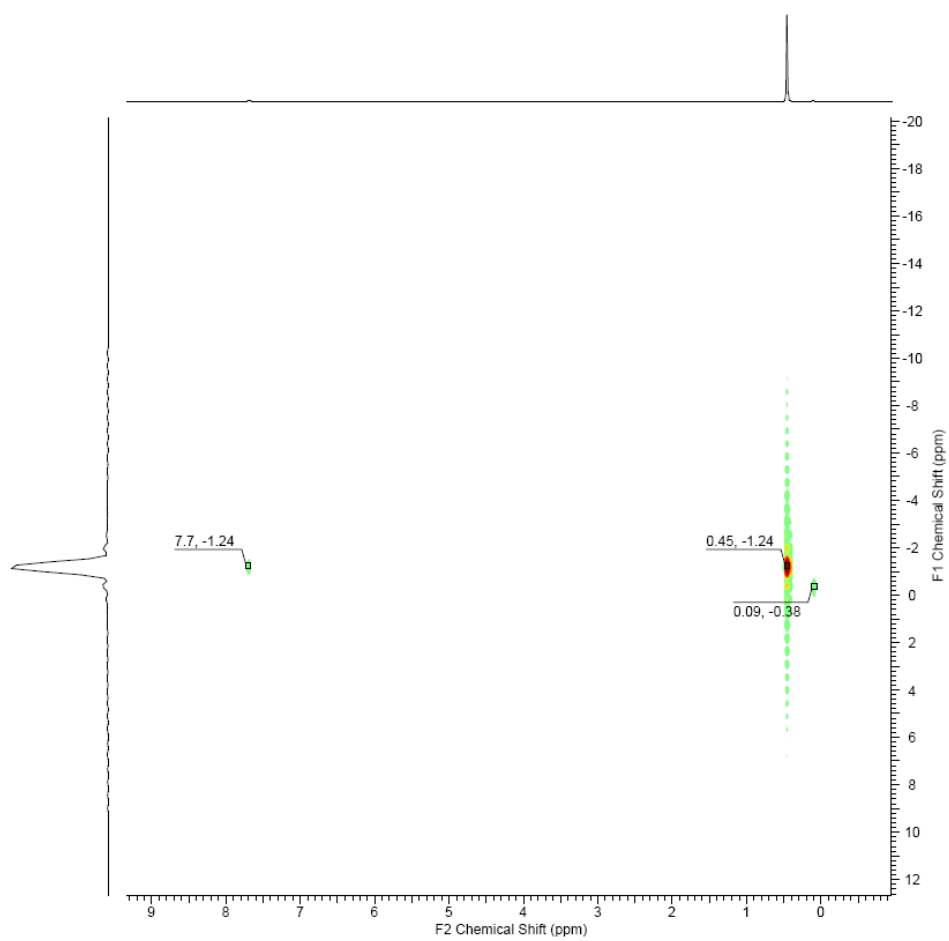




¹H NMR (400 MHz, DICHLOROMETHANE-*d*₂) δ ppm 0.45 (s, 12 H) 7.44 - 7.53 (m, 6 H) 7.64 - 7.73 (m, 4 H)

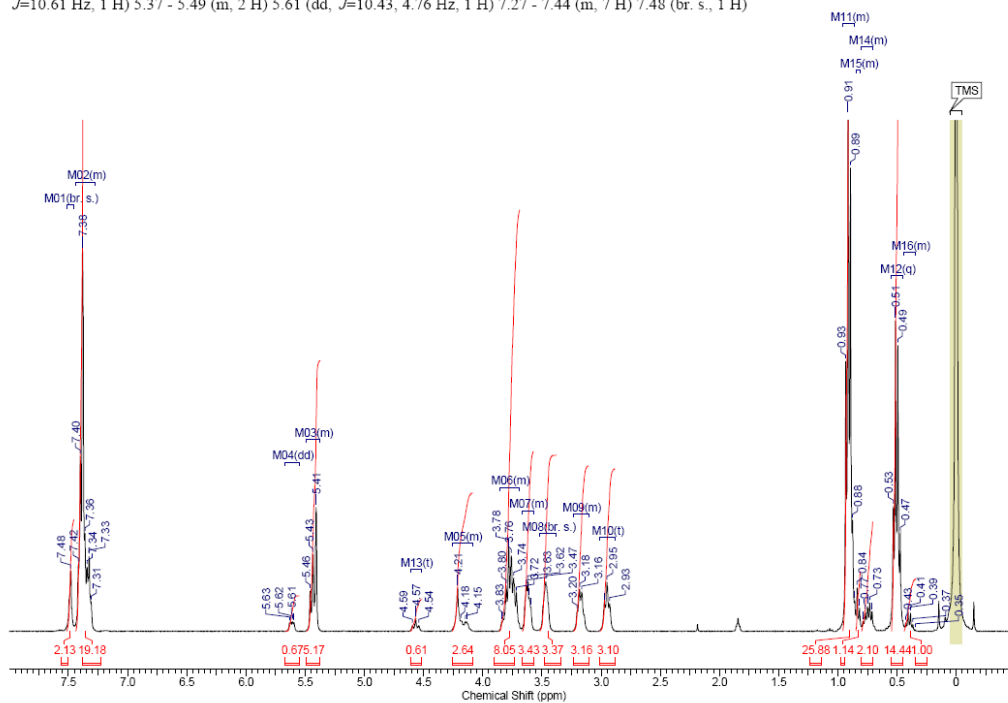


^1H - ^{29}Si gHSQC NMR

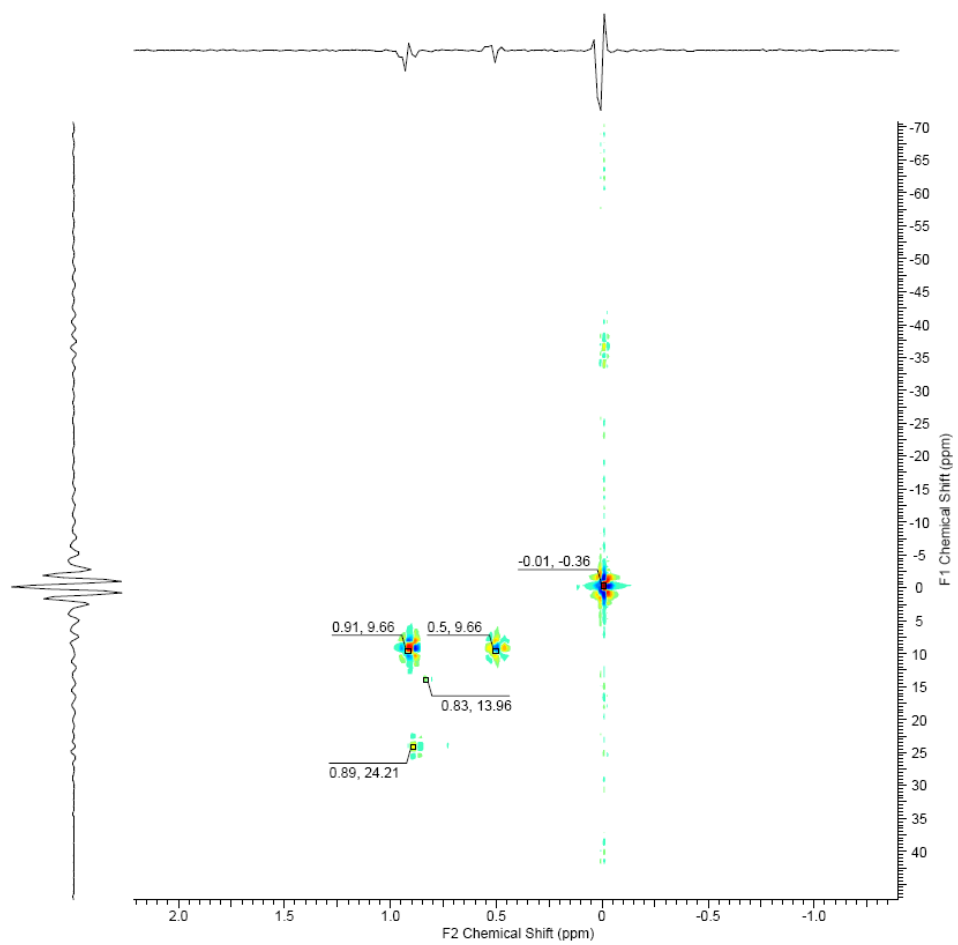


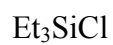
2.12/Et₃SiCl

¹H NMR (400 MHz, DICHLOROMETHANE-*d*₂) δ ppm 0.34 - 0.44 (m, 1 H) 0.50 (q, *J*=7.81 Hz, 5 H) 0.70 - 0.80 (m, 1 H) 0.81 - 0.85 (m, 1 H) 0.86 - 0.96 (m, 9 H) 2.95 (t, *J*=8.87 Hz, 1 H) 3.11 - 3.23 (m, 1 H) 3.47 (br. s., 1 H) 3.57 - 3.66 (m, 1 H) 3.69 - 3.86 (m, 3 H) 4.09 - 4.26 (m, 1 H) 4.57 (t, *J*=10.61 Hz, 1 H) 5.37 - 5.49 (m, 2 H) 5.61 (dd, *J*=10.43, 4.76 Hz, 1 H) 7.27 - 7.44 (m, 7 H) 7.48 (br. s., 1 H)

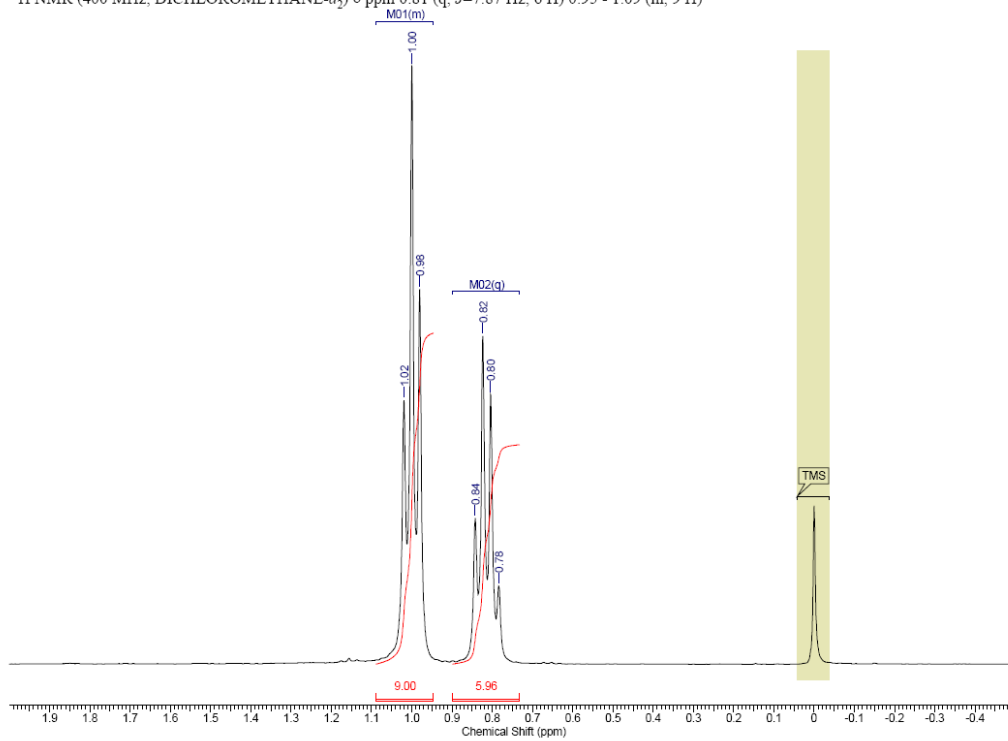


^1H - ^{29}Si gHSQC NMR

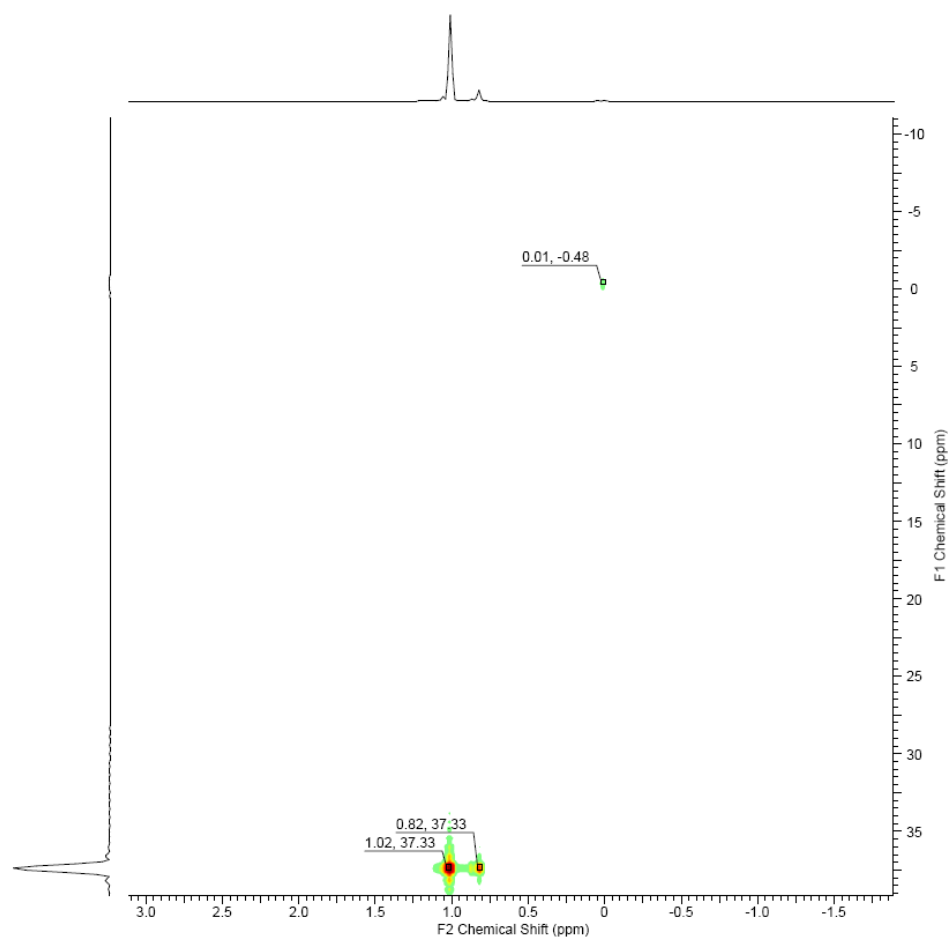




^1H NMR (400 MHz, $\text{DICHLOROMETHANE-}d_2$) δ ppm 0.81 (q, $J=7.87$ Hz, 6 H) 0.95 - 1.09 (m, 9 H)

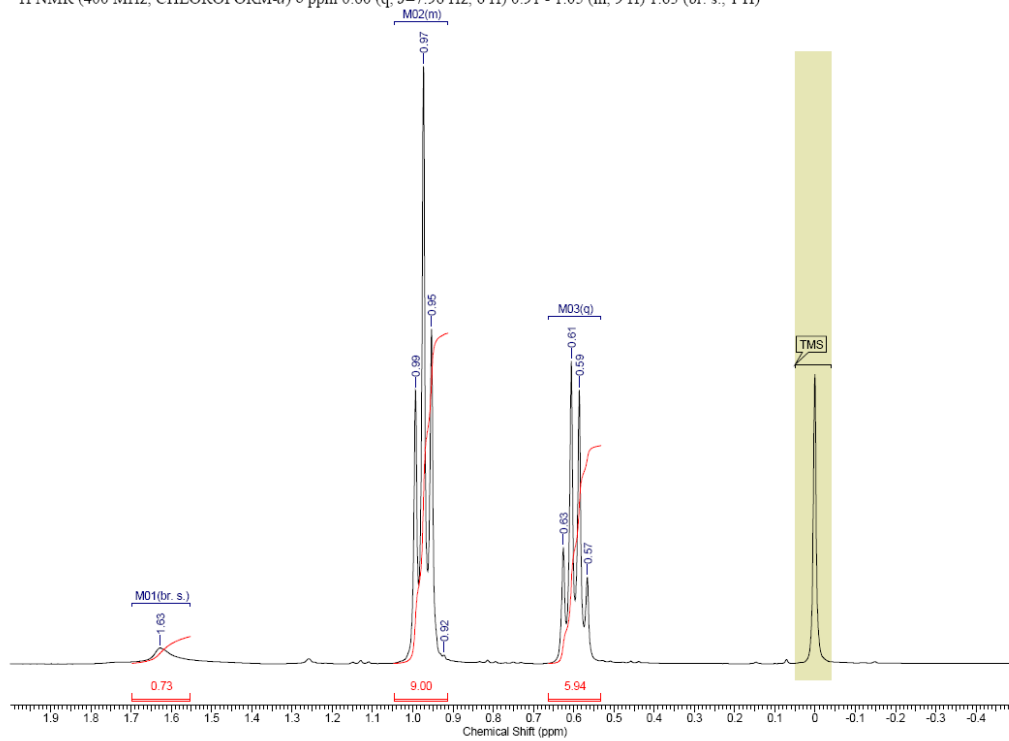


^1H - ^{29}Si gHSQC NMR

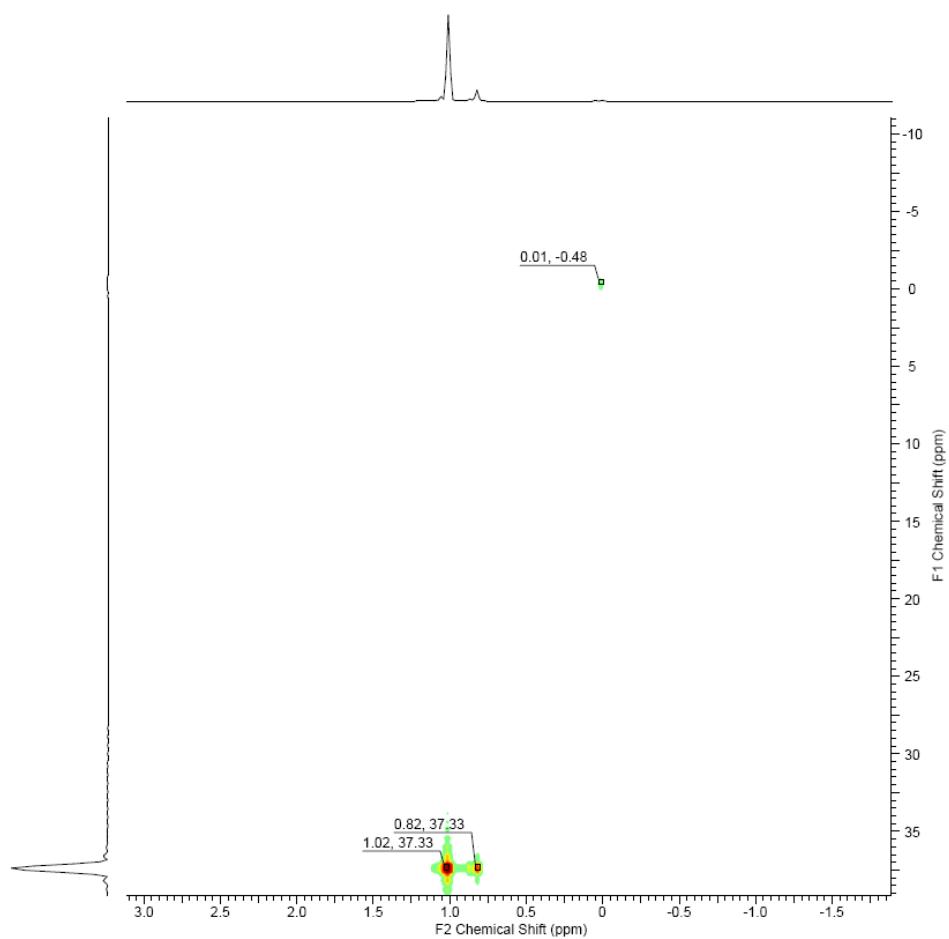


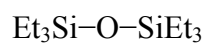


¹H NMR (400 MHz, CHLOROFORM-*d*) δ ppm 0.60 (q, *J*=7.96 Hz, 6 H) 0.91 - 1.05 (m, 9 H) 1.63 (br. s., 1 H)

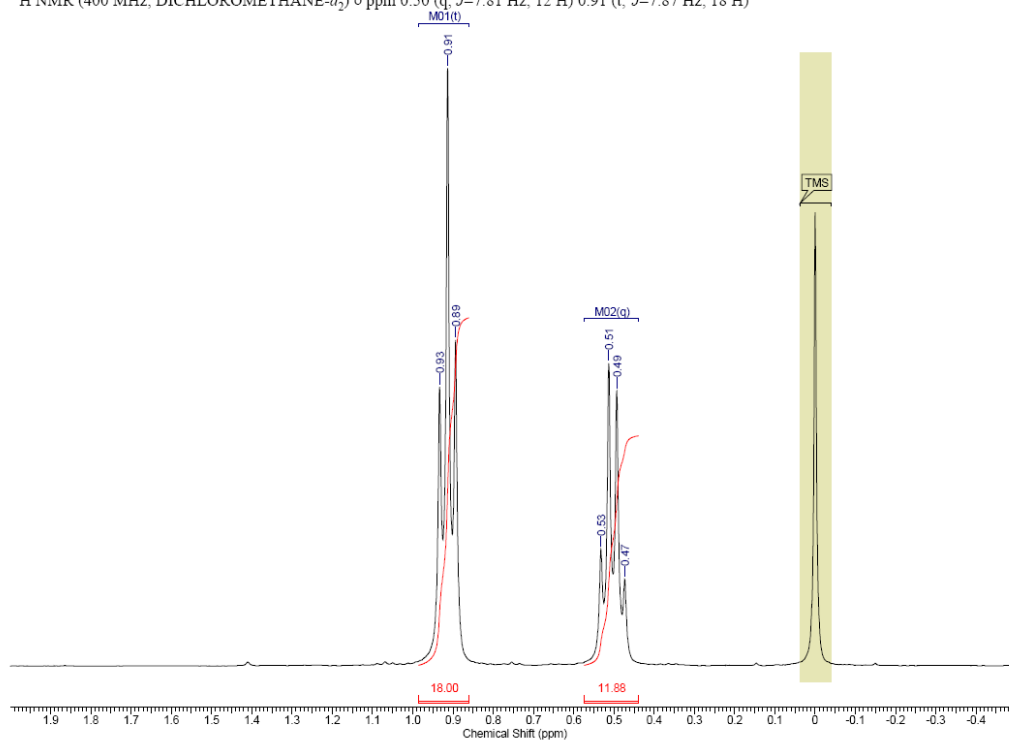


^1H - ^{29}Si gHSQC NMR

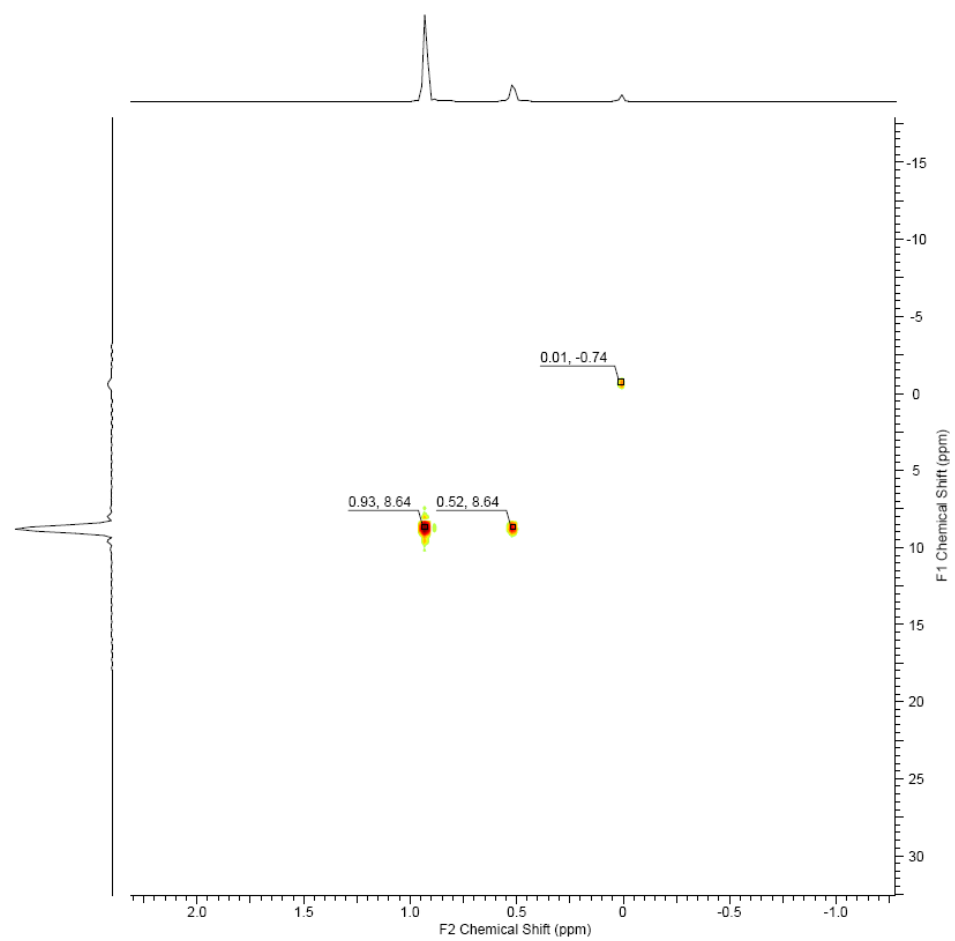




^1H NMR (400 MHz, $\text{DICHLOROMETHANE-}d_2$) δ ppm 0.50 (q, $J=7.81$ Hz, 12 H) 0.91 (t, $J=7.87$ Hz, 18 H)

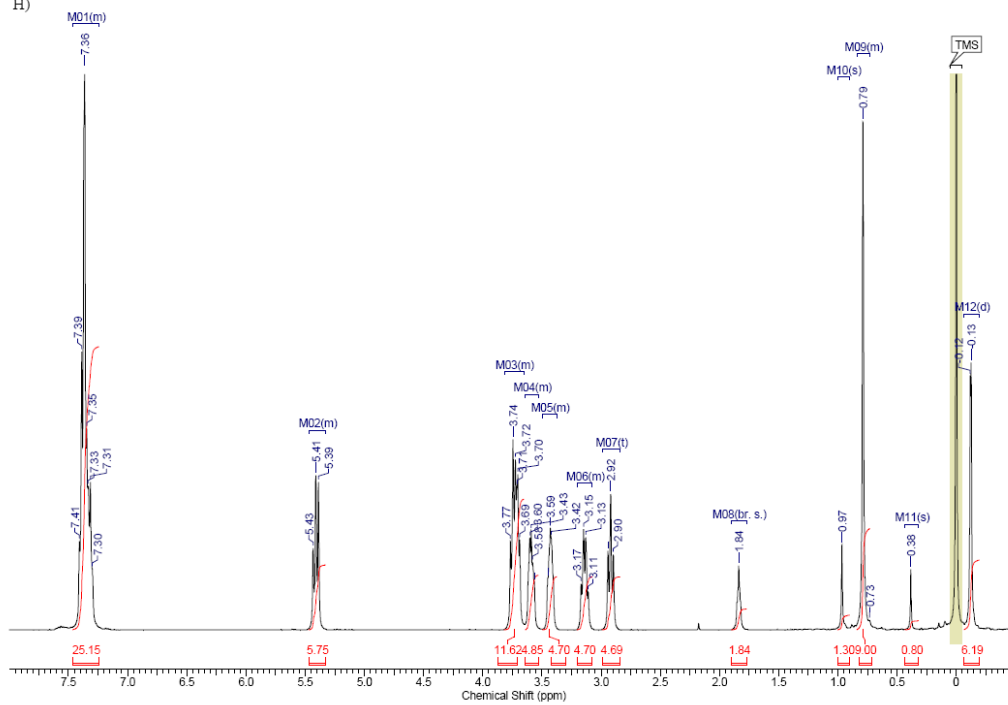


^1H - ^{29}Si gHSQC NMR

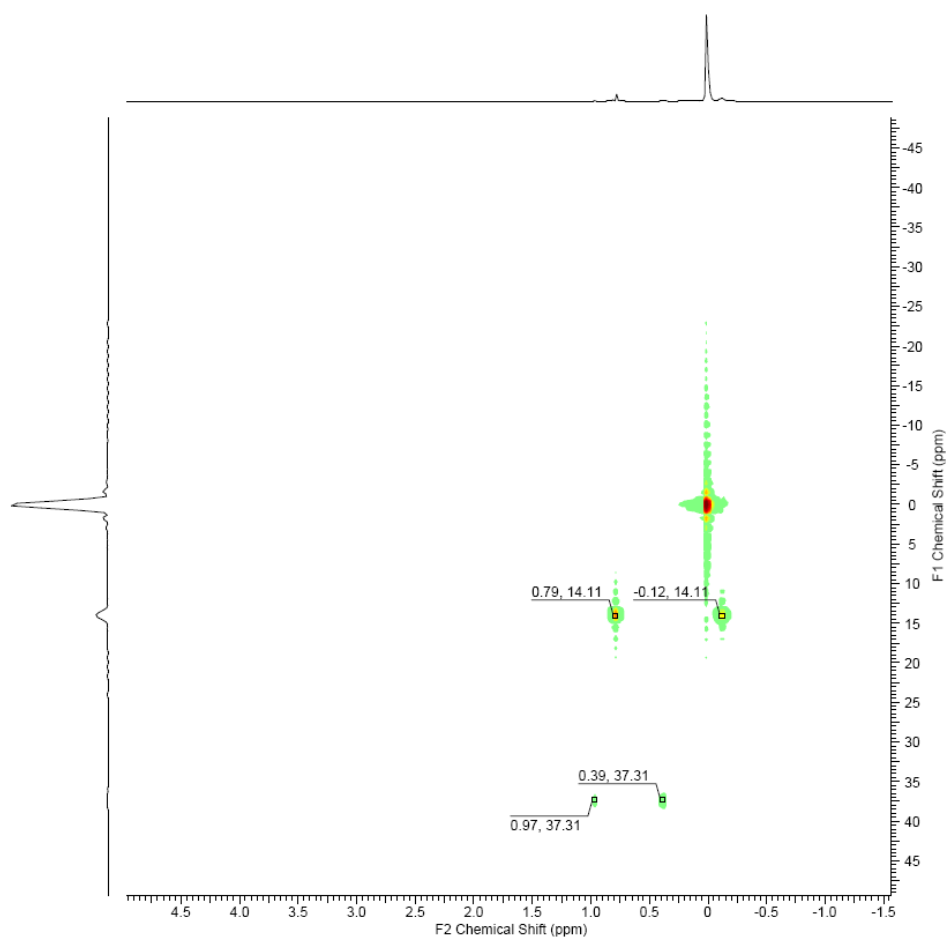


2.12/*t*BuMe₂SiCl

¹H NMR (400 MHz, DICHLOROMETHANE-*d*₂) δ ppm -0.12 (d, *J*=2.74 Hz, 6 H) 0.38 (s, 1 H) 0.73 - 0.84 (m, 9 H) 0.97 (s, 1 H) 1.84 (br. s., 2 H) 2.92 (t, *J*=9.24 Hz, 5 H) 3.08 - 3.20 (m, 5 H) 3.37 - 3.50 (m, 5 H) 3.53 - 3.64 (m, 5 H) 3.65 - 3.82 (m, 12 H) 5.33 - 5.47 (m, 6 H) 7.24 - 7.46 (m, 25 H)

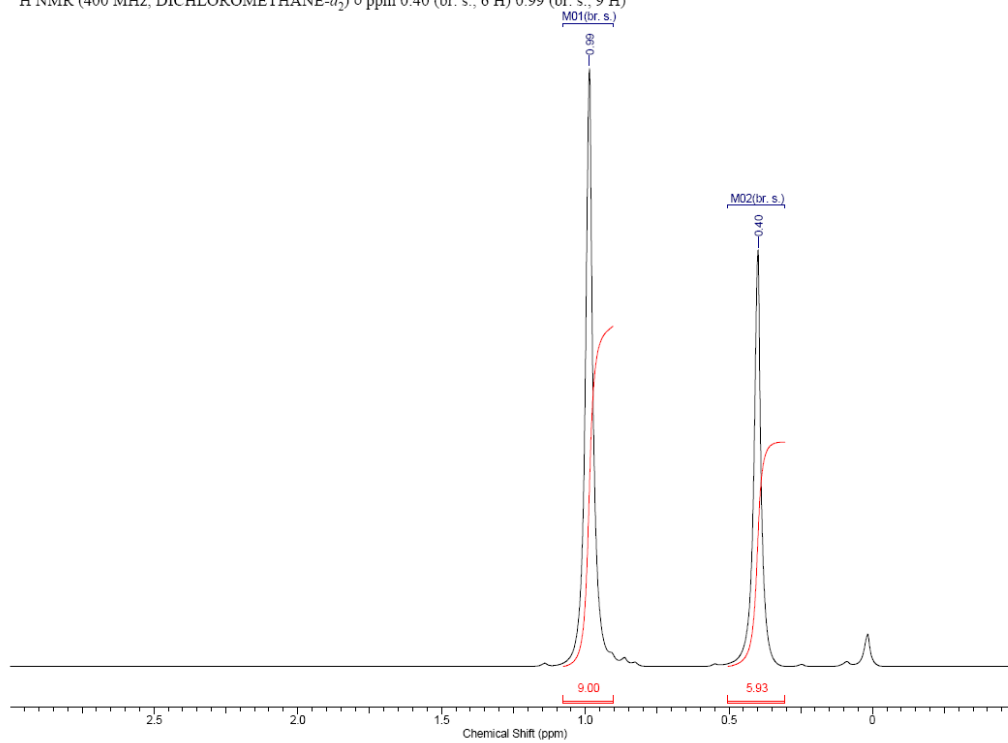


^1H - ^{29}Si gHSQC NMR

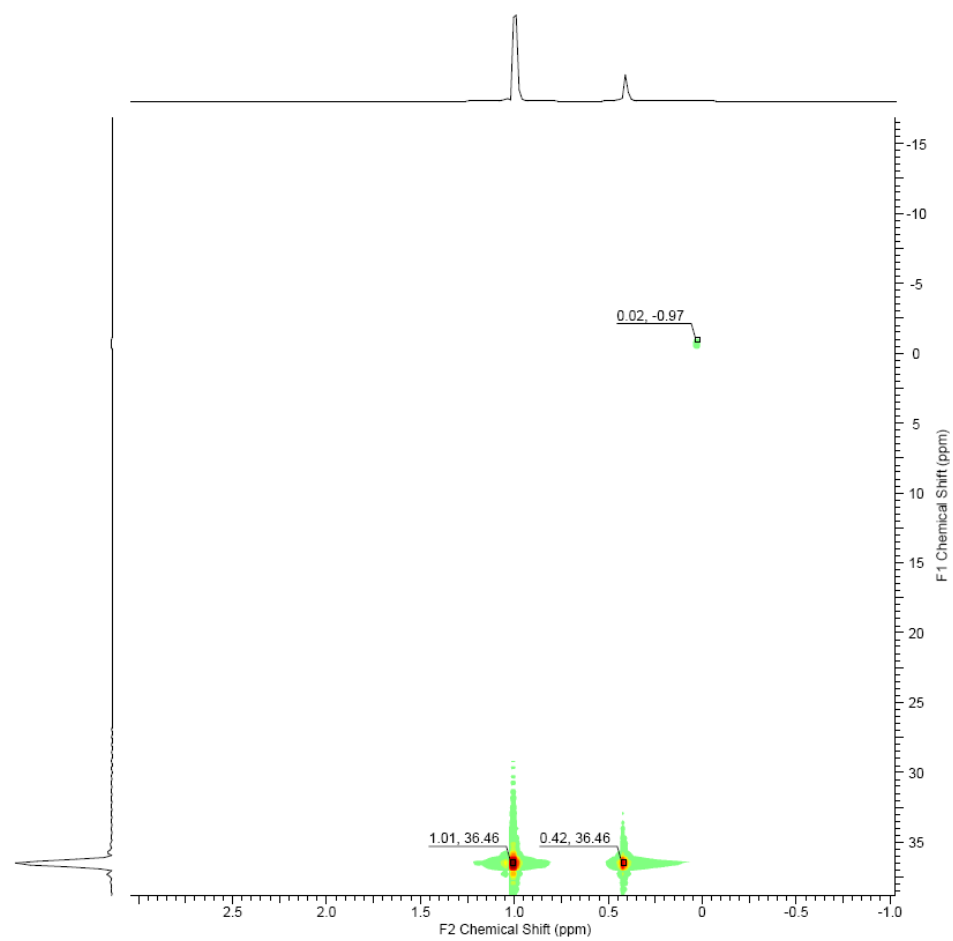


*t*BuMe₂SiCl

¹H NMR (400 MHz, DICHLOROMETHANE-*d*₂) δ ppm 0.40 (br. s., 6 H) 0.99 (br. s., 9 H)

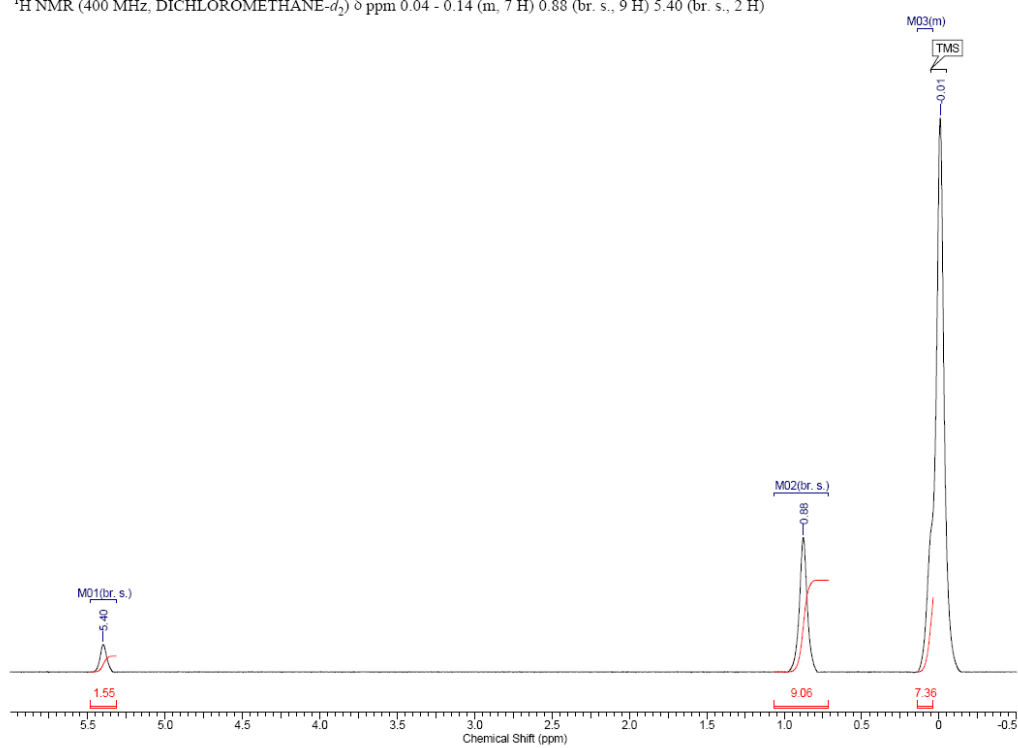


^1H - ^{29}Si gHSQC NMR

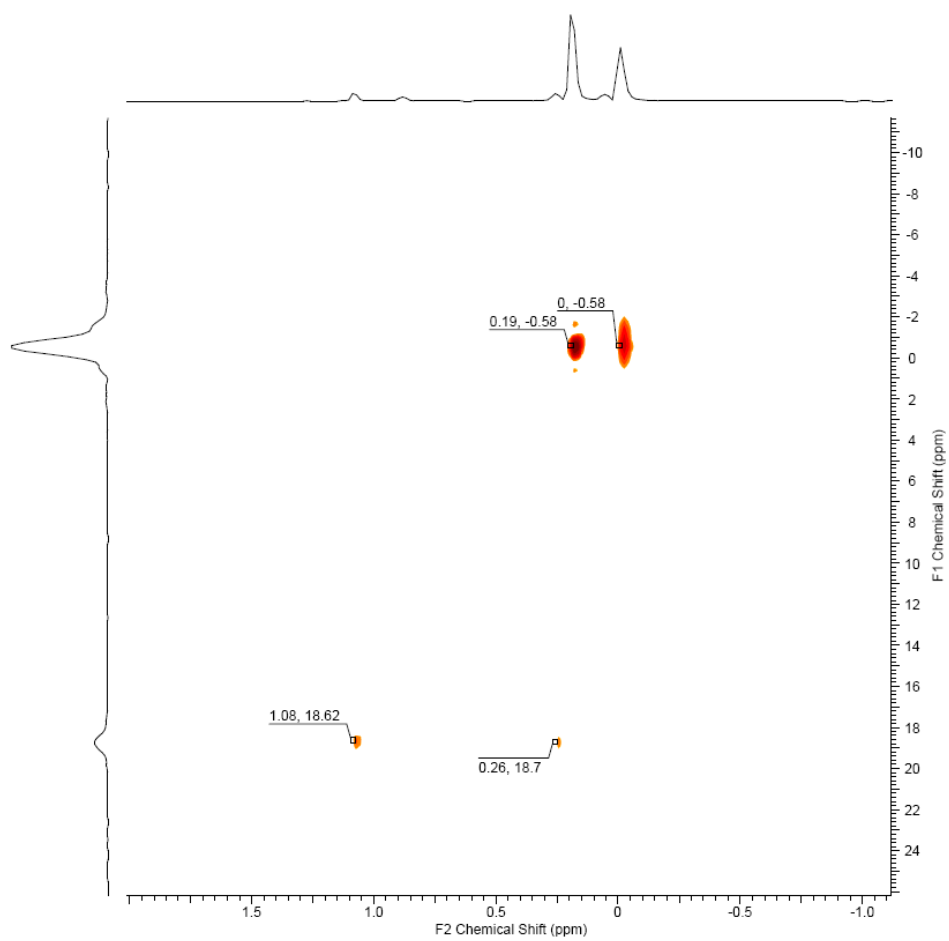


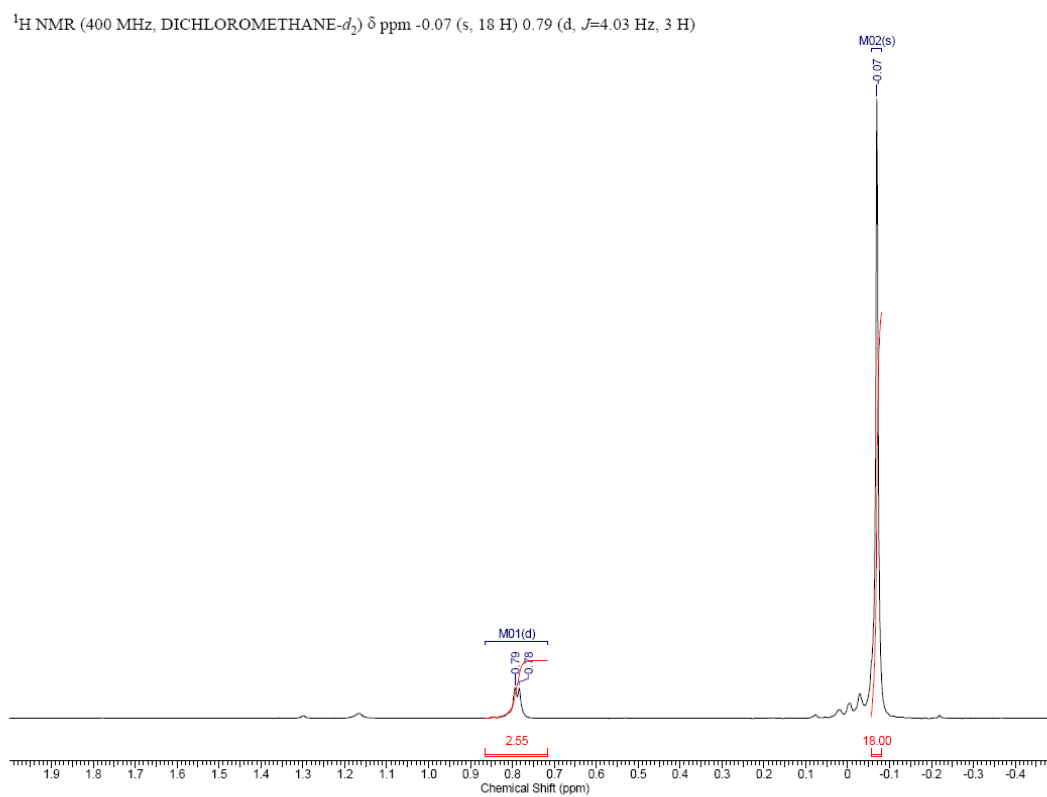
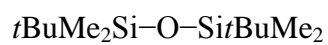
*t*BuMe₂SiOH

¹H NMR (400 MHz, DICHLOROMETHANE-*d*₂) δ ppm 0.04 - 0.14 (m, 7 H) 0.88 (br. s., 9 H) 5.40 (br. s., 2 H)

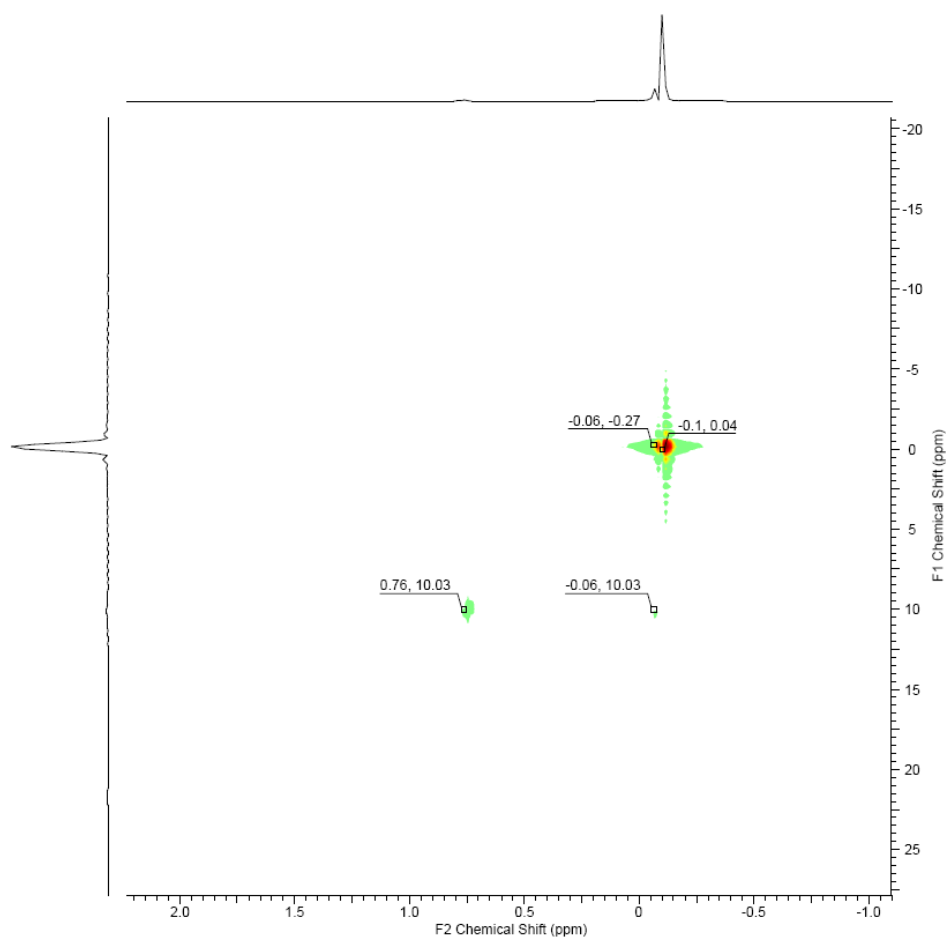


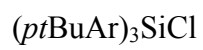
^1H - ^{29}Si gHSQC NMR



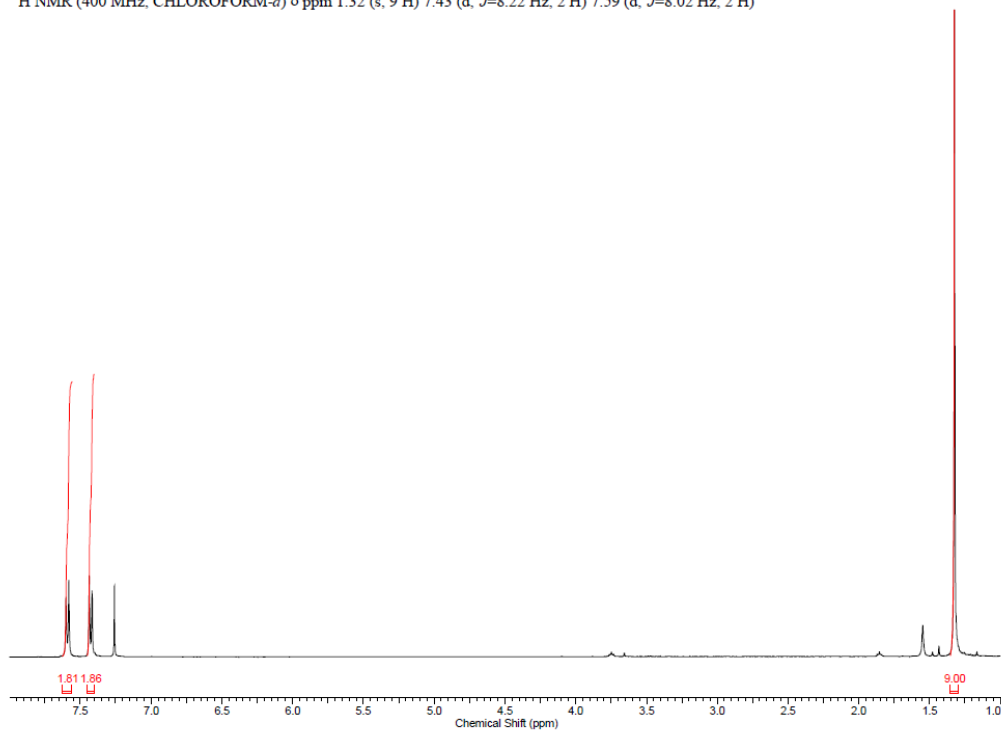


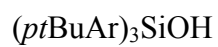
^1H - ^{29}Si gHSQC NMR



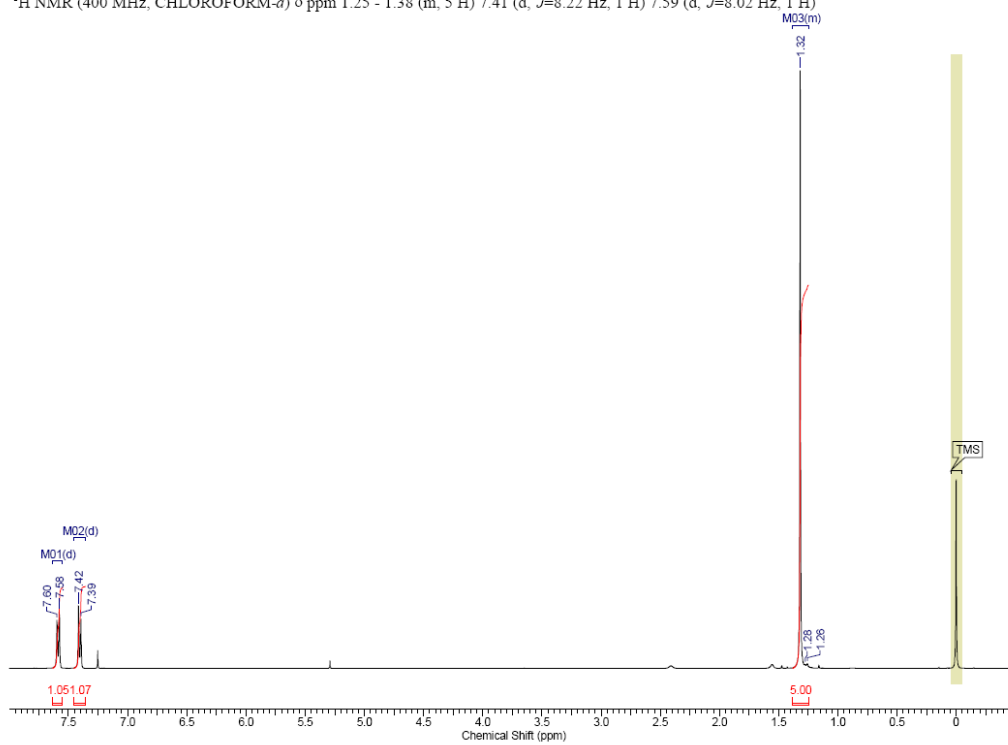


^1H NMR (400 MHz, CHCl_3) δ ppm 1.32 (s, 9 H) 7.43 (d, $J=8.22$ Hz, 2 H) 7.59 (d, $J=8.02$ Hz, 2 H)

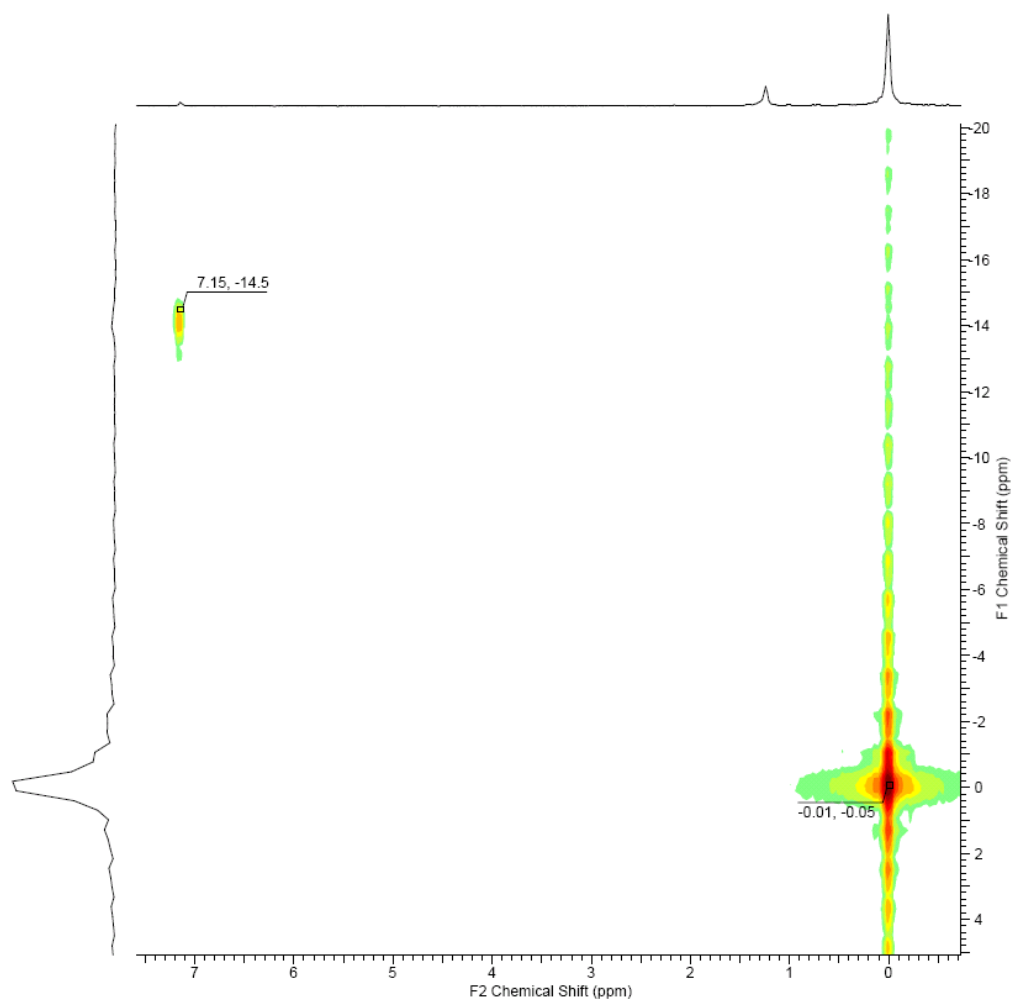


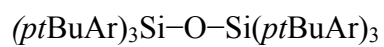


^1H NMR (400 MHz, CHCl_3) δ ppm 1.25 - 1.38 (m, 5 H) 7.41 (d, $J=8.22$ Hz, 1 H) 7.59 (d, $J=8.02$ Hz, 1 H)

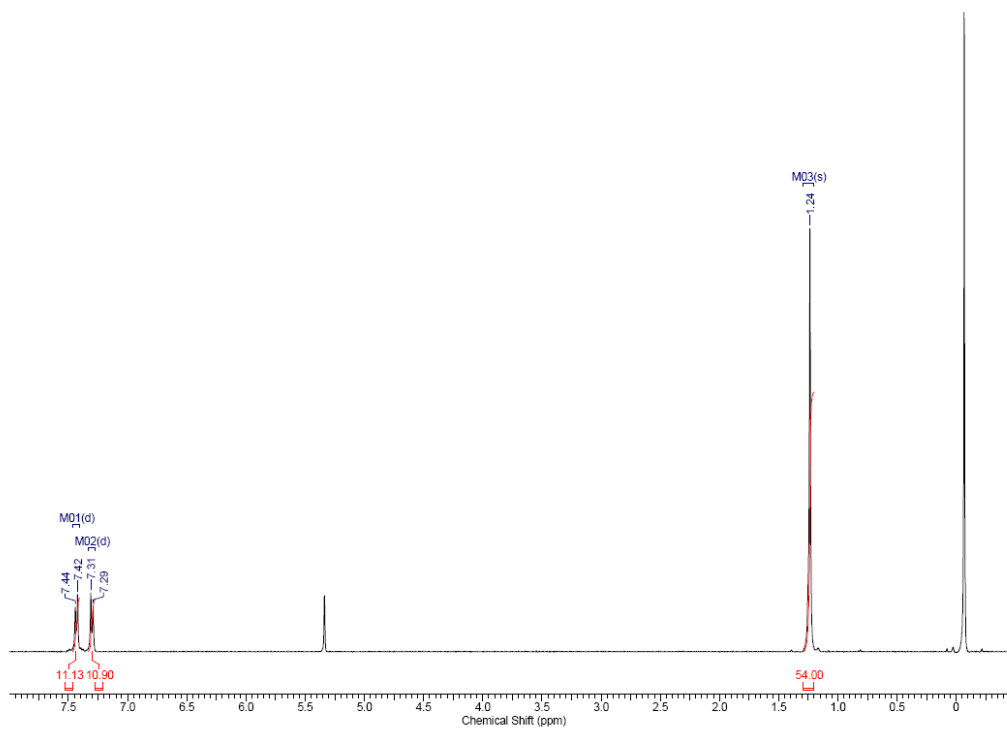


^1H - ^{29}Si gHSQC NMR

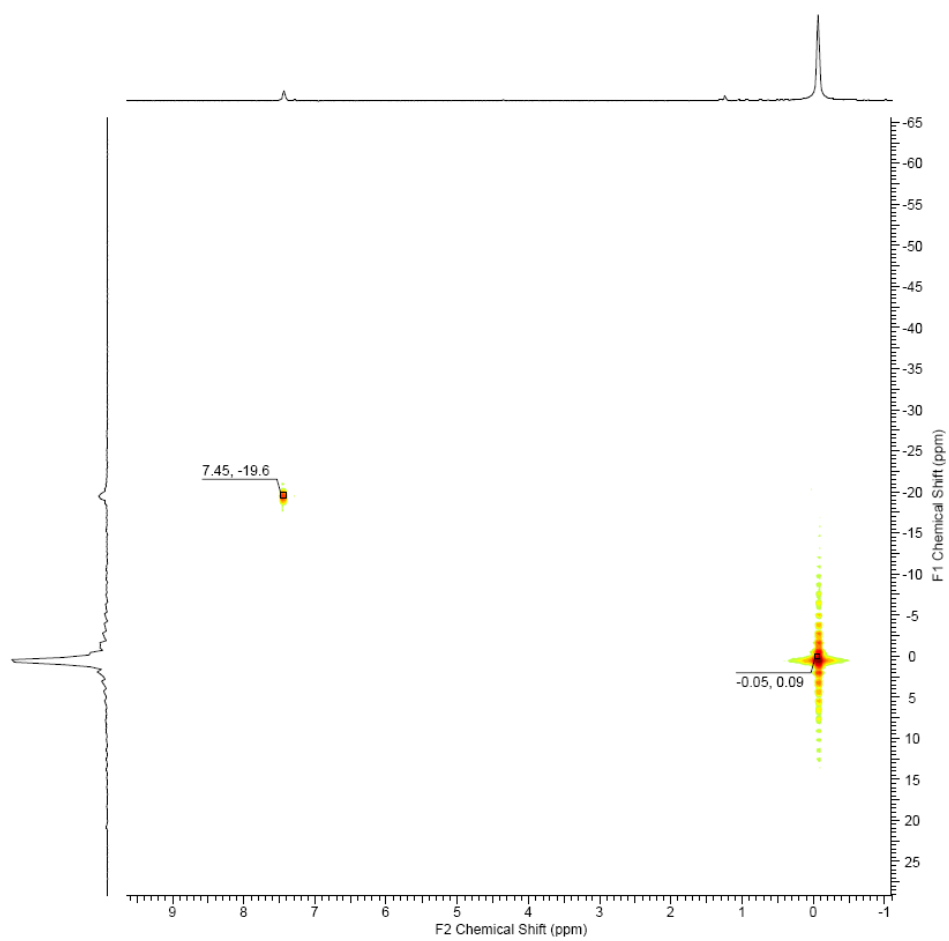




^1H NMR (400 MHz, $\text{DICHLOROMETHANE-}d_2$) δ ppm 1.24 (s, 54 H) 7.30 (d, $J=7.87$ Hz, 11 H) 7.43 (d, $J=7.87$ Hz, 11 H)

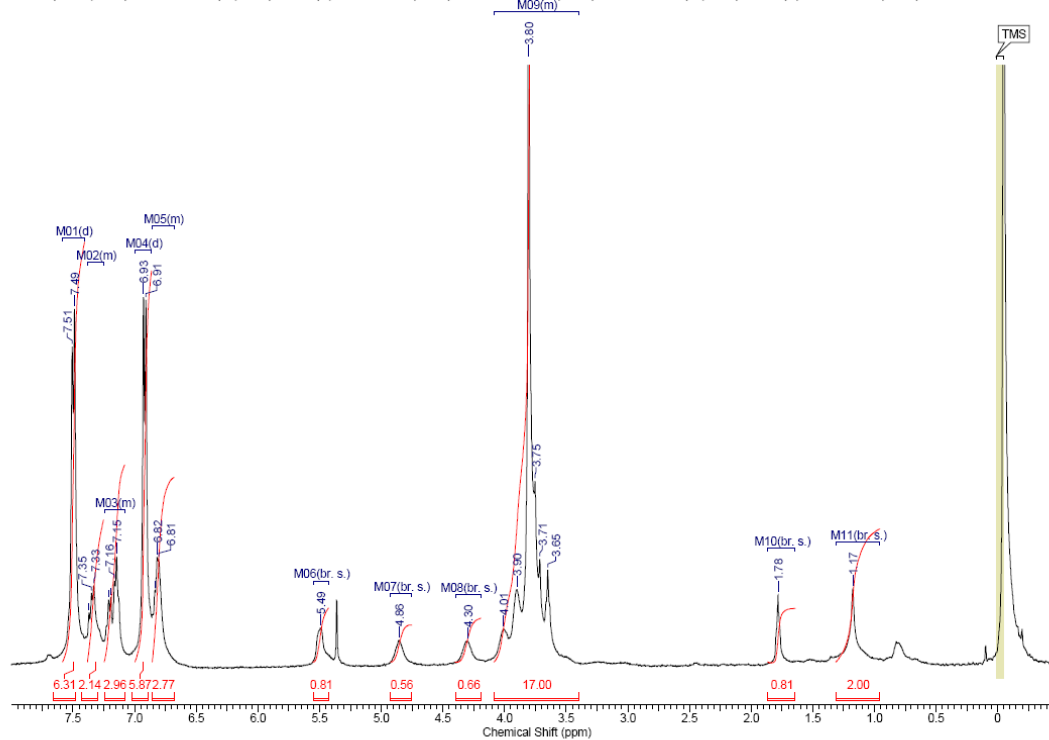


^1H - ^{29}Si gHSQC NMR

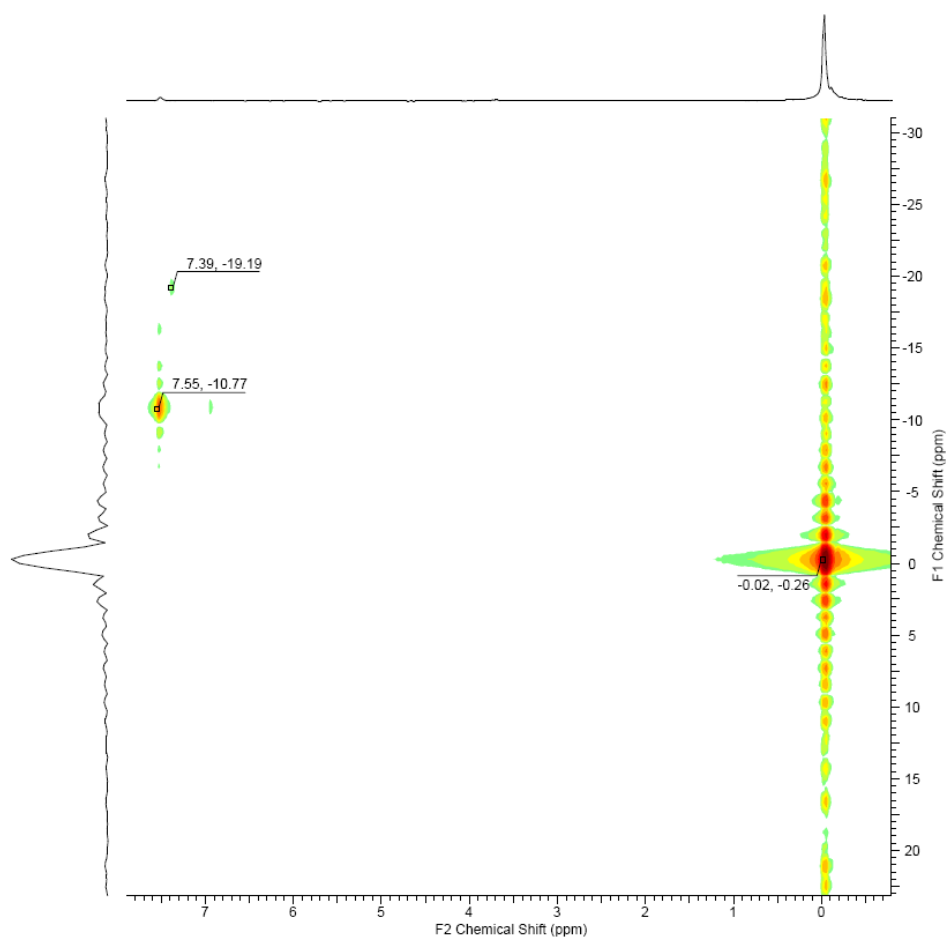


2.12/(pMeOAr)₃SiCl

¹H NMR (400 MHz, DICHLOROMETHANE-*d*₂) δ ppm 1.17 (br. s., 2 H) 1.78 (br. s., 1 H) 3.40 - 4.09 (m, 26 H) 4.30 (br. s., 1 H) 4.86 (br. s., 1 H) 5.49 (br. s., 1 H) 6.68 - 6.86 (m, 1 H) 6.92 (d, *J*=7.87 Hz, 2 H) 7.08 - 7.25 (m, 1 H) 7.25 - 7.38 (m, 1 H) 7.50 (d, *J*=7.68 Hz, 1 H)

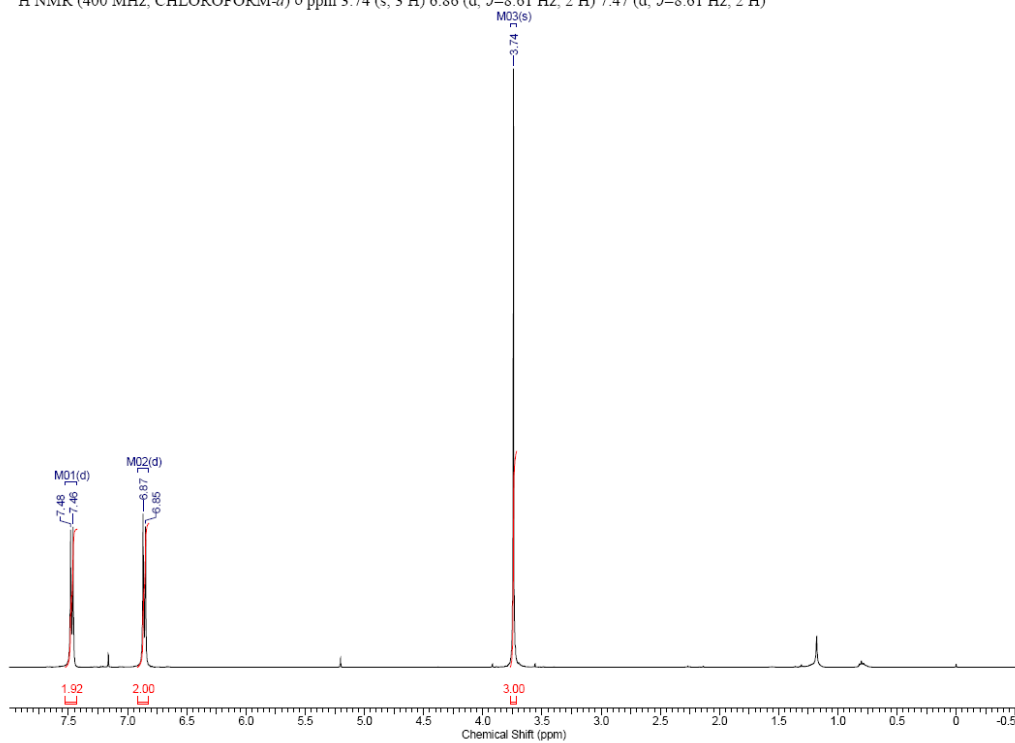


^1H - ^{29}Si gHSQC NMR

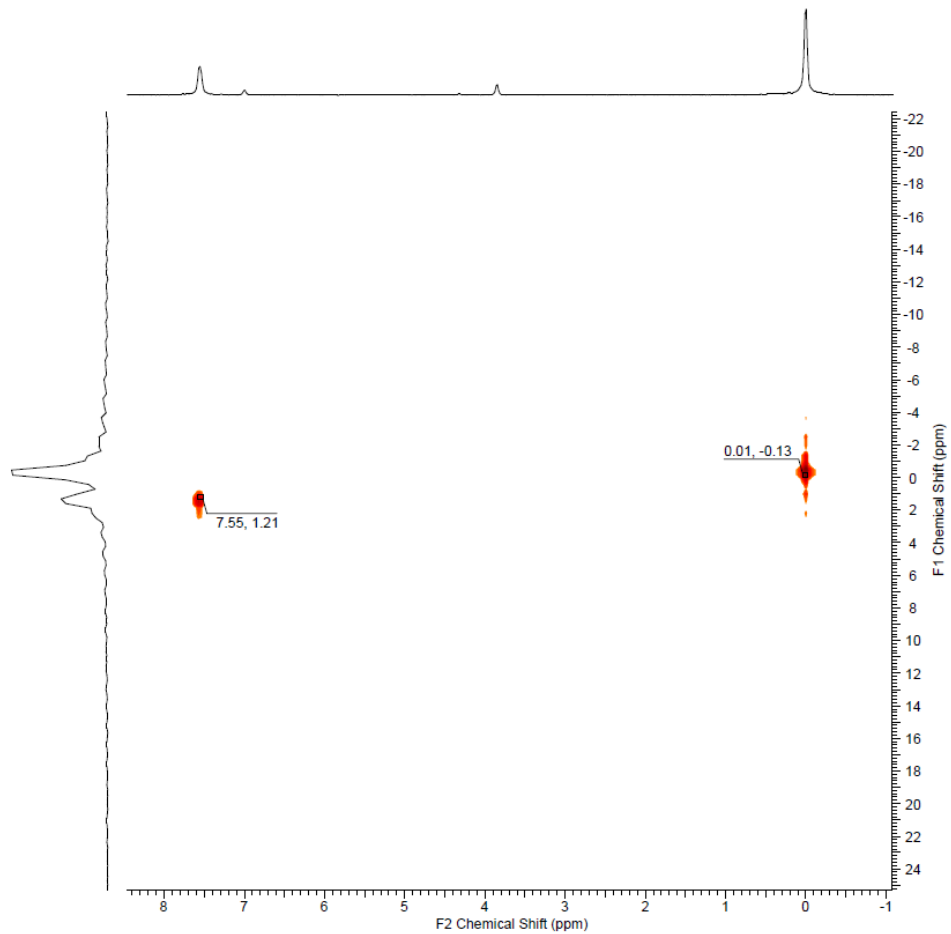




^1H NMR (400 MHz, CHCl_3) δ ppm 3.74 (s, 3 H) 6.86 (d, $J=8.61$ Hz, 2 H) 7.47 (d, $J=8.61$ Hz, 2 H)

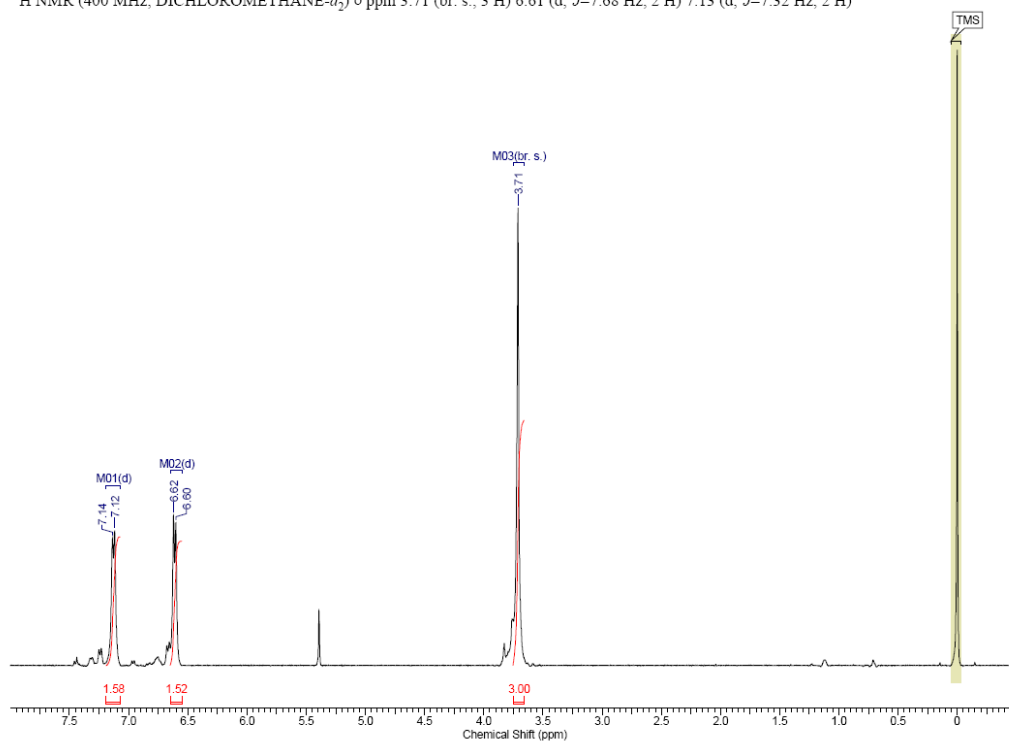


^1H - ^{29}Si gHSQC NMR

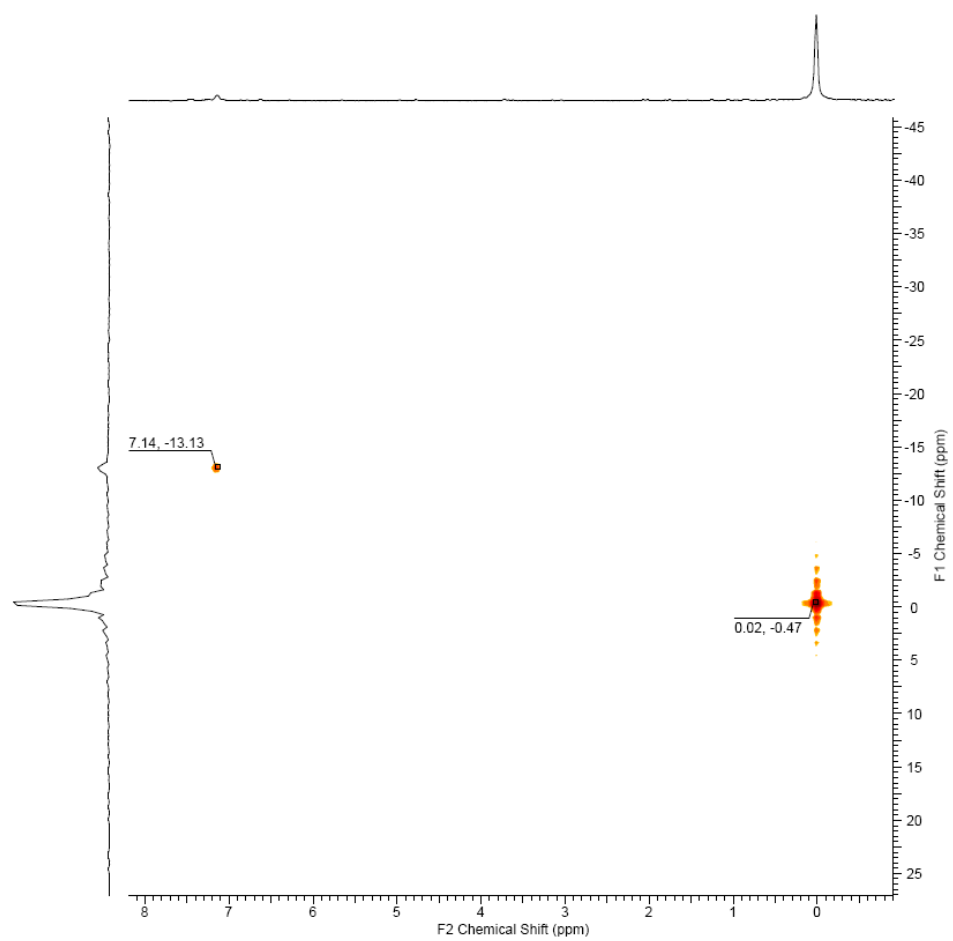


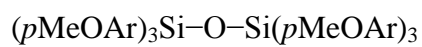


^1H NMR (400 MHz, $\text{DICHLOROMETHANE-}d_2$) δ ppm 3.71 (br. s., 3 H) 6.61 (d, $J=7.68$ Hz, 2 H) 7.13 (d, $J=7.32$ Hz, 2 H)

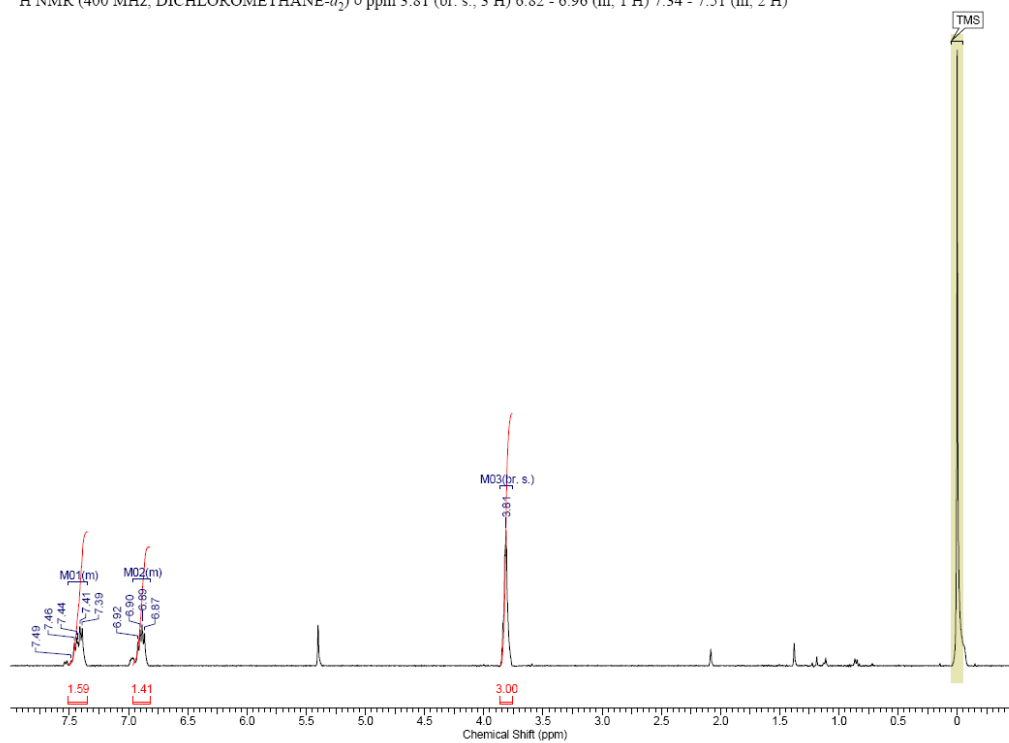


^1H - ^{29}Si gHSQC NMR

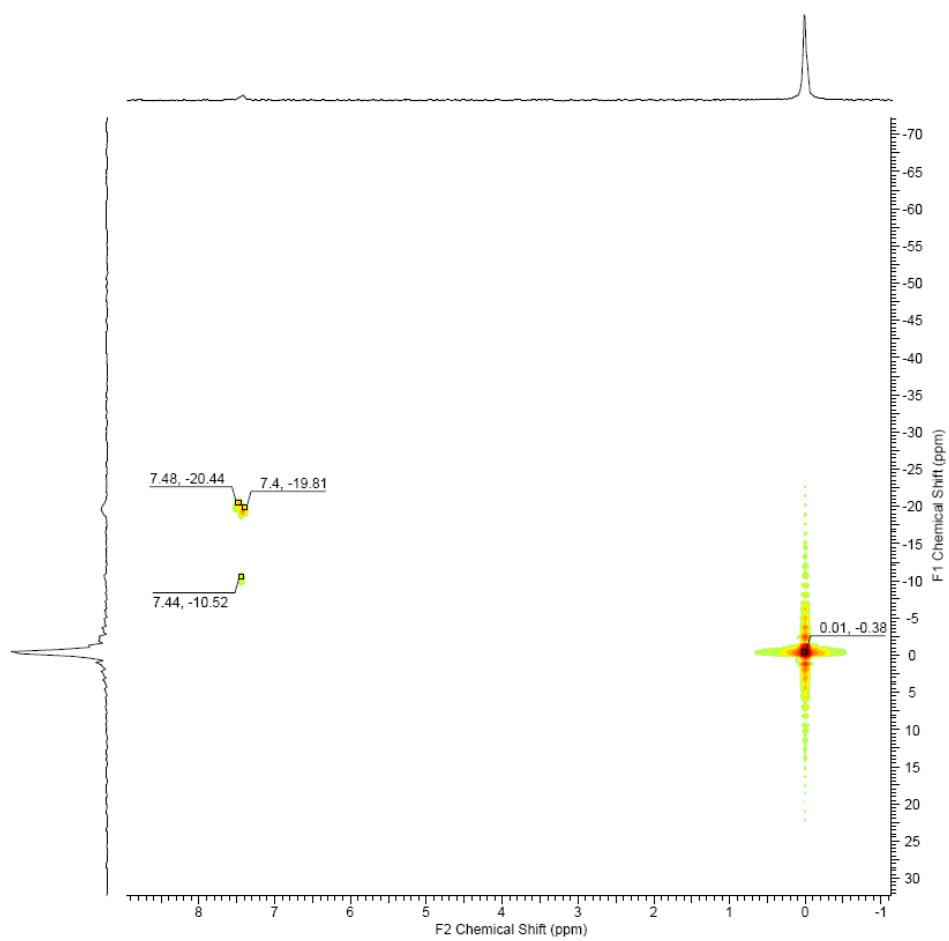




^1H NMR (400 MHz, $\text{DICHLOROMETHANE-}d_2$) δ ppm 3.81 (br. s., 3 H) 6.82 - 6.96 (m, 1 H) 7.34 - 7.51 (m, 2 H)

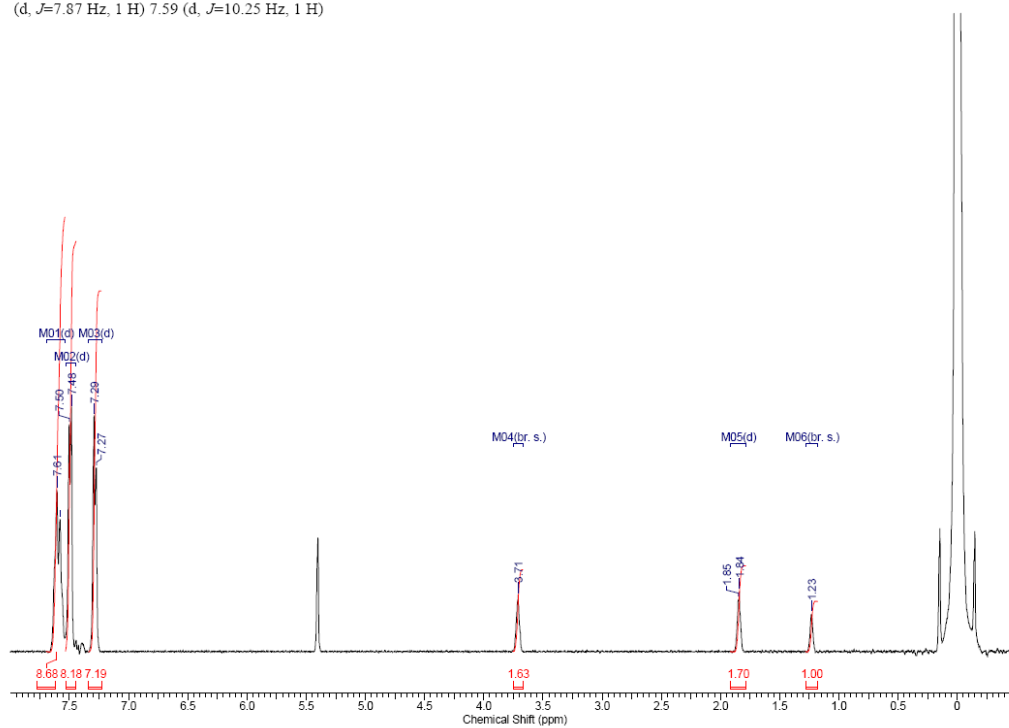


^1H - ^{29}Si gHSQC NMR

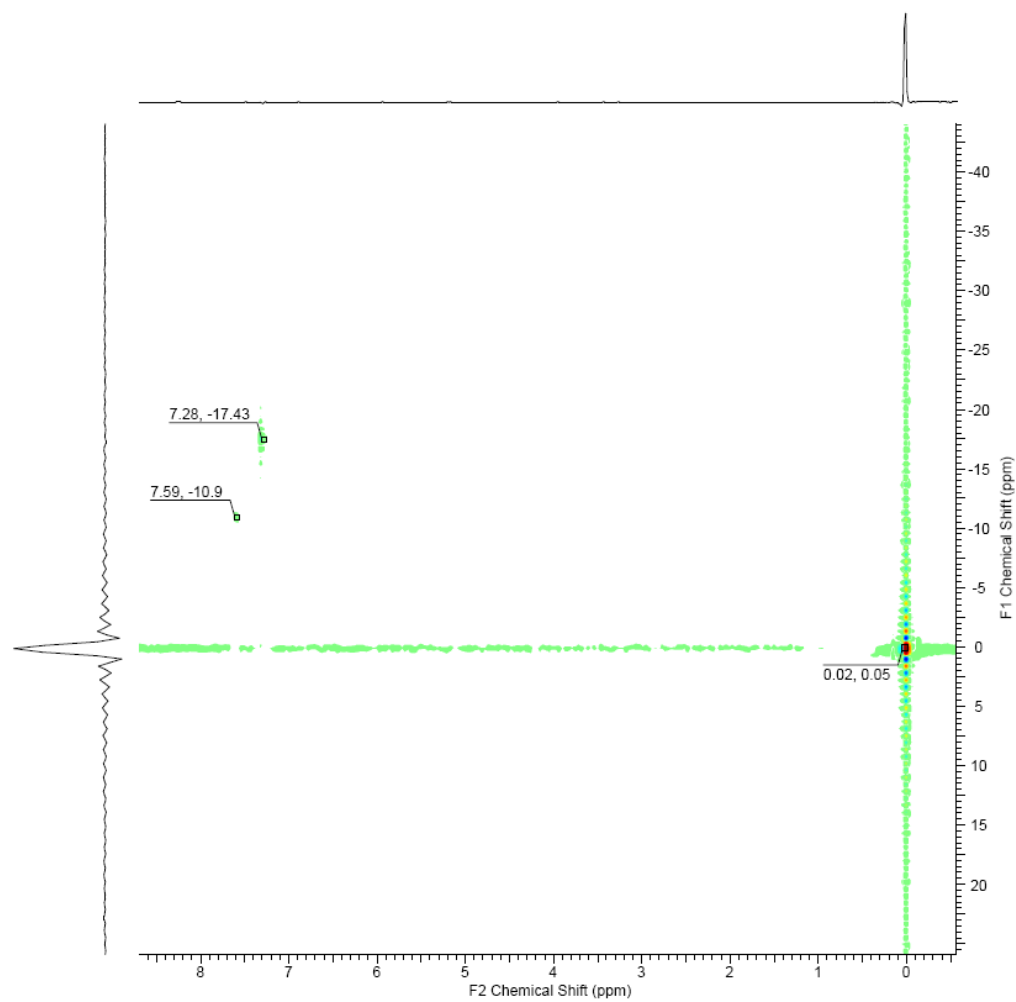


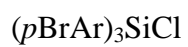
2.12/(pBrAr)₃SiCl

¹H NMR (400 MHz, DICHLOROMETHANE-*d*₂) δ ppm 1.23 (br. s., 1 H) 1.85 (d, *J*=3.11 Hz, 1 H) 3.71 (br. s., 1 H) 7.28 (d, *J*=7.87 Hz, 1 H) 7.49 (d, *J*=7.87 Hz, 1 H) 7.59 (d, *J*=10.25 Hz, 1 H)

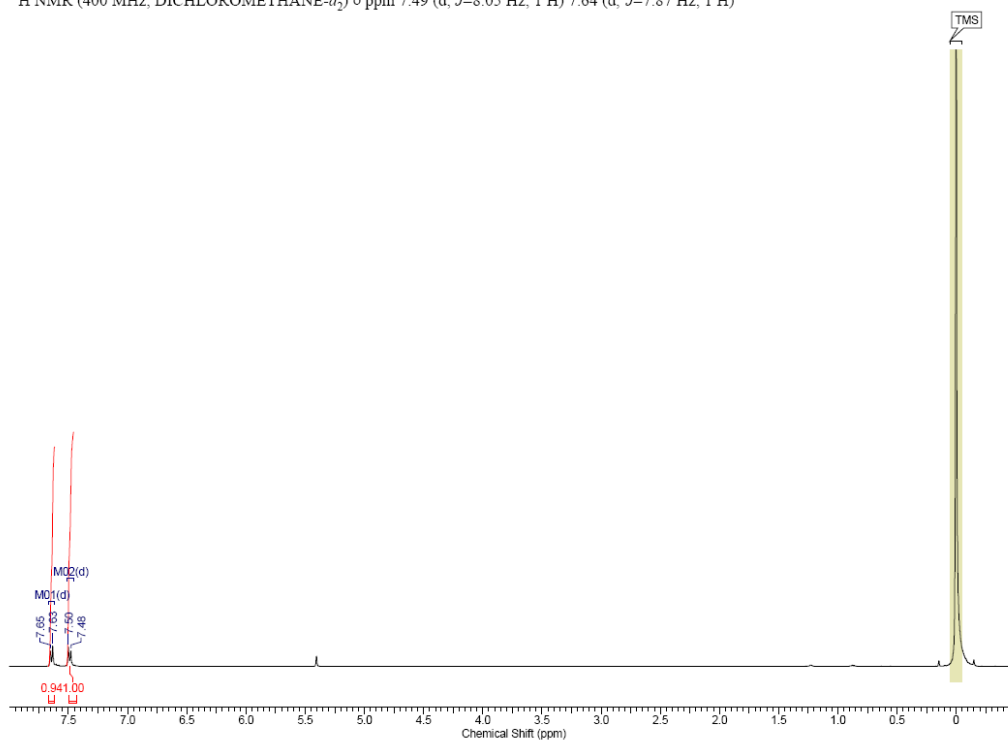


^1H - ^{29}Si gHSQC NMR

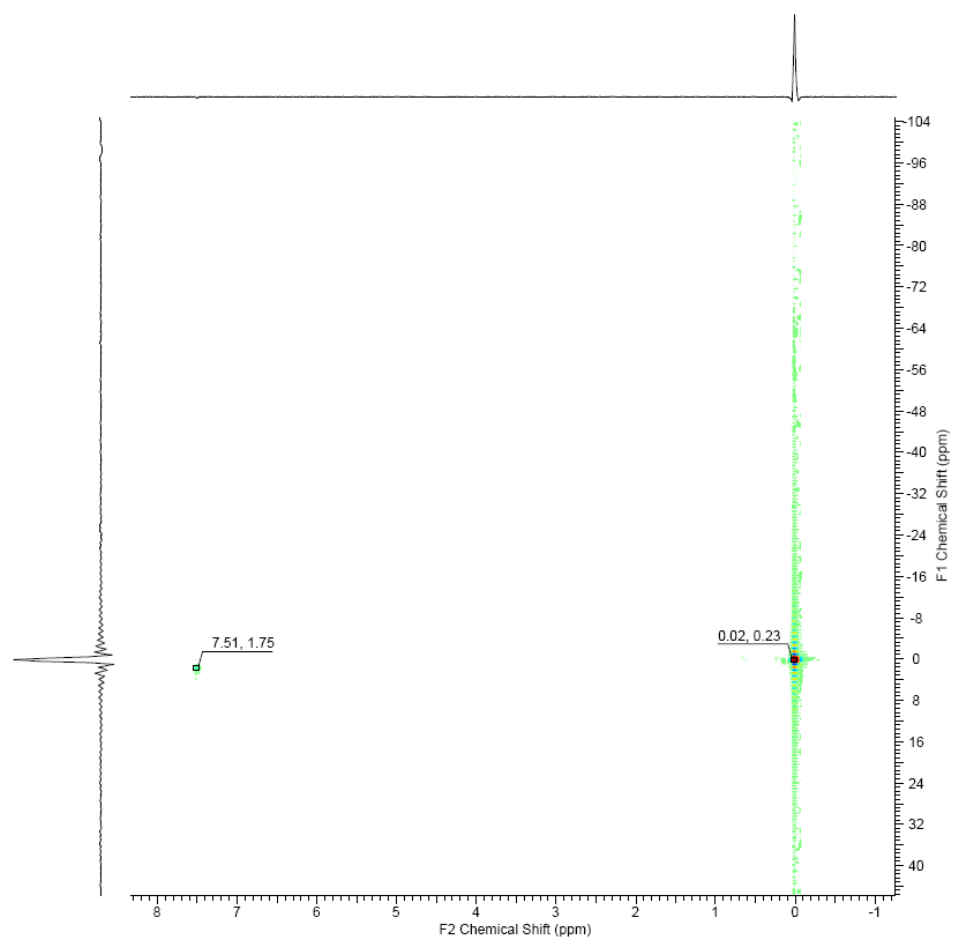


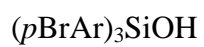


^1H NMR (400 MHz, $\text{DICHLOROMETHANE-}d_2$) δ ppm 7.49 (d, $J=8.05$ Hz, 1 H) 7.64 (d, $J=7.87$ Hz, 1 H)

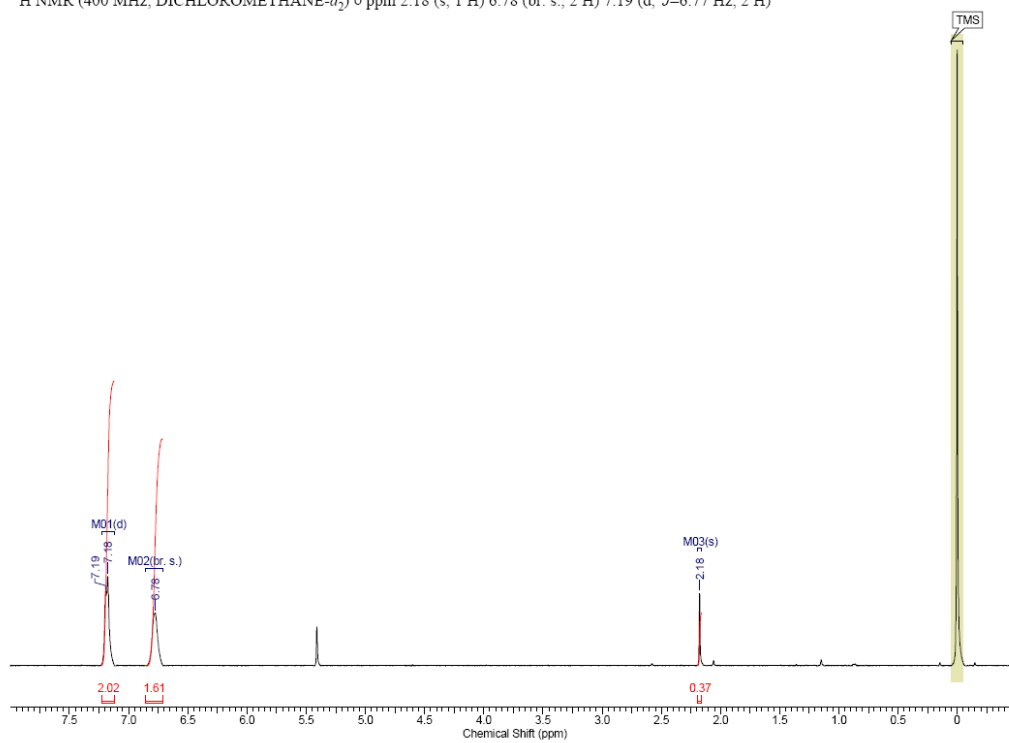


^1H - ^{29}Si gHSQC NMR

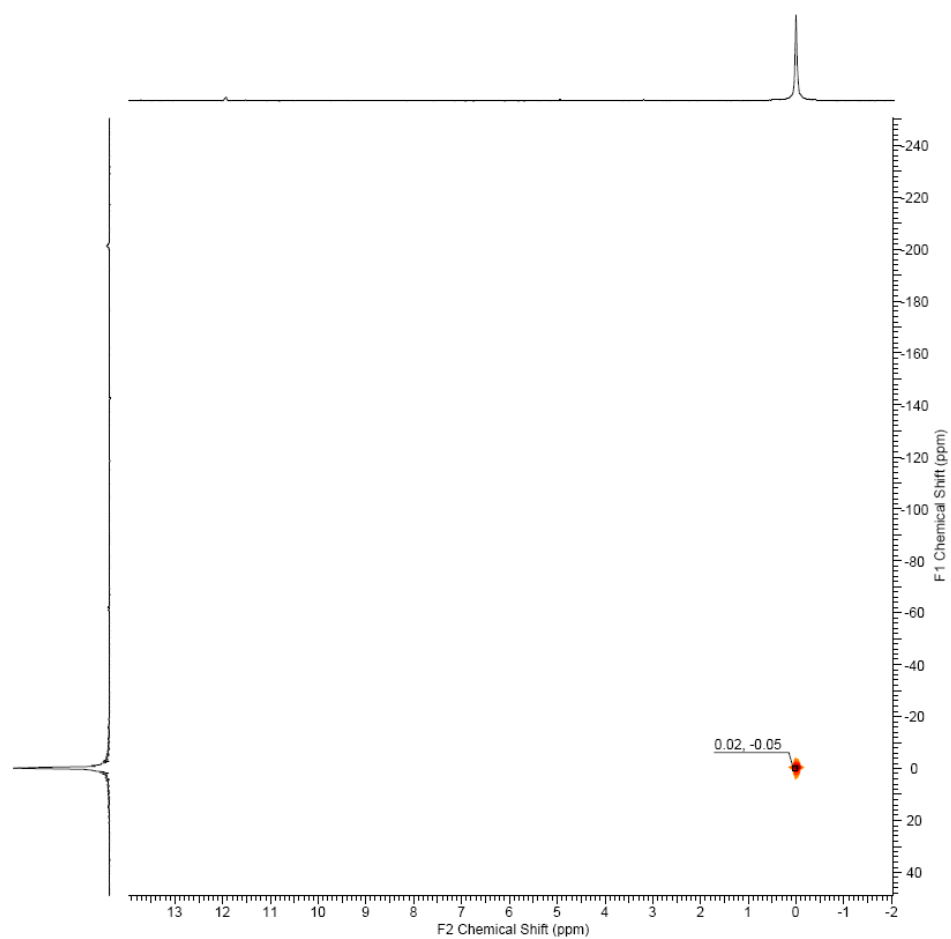




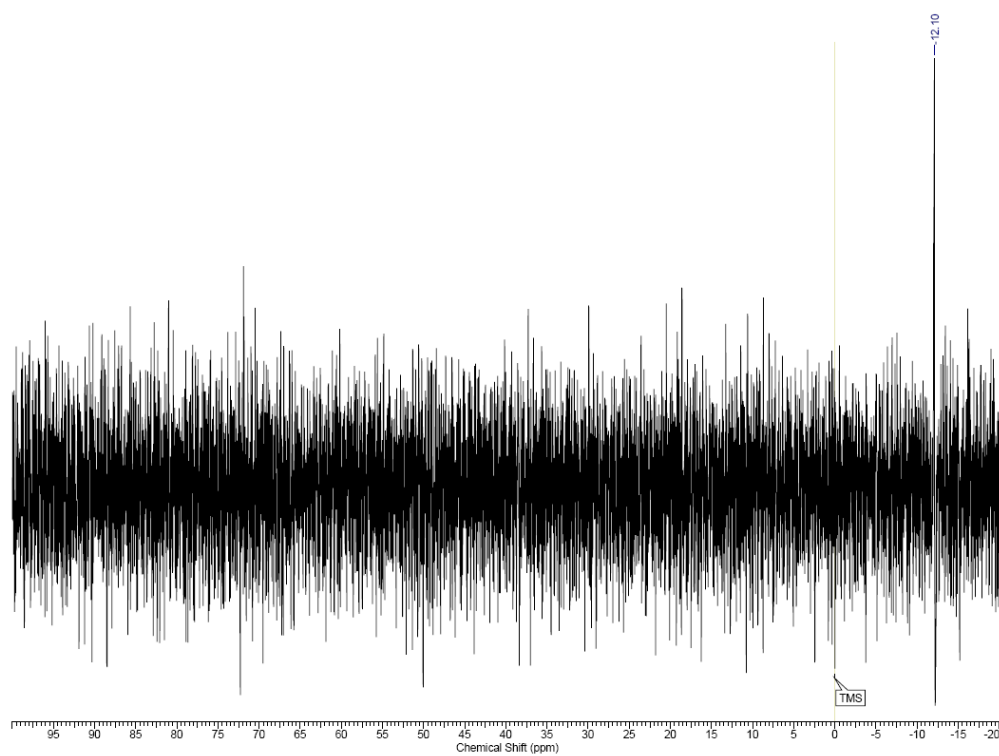
^1H NMR (400 MHz, $\text{DICHLOROMETHANE-}d_2$) δ ppm 2.18 (s, 1 H) 6.78 (br. s., 2 H) 7.19 (d, $J=6.77$ Hz, 2 H)

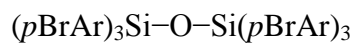


^1H - ^{29}Si gHSQC NMR

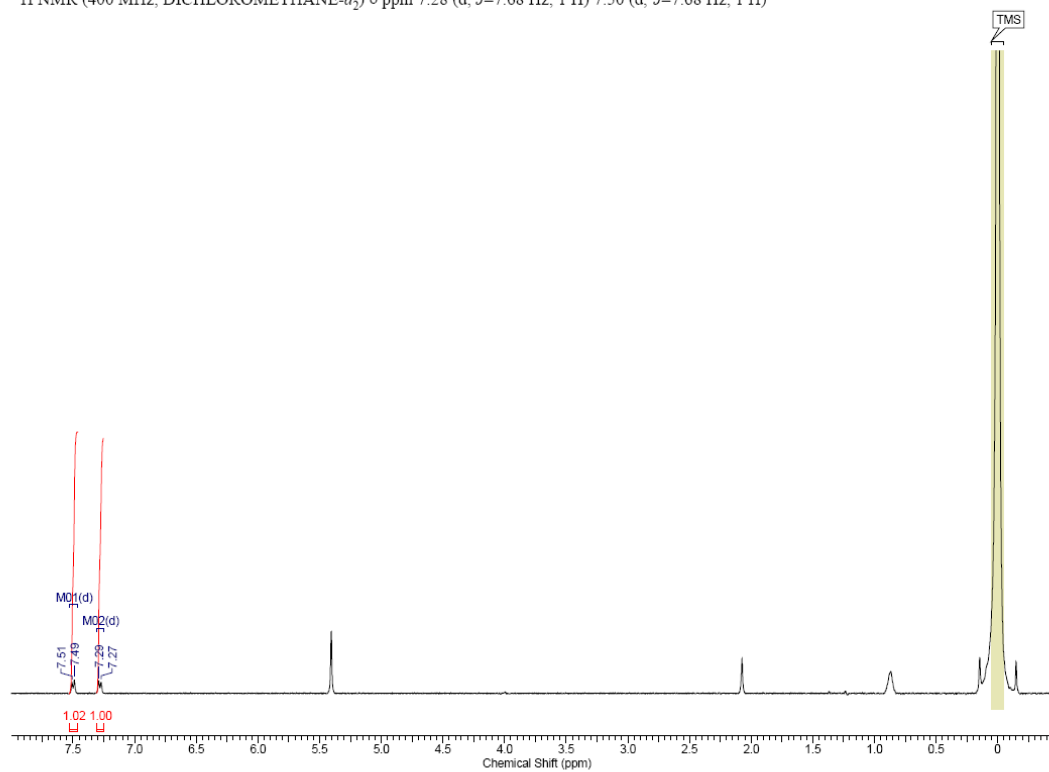


One dimensional ^{29}Si NMR

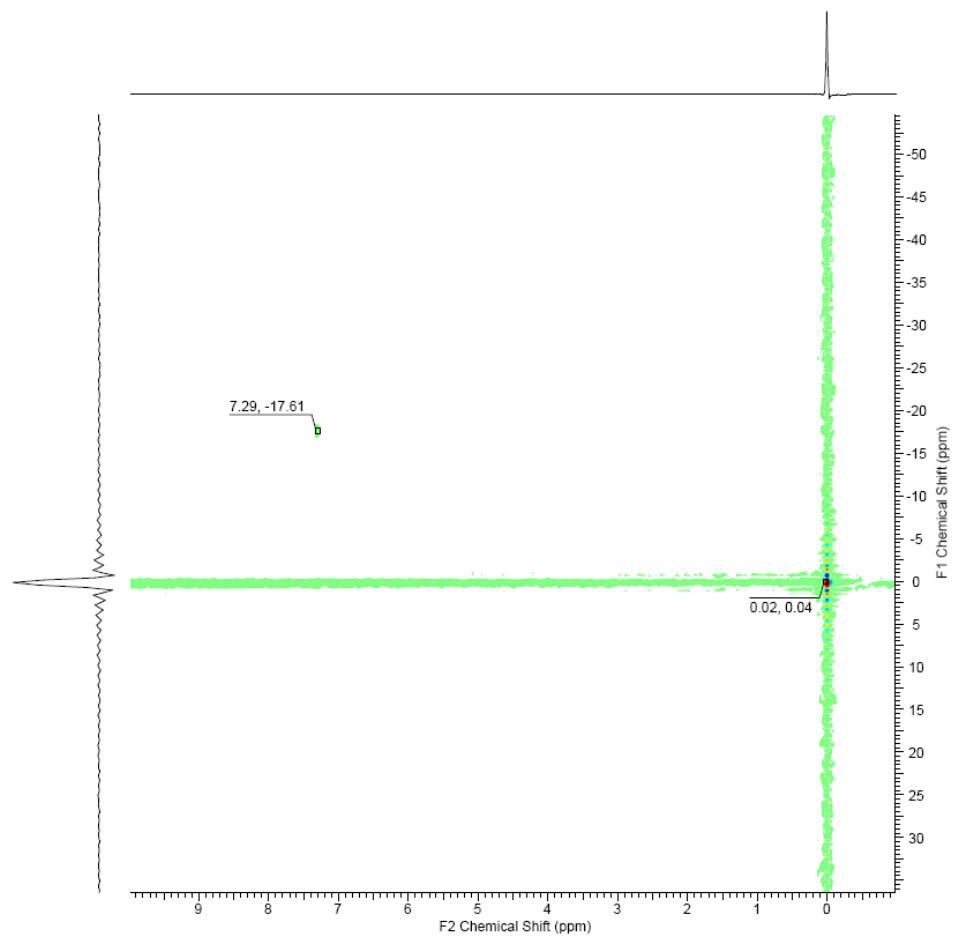




^1H NMR (400 MHz, $\text{DICHLOROMETHANE-}d_2$) δ ppm 7.28 (d, $J=7.68$ Hz, 1 H) 7.50 (d, $J=7.68$ Hz, 1 H)

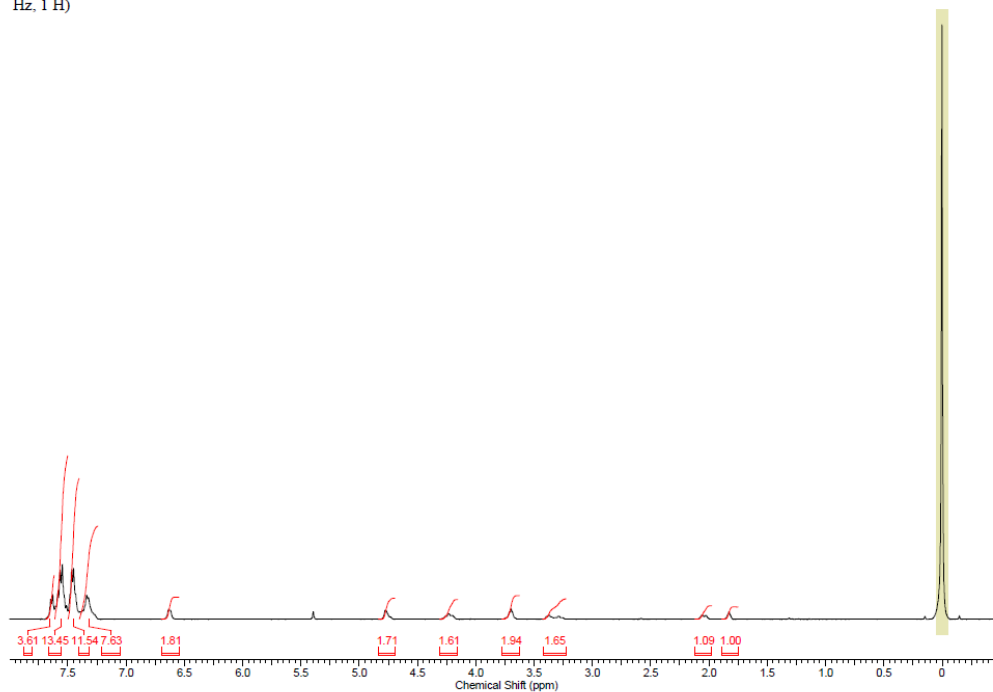


^1H - ^{29}Si gHSQC NMR

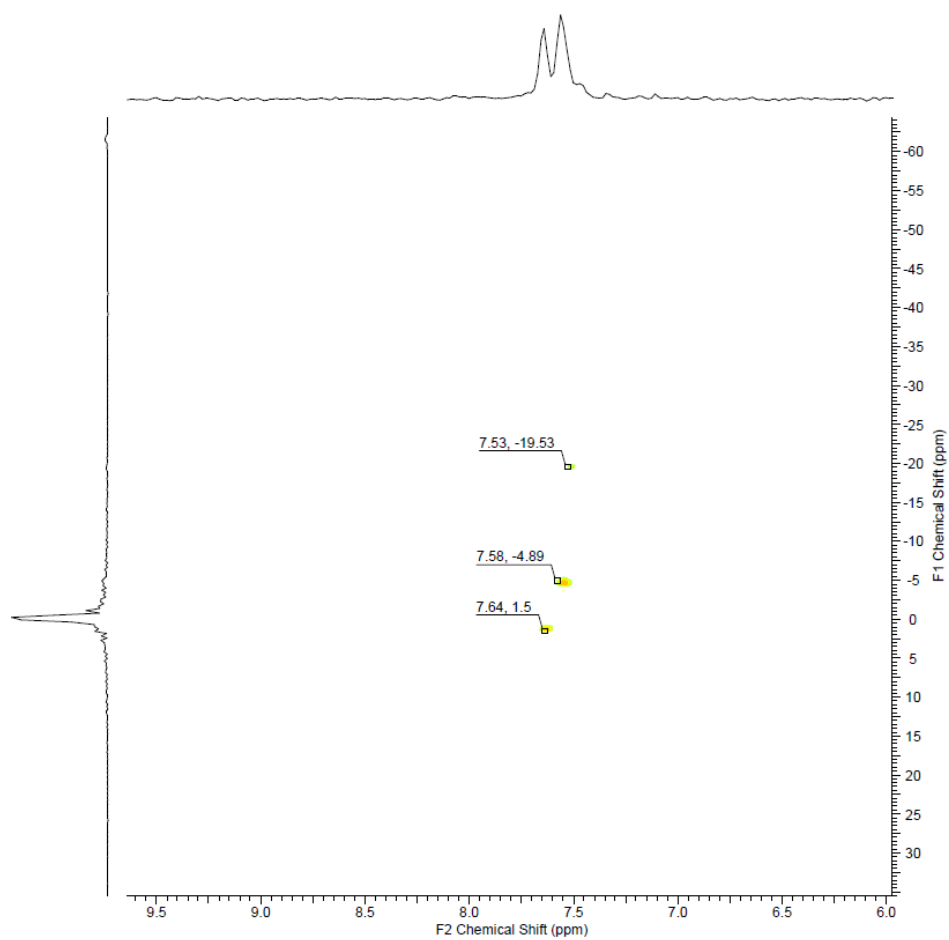


3.7/Ph₃SiCl

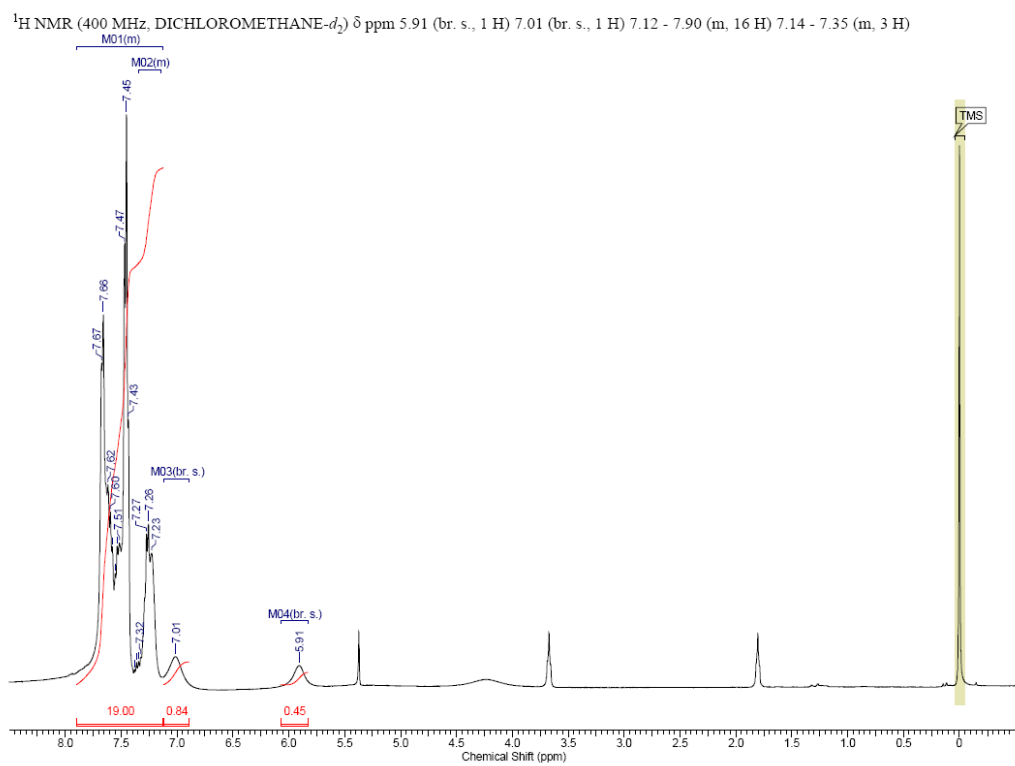
¹H NMR (400 MHz, DICHLOROMETHANE-*d*₂) δ ppm 1.83 (br. s., 1 H) 2.04 (d, *J*=12.44 Hz, 1 H) 3.23 - 3.42 (m, 1 H) 3.70 (d, *J*=6.22 Hz, 1 H) 4.16 - 4.31 (m, 1 H) 4.77 (br. s., 1 H) 6.63 (d, *J*=5.49 Hz, 1 H) 7.24 - 7.40 (m, 2 H) 7.46 (d, *J*=6.59 Hz, 3 H) 7.50 - 7.61 (m, 4 H) 7.64 (d, *J*=6.95 Hz, 1 H)



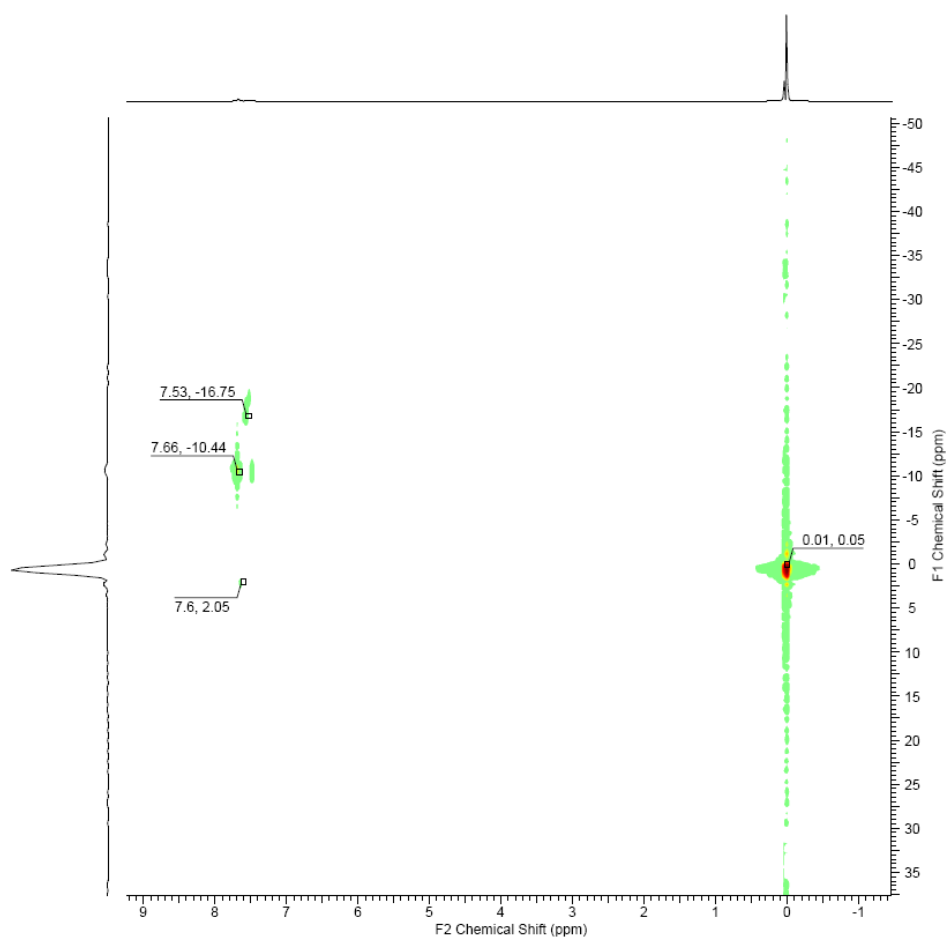
^1H - ^{29}Si gHSQC NMR



3.8/Ph₃SiCl

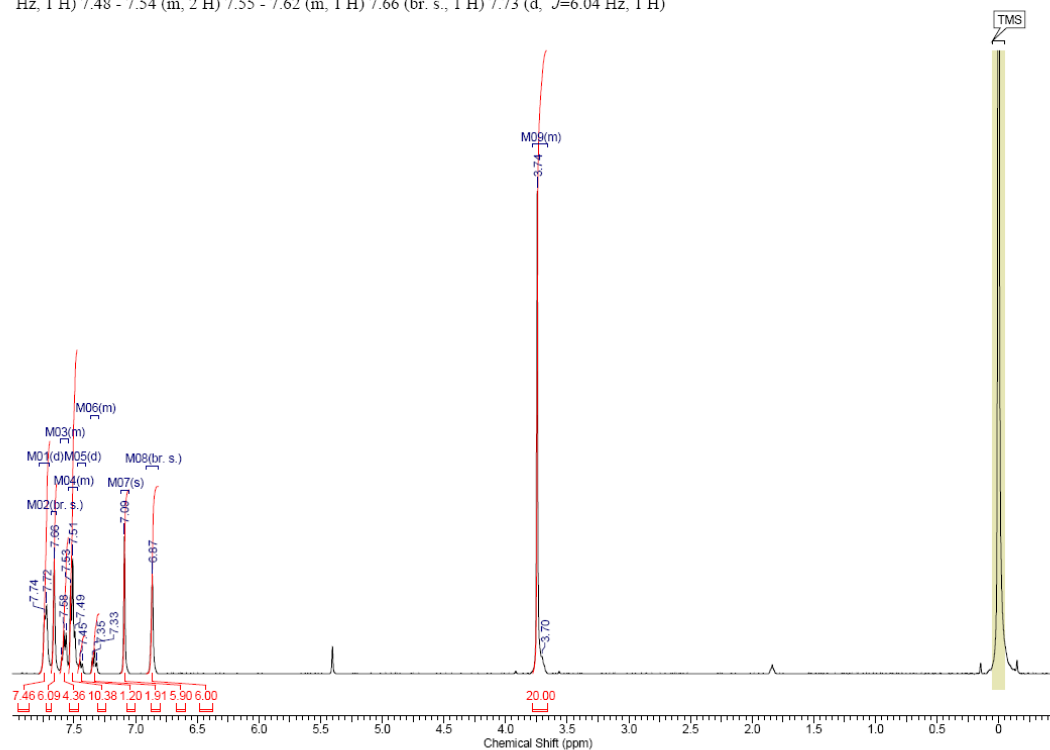


^1H - ^{29}Si gHSQC NMR

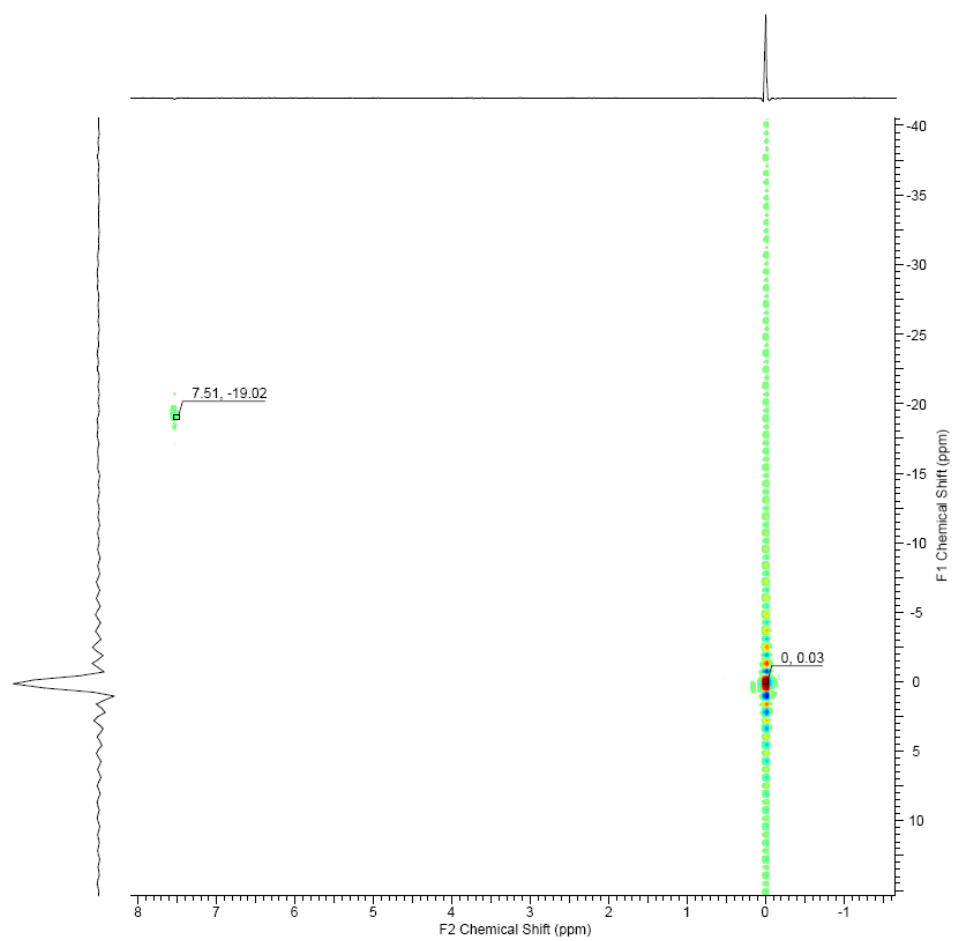


3.9/Ph₃SiCl

¹H NMR (400 MHz, DICHLOROMETHANE-*d*₂) δ ppm 3.66 - 3.78 (m, 20 H) 6.87 (br. s., 6 H) 7.09 (s, 6 H) 7.30 - 7.37 (m, 2 H) 7.44 (d, *J*=7.14 Hz, 1 H) 7.48 - 7.54 (m, 2 H) 7.55 - 7.62 (m, 1 H) 7.66 (br. s., 1 H) 7.73 (d, *J*=6.04 Hz, 1 H)

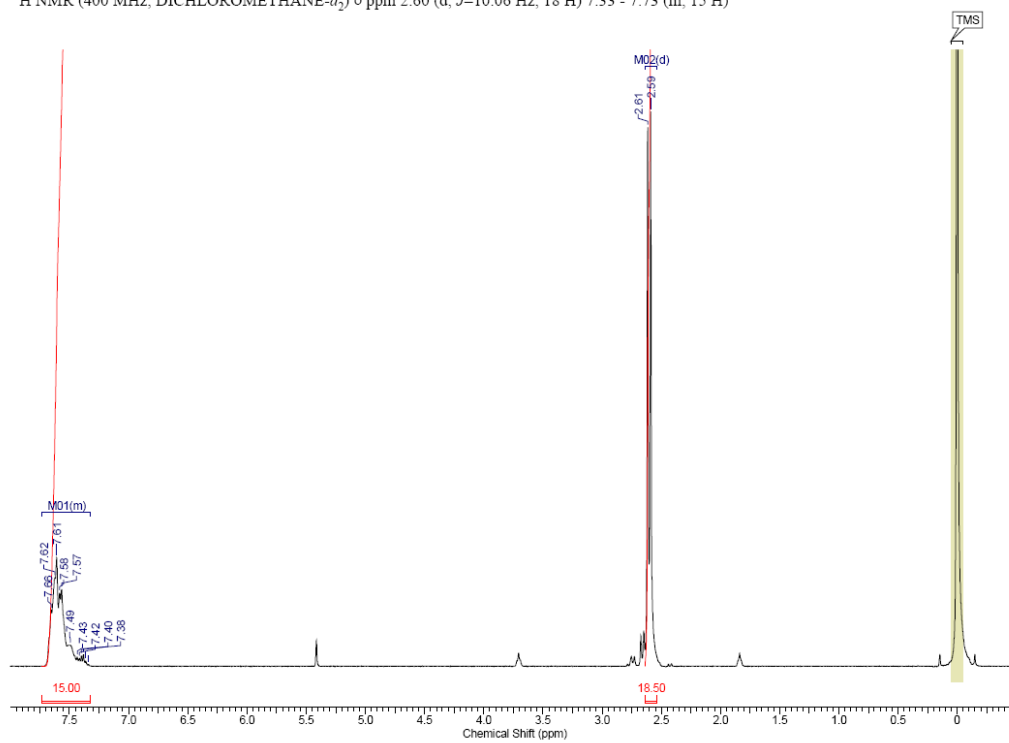


^1H - ^{29}Si gHSQC NMR

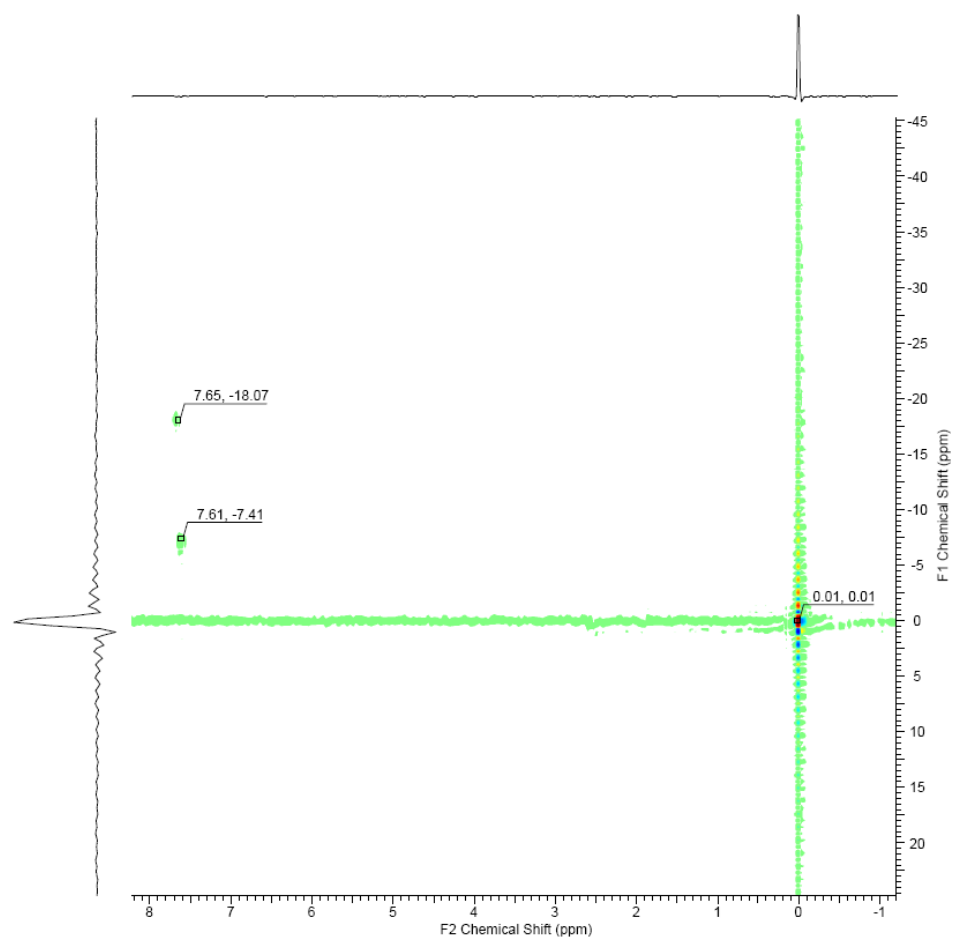


3.10/Ph₃SiCl

¹H NMR (400 MHz, DICHLOROMETHANE-*d*₂) δ ppm 2.60 (d, *J*=10.06 Hz, 18 H) 7.33 - 7.73 (m, 15 H)

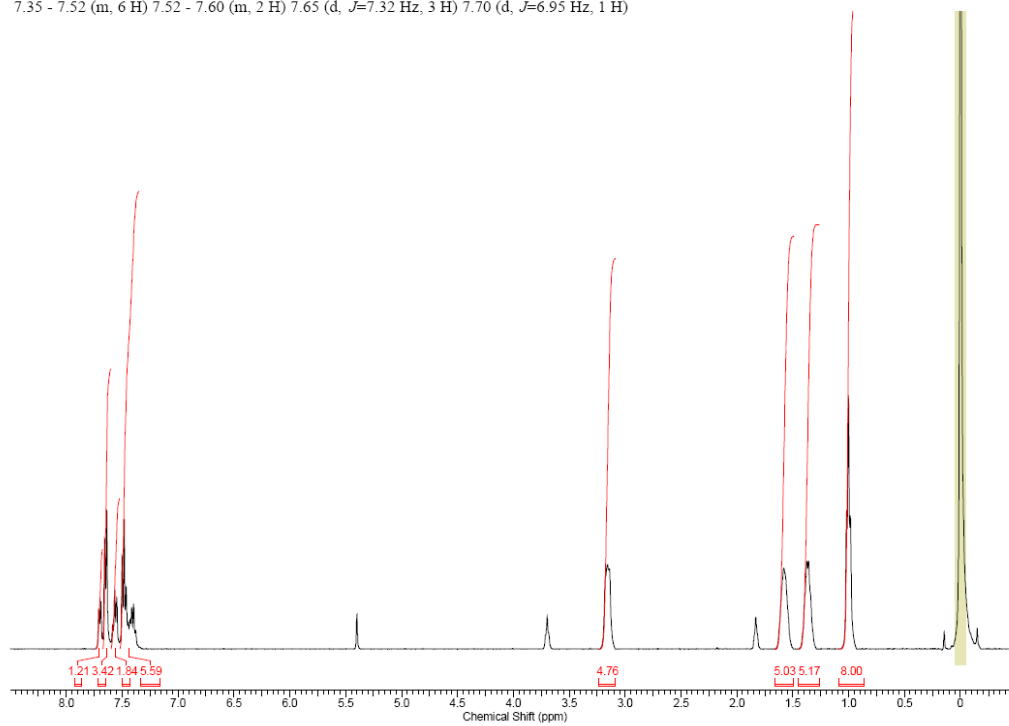


^1H - ^{29}Si gHSQC NMR

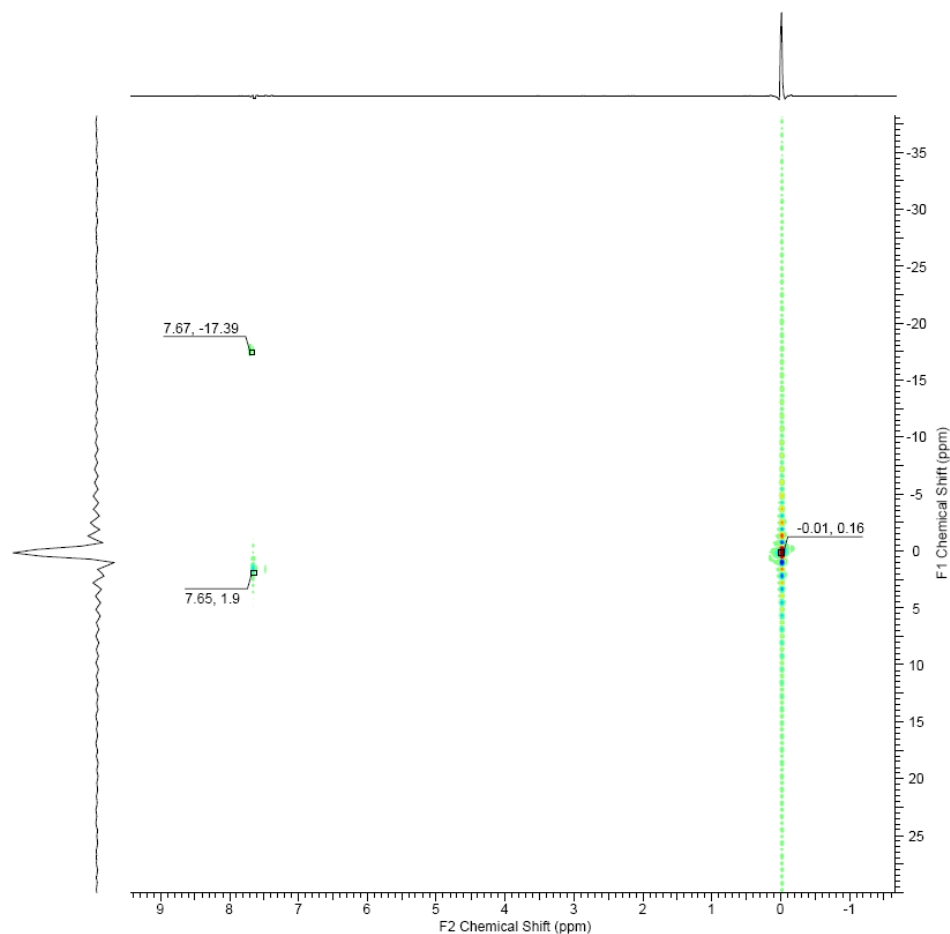


3.11/Ph₃SiCl

¹H NMR (400 MHz, DICHLOROMETHANE-*d*₂) δ ppm 0.87 - 1.09 (m, 8 H) 1.37 (d, *J*=6.40 Hz, 5 H) 1.58 (br. s., 5 H) 3.15 (d, *J*=7.32 Hz, 5 H) 7.35 - 7.52 (m, 6 H) 7.52 - 7.60 (m, 2 H) 7.65 (d, *J*=7.32 Hz, 3 H) 7.70 (d, *J*=6.95 Hz, 1 H)



3.11/Ph₃SiCl



3.7 References

1. Weickgenannt, A.; Mewald, M.; Oestreich, M., Asymmetric Si-O coupling of alcohols. *Org. Biomol. Chem.* **2010**, *8*, 1497-1504.
2. Rodrigo, J. M.; Zhao, Y.; Hoveyda, A. H.; Snapper, M. L., Regiodivergent Reactions through Catalytic Enantioselective Silylation of Chiral Diols. Synthesis of Sapinofuranone A. *Org. Lett.* **2011**, *13*, 3778-3781.
3. Sheppard, C. I.; Taylor, J. L.; Wiskur, S. L., Silylation-Based Kinetic Resolution of Monofunctional Secondary Alcohols. *Org. Lett.* **2011**, *13*, 3794-3797.

4. Worthy, A. D.; Sun, X.; Tan, K. L., Site-Selective Catalysis: Toward a Regiodivergent Resolution of 1,2-Diols. *J. Amer. Chem.Soc.* **2012**, *134*, 7321-7324.
5. Sun, X.; Worthy, A. D.; Tan, K. L., Scaffolding Catalysts: Highly Enantioselective Desymmetrization Reactions. *Angew. Chem. Int. Ed.* **2011**, *50*, 8167-8171.
6. Vedejs, E.; Jure, M., Efficiency in Nonenzymatic Kinetic Resolution. *Angew. Chem. Int. Ed.* **2005**, *44*, 3974-4001.
7. Kagan, H. B.; Fiaud, J. C., In *Topics in Stereochemistry*, Eliel, E. L.; Wilen, S. H., Eds. John Wiley & Sons, Inc.: New York, 1988; Vol. 18, p 249.
8. Li, X.; Jiang, H.; Uffman, E. W.; Guo, L.; Zhang, Y.; Yang, X.; Birman, V. B., Kinetic Resolution of Secondary Alcohols Using Amidine-Based Catalysts. *J. Org. Chem.* **2012**, *77*, 1722-1737.
9. Kobayashi, M.; Okamoto, S., Unexpected reactivity of annulated 3H-benzothiazol-2-ylideneamines as an acyl transfer catalyst. *Tet. Lett* **2006**, *47*, 4347-4350.
10. Li, X.; Liu, P.; Houk, K. N.; Birman, V. B., Origin of Enantioselectivity in CF₃-PIP-Catalyzed Kinetic Resolution of Secondary Benzylic Alcohols. *J. Am. Chem. Soc.* **2008**, *130*, 13836-13837.
11. Liu, P.; Yang, X.; Birman, V. B.; Houk, K. N., Origin of Enantioselectivity in Benzotetramisole-Catalyzed Dynamic Kinetic Resolution of Azlactones. *Org. Lett.* **2012**, *14*, 3288-3291.
12. Larionov, E.; Mahesh, M.; Spivey, A. C.; Wei, Y.; Zipse, H., Theoretical Prediction of Selectivity in Kinetic Resolution of Secondary Alcohols Catalyzed by Chiral DMAP Derivatives. *J. Am. Chem. Soc.* **2012**, *134*, 9390-9399.
13. Chuit, C.; Corriu, R. J. P.; Reye, C.; Young, J. C., Reactivity of penta- and hexacoordinate silicon compounds and their role as reaction intermediates. *Chem. Rev.* **1993**, *93*, 1371-1448.
14. Marciniec, B.; Chojnowski, J., *Progress in Organosilicon Chemistry*. 1st ed.; Gordon and Breach: Amsterdam, 1995.
15. Patai, S.; Apeloig, Y., *The Chemistry of Organic Silicon Compounds*. John Wiley & Sons, Ltd: Chichester, 2001; Vol. 3.
16. Corriu, R. J. P.; Guerin, C.; Stone, F. G. A.; Robert, W., Nucleophilic Displacement at Silicon: Recent Developments and Mechanistic Implications. In *Advances in Organometallic Chemistry*, Academic Press: 1982; Vol. Volume 20, pp 265-312.
17. Patai, S.; Rappoport, Z., *The Chemistry of Organic Silicon Compounds*. Wiley: Chichester: 1989; Vol. 1, p 840-863.

18. Rendler, S.; Oestreich, M., Hypervalent Silicon as a Reactive Site in Selective Bond-Forming Processes. *Synthesis* **2005**, 2005, 1747.
19. Patai, S.; Apeloig, Y., *The Chemistry of Organic Silicon Chemistry*. John Wiley & Sons, Ltd: Chichester, 1998; Vol. 2.
20. Chojnowski, J.; Cypryk, M.; Michalski, J., The nature of the interaction between hexamethyl-phosphortriamide and trimethylhalosilanes; cations containing tetravalent silicon as possible intermediates in nucleophile-induced substitution of silicon halides. *J. Organomet. Chem.* **1978**, 161, C31-C35.
21. Bassindale, A. R.; Stout, T., A ^{29}Si , ^{13}C and ^1H NMR study of the interaction of various halotrimethylsilanes and trimethylsilyl triflate with dimethyl formamide and acetonitrile, a comment on the nucleophile induced racemisation of halosilanes. *J. Organomet. Chem.* **1982**, 238, C41-C45.
22. Chu, H. K.; Johnson, M. D.; Frye, C. L., Tertiary alcoholysis of chlorosilanes via tetracoordinate silylated quaternary ammonium intermediates. *J. Organomet. Chem.* **1984**, 271, 327-336.
23. Akiba, K., *Chemistry of Hypervalent Compounds*. Wiley-VCH: New York, 1999.
24. Cheung, Y.-S.; Ng, C.-Y.; Chiu, S.-W.; Li, W.-K., Application of three-center-four-electron bonding for structural and stability predictions of main group hypervalent molecules: the fulfillment of octet shell rule. *J. Mol. Struct.-THEOCHEM* **2003**, 623, 1-10.
25. Benaglia, M.; Guizzetti, S.; Rossi, S., Silicate-Mediated Stereoselective Reactions Catalyzed by Chiral Lewis Bases. In *Catalytic Methods in Asymmetric Synthesis*, John Wiley & Sons, Inc.: 2011; pp 579-624.
26. Tandura, S.; Voronkov, M.; Alekseev, N., Molecular and electronic structure of penta- and hexacoordinate silicon compounds. *Structural Chemistry of Boron and Silicon*. In Springer Berlin / Heidelberg: 1986; Vol. 131, pp 99-189.
27. Bassindale, A. R.; Jiang, J., The effect of pentacoordination on silicon-29 NMR chemical shifts and silicon-hydrogen coupling constants. *J. Organomet. Chem.* **1993**, 446, C3-C5.
28. Kobayashi, J.; Ishida, K.; Kawashima, T., Synthesis of a heptacoordinate trichlorosilane with a tetradentate ligand and unusual stability for nucleophilic substitution. *Silicon Chemistry* **2002**, 1, 351-354.
29. Scholl, R. L.; Maciel, G. E.; Musker, W. K., Silicon-29 chemical shifts of organosilicon compounds. *J. Am. Chem. Soc.* **1972**, 94, 6376-6385.
30. Bacon, M. R.; Maciel, G. E., Solvent effects on the five shielding constants in tetramethylsilane and cyclohexane. *J. Am. Chem. Soc.* **1973**, 95, 2413-2426.

31. Williams, E. A.; Cargioli, J. D.; Larochelle, R. W., Silicon-29 NMR. Solvent effects on chemical shifts of silanols and silylamines. *J. Organomet. Chem.* **1976**, *108*, 153-158.
32. Campbell-Ferguson, H. J.; Ebsworth, E. A. V., Adducts formed between some halogenosilanes and the organic bases pyridine, trimethylamine, and tetramethylethylenediamine. Part I. Stoichiometry. *J. Chem. Soc. A* **1966**, 1508-1514.
33. Campbell-Ferguson, H. J.; Ebsworth, E. A. V., Adducts of the halogenosilanes. Part II. Physical properties and structures. *J. Chem. Soc. A* **1967**, 705-712.
34. Boudjouk, P.; D. Kloos, S.; Kim, B.-K.; Page, M.; Thweatt, D., An unexpected redistribution of trichlorosilane. Synthesis, structure and bonding of (N,N,N',N'-tetraethylethylenediamine)dichlorosilane. *J. Chem. Soc., Dalton Trans.* **1998**, *6*, 877- 880.
35. Lippmaa, E. T.; Alla, M. A.; Pehk, T. J.; Engelhardt, G., Solid-state high resolution NMR spectroscopy of spin 1/2 nuclei (carbon-13, silicon-29, tin-119) in organic compounds. *J. Am. Chem. Soc.* **1978**, *100*, 1929-1931.
36. Brendler, E.; Heine, T.; Hill, A. F.; Wagler, J., A Pentacoordinate Chlorotrimethylsilane Derivative: A very Polar Snapshot of a Nucleophilic Substitution and its Influence on ²⁹Si Solid State NMR Properties. *Z. Anorg. Allg. Chem.* **2009**, *635*, 1300-1305.
37. Bassindale, A. R.; Stout, T., Interaction of N-trimethylsilylimidazole with electrophilic trimethylsilyl compounds. Part 1. Characterisation of silylimidazolium salts. *J. Chem. Soc., Perkin Transs. 2* **1986**, *2*, 221-225.
38. Aliev, A. E.; Atkinson, C. E.; Harris, K. D. M., Hydrogen Bond Dynamics in Solid Triphenylsilanol. *J. Phys. Chem. B* **2002**, *106*, 9013-9018.
39. Bax, A.; Summers, M. F., Proton and carbon-13 assignments from sensitivity-enhanced detection of heteronuclear multiple-bond connectivity by 2D multiple quantum NMR. *J. Am. Chem. Soc.* **1986**, *108*, 2093-2094.
40. Schraml, J., ²⁹Si NMR Experiments in Solutions of Organosilicon Compounds. In *The Chemistry of Organic Silicon Compounds*, John Wiley & Sons, Ltd: 2001; pp 223-339.
41. Bearpark, M. J.; McGrady, G. S.; Prince, P. D.; Steed, J. W., The First Structurally Characterized Hypervalent Silicon Hydride: Unexpected Molecular Geometry and Si-H Interactions. *J. American Chem. Soc.* **2001**, *123*, 7736-7737.
42. Rot, N.; Nijbacker, T.; Kroon, R.; de Kanter, F. J. J.; Bickelhaupt, F.; Lutz, M.; Spek, A. L., Introduction of Bulky Substituents at the Bridgehead Position of a 9-Silatrypticene: Pentacoordinate Hydridoorganylsilicates as Intermediates. *Organometallics* **2000**, *19*, 1319-1324.

43. Bassindale, A. R.; Stout, T., The preparation and observation by ^{29}Si n.m.r. spectroscopy of simple, acyclic, five-coordinate silicon salts. *J. Chem. Society, Chem. Comm.* **1984**, 21, 1387-1389.
44. Lyčka, A.; Šnobl, D.; Handlř, K.; Holeček, J.; Nádvorník, M., ^{29}Si and ^{13}C NMR spectra of some alkylidiphenylchlorosilanes, alkylidiphenylsilanoles and bis(alkylidiphenylsilyl)chromates. *Collect. Czech. Chem. Commun.* **1982**, 47, 603-612.
45. Negrebetsky, V. V.; Negrebetsky, V. V.; Shipov, A. G.; Kramorova, E. P.; Baukov, Y. I., Intermolecular and intramolecular coordination interactions in solutions of N-(dimethylchlorosilylmethyl) acetamides. *J. Organomet. Chem.* **1995**, 496, 103-107.
46. Kummer, D.; Halim, S. H. A., Beiträge zur Chemie der Halogensilan-Addukte. XXIV. Übergänge zwischen penta- und tetrakoordinierten SiCl - und SiBr -Verbindungen und ihre Abhängigkeit von Lösungsmittel, Temperatur und Konzentration. Direkter spektroskopischer Nachweis des reversiblen Übergangs von einer O-SiCl zu einer OSi-Cl-Koordination. *Z. Anorg. Allg. Chem.* **1996**, 622, 57-66.
47. Cragg, R. H.; Lane, R. D., Contributions to group IV organometallic chemistry: VII. The effect of electronegativity on substituent shifts in silicon-29 NMR. *J. Organomet. Chem.* **1984**, 277, 199-201.
48. Ritchie, C. D.; Sager, W. F., An Examination of Structure-Reactivity Relationships. In *Progress in Physical Organic Chemistry*, John Wiley & Sons, Inc.: 2007; pp 323-400.
49. Akhani, R., *Manuscript in preparation*.
50. Akhani, R., *Manuscript in preparation*.
51. Birman, V. B.; Li, X., Homobenzotetramisole: An Effective Catalyst for Kinetic Resolution of Aryl-Cycloalkanols. *Org. Lett.* **2008**, 10, 1115-1118.
52. Zhang, Y.; Birman, V. B., Effects of Methyl Substituents on the Activity and Enantioselectivity of Homobenzotetramisole-Based Catalysts in the Kinetic Resolution of Alcohols. *Adv. Synth. Catal.* **2009**, 351, 2525-2529.
53. Birman, V. B.; Li, X., Benzotetramisole: A Remarkably Enantioselective Acyl Transfer Catalyst. *Org. Lett.* **2006**, 8, 1351-1354.
54. Hensen, K.; Zengerly, T.; Müller, T.; Pickel, P., Ionische Strukturen von 4- bzw. 5fach koordiniertem Silicium: $[\text{Me}_3\text{Si}(\text{NMI})]^+\text{Cl}^-$, $[\text{Me}_2\text{HSi}(\text{NMI})_2]^+\text{Cl}^-$, $[\text{Me}_2\text{Si}(\text{NMI})_3]_2^{+2}\text{Cl}^- \cdot \text{NMI}$. *Z. Anorg. Allg. Chem.* **1988**, 558, 21-27.
55. Bassindale, A. R.; Stout, T., The preparation and observation by ^{29}Si n.m.r. spectroscopy of simple, acyclic, five-co-ordinate silicon salts. *J. Chem. Soc., Chem. Comm.* **1984**, 21, 1387-1389.

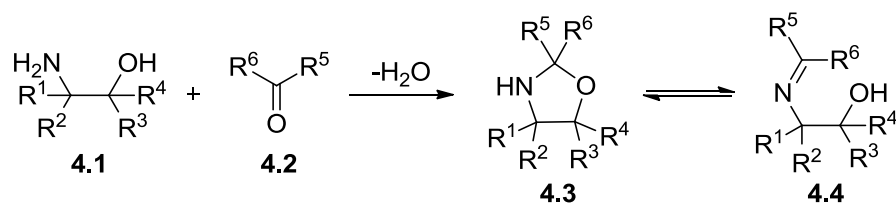
56. Corriu, R. J. P.; Dabosi, G.; Martineau, M., The nature of the interaction of nucleophiles such as HMPT, DMSO, DMF and Ph₃PO with triorganohalo-silanes, germanes, and -stannanes and organophosphorus compounds. Mechanism of nucleophile induced racemization and substitution at metal. *J. Organomet. Chem.* **1980**, *186*, 25-37.
57. Maji, B.; Joannesse, C.; Nigst, T. A.; Smith, A. D.; Mayr, H., Nucleophilicities and Lewis Basicities of Isothiourea Derivatives. *J. Org. Chem.* **2011**, *76*, 5104-5112.
58. Mislow, K., Stereochemical consequences of correlated rotation in molecular propellers. *Acc. Chem. Res.* **1976**, *9*, 26-33.
59. Mislow, K.; Gust, D.; Finocchiaro, P.; Boettcher, R., Stereochemical correspondence among molecular propellers. In *Stereochemistry I*, Springer Berlin Heidelberg: 1974; Vol. 47, pp 1-28.
60. Allen, G. W.; Aroney, M. J.; Hambley, T. W., Conformational analysis of group IVB aryls: An electric birefringence and molecular mechanics study. *J. Mol. Struc.* **1990**, *216*, 227-240.
61. Gust, D.; Mislow, K., Analysis of isomerization in compounds displaying restricted rotation of aryl groups. *J. Am. Chem. Soc.* **1973**, *95*, 1535-1547.
62. Andose, J. D.; Mislow, K., Structure and dynamic stereochemistry of trimesitylmethane. II. Empirical force field calculations. *J. Am. Chem. Soc.* **1974**, *96*, 2168-2176.
63. Kates, M. R.; Andose, J. D.; Finocchiaro, P.; Gust, D.; Mislow, K., Empirical force-field calculations on a model system for trimesityl derivatives of Group IIIa, IVa, and Va elements. Stereoisomerization pathways. *J. Am. Chem. Soc.* **1975**, *97*, 1772-1778.
64. Ściebura, J.; Skowronek, P.; Gawronski, J., Trityl Ethers: Molecular Bevel Gears Reporting Chirality through Circular Dichroism Spectra. *Angew. Chem. Int. Ed.* **2009**, *48*, 7069-7072.
65. Ściebura, J.; Gawroński, J., Double Chirality Transmission in Trityl Amines: Sensing Molecular Dynamic Stereochemistry by Circular Dichroism and DFT Calculations. *Chem. Eur. J.* **2011**, *17*, 13138-13141.
66. DiNitto, J. M.; Kenney, J. M., Noise Characterization in Circular Dichroism Spectroscopy. *Appl. Spectrosc.* **2012**, *66*, 180-187.
67. Savitzky, A.; Golay, M. J. E., Smoothing and Differentiation of Data by Simplified Least Squares Procedures. *Anal. Chem.* **1964**, *36*, 1627-1639.

68. Leslie, F. M.; Demus, D.; Goodby, J.; Gray, G. W.; Spiess, H. W.; Vill, V., Theory of the Liquid Crystalline State. In *Physical Properties of Liquid Crystals*, Wiley-VCH Verlag GmbH: 2007; pp 25-86.

Chapter 4. The synthesis and characterization of 2-pyridyl-oxazolidine ligands and their application as chiral sensors and catalysts

4.1 Introduction

Due to the ever growing demand for enantiomerically pure materials, the development of novel ligands and organocatalysts has been an area of active research. In particular, the oxazolidine functionality (**Scheme 4.1**, (**4.3**)) has shown much promise as a chiral ligand for transition metal catalyzed transformations and as organocatalysts in such reactions as alkylation, alkynylation, Diels-Alder, and Henry reactions.^{1, 2} This functionality has a superficial relationship to the more widely used, privileged ligand, the oxazoline functionality (**Figure 4.1**, (**4.5**)). While oxazolines and their use in asymmetric catalysis has been well documented,³⁻⁶ the completely saturated, oxazolidine functionality has only begun to be explored. The basic 1,3-oxazolidine core is a 5-member ring containing a hemiaminal carbon. The most common method for the synthesis of this functionality (**Scheme 4.1**) is through a dehydration reaction (imine formation) between an α -amino alcohol (**4.1**) and an aldehyde or ketone (**4.2**) (although the development of alternative methods for the synthesis of this functionality is an area of active research^{7, 8}). This synthetic method has the potential for the easy installation of chiral substituents in the 1,3-oxazolidine product (**4.3**) via the use of a chiral amino alcohol starting material.



Scheme 4.1 The most common method for the synthesis of the core structure of the 1,3-oxazolidine functionality (**4.3**) and the open imine form **4.4**.

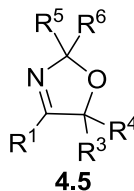
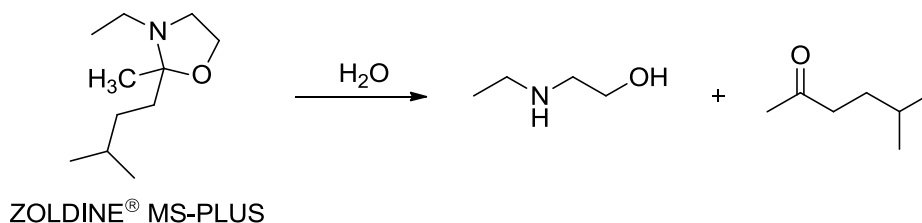


Figure 4.1 The oxazoline functionality

The utility of using the oxazolidine functionality as a ligand for asymmetric catalysis, is due to the presence of up to two chiral centers adjacent to the metal binding nitrogen center. This interesting ligand topography may be the reason the ligands have achieved high enantiomeric excess (ee) for a number of asymmetric reactions.⁹ Despite their great potential for use in asymmetric transformations, their potential as asymmetric catalysts has only just begun to be explored. The paucity of examples is mainly due to the equilibrium that exists between the 1,3-oxazolidine and imine forms (**4.3** and **4.4** respectively), which complicates their isolation and analysis.¹⁰ Interestingly, since the ring closure reaction between the amino alcohol and aldehyde is a 5-endo-trig reaction and therefore formally disfavored,¹¹ there should be a slow equilibrium between **4.3** and **4.4** on the NMR time scale which would allow for easy identification, however this is often not the case. Furthermore, complete formation of the oxazolidine from the imine intermediate seems to depend largely upon the amino alcohol and aldehyde or ketone used. Also, the sensitivity of some oxazolidine containing compounds complicates purification as silica gel can cause degradation.¹² Some oxazolidine compounds can also

be quite moisture sensitive and some compounds containing this functionality have also been employed as moisture scavengers in industrial applications¹³ such as ZOLDINE[®] MS-PLUS sold by Dow chemical company (**Scheme 4.2**).



Scheme 4.2 The commercially available moisture scavenging oxazolidine, ZOLDINE[®] MS-PLUS and its hydrolysis products.¹⁴

Although the aforementioned properties can complicate the synthesis and characterization of some oxazolidine compounds, these ligands have much potential in asymmetric catalysis. Therefore, the successful synthesis of an enantiomerically pure oxazolidine compound which is simple to purify and is not moisture sensitive are key targets for the preparation of oxazolidines. Apart from their use as organocatalysts or chiral ligands for metal catalyzed transformations, another application which was investigated was the application of metal-bisoxazolidine complexes for use as colorimetric¹⁵ sensors. Specifically these complexes were studied for their ability to discriminate between the enantiomers of chiral alcohols and/or chiral amines. By preferentially binding a the analyte (which was a single enantiomer) to the complex, it was assumed that there would be a noticeable color change when one enantiomer binds to the complex, or there would be a detectable difference in the UV-Vis spectrum of the bound complex.

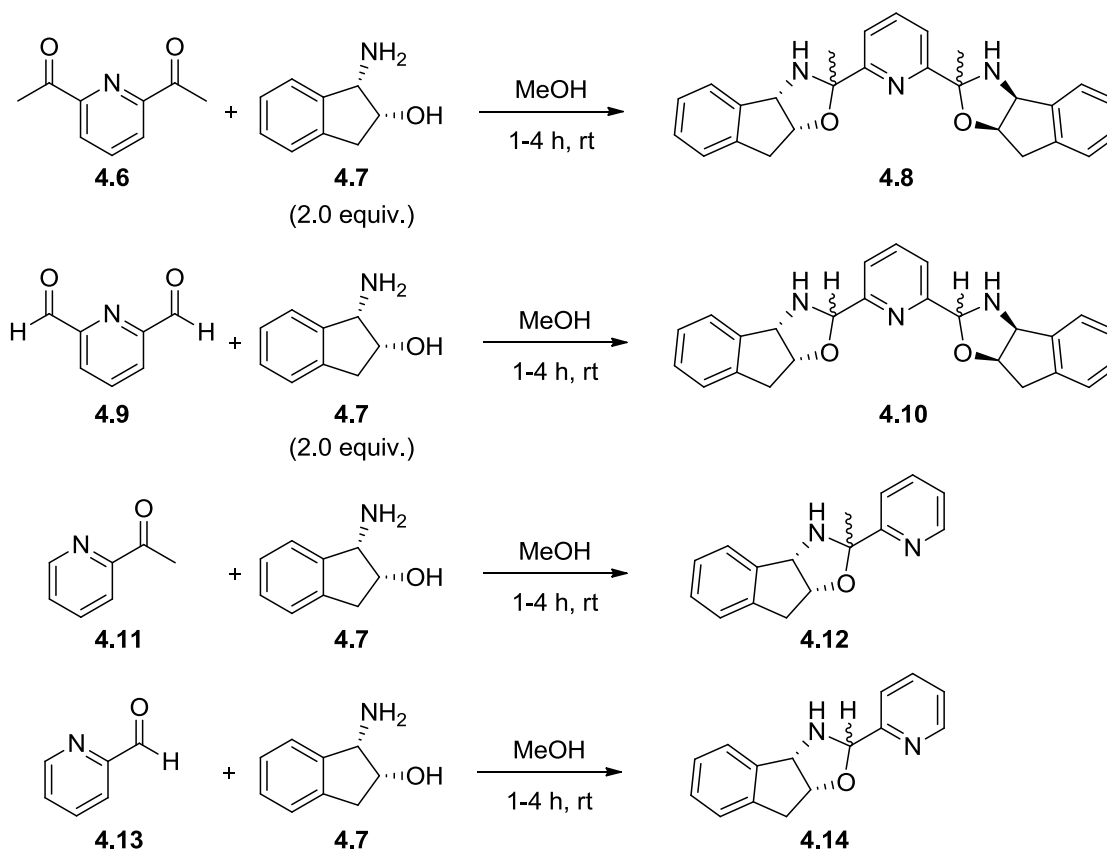
The subsequent metal-oxazolidine and bisoxazolidine complexes presented herein are to the best of our knowledge unique and their properties were analyzed and crystal

structures obtained. NMR studies and calculations were performed to determine first whether the major product is the imine or oxazolidine isomer and the diastereoselectivity of the formed oxazolidine product. Then when crystallized, the physical properties of the crystal structures were also analyzed for such physical properties. Then the application of the metal complexes for use in colorimetric sensing and catalysis will be presented.

4.2 Synthesis and characterization of chiral 2-Pyridyl-oxazolidine (MonOx) and 2-Pyridyl-bisoxazolidine (BisOx) complexes

Due to the growing interest in the oxazolidine functionality as a chiral ligand and organocatalysts, a series of novel bidentate pyridyl-oxazolidine (MonOx) and tridentate pyridyl-bisoxazolidine (BisOx) ligands were synthesized (**Scheme 4.2**). The synthesis of both MonOx and BisOx compounds followed the same general procedure, the focus of this work is primarily on BisOx and resulting complexes, however MonOx was used as a simplified system for several of the studies presented. The addition of 2,6-diacetyl pyridine or 2,6-pyridine carboxaldehyde (**4.6** or **4.9** respectively) to (1*S*,2*R*)-aminoindanol (**4.7**) in methanol afforded dimethyl-BisOx **4.8** as an oil and BisOx **4.10** as a white solid. Both of these compounds were difficult to purify by silica gel column, but did not appear to be moisture sensitive. However, **4.10** was found to be very insoluble in water and during the course of the reaction **4.10** precipitated from solution with relatively high purity. For the synthesis of the MonOx compounds **4.12** and **4.14** a similar procedure was followed for the formation of the BisOx product, but with 2-acetyl

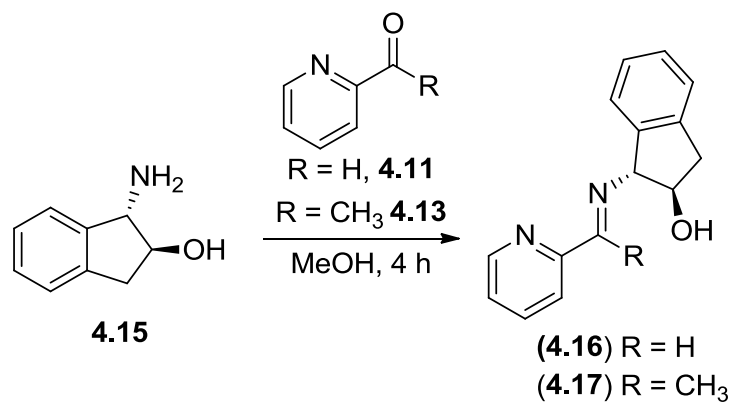
pyridine (**4.11**) to form the methyl-MonOX (**4.12**) and 2-pyridine carboxaldehyde (**4.13**) to form MonOx (**4.14**), both as oils.



Scheme 4.3 Synthesis of BisOx compounds **4.8** and **4.10**, as well as MonOx **4.12** and **4.14**.

Apart from the potential that **4.8**, **4.10**, **4.12**, and **4.14** have to form diastereomers in the ring closed, oxazolidine conformation, there also exists the possibility that the majority of compounds exists in the imine form. To determine whether the isolated compounds are either in the oxazolidine (**4.3**) form or the imine form (**4.4**), $^1\text{H-NMR}$ studies were performed. To simplify the interpretation of the NMR spectrum, the MonOx derivatives were chosen as analogues for the BisOx compounds. Furthermore,

due to the stereoelectronic configuration of the product of trans-aminoindanol (**4.15**) and the 2-pyridyl derivatives (**4.11** and **4.13**), the products (**4.16** and **4.17**) would be unable to form a ring-closed (oxazolidine) conformation (**Scheme 4.4**). This makes these compounds excellent for studying the potential for imine formation and will aid in delineating NMR data to determine whether the reaction forms the oxazolidine product or remains as the imine. Therefore it was determined that the products **4.16** and **4.17** could act as NMR references for the open ring imine form. The resulting ketimine compound (**4.17**) produced from 2-acetylpyridine was found to convert completely to product, however there was a ratio of approximately 4:1 between the Z and E isomers.(in CDCl₃). Interestingly, the ratio between isomers of the ketimine was found to become a 2.5:1 ratio after azeotroping off water three times with benzene. When the carbonyl source was **4.13**, there was also total conversion to the aldimine (**4.16**), and there was almost entirely one isomer of the product, which did not change after azeotroping off any residual water with benzene.



Scheme 4.4 Formation of the imine product (**4.16** and **4.17**) by condensation of (1*S*,2*S*)-trans-aminoindanol (**4.15**) with 2-acetylpyridine (**4.11**) and 2-pyridinecarboxaldehyde (**4.13**)

The MonOx products of the condensation reaction with cis-amino indanol and 2-acetylpyridine or 2-pyridinecarboxaldehyde (**4.11** and **4.13**) were also analyzed by ^1H -NMR. When analyzed in CDCl_3 , the ketone derived methyl-MonOx compound (**4.12**) showed complete conversion of the starting materials (by NMR) and there was a 1:1 ratio of diastereomers in the oxazolidine product with approximately 25% imine present.¹⁶ After using benzene to azeotrope the water that formed as a side product of the condensation reaction four times, the ratio of diastereomers stayed relatively similar at a 1:1 ratio. When forming the aldehyde derived MonOx (**4.13**) product and after removal of water by azeotrope with benzene four times the diastereomeric ratio stayed essentially the same at a 5.5:1 ratio.

To further aid in determining the preferred conformation of the oxazolidine compound, computational studies were performed to aid in determining the preferred stereochemistry of the hemiaminal center. Using the DFT models with the RB3LYP method and the 6-31G(D) basis set,¹⁷ geometry optimization studies were performed. To simplify calculations, all calculations were performed on the MonOx derivatives. It was calculated that the difference between the stereoisomers of the aldehyde derived MonOx (**4.14a** and **4.14b**) was 3.57 kcal/mol in favor of the *S,R,R* stereoisomer of MonOx (**Figure 4.2**). When the methyl-MonOx derivative was modeled (**4.12a** and **4.12b**), the difference between the diastereomeric isomers was only 2.89 kcal/mol, also in favor of the *S,R,R* stereoisomer. With the calculated energy differences for the diastereomers of **4.12** and **4.14** being as great as they are, this should render only a single diastereomer. However, NMR analysis of the resulting compounds showed a much more even distribution of diastereomers. One explanation for this deviation is that because the

formation of the oxazolidine product goes through an imine intermediate (**4.4**), and the resulting E:Z ratio of imine isomers plays a role in the distribution of oxazolidine products, the energy difference between the two isomers of the imine may show a closer correlation to the observed product distribution. With the NMR data and calculation studies suggesting primarily a single diastereomer for the MonOx and methyl-MonOx derivatives, it was decided to move forward with the BisOx and dimethyl-BisOx compounds for use as ligands and organocatalysts.

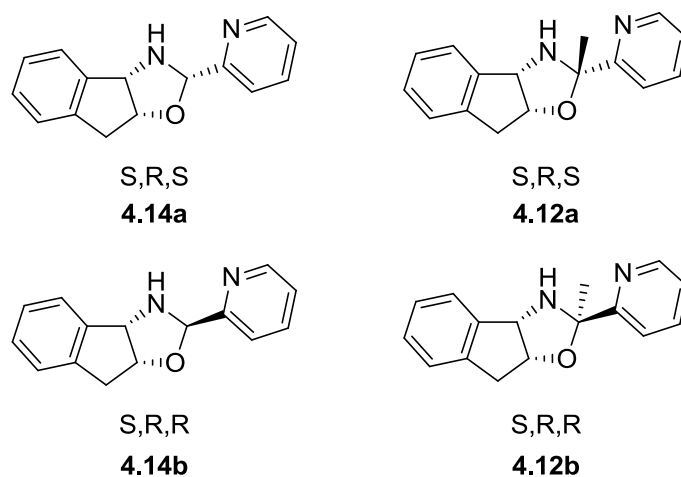


Figure 4.2 The two potential diastereomers of the oxazolidine complexes MonOx and methyl-MonOx.

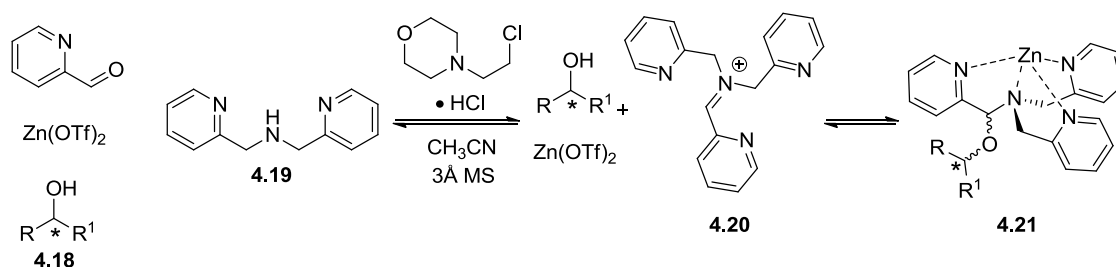
4.3 The synthesis of novel metal complexes with the dimethyl-BisOx ligand and their application in the colorimetric sensing of chiral alcohols

The need for colorimetric sensors that can quickly and accurately measure the enantiomeric excess of a solution is of high importance to the chemical community. When analyzing the enantiomeric excess of a compound, the usual techniques for measuring enantiomeric excess (HPLC and GC on a chiral stationary phase), can usually

be done in less than 5-10 minutes with a high level of accuracy. However, when analyzing large quantities of chiral compounds, the usual screening techniques for measuring enantiomeric excess can become prohibitive. Therefore, the demand for a sensor which can colorimetrically indicate the enantiomeric purity quickly is great.

The initial efforts by the Wiskur group in applying the 1,3-oxazolidine compounds, BisOx and dimethyl-BisOx, were directed towards the synthesis of a colorimetric sensor for the determination of enantiomeric excess of chiral monofunctional amines or alcohols. The chosen analytes for these potential sensors were chiral monofunctional amines and chiral monofunctional alcohols. The choice of chiral alcohols as an analyte for a chiral sensor was made mainly due to their ubiquity in nature and as intermediates in the synthesis of natural products.¹⁸⁻²¹ Despite their abundance, there are few example of sensors for chiral monofunctional alcohols. The development of methods for the analysis of monofunctional alcohols via transition metal complexes is complicated by the poor coordination ability of monofunctional alcohols especially when compared to analytes with multiple binding centers. For this reason, a sensor of extreme sensitivity would be needed in order to obtain any selective binding. So far the only report of a sensor for chiral monofunctional alcohols was by the Anslyn group²² in which a four component dynamic combinatorial approach is undertaken (**Scheme 4.5**). By combining 2-pyridinecarboxaldehyde with $\text{Zn}(\text{OTf})_2$ and the bispyridylamine **4.19** in the presence of a chiral alcohol **4.18** and an acid, the reactive iminium compound **4.20** is formed which then undergoes nucleophilic addition of the chiral alcohol which forms a tridentate ligand that readily binds $\text{Zn}(\text{OTf})_2$ (**4.21**). The bound zinc complex **4.21** has a helical conformation with respect to the pyridyl groups and is active by circular

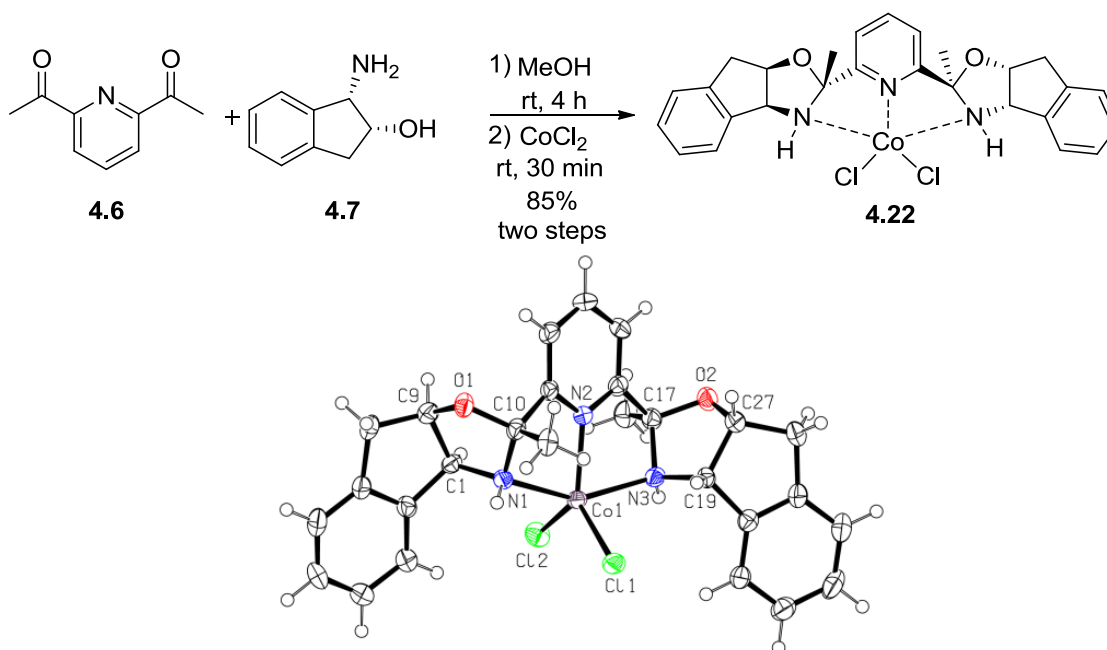
dichroism (CD). The helicity is measured (by a characteristic Cotton effect) and is directly influenced by the chirality of the attached chiral alcohol. This CD active assembly allows for the accurate measurement of the enantiomeric excess (ee) of several secondary monofunctional alcohols. It was reported that the chiral alcohol forced the formation of a propeller conformation with respect to the ligand.



Scheme 4.5 The four component dynamic combinatorial approach to the formation of the CD active compound **4.21**.

The approach taken by the Anslyn group represents a seminal result in the sensing of chiral alcohols. Furthermore, the analytical techniques used allow for a highly accurate determination of ee using relatively facile reaction conditions. However, it is hypothesized by the Wiskur group that if a chiral metal-ligand complex could enantioselectively coordinate a chiral alcohol, there may be enough of an electronic change to allow for colorimetric discrimination of enantiomers. Also, since this approach would not necessarily necessitate the formation of a thermodynamically favored compound (such as **4.21**) but simple coordination of chiral alcohols to the metal center, a colorimetric change could happen considerably faster than was found for **4.21** (the Anslyn group reported that for near complete conversion to **4.21**, the reaction had to stir overnight).

To test whether the BisOx ligand can discriminate between enantiomers that bind to metal centers, the transition metal-BisOx complex **4.22**, was synthesized for use as the sensor. The synthesis of **4.22** proved to be very facile to perform (**Scheme 4.6**). The dimethyl-BisOx ligand was synthesized by combining **4.5** and **4.6** in anhydrous methanol and stirring for 4 hours. The resulting crude dimethyl-BisOx ligand was then treated with CoCl_2 which led to the product **4.22** precipitating immediately in methanol. Purification was through filtration to give **4.22** as a blue solid. It is also worth noting that the crystal structure of dimethyl-BisOx confirms what was calculated to be the lowest energy diastereomer in the methyl-MonOx compound. Also, **4.22** was found to possess a C_2 symmetric point group. The C_2 symmetry of **4.22** may be beneficial as this symmetry can lead to facial selectivity between enantiomers of the analyte.



Scheme 4.6 Synthesis of the CoCl_2 -BisOx transition metal complex and crystal structure of **4.22**. The stereochemistry at C10 and C17 was determined from the known stereochemistry of C1, C9, C19, and C27.

With **4.22** in hand, the complex was then tested for colorimetric sensing of chiral alcohols. Due to the poor solubility of **4.22**, the solvent chosen was DMSO. To the sensor in DMSO was added either the *R* or *S* enantiomer of the alcohol analyte. To help facilitate binding, base (pyridine, Et₃N, or *i*Pr₂EtN) was added and the solution was sonicated or heated for 30 minutes. The alcohols tested included the aliphatic alcohols **4.23-4.26**, the benzylic alcohol **4.27** and **4.28**, as well as the benzylic bicyclic alcohols **4.29** and **4.30** (Figure 4.3). Unfortunately, there was no reproducible colorimetric change, even when the analyte was used in over 100 fold excess. Due to this unfortunate result, it was then decided to change analyte class from monofunctional alcohols to monofunctional amines.

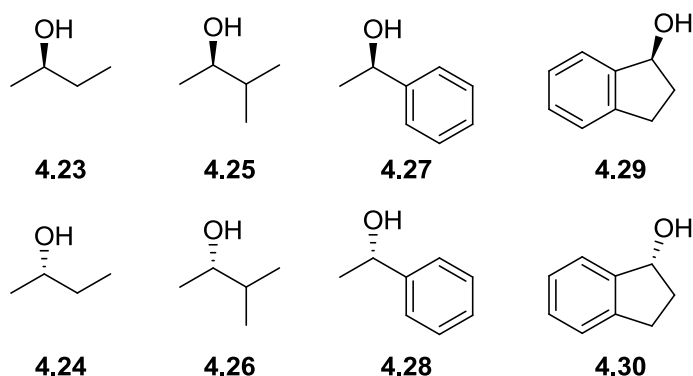


Figure 4.3 Chiral monofunctional alcohols tested as analytes with **4.22**

4.4 The synthesis of novel BisOx-nickel and BisOx-zinc complexes and their use as sensors for monofunctional chiral amines

Amines, when compared to alcohols, have considerably more Lewis basic character and could therefore facilitate binding to a sensor to a much greater extent. Due to the enhanced chemical reactivity inherent in the amine functionality, there have been several colorimetric chiral amine sensors reported. However, examples of colorimetric sensors of monofunctional amines are rare.²³⁻³² Of the methods for colorimetric sensing

of chiral amines that have been reported, a majority of them require a pseudo crown ether motif to facilitate binding of chiral amines (**Figure 4.4**). These sensors are believed to work by the amine forming a hydrogen bonding interaction with the phenolic motif that is then stabilized by the ether linkages in the pseudo crown ether moiety. This is believed to lead to a significant energy difference between the diastereomeric complexes, thereby leading to enantiodiscrimination. One of the major drawbacks of this class of sensors however is the lengthy synthesis required. An alternative method to the pseudo crown ether based sensor, that also ameliorates the lengthy synthesis requirements of the other colorimetric chiral amine sensor types, has been reported by the Anslyn group (**Figure 4.5**).²⁸ The approach taken by the Anslyn group is through the use of an enantioselective indicator displacement assay (eIDA). The indicator (in this case, chrome azurol S) changes color when becoming displaced from the chiral amine ligand-copper complex by the analyte. The eIDA reported has shown to be efficacious in the sensing of most of the chiral α -amino acids. Furthermore, this technique has been found to be successfully applied to high throughput screening techniques offering even greater utility in the screening of large quantities of asymmetric reaction products.³³ However, the sensing of monofunctional chiral amines has never been reported for the eIDA reported by the Anslyn group.

synthesized and can rapidly detect monofunctional chiral amines. The impetus for the development of such a sensor is due to the chiral amine's importance in the preparation of molecules of interest to academia and pharmaceutical companies. Therefore, although the dimethyl-BisOx metal complexes failed to successfully discriminate between enantiomers of monofunctional chiral alcohols, it was determined to test this family of potential sensors with amines.

To test whether **4.22** can enantioselectively discriminate between chiral amines, a series of primary, secondary, and sulfonamides (**Figure 4.6**) were added to the sensor dissolved in pyridine and either DMSO, CHCl_3 , or MeOH. Unfortunately, **4.22** was found to be either incapable of distinguishing between enantiomers, or there was no change in absorbance between the sensor in the presence of either chiral amine. It was then decided to perform an extensive screening of metal salts in the presence of chiral amines and **4.7**.

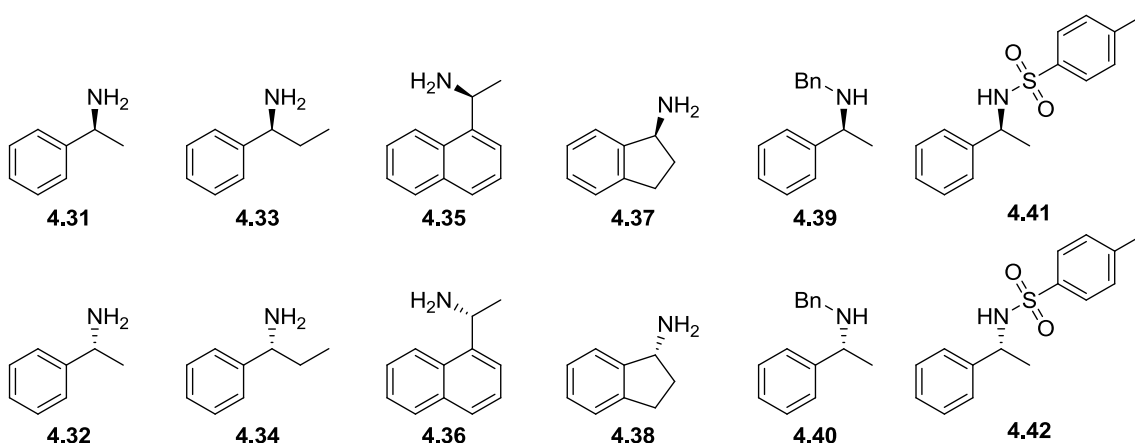


Figure 4.6 Chiral monofunctional amines tested as analytes with **4.22**.

Extensive complex formation with a series of transition metals and lanthanides with **4.7** was performed to test the chiral recognition capabilities of the CoCl_2 -dimethyl-BisOx complex. In a 96 well plate the transition metal or lanthanide salt (**Figure 4.7** was

dissolved in MeOH, treated with **4.8** then with the 1-phenylethylamine enantiomers **4.31** or **4.32** and analyzed by UV-Vis spectroscopy. Unfortunately, all of the **4.8** complexes were found to be incapable of chiral recognition. Therefore, the ligand **4.8** was abandoned and a more targeted approach was made to attempt to colorimetrically discriminate between amine enantiomers. Due to ease of synthesis and purification, the BisOx ligand **4.10** was chosen as well as more azaphilic metals to form the metal-bisoxazolidine complexes.

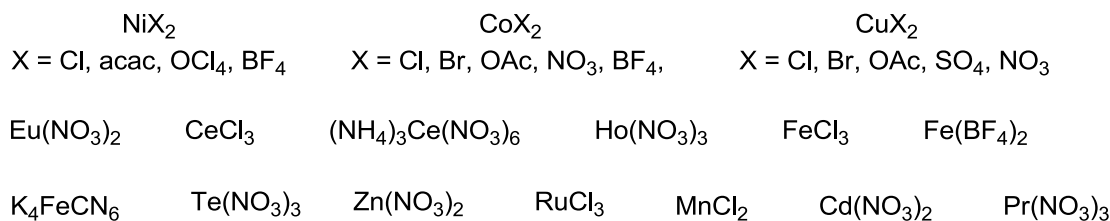
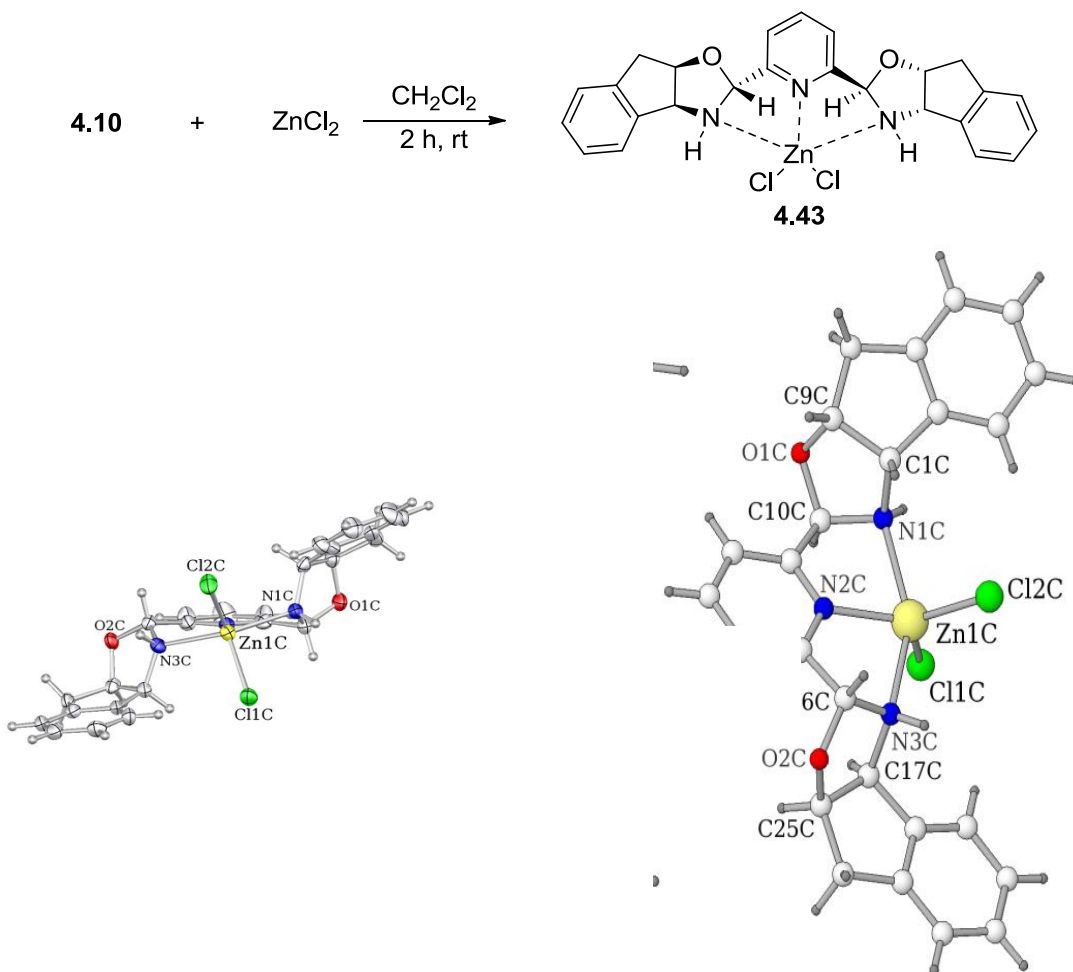


Figure 4.7 The transition metal and lanthanide salts used with **4.8** in the discrimination of **4.31** and **4.22** (acac = acetylacetone).

The BisOx ligand (**4.10**) was synthesized in a similar protocol to that of **4.8** (**Scheme 4.3**). The resulting product was then easily purified by filtration due to the insolubility of the product in water. Therefore, anhydrous conditions were avoided to aid in the precipitant of the desired compound, **4.10**. With the BisOx ligand synthesized, the transition metals nickel and zinc were chosen due to their azaphilicity to form complexes with **4.10**

The first complex which was synthesized with the BisOx ligand (**4.10**) was with ZnCl_2 (**4.43**, **Scheme 4.8**). It is worth highlighting that the crystal structure which was obtained confirms the stereochemistry of the hemiaminal center that was the lower energy calculated orientation of the two diastereomers. Also, the complex shows a C_2 point group symmetry which may help in discriminating between enantiomers when they

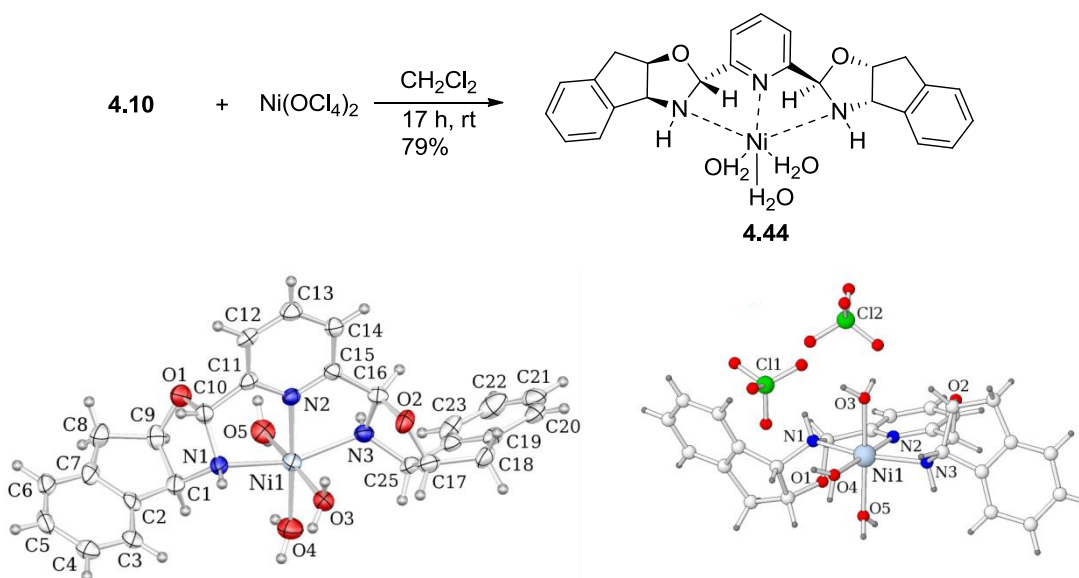
bind to the metal center. Another point of interest resides in the chiral crystal that was obtained from **4.43**. The interesting structure of the ligand (**Scheme 4.8**) and the crystal's chirality may lend this complex interesting physical properties.³⁴



Scheme 4.7 Synthesis of BisOx-ZnCl₂ complex (**4.43**) and observed crystal structure. The stereochemistry of C10 and C16 was determined from the known stereochemistry of C1, C9, C17, and C25.

In addition to the BisOx-ZnCl₂ complex, a BisOx-Ni(OC₄)₂ complex was also synthesized. The synthesis of this ligand metal complex was also straightforward and proceeded with good yields. The addition of BisOx (**4.9**) to Ni(OC₄)₂ in CH₂Cl₂ then stirring overnight allowed the product (**4.44**) to be isolated by filtration (**Scheme 4.8**).

The crystal structure obtained for **4.44** was found to be the trihydrate of the desired complex. It is not believed that the water molecules would interfere with analyte binding so **4.44** was considered suitable for use in sensing of chiral monofunctional amines. The geometry of the nickel atom of the resulting complex is in an octahedral configuration, as opposed to the trigonal bipyramidal of **4.22** or **4.33**. The geometry of the nickel atom and its smaller atomic nuclei, when compared to zinc and cobalt, leads to an interesting twisted conformation of the ligand. It was also observed that **4.44** maintained its C_2 symmetry and the resulting stereochemistry of the hemiaminal center is the same as what was calculated to be the lowest in energy in the case of MonOx (**4.14**).



Scheme 4.8 Synthesis and isolated crystal structure of BisOx-Ni(OC14)₂·3H₂O (**4.44**)
The stereochemistry of C10 and C16 was determined from the known stereochemistry of C1, C9, C17, and C25.

Attempts at the sensing of monofunctional chiral amines were then performed with **4.44**. The analytes tested were both aromatic containing (**4.45** and **4.46**) and aliphatic amines of various steric bulk (**4.47-4.50**) and the secondary amine *N*- α -

dimethylbenzylamine (**4.51** and **4.52**) were also tested (**Figure 4.8**). All attempts to colorimetrically or spectroscopically discriminate between the chiral amines failed. Although for most of these amines, there was a colorimetric change (which increased reproducibly over time), there was no discrimination between the two enantiomers.

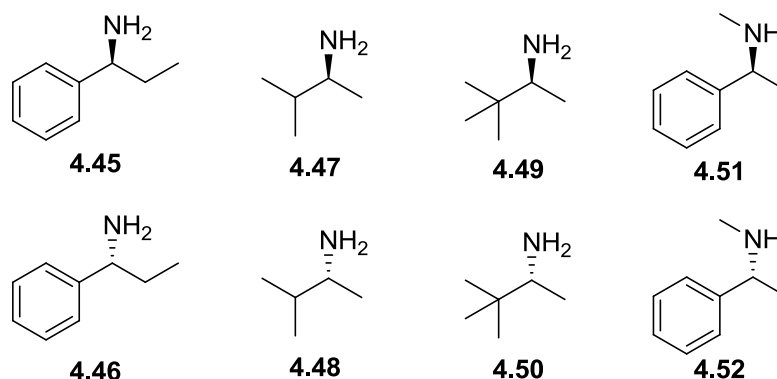
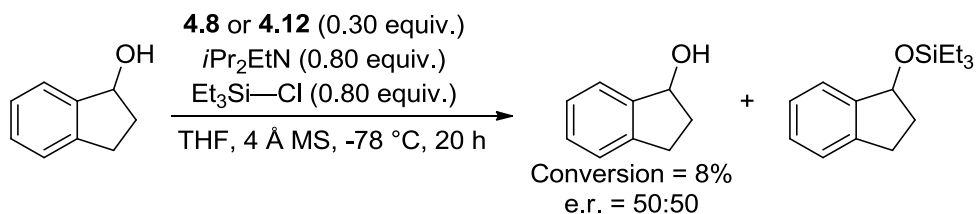


Figure 4.8 The monofunctional chiral amines used as analytes with **4.44**.

4.5 Application of BisOx as an organocatalyst in the kinetic resolution of secondary alcohols via enantioselective silylation

Although the BisOx metal complexes were found to lack the ability to colorimetrically discriminate between enantiomers of monofunctional alcohols and amines, the 1,3-oxazolidine functionality has also been shown to be effective in organocatalysis.³⁵ Because of their reported utility in asymmetric reactions, the dimethyl-BisOx ligand (**4.7**) was employed as a catalyst for the enantioselective silylation of monofunctional secondary alcohols.³⁶ Specifically, **4.7** was used in the kinetic resolution³⁷ reaction described by the Wiskur group³⁸ (**Scheme 4.10**). The kinetic resolution of 1-indanol was catalyzed by **4.7** or **4.11** using the amine base *i*Pr₂EtN with the silyl source of Et₃SiCl. The reactions were carried out at -78 °C and left to react for 20

h in the presence of 4 Å molecular sieves. It was discovered that the recovered starting materials was not enantiomerically enriched and only 8% conversion (determined by HPLC) was observed when either **4.7** or **4.11** was used as the catalyst. It is not clear whether **4.7** or **4.11** actually catalyzed the reaction or whether the reaction was catalyzed by *i*Pr₂EtN, but the reaction conditions described are not effective for the kinetic resolution of 1-indanol by enantioselective silylation.



Scheme 4.10 The kinetic resolution of 1-indanol by enantioselective silylation catalyzed by **4.7** and **4.11**.

4.6 Conclusions

Presented was the synthesis and characterization of the 1,3-oxazolidine compounds: dimethyl-BisOx **4.8**, BisOx **4.10**, methyl-MonOx (**4.12**), and MonOx (**4.14**). Through calculations and NMR studies it was determined that the desired oxazolidine compounds do form and that there is a preference for a single diastereomer. Experimentally, only the oxazolidine ligands derived from 2-pyridinecarboxaldehyde (**4.13**) and 2,6-pyridinedicarboxaldehyde (**4.9**) showed a strong preference for forming a majority of one diastereomer.

With the oxazolidine compounds in hand the CoCl₂-**4.8** complex (**4.22**) was formed and a series of chiral monofunctional alcohol analytes **4.23-4.30** were added in

order to see if a colorimetric change was observed by enantioselective binding of the analytes. The ligand **4.8** was then used with a large quantity of transition metal and lanthanide salts, to these complexes were also added the chiral amine **4.31**, however no enantiodiscrimination was observed. It was then decided to use more azaphilic metals and the metal complexes ZnCl_2 -**4.10** (**4.43**) and $\text{Ni}(\text{OCl}_4)_2$ -**4.10** (**4.44**) were synthesized. The zinc complex **4.43** was found to be unable to colorimetrically discriminate between the enantiomers of chiral monofunctional amines **4.31-4.42**. The nickel complex (**4.44**) was also found to be unable to enantiodiscriminate between the enantiomers of chiral monofunctional amines **4.45-4.52**.

The oxazolidine compounds **4.8** and **4.10** were then tested as organocatalysts in the kinetic resolution of 1-inanol by enantioselective silylation (**Scheme 4.10**). Although the oxazolidine catalysts were not successful in resolving the enantiomers, the oxazolidine compounds are easily synthesized from commercially available starting material and appear to be stable compounds. For this reason and the topology of the ligand, the potential for these compounds in other reactions such as zinc alkylations or cycloaddition reactions.

4.7 Experimental

All reactions were carried out under a dry N_2 or Ar atmosphere in oven-dried glassware and all NMR experiments were performed with oven-dried NMR tubes. Dry tetrahydrofuran (THF), methanol, dichloromethane, and hexanes were obtained by passing the previously degassed solvents through activated alumina columns into a flask

containing activated 4Å molecular sieves. Anhydrous CHCl_3 and dimethylsulfoxide (DMSO) were obtained from Sigma-Aldrich. Triethylamine (Et_3N) and $i\text{Pr}_2\text{EtN}$ were distilled over CaH_2 prior to use. Pyridine was distilled by Kugelrohr apparatus prior to use. All chiral alcohols or amines that were liquids were distilled prior to use. All chemicals were purchased from major suppliers such as Alfa Aesar, Sigma-Aldrich, TCI, or Acros. Unless otherwise stated all reagents were used as received without further purification. 4Å Molecular sieves (4Å MS) were activated by heating and storage at 170 °C for at least 48 hours prior to use. ^1H NMR spectra were recorded on a Varian Mercury/VX (400 and 500MHz). Chemical shifts are reported in ppm with either TMS (0.00 ppm for ^1H and ^{13}C), CD_2Cl_2 (CD_2Cl_2 : δ 5.32 and 53.8 ppm for ^1H and ^{13}C respectively), or CDCl_3 as the internal standard (CDCl_3 : δ 7.26 and 77.0 ppm for ^1H and ^{13}C respectively). Data are reported as follows: chemical shift, multiplicity (s = singlet, d = doublet, t = triplet, q = quartet, dd = doublet of doublet, dt = doublet of triplets, dsep = doublet of septet, m = multiplet, br = broad, ur = unresolved multiplet) and coupling constants (Hz). ^{13}C NMR spectra were recorded on a Varian Mercury/VX (100 MHz) with complete proton decoupling. Reactions were monitored by thin layer chromatography (TLC) using EMD chemicals 60F silica gel plates. Flash column chromatography was performed over silica gel (32-63 μm). High resolution mass spectrometry (**HRMS**) was performed by the mass spectrometry facility at the University of South Carolina. **IR** data were obtained on a Perkin Elmer Spectrum 100 FT-IR ATR spectrophotometer, ν_{max} in cm^{-1} . All enantiomeric ratios were determined by **HPLC** on an Agilent 1200 series using the chiral stationary phases Daicel Chiralcel AD-H, OJ-H, or OD-H (4.6 \times 250 mm \times 5 μm) columns, and monitored by DAD (Diode Array

Detector) in comparison with authentic racemic materials. Melting points (**mp**) were taken with a Laboratory Devices Mel-Temp and were uncorrected. **Optical rotations** were obtained using a JASCO P-1010 polarimeter.

General procedure for the synthesis of 1,3-oxazolidine and 1,3-bisoxazolidine ligands (4.8, 4.10, 4.12, 4.14).

To a 4 dram vial was added (1*S*,2*S*)-cis-1-amino-indanol (**4.2**) (100 mg, 0.67 mmol) and either 2-acetyl pyridine, 2,6-diacetylpyridine, 2-pyridinecarboxaldehyde, or 2,6-pyridinedicarboxaldehyde (0.67 mmol). The vial was then charged with 20 mL of dry methanol. The reaction was then stirred for 4h. In the case of the formation of BisOx (**4.10**) precipitated from solution as a wet cake which can be collected by filtration then dried under vacuum. For the other oxazolidine products, the solution was then evaporated to dryness and then benzene added (5-10 mL) and evaporated off (3-5x) to remove residual water.

General procedure for the synthesis of hydroxy imine compounds 4.16 and 4.17

To an oven dried 50 mL round bottom flask was added (1*S*,2*S*)-trans amino indanol (**4.14**) (80 mg, 0.54 mmol). The flask was then charged with 12 mL dry methanol then treated with either 2-acetylpyridine or 2-pyridinecarboxaldehyde (0.54 mmol). The flask was then stirred for 3h then the solvent was removed under vacuum. The oil was then dissolved in benzene (5-10 mL) then evaporated to dryness (4x) to remove residual water.

Synthesis of dimethyl-BisOx CoCl₂ complex (4.22)

To a 200 mL RBF fitted with a teflon coated stir bar was added 2,6-diacetylpyridine (1.47 g, 9.0 mmol) and cis- α -amino indanol. The flask was then charged with 50 mL of dry methanol and stirred for 3.5 h. To the solution was then added CoCl₂ and the solution was lightly stirred until the solution became homogenous. Then the solution was left to sit for 1 h, during which time a precipitant formed. The suspension was then filtered and washed with methanol to give **4.22** as a blue solid (4.23 g, 7.62 mmol).

Synthesis of (*S*) and (*R*)-*N*-benzyl-1-phenylethanamine (4.39 and 4.40 respectively)

Benzaldehyde (2.22 mL, 20.0 mmol) was added to a 25 mL round bottom flask and the flask was charged with 15 mL dry methanol. To the solution was added (*S*) or (*R*)-1-phenylamine (2.10 mL, 16.5 mmol) and the reaction was stirred for 20 h. The solution was then cooled to 0°C and slowly treated with sodium borohydride (0.815 g, 21.5 mmol). The reaction was then quenched with 1M NaOH until the solution was a pH of 10. The organic layer was then filtered and evaporated to dryness leaving a clear colorless oil. The oil was stored as the HCl salt which was protonated by bubbling HCl gas through a solution of the amine in diethyl ether. The resulting salt was evaporated to dryness, then recrystallized from CH₂Cl₂:hexanes to give white crystals (0.380 g, 9 %). The amine is then deprotonated by washing with sodium hydroxide (1 M, aqueous) and extracting with dichloromethane and evaporating to dryness prior to use.

Synthesis of (S) and (R)-4-methyl-N-(1-phenylethyl)benzenesulfonamide (4.41 and 4.42 respectively)

p-Toluenesulfonylchloride (2.29 g, 12.01 mmol) was added to a 100 mL round bottom flask which was then charged with 30 mL of dry diethyl ether. The flask was then cooled to 0°C and to the flask was then added triethylamine (1.85 mL, 13.24 mmol). The solution was then treated with (S) or (R)-1-phenylethylamine and stirred for 15.5 h. The precipitant was then filtered off and the filtrate was evaporated to dryness. The resulting solid was then purified by flash column chromatography (silica gel; 1:1 hexanes:ethyl acetate) to yield the product as a white solid. (3.15 g, 95%)

Synthesis of dimethyl-BisOx ZnCl₂ complex (4.43)

To a 4 dram vial was added **4.9** (50 mg, 0.126 mmol) and ZnCl₂ (18.9 mg, 0.139 mmol). The vial was then charged with 6 mL of CH₂Cl₂ then stirred for 12 h. Then pentane was added until the turbidity persisted. The resulting suspension was then placed in a freezer for 2 h. The resulting precipitant was then filtered and washed with cold pentane to give an off yellow solid.

Synthesis of dimethyl-BisOx Ni(OCl₄)₂ complex (4.44)

To a 4 dram vial was added **4.9** (60 mg, 0.151 mmol) and Ni(OCl₄)₂ (39.0 mg, 0.151 mmol). The vial was then charged with 6 mL of CH₂Cl₂ then stirred for 16.5 h. During this time, a green precipitant formed. The reaction was then placed in a freezer for 1 h. The resulting precipitant was then filtered off and washed with cold hexanes to yield a green solid (78.1 mg, 79%).

General procedure for the growth of x-ray quality crystals of 1,3-oxazolidine metal complexes.

To a 1 dram vial was added a dilute solution (<5 mg sample in 2 mL methanol) of the ligand-metal complex. The 1 dram vial was then placed in a 4-dram vial charged with 5 mL hexanes. The 4 dram vial was then tightly fitted with a septum and left to crystallize by slow diffusion.

General procedure for colorimetric discrimination of amine and alcohol enantiomers with 1,3-bisoxazolidine-metal complexes.

To a 0.5 dram vial was added 200 μ L of a 10 mM solution of sensor in anhydrous solvent. The solution was then treated with 100 μ L of pyridine then 50 μ L of alcohol or amine analyte. The resulting solution was then sonicated for 30 minutes and analyzed by UV-Vis spectrometer in a quartz cuvette.

General procedure for colorimetric discrimination of amine and alcohol enantiomers with 1,3-bisoxazolidine-metal complexes by 96-well plate.

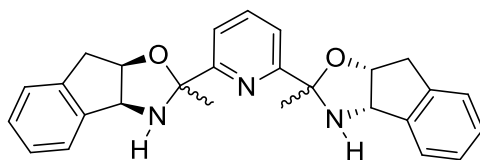
To a well of a 96-well plate was added 50 μ L of a 24 mM solution of metal salt in methanol. The well was then charged with 150 μ L of dry methanol then treated with 100 μ L of 12 mM Bisoxazolidine ligand. The solution was then treated with 50 μ L of distilled chiral amine.

Procedure for the silylation based kinetic resolution of 1-indanol with 4.7 and 4.11

To an oven dried 1 dram vial with activated 4 Å molecular sieves (20-25 mg) was fitted an oven dried Teflon coated stir bar. To the vial was added 1-indanol (30 mg, 0.22 mmol) and either **4.7** or **4.11** (0.067 mmol) then quickly sealed under dry N₂. The vial

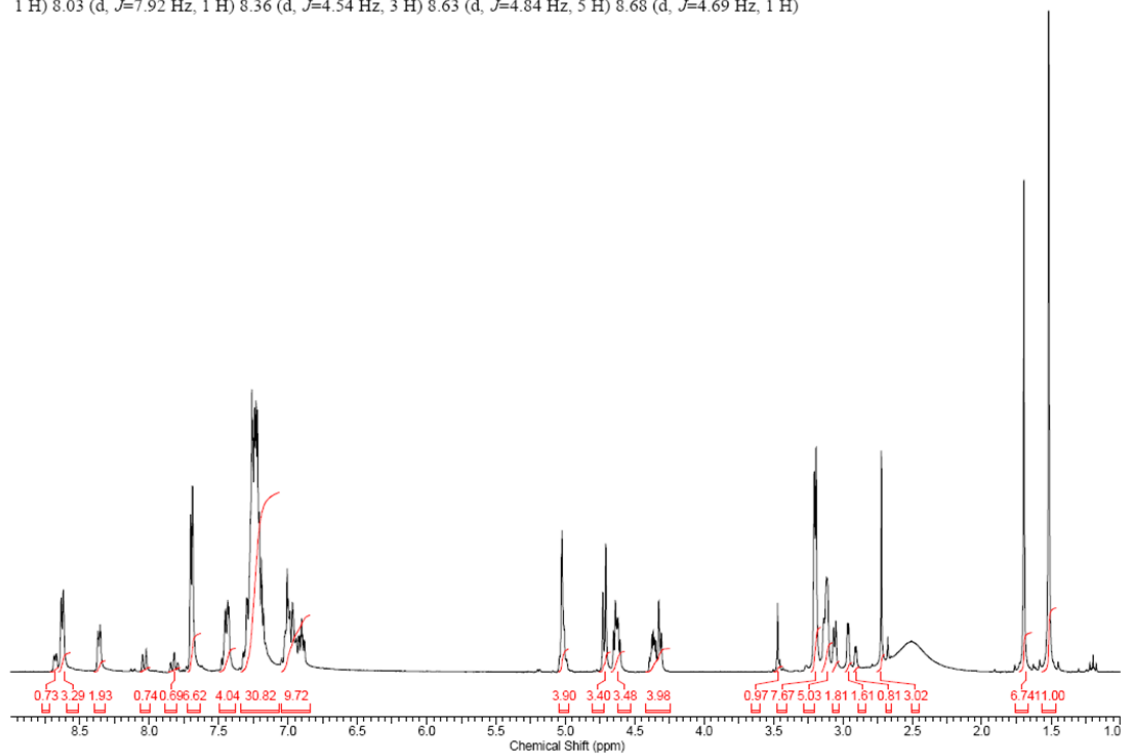
was then charged with 1.0 mL THF to generate a 0.3 M solution and the solution was treated with *i*Pr₂EtN (31 μ L, 0.176 mmol) and cooled to -78 °C in a crycool apparatus for about 30 minutes. The cooled solution was then treated with a 1.19 M solution of Et₃Si-Cl in dry THF and left to react for the 20 h at -78 °C. The reaction was then quenched with 250 μ L MeOH and poured into a 4-dram vial containing 1.5 mL sat. aqueous NH₄Cl and extracted with diethyl ether (3 x 5 mL), the ethereal layer was then dried over sodium sulfate. The crude reaction was then analyzed by HPLC with a chiral stationary phase.

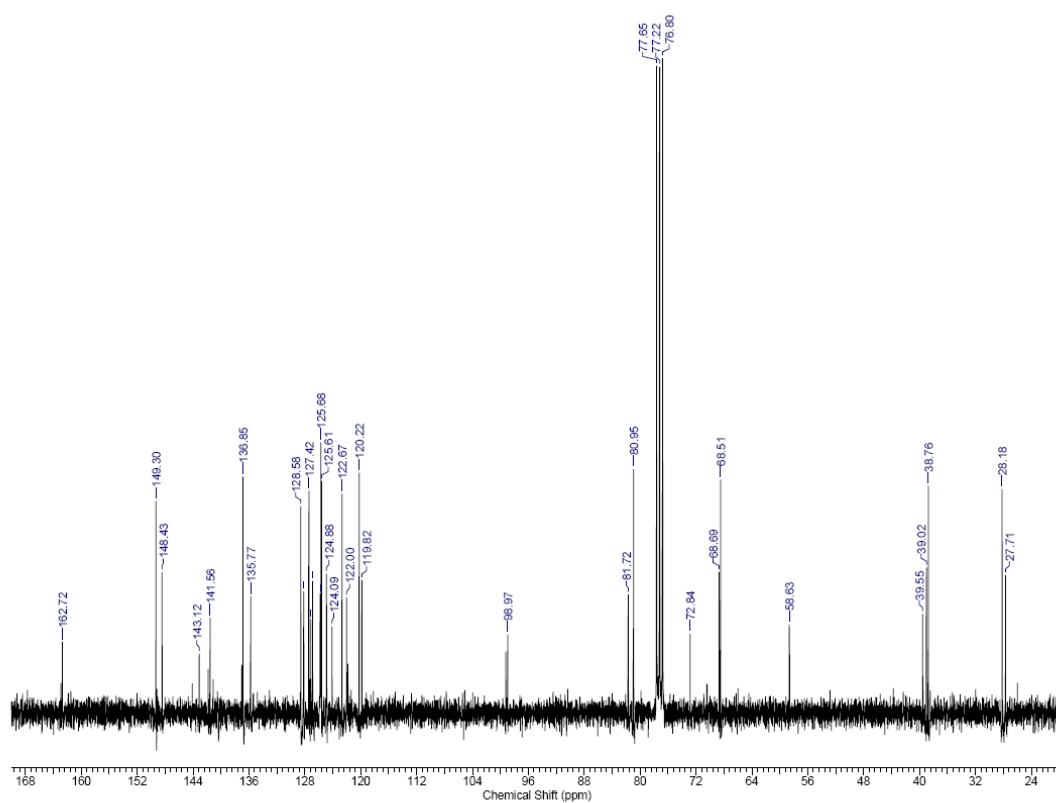
Spectral data

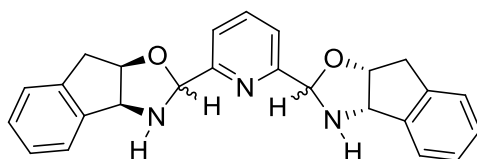


4.8

¹H NMR (300 MHz, CHLOROFORM-*d*) δ ppm 1.52 (s, 11 H) 1.64 - 1.73 (m, 7 H) 2.72 (s, 3 H) 2.91 (d, $J=2.93$ Hz, 1 H) 2.96 (d, $J=2.64$ Hz, 2 H) 3.06 (d, $J=5.28$ Hz, 2 H) 3.08 - 3.15 (m, 5 H) 3.20 (d, $J=3.81$ Hz, 8 H) 3.43 - 3.50 (m, 1 H) 4.25 - 4.42 (m, 6 H) 4.63 (dt, $J=6.19, 4.09$ Hz, 5 H) 4.68 - 4.76 (m, 5 H) 4.98 - 5.05 (m, 6 H) 6.84 - 7.04 (m, 15 H) 7.06 - 7.34 (m, 46 H) 7.38 - 7.49 (m, 6 H) 7.63 - 7.72 (m, 10 H) 7.82 (td, $J=7.70, 1.61$ Hz, 1 H) 8.03 (d, $J=7.92$ Hz, 1 H) 8.36 (d, $J=4.54$ Hz, 3 H) 8.63 (d, $J=4.84$ Hz, 5 H) 8.68 (d, $J=4.69$ Hz, 1 H)

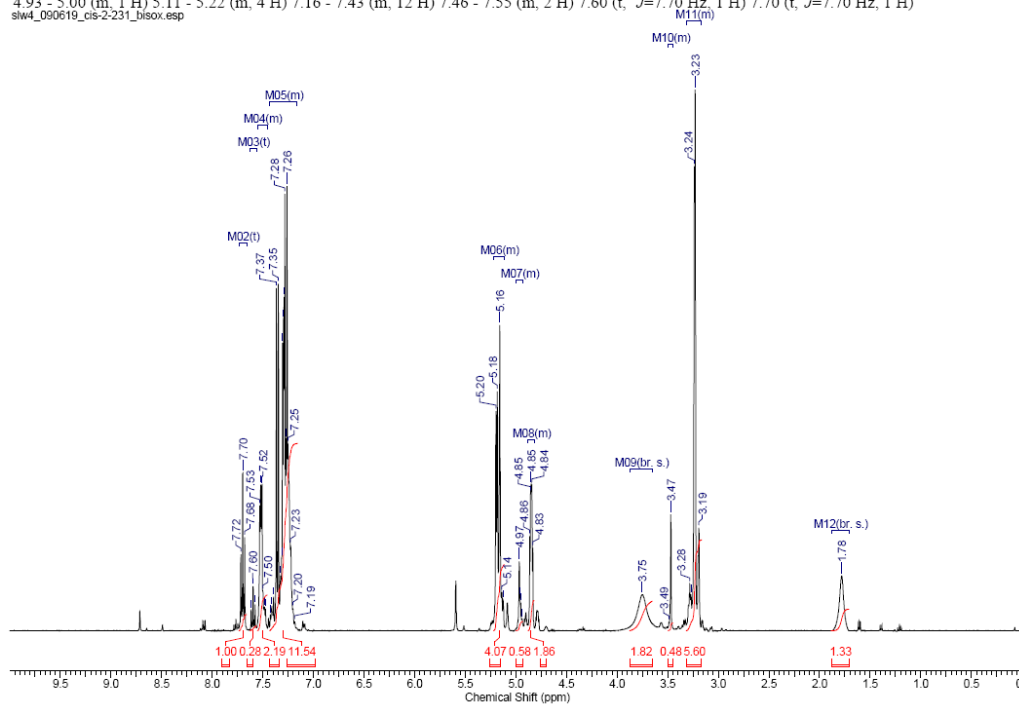






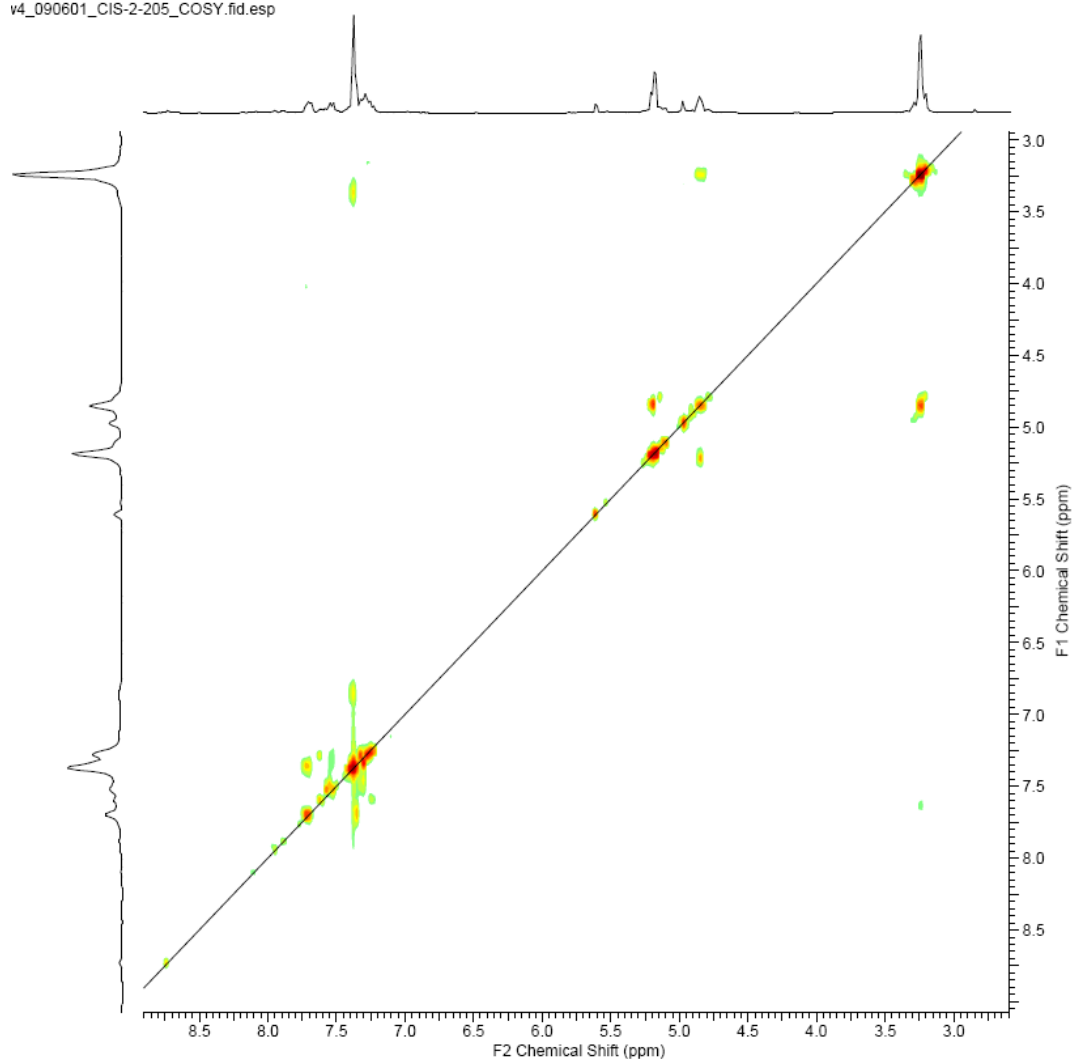
4.10

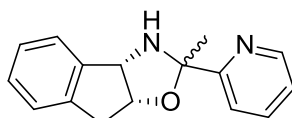
¹H NMR (400 MHz, CHLOROFORM-*d*) δ ppm 1.78 (br. s., 1 H) 3.17 - 3.32 (m, 6 H) 3.45 - 3.50 (m, 1 H) 3.75 (br. s., 2 H) 4.82 - 4.88 (m, 2 H) 4.93 - 5.00 (m, 1 H) 5.11 - 5.22 (m, 4 H) 7.16 - 7.43 (m, 12 H) 7.46 - 7.55 (m, 2 H) 7.60 (t, *J*=7.70 Hz, 1 H) 7.70 (t, *J*=7.70 Hz, 1 H)



^1H - ^1H -COSY

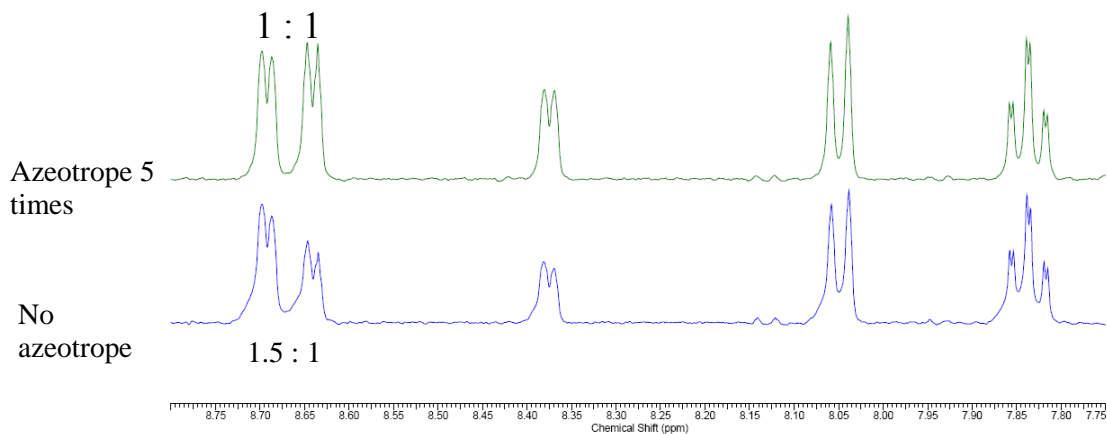
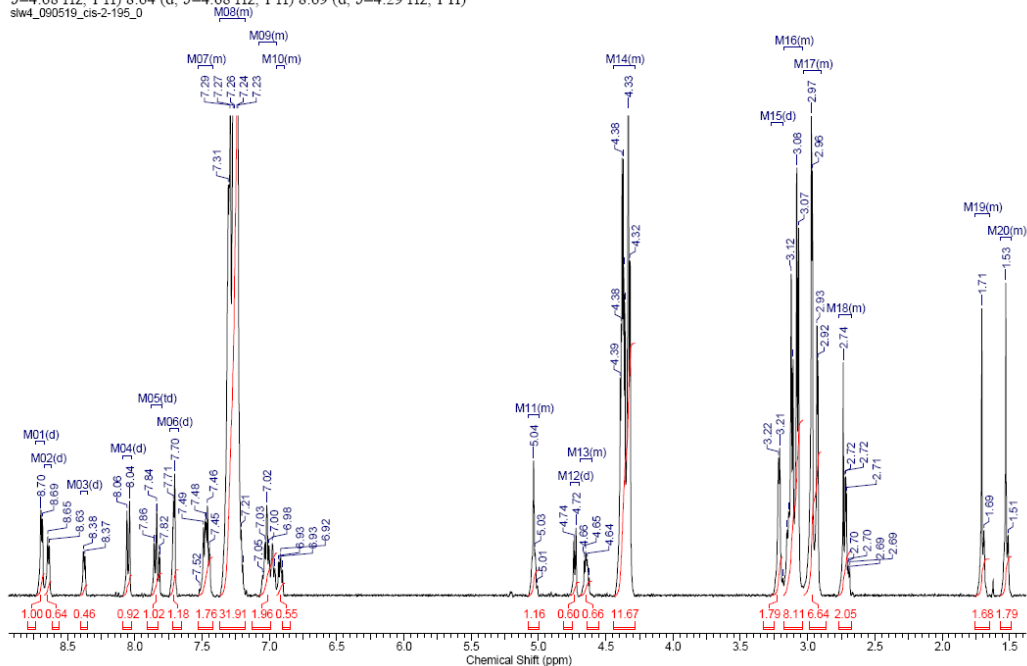
v4_090601_CIS-2-205_COSY.fid.esp

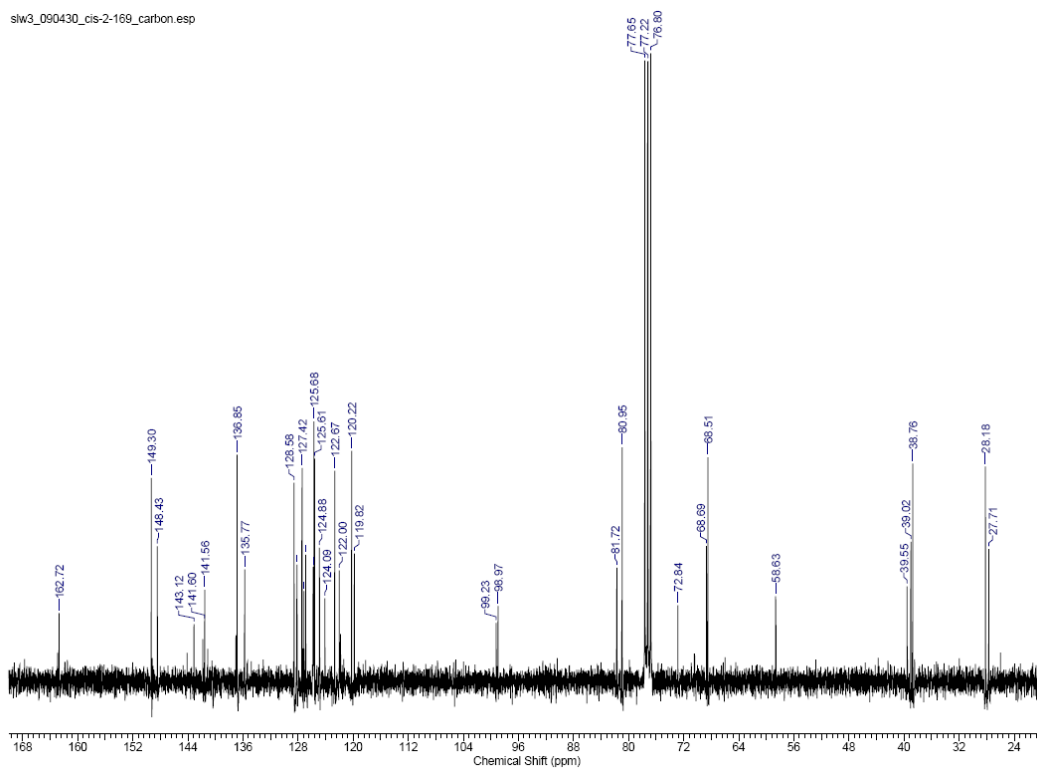


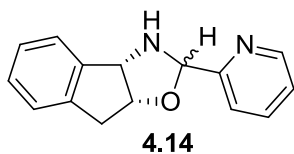


4.12

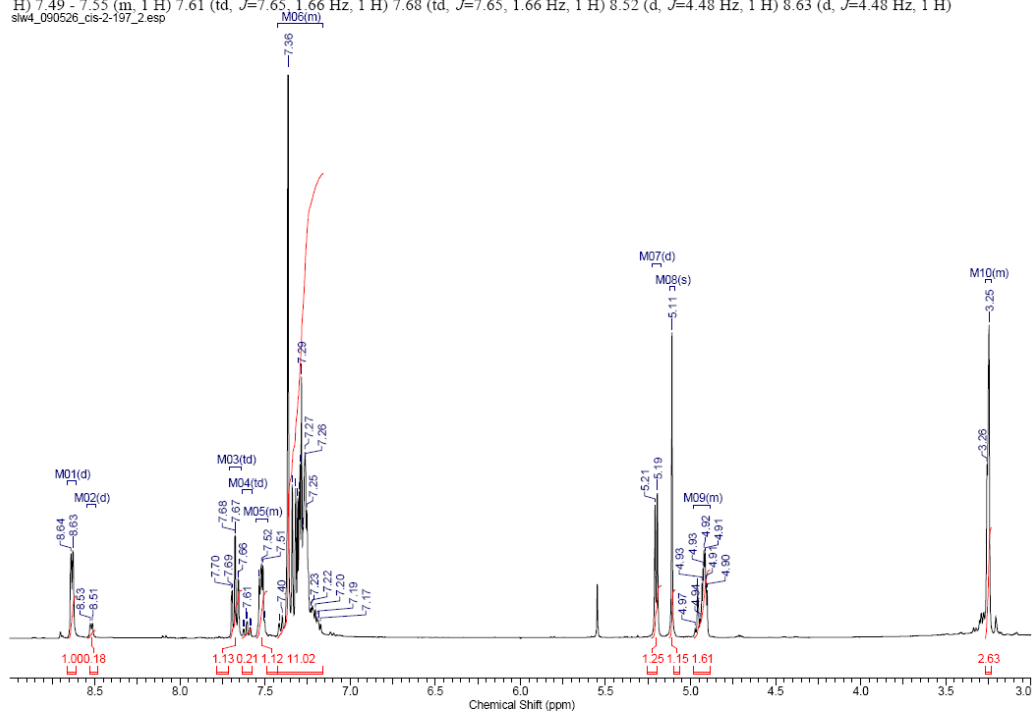
^1H NMR (400 MHz, CHCl_3 - d) δ ppm 1.48 - 1.57 (m, 2 H) 1.65 - 1.76 (m, 2 H) 2.68 - 2.77 (m, 2 H) 2.90 - 3.03 (m, 7 H) 3.04 - 3.18 (m, 8 H) 3.21 (d, $J=3.51$ Hz, 2 H) 4.28 - 4.44 (m, 12 H) 4.60 - 4.69 (m, 1 H) 4.73 (d, $J=6.24$ Hz, 1 H) 4.99 - 5.08 (m, 1 H) 6.89 - 6.95 (m, 1 H) 6.95 - 7.08 (m, 2 H) 7.18 - 7.37 (m, 32 H) 7.42 - 7.53 (m, 2 H) 7.71 (d, $J=3.32$ Hz, 1 H) 7.84 (td, $J=7.70$, 1.56 Hz, 1 H) 8.05 (d, $J=7.80$ Hz, 1 H) 8.38 (d, $J=4.68$ Hz, 1 H) 8.64 (d, $J=4.68$ Hz, 1 H) 8.69 (d, $J=4.29$ Hz, 1 H)

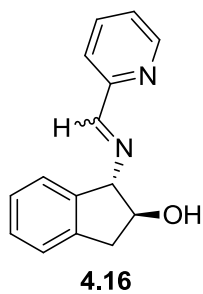




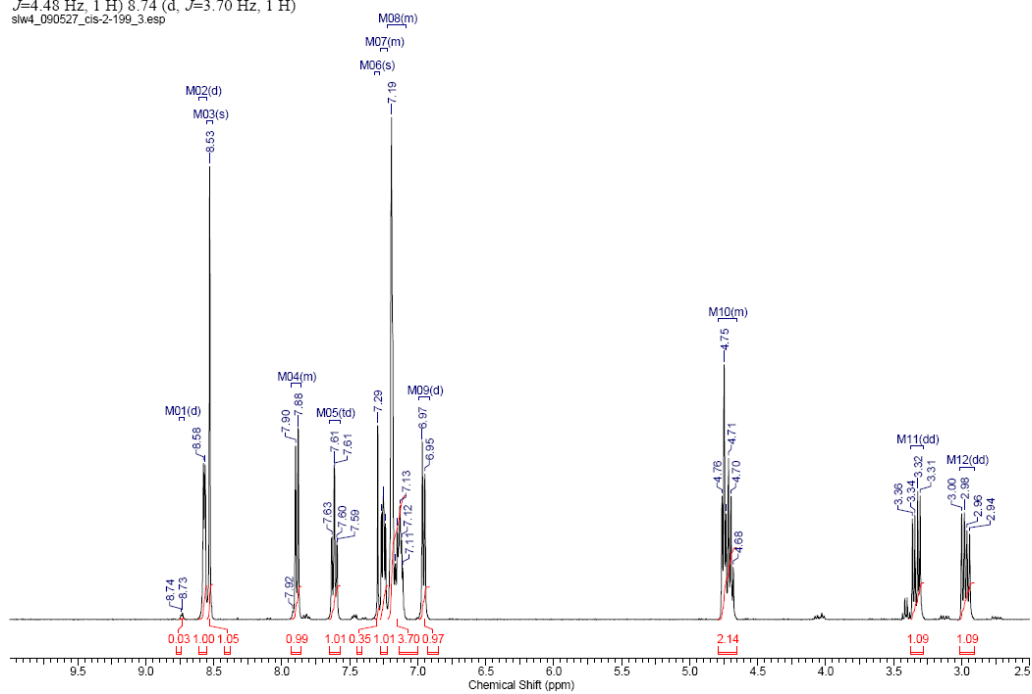


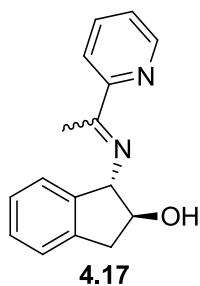
^1H NMR (400 MHz, CHCl_3 - d) δ ppm 3.23 - 3.27 (m, 3 H) 4.88 - 4.98 (m, 2 H) 5.11 (s, 1 H) 5.20 (d, $J=5.46$ Hz, 1 H) 7.16 - 7.43 (m, 11 H) 7.49 - 7.55 (m, 1 H) 7.61 (td, $J=7.65, 1.66$ Hz, 1 H) 7.68 (td, $J=7.65, 1.66$ Hz, 1 H) 8.52 (d, $J=4.48$ Hz, 1 H) 8.63 (d, $J=4.48$ Hz, 1 H)





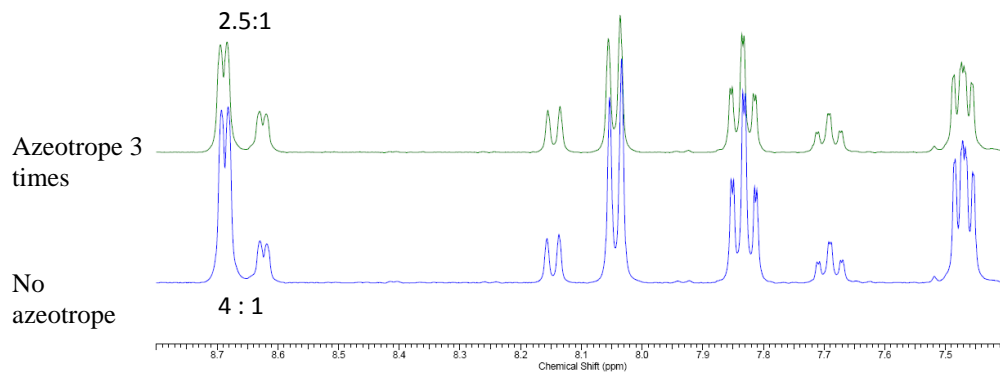
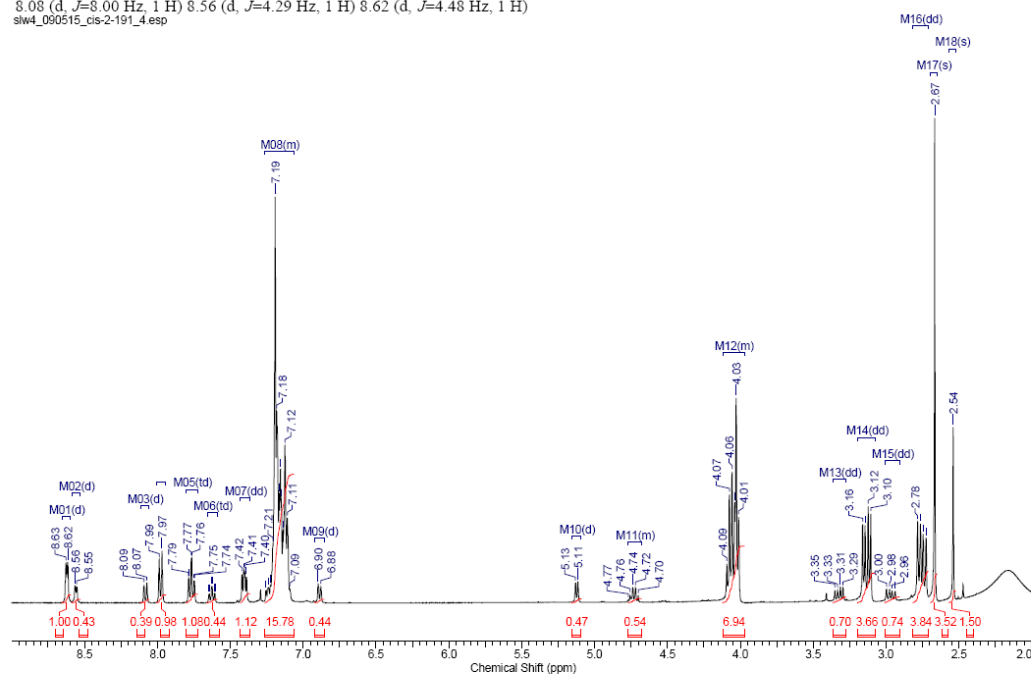
^1H NMR (400 MHz, CHCl_3) δ ppm 2.97 (dd, $J=15.41, 8.00$ Hz, 1 H) 3.33 (dd, $J=15.41, 7.02$ Hz, 1 H) 4.65 - 4.79 (m, 2 H) 6.96 (d, $J=7.41$ Hz, 1 H) 7.09 - 7.22 (m, 4 H) 7.22 - 7.28 (m, 1 H) 7.29 (s, 1 H) 7.61 (td, $J=7.65, 1.27$ Hz, 1 H) 7.86 - 7.93 (m, 1 H) 8.53 (s, 1 H) 8.57 (d, $J=4.48$ Hz, 1 H) 8.74 (d, $J=3.70$ Hz, 1 H)

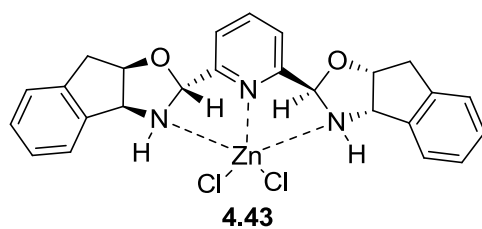




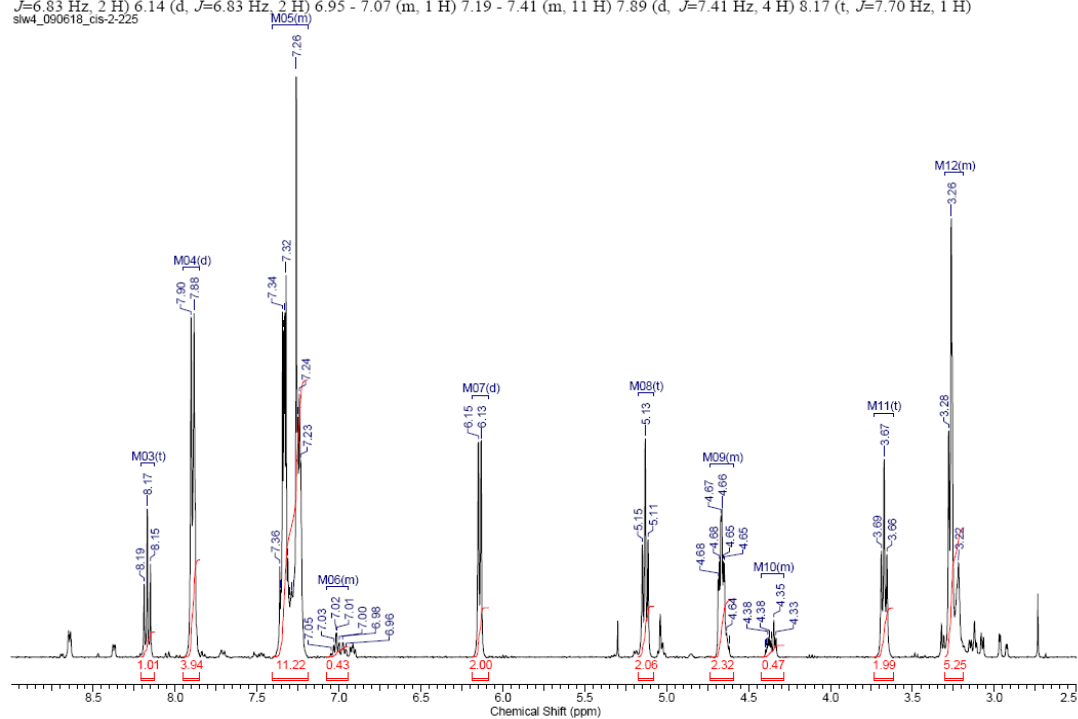
^1H NMR (400 MHz, CHCl_3 - d) δ ppm 2.54 (s, 1 H) 2.67 (s, 4 H) 2.75 (dd, $J=15.31, 7.90$ Hz, 4 H) 2.97 (dd, $J=15.41, 8.39$ Hz, 1 H) 3.13 (dd, $J=15.31, 6.92$ Hz, 4 H) 3.32 (dd, $J=15.41, 7.22$ Hz, 1 H) 3.97 - 4.12 (m, 7 H) 4.68 - 4.77 (m, 1 H) 5.12 (d, $J=6.63$ Hz, 1 H) 6.89 (d, $J=7.41$ Hz, 1 H) 7.06 - 7.26 (m, 16 H) 7.40 (dd, $J=6.63, 4.88$ Hz, 1 H) 7.63 (td, $J=7.70, 1.56$ Hz, 1 H) 7.77 (td, $J=7.70, 1.56$ Hz, 1 H) 7.98 (d, $J=7.80$ Hz, 1 H) 8.08 (d, $J=8.00$ Hz, 1 H) 8.56 (d, $J=4.29$ Hz, 1 H) 8.62 (d, $J=4.48$ Hz, 1 H)

slw4_090515_cis-2-191_4.esp

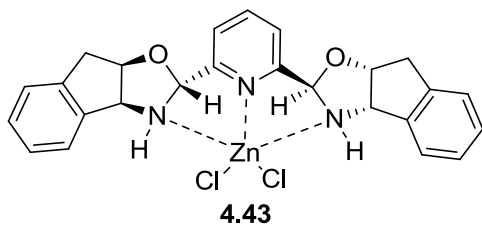




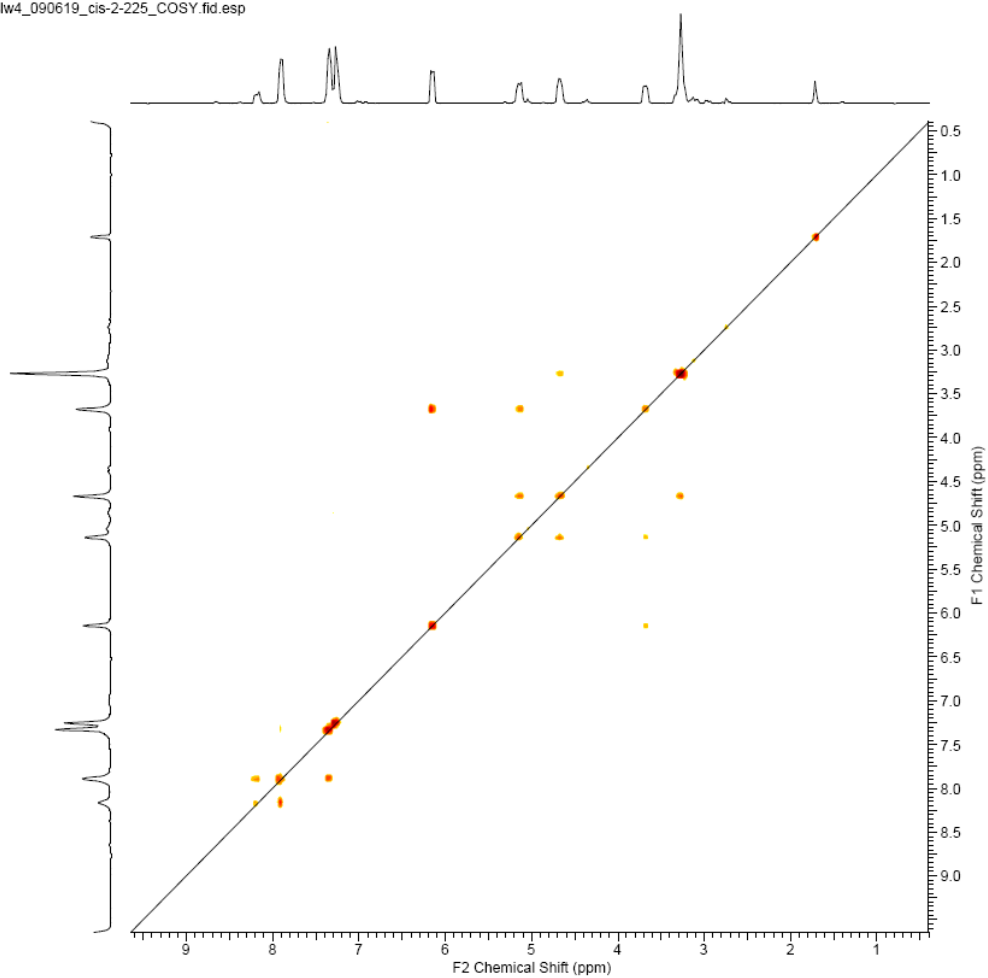
^1H NMR (400 MHz, $\text{CHLOROFORM-}d$) δ ppm 3.19 - 3.30 (m, 5 H) 3.67 (t, $J=6.92$ Hz, 2 H) 4.28 - 4.42 (m, 1 H) 4.59 - 4.73 (m, 2 H) 5.13 (t, $J=6.83$ Hz, 2 H) 6.14 (d, $J=6.83$ Hz, 2 H) 6.95 - 7.07 (m, 1 H) 7.19 - 7.41 (m, 11 H) 7.89 (d, $J=7.41$ Hz, 4 H) 8.17 (t, $J=7.70$ Hz, 1 H)
slw4_090618_cis-2-225

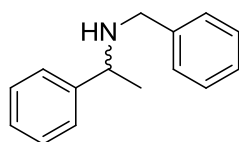


^1H - ^1H -COSY



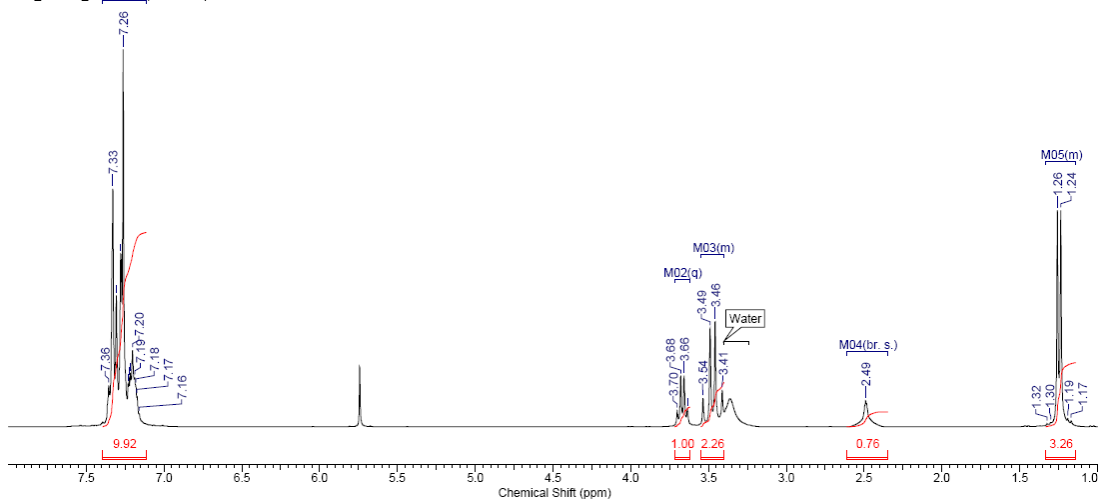
slw4_090619_cis-2-225_COSY.fid.esp

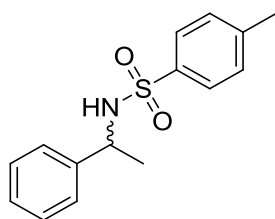




4.39 + 4.40

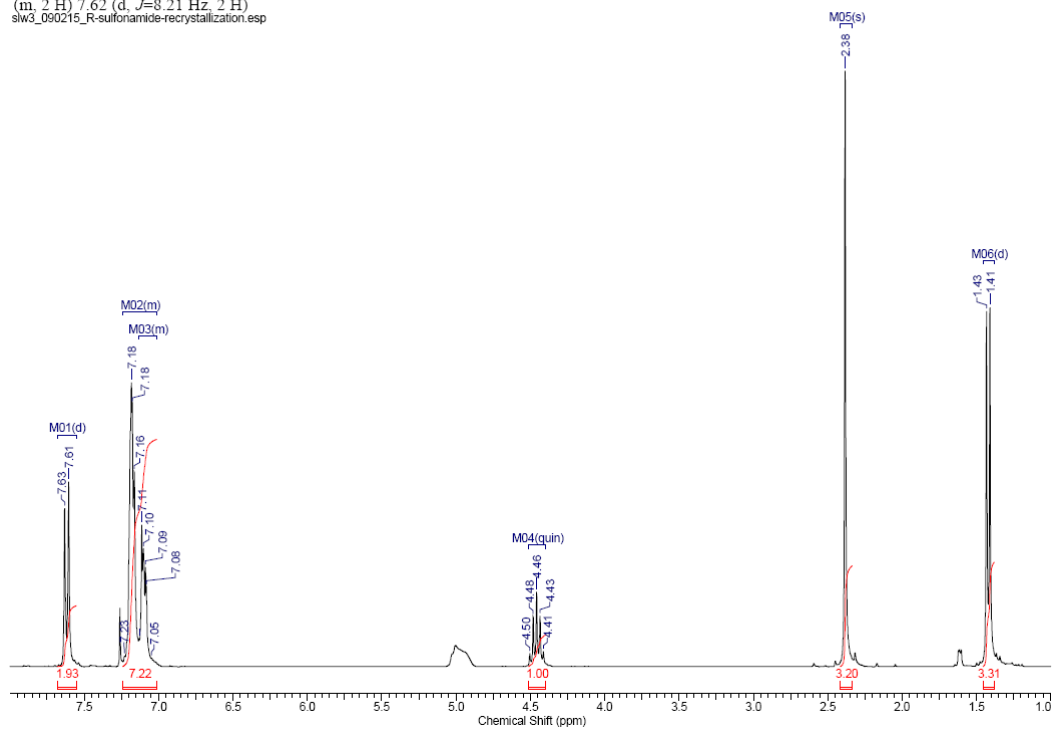
^1H NMR (300 MHz, $\text{DMSO}-d_6$) δ ppm 1.14 - 1.33 (m, 3 H) 2.49 (br. s., 1 H) 3.40 - 3.55 (m, 2 H) 3.67 (q, $J=6.60$ Hz, 1 H) 7.12 - 7.39 (m, 10 H)
 slw3_090112_cis-2.39169_product.esp



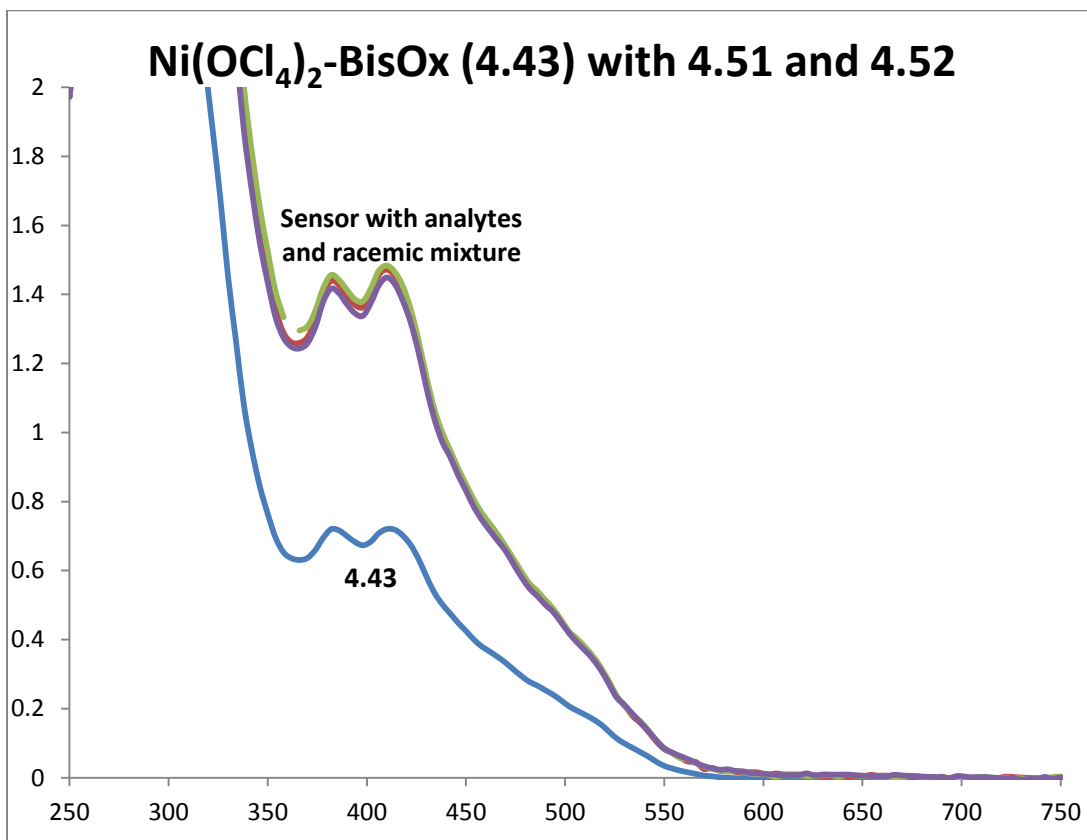


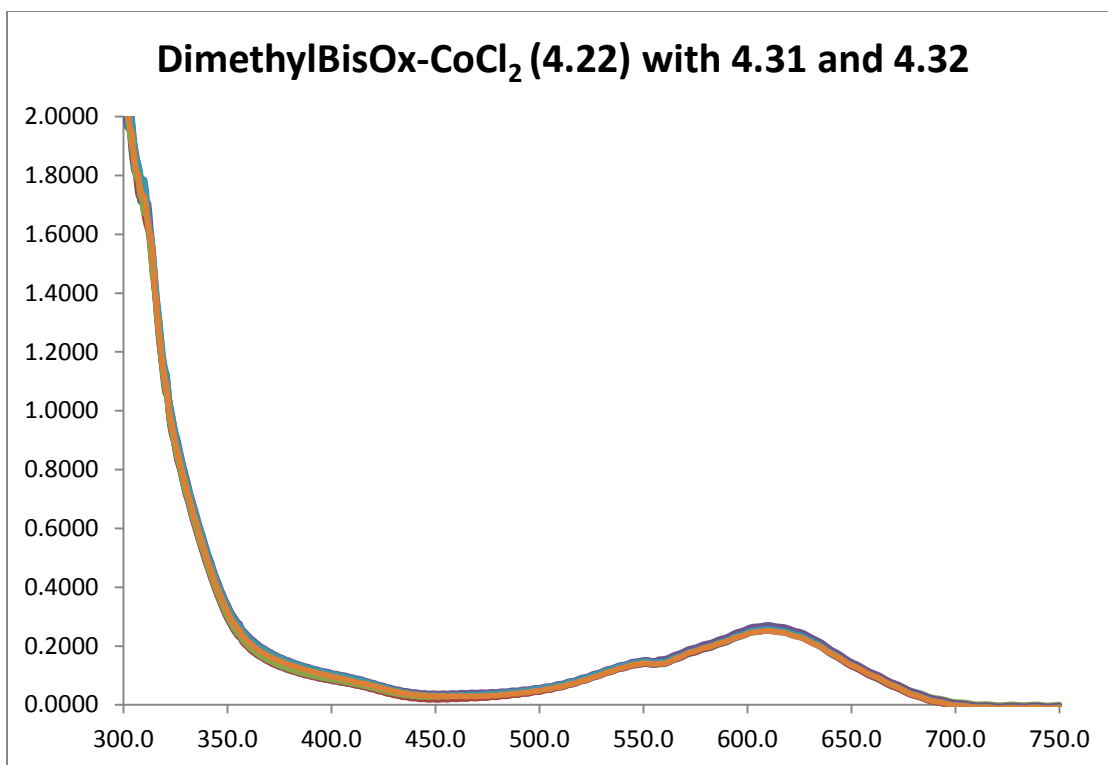
4.41 + 4.42

^1H NMR (300 MHz, CHCl_3) δ ppm 1.42 (d, $J=6.89$ Hz, 3 H) 2.38 (s, 3 H) 4.46 (quin, $J=6.85$ Hz, 1 H) 7.01 - 7.24 (m, 4 H) 7.01 - 7.13 (m, 2 H) 7.62 (d, $J=8.21$ Hz, 2 H)
slw3_090215_R-sulfonamide-recrystallization.esp

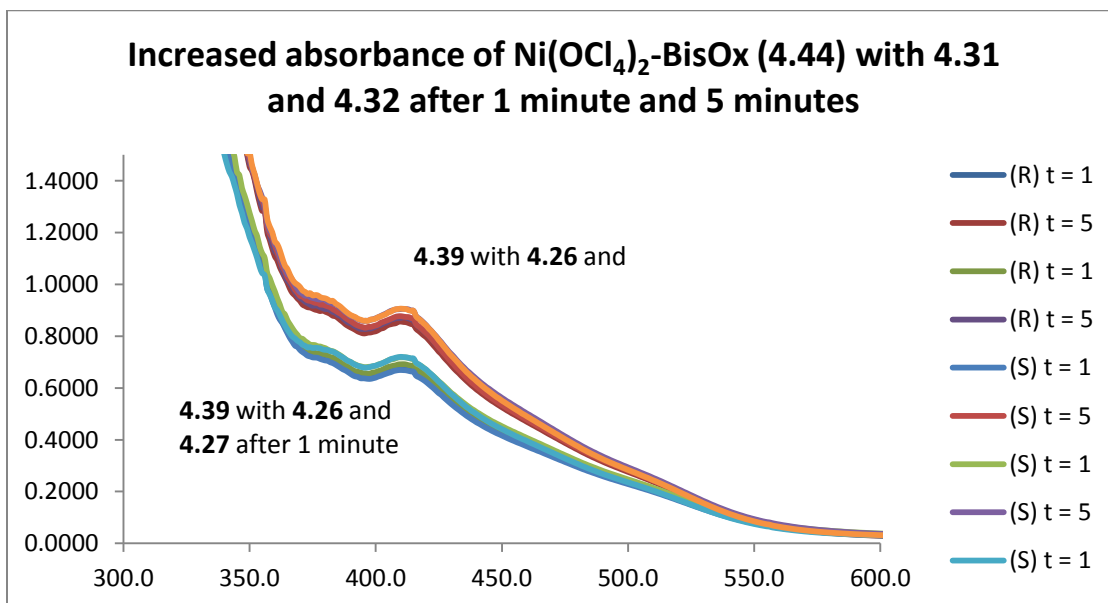


Representative UV spectra:





The observable increase in absorbance of 4.44 over time



4.8 References

1. Wolf, C.; Moskowitz, M., Bisoxazolidine-Catalyzed Enantioselective Reformatsky Reaction. *J. Org. Chem.* **2011**, 76, 6372-6376.
2. Wolf, C.; Xu, H., Asymmetric catalysis with chiral oxazolidine ligands. *Chem. Comm.* **2011**, 47, 3339-3350.
3. Ghosh, A. K.; Mathivanan, P.; Cappiello, J., C2-Symmetric chiral bis(oxazoline)-metal complexes in catalytic asymmetric synthesis. *Tetrahedron: Asymmetry* **1998**, 9, 1-45.
4. Johnson, J. S.; Evans, D. A., Chiral Bis(oxazoline) Copper(II) Complexes: Versatile Catalysts for Enantioselective Cycloaddition, Aldol, Michael, and Carbonyl Ene Reactions. *Acc. Chem. Res.* **2000**, 33, 325-335.
5. Desimoni, G.; Faita, G.; Jorgensen, K. A., Update 1 of: C2-Symmetric Chiral Bis(oxazoline) Ligands in Asymmetric Catalysis. *Chem. Rev.* **2011**, 111, 284-437.
6. Helmchen, G. N.; Pfaltz, A., Phosphinooxazolines A New Class of Versatile, Modular P,N-Ligands for Asymmetric Catalysis. *Acc. Chem. Res.* **2000**, 33, 336-345.

7. Jin, Z.; Huang, H.; Li, W.; Luo, X.; Liang, X.; Ye, J., Enantioselective Organocatalytic Synthesis of Oxazolidine Derivatives through a One-Pot Cascade Reaction. *Adv. Synth. Catal.* **2011**, *353*, 343-348.
8. Fan, Y. C.; Kwon, O., Diversity-Oriented Synthesis Based on the DPPP-Catalyzed Mixed Double-Michael Reactions of Electron-Deficient Acetylenes and Amino Alcohols. *Molecules* **2011**, *16*, 3802-3825
9. Xu, H.; Wolf, C., Asymmetric Synthesis of Chiral 1,3-Diaminopropanols: Bisoxazolidine-Catalyzed C–C Bond Formation with α -Keto Amides. *Angew. Chem. Int Ed.* **2011**, *50*, 12249-12252.
10. Astudillo, M. E. A.; Chokotho, N. C. J.; Jarvis, T. C.; Johnson, C. D.; Lewis, C. C.; McDonnell, P. D., Hydroxy schiff base-oxazolidine tautomerism: Apparent breakdown of baldwin's rules. *Tetrahedron* **1985**, *41*, 5919-5928.
11. Baldwin, J. E.; Cutting, J.; Dupont, W.; Kruse, L.; Silberman, L.; Thomas, R. C., 5-Endo-trigonal reactions: a disfavored ring closure. *J. Chem. Soc., Chem. Comm.* **1976**, *18*, 736-738.
12. Abadallah, H.; Gree, R.; Carrie, R., Syntheses asymetriques a l'aide d'oxazolidines chirales derivees de l'ephedrine. Preparation de formyl cyclopropanes chiraux. *Tet. Lett.* **1982**, *23*, 503-506.
13. Chou, C.-Y.; Raman, P. K.; Malocha, R. E.; Johnson, T. L.; Nocito, V.; Hoffman, M. D.; Brutto, P. E. Iminoalcohol-oxazolidine mixtures and their use. Patent 5,328,635, July 12, 1994.
14. ANGUS Chemical Company Technical Data Sheet
http://sdssearch.dow.com/PublishedLiteratureDOWCOM/dh_003f/0901b8038003f828.pdf?filepath=angus/pdfs/noreg/319-00029.pdf&fromPage=GetDoc
(accessed on March 3rd, 2013).
15. Bicker, K. L.; Wiskur, S. L.; Lavigne, J. J., Colorimetric Sensor Design. In *Chemosensors*, John Wiley & Sons, Inc.: Hoboken, NJ, 2011; pp 275-295.
16. Wiskur, S. L.; Maynor, M. S.; Smith, M. D.; Sheppard, C.; Akhiani, R. K.; Pellechia, P. J.; Vaughn, S. A.; Shieh, C., Chiral pyridinyloxazolidine ligands and copper chloride complexes. *J. Coord. Chem.* **2013**, ASAP.
17. SPARTAN '08 version 1.2 Wavefunction Inc., 18401 Von Karman Avenue, Suite 370, Irvine CA 92612, U.S.A. 2008
18. Turner, N. J., *Nat. Chem. Bio.* **2009**, *5*, (8), 567-573.
19. Nugent, T. C., *Chiral Amine Synthesis. Methods , Developments and Applications*. Wiley-VCH: Weinheim, 2010.

20. Breuer, M.; Ditrich, K.; Habicher, T.; Hauer, B.; Keßeler, M.; Stürmer, R.; Zelinski, T., Industrial Methods for the Production of Optically Active Intermediates. *Angew. Chem. Int. Ed.* **2004**, *43*, 788-824.
21. Henkel, T.; Brunne, R. M.; Müller, H.; Reichel, F., Statistical Investigation into the Structural Complementarity of Natural Products and Synthetic Compounds. *Angew. Chem. Int. Ed.* **1999**, *38*, 643-647.
22. You, L.; Berman, J. S.; Anslyn, E. V., Dynamic multi-component covalent assembly for the reversible binding of secondary alcohols and chirality sensing. *Nat. Chem.* **2011**, *3*, 943-948.
23. Kaneda, T.; Hirose, K.; Misumi, S., Chiral azophenolic acerands: color indicators to judge the absolute configuration of chiral amines. *J. Am. Chem. Soc.* **1989**, *111*, 742-743.
24. Kubo, Y.; Maeda, S. y.; Tokita, S.; Kubo, M., *Nature* **1996**, *382*, 522-524.
25. Misumi, S., Supramolecular Chemistry I Directed Synthesis and Molecular Recognition: Recognitory coloration of cations with chromoacerands. In *Top. Curr. Chem.*, Springer Berlin Heidelberg: 1993; Vol. 165, pp 163-192.
26. Tsubaki, K.; Nuruzzaman, M.; Kusumoto, T.; Hayashi, N.; Bin-Gui, W.; Fuji, K., Visual Enantiomeric Recognition Using Chiral Phenolphthalein Derivatives. *Org. Lett.* **2001**, *3*, 4071-4073.
27. Tsubaki, K.; Tanima, D.; Nuruzzaman, M.; Kusumoto, T.; Fuji, K.; Kawabata, T., Visual Enantiomeric Recognition of Amino Acid Derivatives in Protic Solvents. *J. Org. Chem.* **2005**, *70*, 4609-4616.
28. Leung, D.; Folmer-Andersen, J. F.; Lynch, V. M.; Anslyn, E. V., Using Enantioselective Indicator Displacement Assays To Determine the Enantiomeric Excess of Amino Acids. *J. Am. Chem. Soc.* **2008**, *130*, 12318-12327.
29. Cho, E. N. R.; Li, Y.; Kim, H. J.; Hyun, M. H., A colorimetric chiral sensor based on chiral crown ether for the recognition of the two enantiomers of primary amino alcohols and amines. *Chirality* **2011**, *23*, 349-353.
30. Hirose, K., A Practical Guide for the Determination of Binding Constants. *J. Incl. Phenom. Macro.* **2001**, *39*, 193-209.
31. Kubo, Y., Binaphthyl-appended Chromogenic Receptors: Synthesis and Application to their Colorimetric Recognition of Amines. *Synlett* **1999**, *1999*, 161-174.
32. Hirose, K.; Aksharanandana, P.; Suzuki, M.; Wads, K.; Naemura, K.; Tobe, Y., *Heterocycles* **2005**, *66*, 405-431.

33. Leung, D.; Anslyn, E. V., Transitioning Enantioselective Indicator Displacement Assays for Amino Acids to Protocols Amenable to High-Throughput Screening. *J. Am. Chem. Soc.* **2008**, *130*, 12328-12333.
34. Crassous, J., Chiral transfer in coordination complexes: towards molecular materials. *Chem. Soc. Rev.* **2009**, *38*, 830-845.
35. Nakano, H.; Osone, K.; Takeshita, M.; Kwon, E.; Seki, C.; Matsuyama, H.; Takano, N.; Kohari, Y., A novel chiral oxazolidine organocatalyst for the synthesis of an oseltamivir intermediate using a highly enantioselective Diels-Alder reaction of 1,2- dihydropyridine. *Chem. Comm.* **2010**, *46*, 4827-4829.
36. Weickgenannt, A.; Mewald, M.; Oestreich, M., Asymmetric Si-O coupling of alcohols. *Org. Biomol. Chem.* **2010**, *8*, 1497-1504.
37. Kagan, H. B.; Fiaud, J. C., Kinetic Resolution. In *Topics in Stereochemistry*, John Wiley & Sons, Inc.: 1988; pp 249-330.
38. Sheppard, C. I.; Taylor, J. L.; Wiskur, S. L., Silylation-Based Kinetic Resolution of Monofunctional Secondary Alcohols. *Org. Lett.* **2011**, *13*, 3794-3797.

Works Cited

Collins, A. N.; Sheldrake, G. N.; Crosby, J. E., *Chirality in Industry: The Commercial Manufacture and Applications of Optically Active Compounds*. Wiley-VCH: New York, 1992.

Collins, A. N.; Sheldrake, G. N.; Crosby, J. E., *Chirality in Industry II: Developments in the Commercial Manufacture and Applications of Optically Active Compounds*. Wiley-VCH: New York, 1998.

FDA,
<http://www.fda.gov/drugs/GuidanceComplianceRegulatoryInformation/Guidances/ucm122883.htm> (accessed on April 9, 2012).

Olbe, L.; Carlsson, E.; Lindberg, P., A proton-pump inhibitor expedition: the case histories of omeprazole and esomeprazole. *Nat Rev Drug Discov* **2003**, 2, 132-139.

Harvey, A. L., Natural products in drug discovery. *Drug Discovery Today* **2008**, 13, 894-901.

Shai, Y.; Oren, Z., Diastereomers of Cytolysins, a Novel Class of Potent Antibacterial Peptides. *J. Biol. Chem.* **1996**, 271, 7305-7308.

Kaminski, H. M.; Feix, J. B., Effects of D-Lysine Substitutions on the Activity and Selectivity of Antimicrobial Peptide CM15. *Polymers* **2011**, 3, 2088-2106.

Oren, Z.; Hong, J.; Shai, Y., A comparative study on the structure and function of a cytolytic α -helical peptide and its antimicrobial β -sheet diastereomer. *Eur. J. Biochem.* **1999**, 259, 360-369.

Martínez-Rodríguez, S.; Martínez-Gómez, A. I.; Rodríguez-Vico, F.; Clemente-Jiménez, J. M.; Las Heras-Vázquez, F. J., Natural Occurrence and Industrial Applications of d-Amino Acids: An Overview. *Chem. Biodiversity* **2010**, 7, 1531-1548.

Wani, M. C.; Taylor, H. L.; Wall, M. E.; Coggon, P.; McPhail, A. T., Plant antitumor agents. VI. Isolation and structure of taxol, a novel antileukemic and antitumor agent from *Taxus brevifolia*. *J. Amer. Chem. Soc.* **1971**, 93, 2325-2327.

Patel, R. N., Tour de Paclitaxel: Biocatalysis for Semisynthesis. *Annu. Rev. Microbiol.* **1998**, 52, 361-395.

Ottaggio, L.; Bestoso, F.; Armirotti, A.; Balbi, A.; Damonte, G.; Mazzei, M.; Sancandi, M.; Miele, M., Taxanes from Shells and Leaves of *Corylus avellana*. *J. Nat. Prod.* **2007**, 71, 58-60

- Pellissier, H. I. n., Asymmetric organocatalysis. *Tetrahedron* **2007**, *63*, 9267-9331.
- Jacobsen, E. N., Pfaltz., A.; Yamamoto, H. (Eds.), *Comprehensive Asymmetric Catalysis*. Springer: New York, 1999; Vol. i-iii.
- Jacobsen, E. N. Pfaltz., A.; Yamamoto, H. (Eds.), *Comprehensive Asymmetric Catalysis Supplement*. Springer: New York, 2004; Vol. 1-2.
- Katsuki, T.; Sharpless, K. B., The first practical method for asymmetric epoxidation. *J. Amer. Chem. Soc.* **1980**, *102*, 5974-5976.
- Finn, M. G.; Sharpless, K. B., Mechanism of asymmetric epoxidation. 2. Catalyst structure. *J. Am. Chem. Soc.* **1991**, *113*, 113-126.
- Katsuki, T.; Martin, V., Asymmetric Epoxidation of Allylic Alcohols: the Katsuki–Sharpless Epoxidation Reaction. In *Organic Reactions*, John Wiley & Sons, Inc.: 2004.
- Noyori, R.; Ohkuma, T.; Kitamura, M.; Takaya, H.; Sayo, N.; Kumobayashi, H.; Akutagawa, S., Asymmetric hydrogenation of beta-keto carboxylic esters. A practical, purely chemical access to beta-hydroxy esters in high enantiomeric purity. *J. Am. Chem. Soc.* **1987**, *109*, 5856-5858
- Ager, D. J.; Laneman, S. A., Reductions of 1,3-dicarbonyl systems with ruthenium-biarylphosphine catalysts. *Tetrahedron: Asymmetry* **1997**, *8*, 3327-3355.
- Noyori, R.; Ohta, M.; Hsiao, Y.; Kitamura, M.; Ohta, T.; Takaya, H., Asymmetric synthesis of isoquinoline alkaloids by homogeneous catalysis. *J. Am. Chem. Soc.* **1986**, *108*, 7117-7119.
- Chi, Y.; Tang, W.; Zhang, X., Rhodium-Catalyzed Asymmetric Hydrogenation. In *Modern Rhodium-Catalyzed Organic Reactions*, Wiley-VCH Verlag GmbH & Co. KGaA: 2005; pp 1-31.
- Knowles, W. S.; Sabacky, M. J., Catalytic asymmetric hydrogenation employing a soluble, optically active, rhodium complex. *Chem. Comm.* **1968**, *22*, 1445-1446.
- Knowles, W. S., Asymmetric hydrogenation. *Acc. of Chem. Res.* **1983**, *16*, 106-112.
- Knowles, W. S., Asymmetric Hydrogenations (Nobel Lecture 2001). *Adv. Synt. & Catal.* **2003**, *345*, 3-13.
- Giacalone, F.; Gruttadauria, M.; Agrigento, P.; Noto, R., Low-loading asymmetric organocatalysis. *Chem. Soc. Rev.* **2012**, *41*, 2406-2447.
- Collet, A., Resolution of Racemates: Did You Say “Classical”? *Angew. Chem. Int. Ed.* **1998**, *37*, 3239-3241.
- Dalmolen, J.; Tiemersma-Wegman, T. D.; Nieuwenhuijzen, J. W.; van der Sluis, M.; van Echten, E.; Vries, T. R.; Kaptein, B.; Broxterman, Q. B.; Kellogg, R. M., The Dutch Resolution Variant of the Classical Resolution of Racemates by Formation of Diastereomeric Salts: Family Behaviour in Nucleation Inhibition. *Chem. Eur. J.* **2005**, *11*, 5619-5624.

Kagan, H. B.; Fiaud, J. C., Kinetic Resolution. In *Topics in Stereochemistry*, John Wiley & Sons, Inc.: 1988; pp 249-330.

Kagan, H. B., Various aspects of the reaction of a chiral catalyst or reagent with a racemic or enantiopure substrate. *Tetrahedron* **2001**, *57*, 2449-2468.

Keith, J. M.; Larrow, J. F.; Jacobsen, E. N., Practical Considerations in Kinetic Resolution Reactions. *Adv. Synth. Catal.* **2001**, *343*, 5-26.

Vedejs, E.; Jure, M., Efficiency in Nonenzymatic Kinetic Resolution. *Angew. Chem. Int. Ed.* **2005**, *44*, 3974-4001.

Anslyn, E. V.; Dougherty, D. A., *Modern Physical Organic Chemistry*. University Science Books: Sausalito, California, 2006.

Liu, H.-L.; Anthonsen, T., Enantiopure building blocks for chiral drugs from racemic mixtures of secondary alcohols by combination of lipase catalysis and Mitsunobu esterification. *Chirality* **2002**, *14*, 25-27.

Pellissier, H., Catalytic Non-Enzymatic Kinetic Resolution. *Adv. Synth. Catal.* **2011**, *353*, 1613-1666.

Spivey, A.; Arseniyadis, S.; List, B., Amine, Alcohol and Phosphine Catalysts for Acyl Transfer Reactions Asymmetric Organocatalysis. In Springer Berlin / Heidelberg: 2009; Vol. 291, 233-280.

Müller, C. E.; Schreiner, P. R., Organocatalytic Enantioselective Acyl Transfer onto Racemic as well as meso Alcohols, Amines, and Thiols. *Angew. Chem. Int. Ed.* **2011**, *50*, 6012-6042.

Vedejs, E.; Daugulis, O.; Diver, S. T., Enantioselective Acylations Catalyzed by Chiral Phosphines. *J. Org. Chem.* **1996**, *61*, 430-431.

Vedejs, E.; Daugulis, O., A Highly Enantioselective Phosphabicyclooctane Catalyst for the Kinetic Resolution of Benzylic Alcohols. *J. Am. Chem. Soc.* **2003**, *125*, 4166-4173.

Klare, H. F. T.; Oestreich, M., Chiral Recognition with Silicon-Stereogenic Silanes: Remarkable Selectivity Factors in the Kinetic Resolution of Donor-Functionalized Alcohols. *Angew. Chem. Int. Ed.* **2007**, *46*, 9335-9338.

Vedejs, E.; Chen, X., Kinetic Resolution of Secondary Alcohols. Enantioselective Acylation Mediated by a Chiral (Dimethylamino)pyridine Derivative. *J. Am. Chem. Soc.* **1996**, *118*, 1809-1810.

Wurz, R. P., Chiral Dialkylaminopyridine Catalysts in Asymmetric Synthesis. *Chem. Rev.* **2007**, *107*, 5570-5595.

Ruble, J. C.; Tweddell, J.; Fu, G. C., Kinetic Resolution of Arylalkylcarbinols Catalyzed by a Planar-Chiral Derivative of DMAP: A New Benchmark for Nonenzymatic Acylation. *J. Org. Chem.* **1998**, *63*, 2794-2795.

Tao, B.; Ruble, J. C.; Hoic, D. A.; Fu, G. C., Nonenzymatic Kinetic Resolution of Propargylic Alcohols by a Planar Chiral DMAP Derivative: Crystallographic Characterization of the Acylated Catalyst. *J. Am. Chem. Soc.* **1999**, *121*, 5091-5092.

Ruble, J. C.; Latham, H. A.; Fu, G. C., Effective Kinetic Resolution of Secondary Alcohols with a Planar Chiral Analogue of 4-(Dimethylamino)pyridine. Use of the Fe(C₅Ph₅) Group in Asymmetric Catalysis. *J. Am. Chem. Soc.* **1997**, *119*, 1492-1493.

Fu, G. C., Enantioselective Nucleophilic Catalysis with Planar-Chiral • Heterocycles. *Acc. Chem. Res.* **2000**, *33*, 412-420.

Fu, G. C., Asymmetric Catalysis with Planar-Chiral • Derivatives of 4-(Dimethylamino)pyridine. *Acc. Chem. Res.* **2004**, *37*, 542-547.

Sinha, S. C.; Barbas, C. F.; Lerner, R. A., The antibody catalysis route to the total synthesis of epothilones. *Proc. Natl. Acad. Sci. USA* **1998**, *95*, 14603-14608.

Miller, S. J.; Copeland, G. T.; Papaioannou, N.; Horstmann, T. E.; Ruel, E. M., Kinetic Resolution of Alcohols Catalyzed by Tripeptides Containing the N-Alkylimidazole Substructure. *J. Am. Chem. Soc.* **1998**, *120*, 1629-1630.

Jarvo, E. R.; Copeland, G. T.; Papaioannou, N.; Bonitatebus, P. J.; Miller, S. J., A Biomimetic Approach to Asymmetric Acyl Transfer Catalysis. *J. Am. Chem. Soc.* **1999**, *121*, 11638-11643.

Davie, E. A. C.; Mennen, S. M.; Xu, Y.; Miller, S. J., Asymmetric Catalysis Mediated by Synthetic Peptides. *Chem. Rev.* **2007**, *107*, 5759-5812.

Formaggio, F.; Barazza, A.; Bertocco, A.; Toniolo, C.; Broxterman, Q. B.; Kaptein, B.; Brasola, E.; Pengo, P.; Pasquato, L.; Scrimin, P., Role of Secondary Structure in the Asymmetric Acylation Reaction Catalyzed by Peptides Based on Chiral Tetrasubstituted Amino Acids. *J. Org. Chem.* **2004**, *69*, 3849-3856.

Taylor, J. E.; Bull, S. D.; Williams, J. M. J., Amidines, isothioureas, and guanidines as nucleophilic catalysts. *Chem. Soc. Rev.* **2012**, *41*, 2109-2121.

Birman, V. B.; Uffman, E. W.; Jiang, H.; Li, X.; Kilbane, C. J., 2,3-Dihydroimidazo[1,2-a]pyridines: A New Class of Enantioselective Acyl Transfer Catalysts and Their Use in Kinetic Resolution of Alcohols. *J. Am. Chem. Soc.* **2004**, *126*, 12226-12227.

Li, X.; Liu, P.; Houk, K. N.; Birman, V. B., Origin of Enantioselectivity in CF₃-PIP-Catalyzed Kinetic Resolution of Secondary Benzylic Alcohols. *J. Am. Chem. Soc.* **2008**, *130*, 13836-13837.

Birman, V. B.; Li, X., Benzotetramisole: A Remarkably Enantioselective Acyl Transfer Catalyst. *Org. Lett.* **2006**, *8*, 1351-1354.

Birman, V. B.; Li, X., Homobenzotetramisole: An Effective Catalyst for Kinetic Resolution of Aryl-Cycloalkanols. *Org. Lett.* **2008**, *10*, 1115-1118.

Zhang, Y.; Birman, V. B., Effects of Methyl Substituents on the Activity and Enantioselectivity of Homobenzotetramisole-Based Catalysts in the Kinetic Resolution of Alcohols. *Adv. Synth. Catal.* **2009**, *351*, 2525-2529.

Li, X.; Jiang, H.; Uffman, E. W.; Guo, L.; Zhang, Y.; Yang, X.; Birman, V. B., Kinetic Resolution of Secondary Alcohols Using Amidine-Based Catalysts. *J. Org. Chem.* **2012**, *77*, 1722-1737.

Hu, B.; Meng, M.; Wang, Z.; Du, W.; Fossey, J. S.; Hu, X.; Deng, W.-P., A Highly Selective Ferrocene-Based Planar Chiral PIP (Fc-PIP) Acyl Transfer Catalyst for the Kinetic Resolution of Alcohols. *J. Am. Chem. Soc.* **2010**, *132*, 17041-17044.

Weickgenannt, A.; Mewald, M.; Oestreich, M., Asymmetric Si-O coupling of alcohols. *Organic & Biomolecular Chemistry* **2010**, *8*, 1497-1504.

Greene, T. W.; Wuts, P. G. M., *Protective Groups in Organic Synthesis*. 3rd ed.; John Wiley & Sons: New York, 1999.

Sheppard, C. I.; Taylor, J. L.; Wiskur, S. L., Silylation-Based Kinetic Resolution of Monofunctional Secondary Alcohols. *Org. Lett.* **2011**, *13*, 3794-3797.

Rendler, S.; Auer, G.; Oestreich, M., Kinetic Resolution of Chiral Secondary Alcohols by Dehydrogenative Coupling with Recyclable Silicon-Stereogenic Silanes. *Angew. Chem. Int. Ed.* **2005**, *44*, (46), 7620-7624.

Klare, H. F. T.; Oestreich, M., Chiral Recognition with Silicon-Stereogenic Silanes: Remarkable Selectivity Factors in the Kinetic Resolution of Donor-Functionalized Alcohols. *Angew. Chem. Int. Ed.* **2007**, *46*, 9335-9338.

Weickgenannt, A.; Mewald, M.; Muesmann, T. W. T.; Oestreich, M., Catalytic Asymmetric Si-O Coupling of Simple Achiral Silanes and Chiral Donor-Functionalized Alcohols. *Ang. Chem. Int. Ed.* **2010**, *49*, 2223-2226.

Rendler, S.; Oestreich, M., Polishing a Diamond in the Rough: "Cu-H" Catalysis with Silanes. *Angew. Chem. Int. Ed.* **2007**, *46*, 498-504.

Rendler, S.; Plefka, O.; Karatas, B.; Auer, G.; Fröhlich, R.; Mück-Lichtenfeld, C.; Grimme, S.; Oestreich, M., Stereoselective Alcohol Silylation by Dehydrogenative Si-O Coupling: Scope, Limitations, and Mechanism of the Cu-H-Catalyzed Non-Enzymatic Kinetic Resolution with Silicon-Stereogenic Silanes. *Chem. Eur. J.* **2008**, *14*, 11512-11528.

Isobe, T.; Fukuda, K.; Araki, Y.; Ishikawa, T., Modified guanidines as chiral superbases: the first example of asymmetric silylation of secondary alcohols. *Chem. Comm.* **2001**, 243-244.

Jarvo, E. R.; Copeland, G. T.; Papaioannou, N.; Bonitatebus, P. J.; Miller, S. J., A Biomimetic Approach to Asymmetric Acyl Transfer Catalysis. *J. Am. Chem. Soc.* **1999**, *121*, 11638-11643.

Zhao, Y.; Rodrigo, J.; Hoveyda, A. H.; Snapper, M. L., Enantioselective silyl protection of alcohols catalysed by an amino-acid-based small molecule. *Nature* **2006**, *443*, 67-70.

Zhao, Y.; Mitra, A. W.; Hoveyda, A. H.; Snapper, M. L., Kinetic Resolution of 1,2-Diols through Highly Site- and Enantioselective Catalytic Silylation. *Angew. Chem. Int. Ed.* **2007**, *46*, 8471-8474.

You, Z.; Hoveyda, A. H.; Snapper, M. L., Catalytic Enantioselective Silylation of Acyclic and Cyclic Triols: Application to Total Syntheses of Cleroindicans D, F, and C. *Angew. Chem. Int. Ed.* **2009**, *48*, 547-550.

Rodrigo, J. M.; Zhao, Y.; Hoveyda, A. H.; Snapper, M. L., Regiodivergent Reactions through Catalytic Enantioselective Silylation of Chiral Diols. Synthesis of Sapinofuranone A. *Org. Lett.* **2011**, *13*, 3778-3781.

Vedejs, E.; Jure, M., Efficiency in Nonenzymatic Kinetic Resolution. *Angew. Chem. Int. Ed.* **2005**, *44*, 3974-4001.

Vedejs, E.; Chen, X., Parallel Kinetic Resolution. *J. Am. Chem. Soc.* **1997**, *119*, 2584- 2585.

Tan, K. L.; Sun, X.; Worthy, A. D., Scaffolding Catalysis: Expanding the Repertoire of Bifunctional Catalysts. *Synlett* **2012**, *2012*, 321-325.

Sun, X.; Worthy, A. D.; Tan, K. L., Scaffolding Catalysts: Highly Enantioselective Desymmetrization Reactions. *Angew. Chem. Int. Ed.* **2011**, *50*, 8167-8171.

Worthy, A. D.; Sun, X.; Tan, K. L., Site-Selective Catalysis: Toward a Regiodivergent Resolution of 1,2-Diols. *J. Am. Chem. Soc.* **2012**, *134*, 7321-7324.

Patel, S. G.; Wiskur, S. L., Mechanistic investigations of the Mukaiyama aldol reaction as a two part enantioselective reaction. *Tet. Lett.* **2009**, *50*, 1164-1166.

Song, C. E., *Cinchona Alkaloids in Synthesis & Catalysis*. Wiley-VCH Verlag GmbH & Co.: Weinheim, Germany, 2009.

Kagan, H. B.; Fiaud, J. C., Kinetic Resolution. In *Topics in Stereochemistry*, John Wiley & Sons, Inc.: 1988; pp 249-330.

Birman, V. B.; Li, X., Benzotetramisole: A Remarkably Enantioselective Acyl Transfer Catalyst. *Org. Lett.* **2006**, *8*, 1351-1354.

Li, X.; Jiang, H.; Uffman, E. W.; Guo, L.; Zhang, Y.; Yang, X.; Birman, V. B., Kinetic Resolution of Secondary Alcohols Using Amidine-Based Catalysts. *J. Org. Chem.* **2012**, *77*, 1722-1737.

Kim, S.; Chang, H., 1,8-Diazabicyclo[5.4.0]undec-7-ene. An Effective and Selective Catalyst for the *t*-Butyldimethylsilylation of Alcohols. *Bull. Chem. Soc. Jpn.* **1985**, *58*, 3669-3670.

Corriu, R. J. P.; Dabosi, G.; Martineau, M., Macanisme de l'hydrolyse des chlorosilanes, catalysée par un nucléophile: étude cinétique et mise en évidence d'un intermédiaire hexacoordonné. *J. Organomet. Chem.* **1978**, *150*, 27-38.

Bassindale, A. R.; Stout, T., The interaction of electrophilic silanes (Me_3SiX , $\text{X} = \text{ClO}_4, \text{I}, \text{CF}_3\text{SO}_3, \text{Br}, \text{Cl}$) with nucleophiles. The nature of silylation mixtures in solution. *Tet. Lett.* **1985**, 26, 3403-3406.

Fujio, M.; Keeffe, J. R.; More O'Ferrall, R. A.; O'Donoghue, A. C., Unexpectedly Small Ortho-Oxygen Substituent Effects on Stabilities of Benzylic Carbocations. *J. Am. Chem. Soc.* **2004**, 126, 9982-9992.

Jarvo, E. R.; Evans, C. A.; Copeland, G. T.; Miller, S. J., Fluorescence-Based Screening of Asymmetric Acylation Catalysts through Parallel Enantiomer Analysis. Identification of a Catalyst for Tertiary Alcohol Resolution. *J. Org. Chem.* **2001**, 66, 5522-5527.

Angione, M. C.; Miller, S. J., Dihedral angle restriction within a peptide-based tertiary alcohol kinetic resolution catalyst. *Tetrahedron* **2006**, 62, 5254-5261.

Karatas, B.; Rendler, S.; Frohlich, R.; Oestreich, M., Kinetic resolution of donor-functionalised tertiary alcohols by Cu-H-catalysed stereoselective silylation using a strained silicon-stereogenic silane. *Org. Biomol. Chem.* **2008**, 6, 1435-1440.

Breuer, M.; Ditrich, K.; Habicher, T.; Hauer, B.; Keßeler, M.; Stürmer, R.; Zelinski, T., Industrial Methods for the Production of Optically Active Intermediates. *Angew. Chem. Int. Ed.* **2004**, 43, 788-824.

Nicolaou, K. C.; Sorensen, E. K., Classics in Total Synthesis. VCH Publishers: New York, 1996; pp 41-53.

Burchat, A. F.; Chong, J. M.; Nielsen, N., Titration of alkyllithiums with a simple reagent to a blue endpoint. *J. Organomet. Chem.* **1997**, 542, 281-283.

Lindholm, A.; Maki-Arvela, P.; Toukoniitty, E.; Pakkanen, T. A.; Hirvi, J. T.; Salmi, T.; Murzin, D. Y.; Sjöholm, R.; Leino, R., Hydrosilylation of cinchonidine and 9-O-TMS-cinchonidine with triethoxysilane: application of 11-(triethoxysilyl)-10,11-dihydrocinchonidine as a chiral modifier in the enantioselective hydrogenation of 1-phenylpropane-1,2-dione. *J. Chem. Soc., Perkin Trans. 1* **2002**, 23, 2605-2612.

Yamashita, A.; Norton, E. B.; Hanna, C.; Shim, J.; Salaski, E. J.; Zhou, D.; Mansour, T. S., Synthesis of 3,3-Dimethyl-4-chromanones: Improved Procedures Without Ring Opening. *Synth. Commun.* **2006**, 36, 465 - 472.

Breschi, M. C.; Calderone, V.; Martelli, A.; Minutolo, F.; Rapposelli, S.; Testai, L.; Tonelli, F.; Balsamo, A., New Benzopyran-Based Openers of the Mitochondrial ATP-Sensitive Potassium Channel with Potent Anti-Ischemic Properties. *J. Med. Chem.* **2006**, 49, 7600-7602.

Bonvallet, P. A.; Todd, E. M.; Kim, Y. S.; McMahon, R. J., Access to the Naphthylcarbene Rearrangement Manifold via Isomeric Benzodiazocycloheptatrienes. *J. Org. Chem.* **2002**, 67, 9031-9042.

Yamada, T.; Nagata, T.; Sugi, K. D.; Yoroze, K.; Ikeno, T.; Ohtsuka, Y.; Miyazaki, D.; Mukaiyama, T., Enantioselective Borohydride Reduction Catalyzed by Optically Active Cobalt Complexes. *Chem. Eur. J.* **2003**, 9, 4485-4509.

Inagaki, T.; Ito, A.; Ito, J.-i.; Nishiyama, H., Asymmetric Iron-Catalyzed Hydrosilane Reduction of Ketones: Effect of Zinc Metal upon the Absolute Configuration. *Angew. Chem. Int. Ed.* **2010**, 49, 9384-9387.

Mao, J.; Guo, J., Chiral amino amides for the ruthenium(II)-catalyzed asymmetric transfer hydrogenation reaction of ketones in water. *Chirality* **2010**, 22, 173-181.

Zeror, S.; Collin, J.; Fiaud, J.-C.; Zouiouche, L. A., Evaluation of Ligands for Ketone Reduction by Asymmetric Hydride Transfer in Water by Multi-Substrate Screening. *Adv. Synth. Catal.* **2008**, 350, (1), 197-204.

Nolin, K. A.; Ahn, R. W.; Kobayashi, Y.; Kennedy-Smith, J. J.; Toste, F. D., Enantioselective Reduction of Ketones and Imines Catalyzed by (CN-Box)ReV-Oxo Complexes. *Chem. Eur. J.* **2010**, 16, 9555-9562.

Bouzemi, N.; Aribi-Zouiouche, L.; Fiaud, J.-C., Combined lipase-catalyzed resolution/Mitsunobu esterification for the production of enantiomerically enriched arylalkyl carbinols. *Tetrahedron: Asymmetry* **2006**, 17, 797-800.

Zeror, S.; Collin, J.; Fiaud, J.-C.; Zouiouche, L. A., A recyclable multi-substrates catalytic system for enantioselective reduction of ketones in water. *J. Mol. Catal. A: Chem.* **2006**, 256, 85-89.

Ohkuma, T.; Hattori, T.; Ooka, H.; Inoue, T.; Noyori, R., BINAP/1,4-Diamine-Ruthenium(II) Complexes for Efficient Asymmetric Hydrogenation of 1-Tetralones and Analogues. *Org. Lett.* **2004**, 6, 2681-2683.

Glynn, D.; Shannon, J.; Woodward, S., On the Scope of Trimethylaluminium-Promoted 1,2-Additions of ArZnX Reagents to Aldehydes. *Chem. Eur. J.* **2010**, 16, 1053-1060.

Yang, F.; Xi, P.; Yang, L.; Lan, J.; Xie, R.; You, J., Facile, Mild, and Highly Enantioselective Alkynylzinc Addition to Aromatic Aldehydes by BINOL/N-Methylimidazole Dual Catalysis. *J. Org. Chem.* **2007**, 72, 5457-5460.

Chang, S.-Y.; Jiaang, W.-T.; Cherng, C.-D.; Tang, K.-H.; Huang, C.-H.; Tsai, Y.-M., The Scope and Limitations of Intramolecular Radical Cyclizations of Acylsilanes with Alkyl, Aryl, and Vinyl Radicals. *J. Org. Chem.* **1997**, 62, 9089-9098.

Weickgenannt, A.; Mewald, M.; Oestreich, M., Asymmetric Si-O coupling of alcohols. *Org. Biomol. Chem.* **2010**, 8, 1497-1504.

Rodrigo, J. M.; Zhao, Y.; Hoveyda, A. H.; Snapper, M. L., Regiodivergent Reactions through Catalytic Enantioselective Silylation of Chiral Diols. Synthesis of Sapinofuranone A. *Org. Lett.* **2011**, *13*, 3778-3781.

Worthy, A. D.; Sun, X.; Tan, K. L., Site-Selective Catalysis: Toward a Regiodivergent Resolution of 1,2-Diols. *J. Amer. Chem. Soc.* **2012**, *134*, 7321-7324.

Sun, X.; Worthy, A. D.; Tan, K. L., Scaffolding Catalysts: Highly Enantioselective Desymmetrization Reactions. *Angew. Chem. Int. Ed.* **2011**, *50*, 8167-8171.

Vedejs, E.; Jure, M., Efficiency in Nonenzymatic Kinetic Resolution. *Angew. Chem. Int. Ed.* **2005**, *44*, 3974-4001.

Kagan, H. B.; Fiaud, J. C., In *Topics in Stereochemistry*, Eliel, E. L.; Wilen, S. H., Eds. John Wiley & Sons, Inc.: New York, 1988; Vol. 18, p 249.

Li, X.; Jiang, H.; Uffman, E. W.; Guo, L.; Zhang, Y.; Yang, X.; Birman, V. B., Kinetic Resolution of Secondary Alcohols Using Amidine-Based Catalysts. *J. Org. Chem.* **2012**, *77*, 1722-1737.

Kobayashi, M.; Okamoto, S., Unexpected reactivity of annulated 3H-benzothiazol-2-ylideneamines as an acyl transfer catalyst. *Tet. Lett.* **2006**, *47*, 4347-4350.

Li, X.; Liu, P.; Houk, K. N.; Birman, V. B., Origin of Enantioselectivity in CF₃-PIP-Catalyzed Kinetic Resolution of Secondary Benzylic Alcohols. *J. Am. Chem. Soc.* **2008**, *130*, 13836-13837.

Liu, P.; Yang, X.; Birman, V. B.; Houk, K. N., Origin of Enantioselectivity in Benzotetramisole-Catalyzed Dynamic Kinetic Resolution of Azlactones. *Org. Lett.* **2012**, *14*, 3288-3291.

Larionov, E.; Mahesh, M.; Spivey, A. C.; Wei, Y.; Zipse, H., Theoretical Prediction of Selectivity in Kinetic Resolution of Secondary Alcohols Catalyzed by Chiral DMAP Derivatives. *J. Am. Chem. Soc.* **2012**, *134*, 9390-9399.

Chuit, C.; Corriu, R. J. P.; Reye, C.; Young, J. C., Reactivity of penta- and hexacoordinate silicon compounds and their role as reaction intermediates. *Chem. Rev.* **1993**, *93*, 1371-1448.

Marciniec, B.; Chojnowski, J., *Progress in Organosilicon Chemistry*. 1st ed.; Gordon and Breach: Amsterdam, 1995.

Patai, S.; Apeloig, Y., *The Chemistry of Organic Silicon Compounds*. John Wiley & Sons, Ltd: Chichester, 2001; Vol. 3.

Corriu, R. J. P.; Guerin, C.; Stone, F. G. A.; Robert, W., Nucleophilic Displacement at Silicon: Recent Developments and Mechanistic Implications. In *Advances in Organometallic Chemistry*, Academic Press: 1982; Vol. Volume 20, pp 265-312.

Patai, S.; Rappoport, Z., *The Chemistry of Organic Silicon Compounds*. Wiley: Chichester: 1989; Vol. 1, p 840-863.

Rendler, S.; Oestreich, M., Hypervalent Silicon as a Reactive Site in Selective Bond-Forming Processes. *Synthesis* **2005**, 2005, 1747.

Patai, S.; Apeloig, Y., *The Chemistry of Organic Silicon Chemistry*. John Wiley & Sons, Ltd: Chichester, 1998; Vol. 2.

Chojnowski, J.; Cypryk, M.; Michalski, J., The nature of the interaction between hexamethyl-phosphortriamide and trimethylhalosilanes; cations containing tetravalent silicon as possible intermediates in nucleophile-induced substitution of silicon halides. *J. Organomet. Chem.* **1978**, 161, C31-C35.

Bassindale, A. R.; Stout, T., A ^{29}Si , ^{13}C and ^1H NMR study of the interaction of various halotrimethylsilanes and trimethylsilyl triflate with dimethyl formamide and acetonitrile, a comment on the nucleophile induced racemisation of halosilanes. *J. Organomet. Chem.* **1982**, 238, C41-C45.

Chu, H. K.; Johnson, M. D.; Frye, C. L., Tertiary alcoholysis of chlorosilanes via tetracoordinate silylated quaternary ammonium intermediates. *J. Organomet. Chem.* **1984**, 271, 327-336.

Akiba, K., *Chemistry of Hypervalent Compounds*. Wiley-VCH: New York, 1999.

Cheung, Y.-S.; Ng, C.-Y.; Chiu, S.-W.; Li, W.-K., Application of three-center-four-electron bonding for structural and stability predictions of main group hypervalent molecules: the fulfillment of octet shell rule. *J. Mol. Struct-THEOCHEM* **2003**, 623, 1-10.

Benaglia, M.; Guizzetti, S.; Rossi, S., Silicate-Mediated Stereoselective Reactions Catalyzed by Chiral Lewis Bases. In *Catalytic Methods in Asymmetric Synthesis*, John Wiley & Sons, Inc.: 2011; pp 579-624.

Tandura, S.; Voronkov, M.; Alekseev, N., Molecular and electronic structure of penta- and hexacoordinate silicon compounds. *Structural Chemistry of Boron and Silicon*. In Springer Berlin / Heidelberg: 1986; Vol. 131, pp 99-189.

Bassindale, A. R.; Jiang, J., The effect of pentacoordination on silicon-29 NMR chemical shifts and silicon-hydrogen coupling constants. *J. Organomet. Chem.* **1993**, 446, C3-C5.

Kobayashi, J.; Ishida, K.; Kawashima, T., Synthesis of a heptacoordinate trichlorosilane with a tetradentate ligand and unusual stability for nucleophilic substitution. *Silicon Chemistry* **2002**, *1*, 351-354.

Scholl, R. L.; Maciel, G. E.; Musker, W. K., Silicon-29 chemical shifts of organosilicon compounds. *J. Am. Chem. Soc.* **1972**, *94*, 6376-6385.

Bacon, M. R.; Maciel, G. E., Solvent effects on the five shielding constants in tetramethylsilane and cyclohexane. *J. Am. Chem. Soc.* **1973**, *95*, 2413-2426.

Williams, E. A.; Cargioli, J. D.; Larochelle, R. W., Silicon-29 NMR. Solvent effects on chemical shifts of silanols and silylamines. *J. Organomet. Chem.* **1976**, *108*, 153-158.

Campbell-Ferguson, H. J.; Ebsworth, E. A. V., Adducts formed between some halogenosilanes and the organic bases pyridine, trimethylamine, and tetramethylethylenediamine. Part I. Stoichiometry. *J. Chem. Soc. A* **1966**, 1508-1514.

Campbell-Ferguson, H. J.; Ebsworth, E. A. V., Adducts of the halogenosilanes. Part II. Physical properties and structures. *J. Chem. Soc. A* **1967**, 705-712.

Boudjouk, P.; D. Kloos, S.; Kim, B.-K.; Page, M.; Thweatt, D., An unexpected redistribution of trichlorosilane. Synthesis, structure and bonding of (N,N,N',N'-tetraethylethylenediamine)dichlorosilane. *J. Chem. Soc., Dalton Trans.* **1998**, *6*, 877- 880.

Lippmaa, E. T.; Alla, M. A.; Pehk, T. J.; Engelhardt, G., Solid-state high resolution NMR spectroscopy of spin 1/2 nuclei (carbon-13, silicon-29, tin-119) in organic compounds. *J. Am. Chem. Soc.* **1978**, *100*, 1929-1931.

Brendler, E.; Heine, T.; Hill, A. F.; Wagler, J., A Pentacoordinate Chlorotrimethylsilane Derivative: A very Polar Snapshot of a Nucleophilic Substitution and its Influence on ^{29}Si Solid State NMR Properties. *Z. Anorg. Allg. Chem.* **2009**, *635*, 1300-1305.

Bassindale, A. R.; Stout, T., Interaction of N-trimethylsilylimidazole with electrophilic trimethylsilyl compounds. Part 1. Characterisation of silylimidazolium salts. *J. Chem. Soc., Perkin Transs. 2* **1986**, *2*, 221-225.

Aliev, A. E.; Atkinson, C. E.; Harris, K. D. M., Hydrogen Bond Dynamics in Solid Triphenylsilanol. *J. Phys. Chem. B* **2002**, *106*, 9013-9018.

Bax, A.; Summers, M. F., Proton and carbon-13 assignments from sensitivity-enhanced detection of heteronuclear multiple-bond connectivity by 2D multiple quantum NMR. *J. Am. Chem. Soc.* **1986**, *108*, 2093-2094.

Schraml, J., ^{29}Si NMR Experiments in Solutions of Organosilicon Compounds. In *The Chemistry of Organic Silicon Compounds*, John Wiley & Sons, Ltd: 2001; pp 223-339.

Bearpark, M. J.; McGrady, G. S.; Prince, P. D.; Steed, J. W., The First Structurally Characterized Hypervalent Silicon Hydride: Unexpected Molecular Geometry and Si-H Interactions. *J. American Chem. Soc.* **2001**, *123*, 7736-7737.

Rot, N.; Nijbacker, T.; Kroon, R.; de Kanter, F. J. J.; Bickelhaupt, F.; Lutz, M.; Spek, A. L., Introduction of Bulky Substituents at the Bridgehead Position of a 9-Silatriptycene: Pentacoordinate Hydridoorganosilicates as Intermediates. *Organometallics* **2000**, *19*, 1319-1324.

Bassindale, A. R.; Stout, T., The preparation and observation by ^{29}Si n.m.r. spectroscopy of simple, acyclic, five-coordinate silicon salts. *J. Chem. Society, Chem. Comm.* **1984**, *21*, 1387-1389.

Lyčka, A.; Šnobl, D.; Handlíř, K.; Holeček, J.; Nádvorník, M., ^{29}Si and ^{13}C NMR spectra of some alkyl-diphenylchlorosilanes, alkyl-diphenylsilanols and bis(alkyl-diphenylsilyl)chromates. *Collect. Czech. Chem. Commun.* **1982**, *47*, 603-612.

Negrebetsky, V. V.; Negrebetsky, V. V.; Shipov, A. G.; Kramorova, E. P.; Baukov, Y. I., Intermolecular and intramolecular coordination interactions in solutions of N-(dimethylchlorosilylmethyl) acetamides. *J. Organomet. Chem.* **1995**, *496*, 103-107.

Kummer, D.; Halim, S. H. A., Beiträge zur Chemie der Halogensilan-Addukte. XXIV. Übergänge zwischen penta- und tetrakoordinierten SiCl - und SiBr -Verbindungen und ihre Abhängigkeit von Lösungsmittel, Temperatur und Konzentration. Direkter spektroskopischer Nachweis des reversiblen Übergangs von einer O-SiCl zu einer OSi-Cl-Koordination. *Z. Anorg. Allg. Chem.* **1996**, *622*, 57-66.

Cragg, R. H.; Lane, R. D., Contributions to group IV organometallic chemistry: VII. The effect of electronegativity on substituent shifts in silicon-29 NMR. *J. Organomet. Chem.* **1984**, *277*, 199-201.

Ritchie, C. D.; Sager, W. F., An Examination of Structure-Reactivity Relationships. In *Progress in Physical Organic Chemistry*, John Wiley & Sons, Inc.: 2007; pp 323-400.

Birman, V. B.; Li, X., Homobenzotetramisole: An Effective Catalyst for Kinetic Resolution of Aryl-Cycloalkanols. *Org. Lett.* **2008**, *10*, 1115-1118.

Zhang, Y.; Birman, V. B., Effects of Methyl Substituents on the Activity and Enantioselectivity of Homobenzotetramisole-Based Catalysts in the Kinetic Resolution of Alcohols. *Adv. Synth. Catal.* **2009**, *351*, 2525-2529.

Birman, V. B.; Li, X., Benzotetramisole: A Remarkably Enantioselective Acyl Transfer Catalyst. *Org. Lett.* **2006**, 8, 1351-1354.

Hensen, K.; Zengerly, T.; Müller, T.; Pickel, P., Ionische Strukturen von 4- bzw. 5fach koordiniertem Silicium: $[\text{Me}_3\text{Si}(\text{NMI})]^+\text{Cl}^-$, $[\text{Me}_2\text{HSi}(\text{NMI})_2]^+\text{Cl}^-$, $[\text{Me}_2\text{Si}(\text{NMI})_3]_2^{+2}\text{Cl}^- \cdot \text{NMI}$. *Z. Anorg. Allg. Chem.* **1988**, 558, 21-27.

Bassindale, A. R.; Stout, T., The preparation and observation by ^{29}Si n.m.r. spectroscopy of simple, acyclic, five-co-ordinate silicon salts. *J. Chem. Soc., Chem. Comm.* **1984**, 21, 1387-1389.

Corriu, R. J. P.; Dabosi, G.; Martineau, M., The nature of the interaction of nucleophiles such as HMPT, DMSO, DMF and Ph_3PO with triorganohalo-silanes, germanes, and -stannanes and organophosphorus compounds. Mechanism of nucleophile induced racemization and substitution at metal. *J. Organomet. Chem.* **1980**, 186, 25-37.

Maji, B.; Joannesse, C.; Nigst, T. A.; Smith, A. D.; Mayr, H., Nucleophilicities and Lewis Basicities of Isothiourea Derivatives. *J. Org. Chem.* **2011**, 76, 5104-5112.

Mislow, K., Stereochemical consequences of correlated rotation in molecular propellers. *Acc. Chem. Res.* **1976**, 9, 26-33.

Mislow, K.; Gust, D.; Finocchiaro, P.; Boettcher, R., Stereochemical correspondence among molecular propellers. In *Stereochemistry I*, Springer Berlin Heidelberg: 1974; Vol. 47, pp 1-28.

Allen, G. W.; Aroney, M. J.; Hambley, T. W., Conformational analysis of group IVB aryls: An electric birefringence and molecular mechanics study. *J. Mol. Struc.* **1990**, 216, 227-240.

Gust, D.; Mislow, K., Analysis of isomerization in compounds displaying restricted rotation of aryl groups. *J. Am. Chem. Soc.* **1973**, 95, 1535-1547.

Andose, J. D.; Mislow, K., Structure and dynamic stereochemistry of trimesitylmethane. II. Empirical force field calculations. *J. Am. Chem. Soc.* **1974**, 96, 2168-2176.

Kates, M. R.; Andose, J. D.; Finocchiaro, P.; Gust, D.; Mislow, K., Empirical force-field calculations on a model system for trimesityl derivatives of Group IIIa, IVa, and Va elements. Stereoisomerization pathways. *J. Am. Chem. Soc.* **1975**, 97, 1772-1778.

Ściebura, J.; Skowronek, P.; Gawronski, J., Trityl Ethers: Molecular Bevel Gears Reporting Chirality through Circular Dichroism Spectra. *Angew. Chem. Int. Ed.* **2009**, 48, 7069-7072.

Ściebura, J.; Gawroński, J., Double Chirality Transmission in Trityl Amines: Sensing Molecular Dynamic Stereochemistry by Circular Dichroism and DFT Calculations. *Chem. Eur. J.* **2011**, *17*, 13138-13141.

DiNitto, J. M.; Kenney, J. M., Noise Characterization in Circular Dichroism Spectroscopy. *Appl. Spectrosc.* **2012**, *66*, 180-187.

Savitzky, A.; Golay, M. J. E., Smoothing and Differentiation of Data by Simplified Least Squares Procedures. *Anal. Chem.* **1964**, *36*, 1627-1639.

Leslie, F. M.; Demus, D.; Goodby, J.; Gray, G. W.; Spiess, H. W.; Vill, V., Theory of the Liquid Crystalline State. In *Physical Properties of Liquid Crystals*, Wiley-VCH Verlag GmbH: 2007; pp 25-86.

Wolf, C.; Moskowicz, M., Bisoxazolidine-Catalyzed Enantioselective Reformatsky Reaction. *J. Org. Chem.* **2011**, *76*, 6372-6376.

Wolf, C.; Xu, H., Asymmetric catalysis with chiral oxazolidine ligands. *Chem. Comm.* **2011**, *47*, 3339-3350.

Ghosh, A. K.; Mathivanan, P.; Cappiello, J., C₂-Symmetric chiral bis(oxazoline)-metal complexes in catalytic asymmetric synthesis. *Tetrahedron: Asymmetry* **1998**, *9*, 1-45.

Johnson, J. S.; Evans, D. A., Chiral Bis(oxazoline) Copper(II) Complexes: Versatile Catalysts for Enantioselective Cycloaddition, Aldol, Michael, and Carbonyl Ene Reactions. *Acc. Chem. Res.* **2000**, *33*, 325-335.

Desimoni, G.; Faita, G.; Jorgensen, K. A., Update 1 of: C₂-Symmetric Chiral Bis(oxazoline) Ligands in Asymmetric Catalysis. *Chem. Rev.* **2011**, *111*, 284-437.

Helmchen, G. N.; Pfaltz, A., Phosphinooxazolines A New Class of Versatile, Modular P,N-Ligands for Asymmetric Catalysis. *Acc. Chem. Res.* **2000**, *33*, 336-345.

Jin, Z.; Huang, H.; Li, W.; Luo, X.; Liang, X.; Ye, J., Enantioselective Organocatalytic Synthesis of Oxazolidine Derivatives through a One-Pot Cascade Reaction. *Adv. Synth. Catal.* **2011**, *353*, 343-348.

Fan, Y. C.; Kwon, O., Diversity-Oriented Synthesis Based on the DPPP-Catalyzed Mixed Double-Michael Reactions of Electron-Deficient Acetylenes and Amino Alcohols. *Molecules* **2011**, *16*, 3802-3825

Xu, H.; Wolf, C., Asymmetric Synthesis of Chiral 1,3-Diaminopropanols: Bisoxazolidine-Catalyzed C–C Bond Formation with α -Keto Amides. *Angew. Chem. Int Ed.* **2011**, *50*, 12249-12252.

- Astudillo, M. E. A.; Chokotho, N. C. J.; Jarvis, T. C.; Johnson, C. D.; Lewis, C. C.; McDonnell, P. D., Hydroxy schiff base-oxazolidine tautomerism: Apparent breakdown of baldwin's rules. *Tetrahedron* **1985**, *41*, 5919-5928.
- Baldwin, J. E.; Cutting, J.; Dupont, W.; Kruse, L.; Silberman, L.; Thomas, R. C., 5-Endo-trigonal reactions: a disfavored ring closure. *J. Chem. Soc., Chem. Comm.* **1976**, *18*, 736-738.
- Abadallah, H.; Gree, R.; Carrie, R., Syntheses asymetriques a l'aide d'oxazolidines chirales derivees de l'ephedrine. Preparation de formyl cyclopropanes chiraux. *Tet. Lett.* **1982**, *23*, 503-506.
- Chou, C.-Y.; Raman, P. K.; Malocha, R. E.; Johnson, T. L.; Nocito, V.; Hoffman, M. D.; Brutto, P. E. Iminoalcohol-oxazolidine mixtures and their use. Patent 5,328,635, July 12, 1994.
- ANGUS Chemical Company Technical Data Sheet
http://sdssearch.dow.com/PublishedLiteratureDOWCOM/dh_003f/0901b8038003f828.pdf?filepath=angus/pdfs/noreg/319-00029.pdf&fromPage=GetDoc
 (accessed on March 3rd, 2013).
- Bicker, K. L.; Wiskur, S. L.; Lavigne, J. J., Colorimetric Sensor Design. In *Chemosensors*, John Wiley & Sons, Inc.: Hoboken, NJ, 2011; pp 275-295.
- Wiskur, S. L.; Maynor, M. S.; Smith, M. D.; Sheppard, C.; Akhani, R. K.; Pellechia, P. J.; Vaughn, S. A.; Shieh, C., Chiral pyridinyloxazolidine ligands and copper chloride complexes. *J. Coord. Chem.* **2013**, ASAP.
- SPARTAN '08 version 1.2 Wavefunction Inc., 18401 Von Karman Avenue, Suite 370, Irvine CA 92612, U.S.A. 2008
- Turner, N. J., *Nat. Chem. Bio.* **2009**, *5*, (8), 567-573.
- Nugent, T. C., *Chiral Amine Synthesis. Methods , Developments and Applications*. Wiley-VCH: Weinheim, 2010.
- Breuer, M.; Ditrach, K.; Habicher, T.; Hauer, B.; Keßeler, M.; Stürmer, R.; Zelinski, T., Industrial Methods for the Production of Optically Active Intermediates. *Angew. Chem. Int. Ed.* **2004**, *43*, 788-824.
- Henkel, T.; Brunne, R. M.; Müller, H.; Reichel, F., Statistical Investigation into the Structural Complementarity of Natural Products and Synthetic Compounds. *Angew. Chem. Int. Ed.* **1999**, *38*, 643-647.
- You, L.; Berman, J. S.; Anslyn, E. V., Dynamic multi-component covalent assembly for the reversible binding of secondary alcohols and chirality sensing. *Nat. Chem.* **2011**, *3*, 943-948.

Kaneda, T.; Hirose, K.; Misumi, S., Chiral azophenolic acerands: color indicators to judge the absolute configuration of chiral amines. *J. Am. Chem. Soc.* **1989**, *111*, 742-743.

Kubo, Y.; Maeda, S. y.; Tokita, S.; Kubo, M., *Nature* **1996**, *382*, 522-524.

Misumi, S., Supramolecular Chemistry I Directed Synthesis and Molecular Recognition: Recognitory coloration of cations with chromoacerands. In *Top. Curr. Chem.*, Springer Berlin Heidelberg: 1993; Vol. 165, pp 163-192.

Tsubaki, K.; Nuruzzaman, M.; Kusumoto, T.; Hayashi, N.; Bin-Gui, W.; Fuji, K., Visual Enantiomeric Recognition Using Chiral Phenolphthalein Derivatives. *Org. Lett.* **2001**, *3*, 4071-4073.

Tsubaki, K.; Tanima, D.; Nuruzzaman, M.; Kusumoto, T.; Fuji, K.; Kawabata, T., Visual Enantiomeric Recognition of Amino Acid Derivatives in Protic Solvents. *J. Org. Chem.* **2005**, *70*, 4609-4616.

Leung, D.; Folmer-Andersen, J. F.; Lynch, V. M.; Anslyn, E. V., Using Enantioselective Indicator Displacement Assays To Determine the Enantiomeric Excess of Amino Acids. *J. Am. Chem. Soc.* **2008**, *130*, 12318-12327.

Cho, E. N. R.; Li, Y.; Kim, H. J.; Hyun, M. H., A colorimetric chiral sensor based on chiral crown ether for the recognition of the two enantiomers of primary amino alcohols and amines. *Chirality* **2011**, *23*, 349-353.

Hirose, K., A Practical Guide for the Determination of Binding Constants. *J. Incl. Phenom. Macro.* **2001**, *39*, 193-209.

Kubo, Y., Binaphthyl-appended Chromogenic Receptors: Synthesis and Application to their Colorimetric Recognition of Amines. *Synlett* **1999**, *1999*, 161-174.

Hirose, K.; Aksharanandana, P.; Suzuki, M.; Wads, K.; Naemura, K.; Tobe, Y., *Heterocycles* **2005**, *66*, 405-431.

Leung, D.; Anslyn, E. V., Transitioning Enantioselective Indicator Displacement Assays for Amino Acids to Protocols Amenable to High-Throughput Screening. *J. Am. Chem. Soc.* **2008**, *130*, 12328-12333.

Crassous, J., Chiral transfer in coordination complexes: towards molecular materials. *Chem. Soc. Rev.* **2009**, *38*, 830-845.

Nakano, H.; Osone, K.; Takeshita, M.; Kwon, E.; Seki, C.; Matsuyama, H.; Takano, N.; Kohari, Y., A novel chiral oxazolidine organocatalyst for the synthesis of an oseltamivir intermediate using a highly enantioselective Diels-Alder reaction of 1,2- dihydropyridine. *Chem. Comm.* **2010**, *46*, 4827-4829.

Weickgenannt, A.; Mewald, M.; Oestreich, M., Asymmetric Si-O coupling of alcohols. *Org. Biomol. Chem.* **2010**, *8*, 1497-1504.